AN INVESTIGATION OF POLYOLEFIN MANUFACTURING TECHNOLOGY - MATHEMATICAL MODELLING OF POLYMERIZATION AND POLYMER MODIFICATION PROCESSES

by

PAUL EDWIN GLOOR, B. Eng.

A Thesis
Submitted to the School of Graduate Studies
in Partial Fulfillment of the Requirements
for the Degree of
Doctor of Philosophy

McMaster University

AN INVESTIGATION OF POLYOLEFIN MANUFACTURING TECHNOLOGY

DOCTOR OF PHILOSOPHY (1993)
(Chemical Engineering)

McMASTER UNIVERSITY
Hamilton, Ontario, Canada.

TITLE:	An investigation of polyolefin manufacturing technology - Mathematical modelling of polymerization and polymer modification processes
AUTHOR:	Paul Edwin Gloor, B. Eng. (McMaster University)
ADVISORS:	Professor Archie E. Hamielec Professor John F. MacGregor
NUMBER OF PAGES:	xii,281

Abstract

Polyolefins have been manufactured as commodity polymers for over 50 years and yet technological details, at the molecular level, of the manufacturing processes available in the open literature are sparse at best. The objectives of the present investigations were therefore to use modern mathematical modelling techniques to elucidate relevant phenomena at the molecular level that are crucial to the success of key manufacturing processes used commercially.

The work described in this thesis can be broken down into two separate parts. The first deals with the mathematical and computer modelling of industrially important methods for the production of polyolefins, specifically: a) the high pressure tubular reactor process, b) the high pressure autoclave type reactor process, and c) the low pressure Ziegler Natta reactor process using heterogeneous catalysts. The second part deals with the chemical modification of these polymers by free radical methods during the extrusion process.

Free radical copolymerization of ethylene in high pressure reactors is considered. Kinetic mechanisms to describe the polymerization rate and polymer properties, including copolymer composition, molecular weight, branching frequencies, melt flow index and polymer density, have been proposed. The method of moments is used, in conjunction with pseudo kinetic rate constants to allow for copolymerization, to calculate the molecular weight averages Based upon this kinetic scheme, a mathematical model has been derived and implemented as computer programs to simulate commercial tubular and autoclave type reactors. The model parameters were fit to steady state data from industrial reactors.

The steady state tubular reactor model allows for multiple feed points, multiple initiators (including oxygen) and non-isothermal polymerization. The effects of the pulse valve and the product cooler are incorporated.

The dynamic autoclave reactor model also includes the two phase kinetics due to polymer-monomer solubilities and phase separation in the reaction mixture. Gel formation from crosslinking reactions is also analyzed. A mixing model is developed to represent the flow inside the reactor. In the simulation PID control equations are used to maintain operation at the unstable steady state. A sensitivity study is performed on the mixing model parameters and on some of the kinetic parameters. The model is compared to steady state temperature, initiator flow and conversion data from commercial reactors.

Many polyolefins are produced using heterogeneous Ziegler Natta catalysts either in gas phase, bulk or slurry type reactors. A multiple active site model is necessary in order to account for the broad properties of polymer produced on these catalysts. These properties include broad molecular weight and copolymer composition distributions. A kinetic model has been derived, based upon multiple catalyst sites of differing reactivities, for the Ziegler-Natta copolymerization of olefins. The model predicts the rate of polymerization, the copolymer composition and the molecular weight distribution of the polymer produced as well as accounting for the observed broad copolymer composition and molecular weight distributions.

In addition to producing polyolefins in reactors, industry is now chemically modifying commodity polyolefins to produce higher priced specialty materials. Several of the reactive processing techniques to modify polyolefins involve the introduction of a free radical initiator into the polymer melt which produce the radicals that modify the molecular structure of the polymer. In general, in reactive processing, scission, grafting, branching and crosslinking may all occur simultaneously.

This dissertation deals with the development of mathematical models to relate the molecular modifications, scission, branching, crosslinking and grafting. The models, based upon generally accepted kinetic mechanisms and certain assumptions about the nature of simultaneous scission and crosslinking, can predict the molecular weight averages, degrees of crosslinking, scission and grafting, and the sol/gel ratio. A mathematical formulation to describe simultaneous random scission and crosslinking has been presented in the literature but only solved by assuming that scission and crosslinking occur serially. For this work, an algorithm to numerically solve this equation was developed. The results of these calculations were compared to the classical solutions to this problem and to the experimental data gathered in this project. This model, although applied to polyolefin modification, has applications for other systems where simultaneous random scission and crosslinking of polymers is encountered.

Acknowledgments

In most facets of our lives, we do not exist in isolation, but interact with the people around us. This collaboration can be rewarding and in my experience, vital. I wish to point out a few of the people who contributed to my life and work.

Firstly my family, Julie and Megan, who have given me the much needed love, support and encouragement. I love you both. And my parents, Ralph and Dorothy, who started me down this path, many years ago.

My supervisors, A. E. Hamielec, and J. F. MacGregor, who truly created the opportunity, and provided the guidance and much of the inspiration for my perspiration. Thanks to A. N. Hrymak for discussions about extruders and numerical methods and life.

Due to the industrial nature of these projects, collaboration was inevitable, indeed desired. Wai Man Chan and Rodolfo Zabisky, supplied their industrial knowledge for the high pressure polyethylene processes. Both provided much needed critical evaluation of the model and software. Bruno de Carvalho and I worked quite closely on the Ziegler Natta polymerization sections. Bruno's industrial knowledge and background in the chemistry of Ziegler Natta polymerization was invaluable. Bruno was instrumental in getting me to Brazil to see their process in operation. *Molto obrigado.*

Lisa Morine, Doug Keller, Stienna Thomas, Greg Emery, Mary Ann Barban and Dean Anderson. Thanks for taking care of most of the logistics and cheerfully helping out when I needed you. You are indispensable. Bill Warriner, everything was *dead nuts*. Yinnan Tang, Aleksandra Kostanska, Kris Kostanski, and Patrick Wong helped with many of the analyses and experiments. Mike Butler for his help in the hot cell experiments, Brian Sayer for the NMR, and João Soares and Jesus Vela Estrada for help with the GPC. Shiping Zhu for initiating countless stimulating discussions. *Gambay!*

McMaster Institute for Polymer Production Technology, National Sciences and Engineering Research Council of Canada, and Department of Chemical Engineering for their financial support.

And to everyone in the chemical engineering department. You have provided an environment in which I could live, learn, explore, grow and contribute. I am honoured to call each of you, my friend.

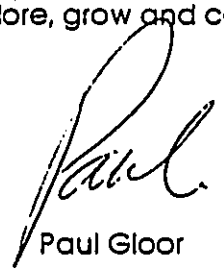

Paul Gloor
Hamilton, Ontario.
April 13, 1993

Table of Contents

Table of Figures

Table of Tables

Chapter 1 Introduction

There can be no doubt that polymeric materials greatly influence our lives. We use them for our clothing, our houses, our automobiles, our electronics, to package our food... The list is virtually endless. The polymers made from the alkenes (polyolefins), especially polyethylene, polypropylene and copolymers, are some of the most useful and are produced in vast quantities. In fact, the world wide production of polyethylene is over 15 million tons per year (Elias 1989).

Polyethylenes have been manufactured since 1933 and polypropylene since the discovery of the Ziegler-Natta catalysts in the early fifties. Much effort has been made to produce materials with the desired densities and flow characteristics by manipulating the reaction conditions or by the addition of comonomers and other modifiers. Even though we have been making these polymers for some time, we still can not exactly quantify just how the process operating conditions influence the molecular and physical properties.

On the other hand, a relatively new process called reactive extrusion, is allowing us to modify existing polyolefin chains to produce materials with a wide variety of properties. We can increase or decrease the molecular weight, add branches, produce a crosslinked structure, graft functional groups to the back bone or graft two different polymers together, all in the melt during the extrusion process. By changing the molecular weights or amounts of branching we can tailor the flow characteristics of the polymer to the application. By grafting special groups onto the backbone of the polymer we can influence the surface properties, like adhesion, to allow for better bonding to reinforcing materials. These special groups may also be used for further reaction as in the case of silane crosslinking of polyethylenes. Alloys of usually immiscible polymers are made by in situ compatibilization, by creating polymer chains with blocks of each polymer type. Whereas, in the past new products were made by designing new polymers by the addition of comonomers or new reaction systems, reactive processing offers a new path to novel materials. Since extruders are high throughput, relatively inexpensive, pieces of equipment even small manufacturers can create a line of low volume, higher priced, specialty polymers all based upon cheaper commodity polymers.

Let us consider the major events in the life of polymer (figure 1). Polymer producers manufacture the polyolefins from monomer. Nearly all of the polymer created is extruded by the polymer producer to at least pelletize the product. The polymer producers earn their living by selling their polymer at a high enough price to pay for the monomer and all the operating costs. Raw material costs and product variability can be reduced through

more efficient reactor operation. Companies that reduce the variability of their product properties, may be able to charge a premium. Another of the costs associated with production occurs when a grade change or a mistake is made. The off specification material produced, if it can't be blended and sold at a discount, must be discarded. Proper operation of the reactor system can minimize the off spec material produced, and thus significantly improve profits.

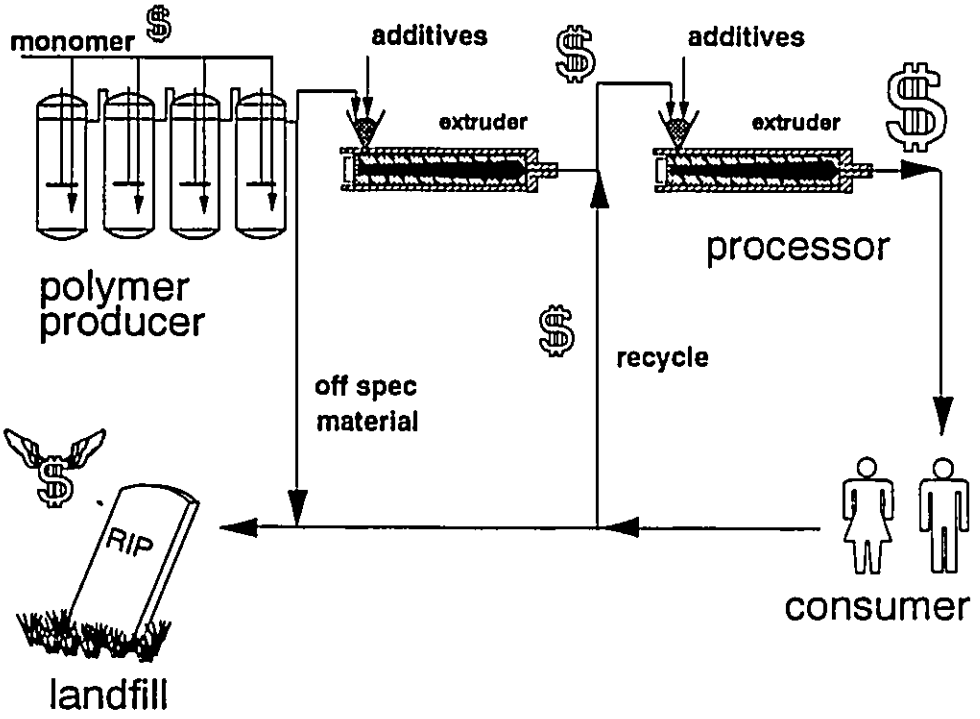

Figure 1. A life cycle diagram for polymers.

The polymer is then shipped from the producer to the processor who extrudes it into a useful shape by, for example, molding, casting or spinning it into fibers and thus increasing its value. These products are then used by the consumer, who traditionally discarded the product to land fill when it was no longer desired. Recent public opinion is now forcing a trend to recycling these polymer products. There are several obstacles associated with this enterprise, not the least of which is that much of the material in the recycle stream is a mixture of different plastics, which must be sorted since their blends do not have adequate mechanical properties.

Let us now introduce reactive extrusion into the picture. If polymer producers can learn to modify their product during the extrusion process, a variety of grades can be produced by simply changing the extruder conditions and the additives. Grade changes would no longer require several hours but could be accomplished in a few minutes, thus reducing the amount of off specification material. Off specification material might even be saved by the appropriate reactive extrusion method. The polymer processors can, using reactive processing, create a host of novel materials based upon modified structures and blends, increasing the value of the product that they sell. Moreover mixtures of recycled plastics may be *compatibilized* into materials with good mechanical properties using reactive extrusion.

Well, how does the work at hand fit into this picture? We have pointed out the value in learning how to better operate our polyolefin producing reactors and learning more about reactive extrusion. One useful framework for studying these systems is to develop mathematical models. We learn a great deal about the process during model development, because we are forced to systematically ask the important questions. When the model is complete, it then becomes convenient storage for all that we have learned. To retrieve the knowledge simply give the process conditions to the computer program.

The work described in this manuscript deals with the mathematical and computer modelling of the chemical and physical phenomena involved in the production of polyolefins in the high pressure free radical process and applied to tubular and autoclave type reactors. A model for the low pressure Ziegler - Natta process is developed which should be applicable to slurry, bulk and gas phase reactors. In addition models are developed for chemical modification of polyolefins by free radical mechanisms in the melt.

Since "the virtue of a computer is speed, not intelligence" (Reid et al. 1986) we must compare our mathematical results to the real world. We have been fortunate to be able to obtain data from industrial autoclave and tubular reactors (Poliolefinas S. A. São Paulo Brazil). Moreover, an experimental study of the reactive extrusion of polyolefins has been completed for this thesis.

1.1 Overview of polyolefins

Before we get into the heart of this work, it is important to outline some of the important properties, uses and concepts associated with polyolefins. Polyolefins are produced either by high pressure, free radical processes, or by processes using Ziegler-Natta catalysts at lower pressures.

In free radical polymerization, an initiator is added to the monomer and it thermally decomposes to form free radicals. These radicals attack and subsequently add on to the double bond on a monomer molecule. This new radical species will then attack and add on to another monomer molecule. This process continues, building up high molecular weight material, until two radicals meet to terminate or a transfer reaction initiates a new chain.

Ziegler-Natta catalysts are mostly complexes of compounds of group IV to group VIII elements (transition metals) and compounds from groups I to IV. The first compound is the catalyst, the second is a cocatalyst. Some of these catalysts are supported on materials like silica. The manufacture, i.e. order of addition, grinding, mixing, of the catalysts has a great effect on the catalyst performance and is still somewhat of an art. These catalysts are very sensitive to impurities like water, CO, and oxygen and can be poisoned by them. The catalysts seem to have a distribution of active site types and some impurities, like CO, can preferentially poison certain sites changing the overall character of the catalyst.

The conceptual model for the polymerization that has stood the test of time is the monomer insertion mechanism of Cossee (1964) as is shown in figure 2. The monomer is inserted at the catalyst site and the polymer grows outward by adding units at the catalyst end, just like hair grows, from the root. The catalyst controls the stereoregularity of the growing chain, by adding the monomer units in a specific orientation.

The rates of polymerization with time can follow several paths, some initially increasing and then declining, some always declining and some constant (see figure 3 and Tait 1986). These different profiles are possibly due to the presence of initiation reactions that cause the formation of new active centers with time, catalyst breakup which exposes new catalyst surface, and catalyst decay which is the destruction of active centers with time. The polymer chain continues to grow by inserting new monomer units until a reaction, like transfer to hydrogen displaces the growing chain from the catalyst site.

Monometallic Mechanism

(Cossee (1964))

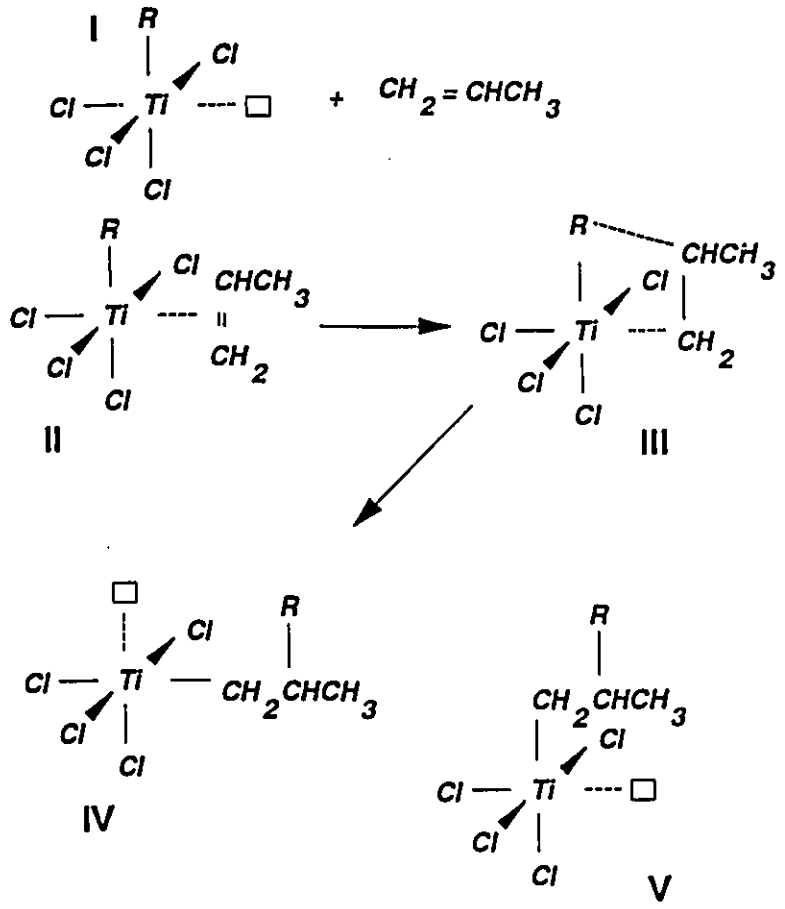

---- □ *denotes a vacancy*

Structures I & V are equivalent - only "R" is different

Figure 2 The monometallic mechanism of Cossee (1964) for Ziegler-Natta catalysts.

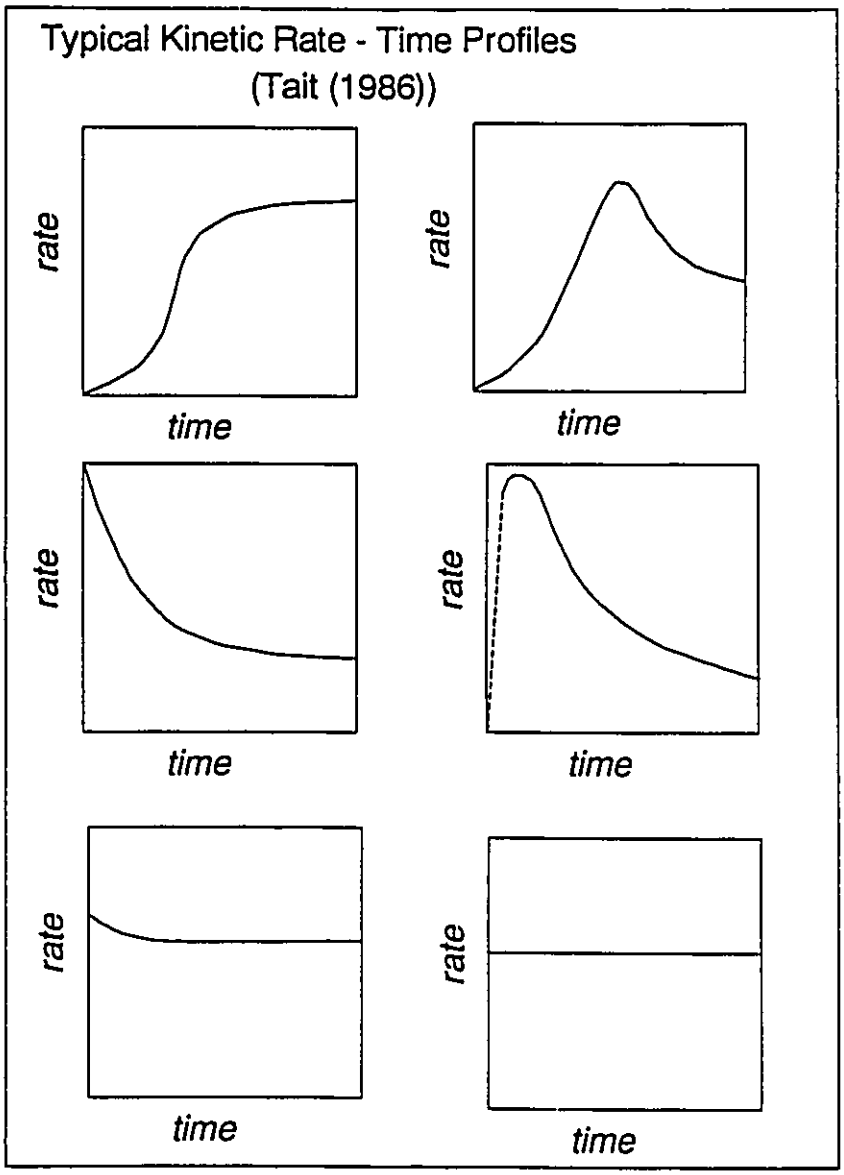

Figure 3 Typical kinetic rate time profiles for Ziegler-Natta catalysts.

1.1.1 Polyethylenes

Polyethylenes are manufactured via free radical and Ziegler-Natta polymerization of ethylene and comonomers. The free radical method, usually at high pressures (up to 3500 atm.) and temperatures (up to 300°C), is the oldest of the two

methods. The Ziegler-Natta processes usually have much milder conditions (lower pressures and temperatures). The common property which distinguishes different polyethylenes is polymer density. Although the distinction is somewhat approximate we usually say that low density PE has a density below 0.94 g/cm^3 while high density is above 0.94 g/cm^3, the density being determined by the polymer structure.

Low density polyethylene (LDPE or HP-LDPE): Polyethylene made in the high pressure process is almost always of low density. The free radical mechanism promotes the formation of short chain branches (typically about 4 carbon atoms long) and long chain branches of length comparable to the length of a typical polymer molecule. Typical branching frequencies are 7-17 short chain branches per thousand backbone carbon atoms, for long chain branches about 0.5 - 2.2 per thousand backbone carbon atoms.

Ethylene vinyl acetate (EVA) copolymers can be produced only by the free radical process, since vinyl acetate destroys the Ziegler-Natta catalyst activity.

High density polyethylene (HDPE): is produced by the homopolymerization of ethylene using Ziegler-Natta catalysts. In 1980, HDPE was the number three thermoplastic produced in the world, surpassed only by LDPE and polyvinyl chloride and followed by polypropylene, polystyrene and expanded polystyrene.

Linear low density polyethylene (LLDPE): A low density polyethylene can also be produced by the Ziegler-Natta processes by incorporating an α-olefins as a comonomer to provide short chain branches. The density is therefore determined by the copolymer composition and by the size of the α-olefin. Most commodity-type applications incorporate butene-1 as the comonomer but higher molecular weight olefin comonomers produce resins with significant strength advantages, including tear, impact, and puncture resistance, relative to butene copolymers.

Compared to a HP-LDPE resin of similar density and melt index, the LLDPE will have higher tensile and impact strength, elongation, environmental stress crack resistance, heat resistance, and stiffness The greater strength of LLDPE allows for a reduction in the product thickness, relative to HP-LDPE and still maintain good end use properties but existing extruders must be modified to convert from HP-LDPE to LLDPE due to the higher shear viscosity of the narrow MWD LLDPE (Yi and Pacala, 1988).

An even lower density polyethylene, produced by Ziegler-Natta processes, is aptly named very low density polyethylene (VLDPE) and has properties such that it may replace ethylene vinyl acetate copolymer or even polyvinyl chloride in applications like flexible hose and tubing, speciality and medical film, and tie and sealing layers in multilayer film constructions (Yi and Pacala, 1988).

UHMWPE: produced by low pressure Ziegler-Natta processes has a molecular weight of greater than about 3 million, and intrinsic viscosity of 20 or more. (Birnkraut et al. 1981). As with other polyethylenes, UHMWPE provides a good non- adherent surface, low coefficient of friction, and good chemical resistance. Moreover UHMWPE exhibits good high abrasion and impact resistance. The large amorphous areas are responsible for the excellent impact properties, and for a lower density. Impact strength decreases with decreases in molecular weight, and may be due to decreasing intermolecular forces and chain entanglement. The melt viscosity of UHMWPE is quite high and as such extrusion on ordinary equipment may not be possible, one must use processing based on powdered metallurgy techniques, or machining from rods or sheets. The most common techniques are compression molding and ram extrusion. Injection molding may not work because the melt viscosity is too high. Nevertheless its desirable properties are causing innovations in the machinery making UHMWPE easier to process (Smoluk, 1989).

1.1.2 Polypropylenes

Propylene will not polymerize at commercial rates via free radical mechanism due to the high transfer to monomer rate and the relatively low reactivity of the double bond. However polymers of propylene can be produced using the organometallic Ziegler-Natta catalysts. Polypropylene homopolymers are characterized by high stiffness and high heat deflection temperatures but show lower impact resistance when compared with equivalent melt flow polymers. Polypropylene can be copolymerized, with ethylene for instance, as a random polymer, or as a 'block' copolymer. Random copolymers are produced by providing both comonomers to the reactor during the entire course of reaction. Block copolymers are produced by forming a homopolymer and then in a subsequent reactor adding both monomers. It was believed that the chains would consist of homopolymer block attached to a random copolymer block. However it is more likely that the block copolymer is a very intimate blend of homopolymer and random copolymer. Block copolymers display a good balance of stiffness and impact properties, while random copolymers combine good impact

resistance with superior contact clarity and improved low-temperature heat sealability. Random copolymers have lower melting point that polypropylene homopolymer, every one percent ethylene reduces melting point by 5°C. In older process three percent ethylene was the limit due to the 'stickiness' problem, but new processes can take up to seven percent. Homopolymers find use in general injection molding and extrusion, random copolymers are mostly used in blow molding and films while the block copolymers are employed in the injection molding of impact resistant products.

In order to increase conventional PP's processability, suppliers apply controlled rheology, a post-reactor technique in which peroxide is used to enhance melt flow rate (MFR). This is a fine example of chemical modification of polymers in the melt. This allows extension of a conventional polypropylene to a 50 or even to a 300 MFR. However controlled rheology, while providing appropriate molecular weight, and molecular weight distribution for many applications, also narrows MWD, thus reducing stiffness and adding to cost. Some polyolefin manufacturers are now making different grades of polymer, not by changing the operating conditions of their reactors, but by simply adding peroxides to the extruders during the pelletizing process.

A polymer's MFR is inversely related to its molecular weight or chain length. MFR is controlled by feeding hydrogen, a chain transfer agent, into the reactor; higher levels produce shorter, lower MW chains, which in turn have a higher MFR. Conventionally, the achievable MFR ranges from less than 1.0 to 20 MFR the limit being the volume of hydrogen incorporated. Union Carbide and Himont claim that their processes can feed hydrogen in volumes high enough to get MFRs of 1000 or more. (Leaversuch, 1988).

1.1.3 Polymer Structures and Characteristics

The predominant measured characteristics of polyethylene and copolymers are density and melt flow index. The density is a rough measure of the short chain branching frequency. As the short chain branching frequency increases, the density decreases. Long chain branches, since there are so few of them, make a very small contribution to the density, but may affect the melt flow index. The melt flow index is a rough measure of the molecular weight. Different polyethylenes have different branching structures as shown in Figure 4.

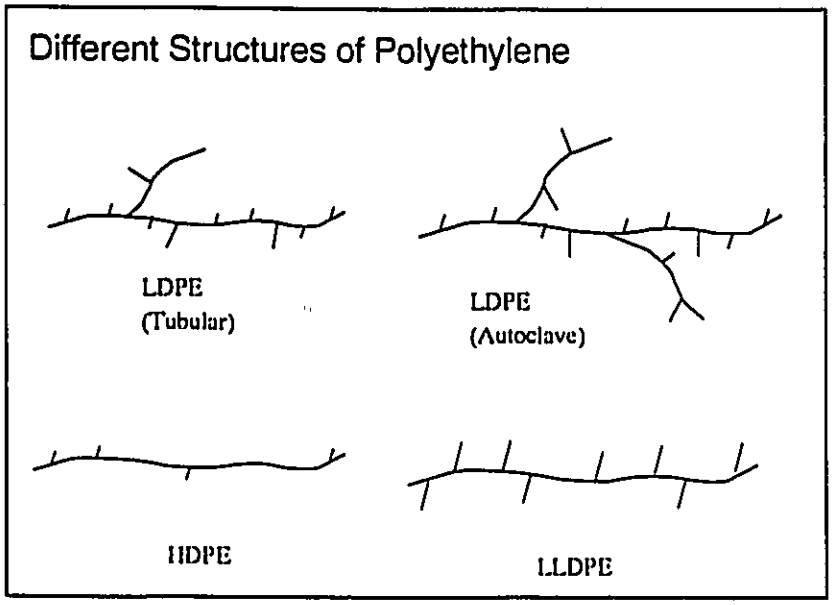

Figure 4 Branching Structures for Polyethylene

Polypropylenes are also characterized by their solubility in various solvents, thus determining their crystallinity. The crystallinity of polypropylene is due to the stereoregularity of the chain, stereoregular (isotactic) polymer is more crystalline, whereas the stereo irregular (atactic) polymer is less so (See Figure 5). Syndiotactic polypropylene, where the methyl group appears on opposite sides of the chain for adjacent repeat units, may also be made. The crystalline polymer is much less soluble than the amorphous polymer. Therefore the soluble fractions are usually assumed to be atactic, whereas the insoluble are isotactic. This is the basis for the technique of Temperature Rising Elution Fractionation (TREF), whereby polymer is fractionated with respect to its solubility, and thus its crystallizability. There are certainly molecular weight effects involved with this measurement but these are not usually considered to be important.

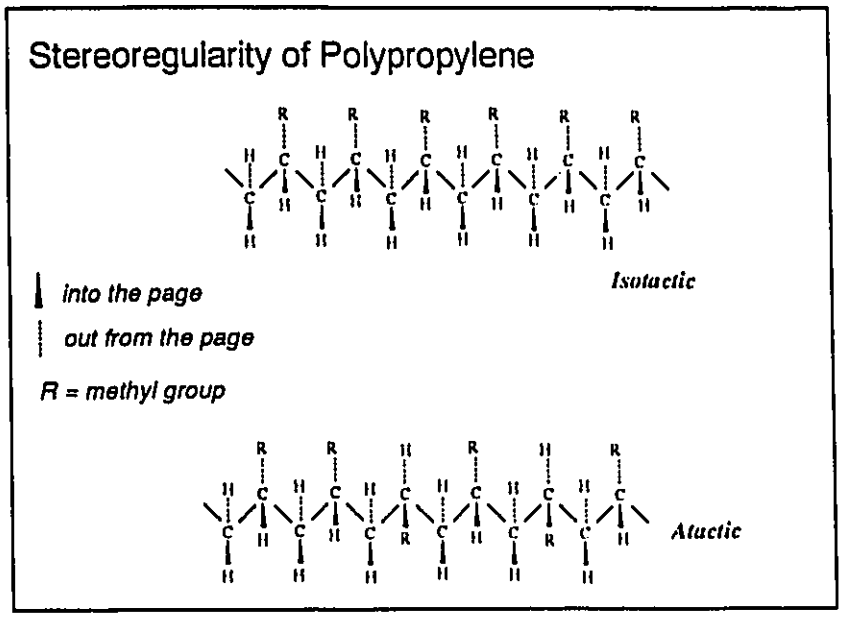

Figure 5 Stereoregularity of Polypropylene

1.1.4 Molecular Weights and Distributions

Polyolefins made from heterogeneous Ziegler-Natta processes have a broad molecular weight distribution, even when produced under steady state conditions. The polydispersities range from 5 - 20 (Floyd et al. 1988). This broad molecular weight distribution has been attributed to diffusion resistance (Floyd et al. 1987; and Zucchini and Cecchin, 1983) but is more likely due to the presence of multiple active site types (Floyd et al. 1988)

The high pressure processes, both autoclave and tubular reactors also make broad MWD material, the autoclave because of a broad residence time distribution, the tubular reactor because of the changing conditions, especially temperature and initiator levels, along the tube. Moreover the long chain branching tends to broaden the molecular weight distribution and may even lead to gel of effectively infinite molecular weight.

1.1.5 Copolymer Composition Distributions

The composition of copolymers made via free radical methods are random as calculated by the reactivity ratios. On the other hand the copolymer composition

distribution for Ziegler-Natta produced polymers may be quite broad, indicating the presence of active sites having different reactivity ratios, and thus producing a polymer that has a mix of copolymer compositions.

1.1.6 Stereoregularity

Z-N polymerization of propylene tends to produce very isotactic material that is insoluble in a solvent like xylene. The old titanium based Ziegler-Natta types (early 1980's) produced about 1000 gram of polymer per gram of catalyst, about 90 to 92% insoluble. New super-high-activity catalysts yield 40,000 gram polymer /gram catalyst with about 99% being insoluble in xylene (Leaversuch, 1988). The stereoregulating power of the catalyst may be a function of active site type where some sites produce atactic polymer and the majority produce isotactic. Free radical methods have little or no stereoregulating control especially at the high temperatures usually employed.

1.1.7 Branching Frequencies

HP- Low density polyethylene, whether made in a tubular or an autoclave type reactor have both short and long chain branches. Increasing LCB will make the melt flow more non- Newtonian, and change the behavior of the material during processing (Hamielec and Vlachopoulos, 1983). The molecular properties of the LDPE made in each type reactor will be different. Typical branching frequencies are 7-17 SCB/1000 carbon atoms, for long chain branches about 0.5 - 2.2 LCB/1000 carbon atoms (Beasley, 1989).

Homopolymer in the low pressure Ziegler-Natta processes are predominantly linear, and lower density polymers are made by adding an α-olefin comonomer (like butene-1) to add short branches along the chain. The number of branches depends upon the copolymer composition and the length of the branch depends on the size of the comonomer. There are very few or no long chain branches.

1.2 Overview of some production technologies

LDPE was developed by ICI in 1933 (Fawcett et al. 1934) and was an established segment of the plastics industry in the early 1960's when Du Pont introduced a low pressure solution polymerization process for the production of LLDPE. Union Carbide started to

make HDPE in 1968 using the Unipol fluidized bed technology and 1977 they announced that UNIPOL could produce LLDPE. In 1978 Dow introduced octene based LLDPE made in low pressure solution technology.

LLDPE has replaced HP-LDPE in many markets and found application in new areas. In 1986 about 1/2 of the LDPE sales was from LLDPE and gains are largely at the expense of HP-LDPE. New higher α-olefins are playing a major role in the growth spurt since 1982 (Yi and Pacala, 1988). LDPE is still added to LLDPE by some processors to improve the film properties.

1.2.1 High pressure free radical processes

Since 1933 ICI has been producing LDPE in autoclave type and tubular type reactors. Up to 36% single pass conversion can be obtained in tubular reactors, using only oxygen as initiator. The polymer produced in these reactors can have a density from 0.915 to 0.93 g/cm^3 and melt flow index from 0.1 to 50 g/10-min. This process can also produce EVA.

Vessel type reactors produce a polymer with some very high molecular weight material, making it unsuitable for the manufacture of films (due to haziness), but this material is good for molding because of its toughness (Gupta, 1987). The polymer is more highly branched and gel may be formed.

1.2.2 Ziegler-Natta catalyzed processes

Karl Ziegler and co-workers invented low pressure polymerization of PE in 1953 using transition metal catalysts. The Ziegler catalysts are combinations of aluminum alkyls with chemical derivatives of titanium, zirconium, hafnium, niobium, tantalum, chromium, molybdenum, tungsten. Soon thereafter, in Italy, Giulio Natta brought about the modification of the titanium-chloride -aluminum alkyl catalyst into a stereospecific catalyst capable of producing polypropylene of high isotacticity. For their work, and thus demonstrating the importance of the production of polyolefins using these catalysts, both Ziegler and Natta received the Nobel prize for chemistry in 1963.

The first industrial scale Ziegler plant started in 1955 at Hoechst in Frankfurt, West Germany (500 metric ton per annum). Chromium based Phillips catalysts and Molybdenum catalysts of Standard Oil were the basis for plants built soon after (Schulz,

1981). Some of the processes based upon these catalysts are briefly outlined below, for a more complete list one should consult Tait (1989) and Short (1983). Ziegler-Natta catalysts can be used in gas or liquid phase reactors.

Gas phase reactors

The gas phase reactors are usually either fluidized bed reactors or transported bed reactors. The Union Carbide UNIPOL process is a fluidized bed that was developed in the 60's to make HDPE. The original catalyst used a chromium type silica supported catalyst in a fluidized bed reactor design (Tait, 1989). UNIPOL typically operates at 100-300 psi (6.8 to 20.5 atm) psi and at temperatures less than 100°C. This process was modified in about 1975 to allow for the production of LLDPE. The major modification was the development of new high activity catalysts that operate at low temperatures and pressures. Since the melting temperature of copolymers is lower, the reaction temperature must be lower to prevent agglomeration in the fluidized bed reactor. The molecular weight is controlled by the addition of hydrogen. Gas phase is generally accepted to provide the greatest product versatility providing a broad range of LLDPE products for film and injection molding (Yi and Pacala, 1988). This process has been licensed and now more than 40 reactors operate in 15 countries (Tait, 1989). See Figure 6 and McAuley et al. (1990) for a schematic of the UNIPOL process

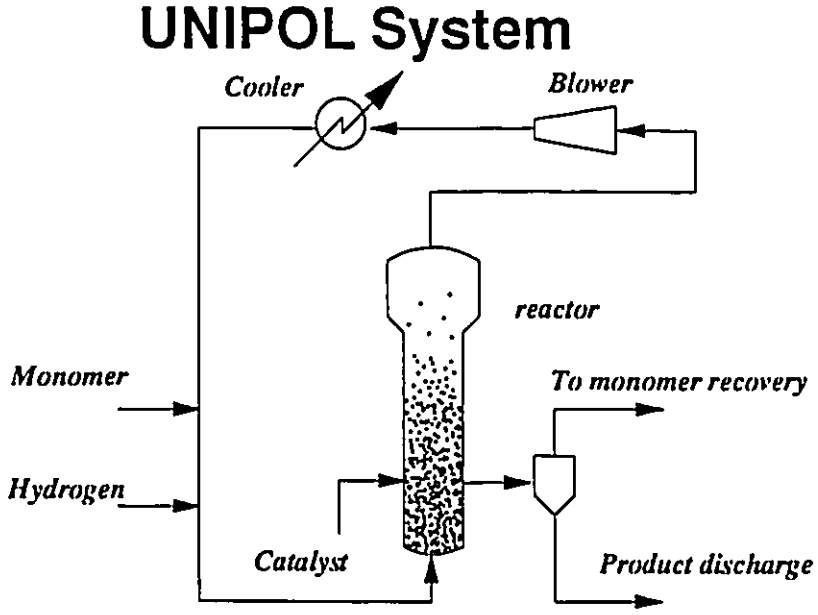

Figure 6 A Schematic of UNIPOL Process

UNIPOL technology was further extended with the development of the Shell High Activity Catalyst (SHAC) in 1985, to allow for the polymerization of propylene and random copolymers. These reactors can be built in series to produce high impact polypropylenes, a special copolymer incorporating ethylene.

The BP process is also carried out under mild conditions (60-100°C and 15-30 atm.) in a fluidized bed reactor. This process can make polyethylene and α-olefin comonomers, using hydrogen to control the molecular weight. The catalysts are high activity titanium and magnesium.

The BASF process to make polypropylene was first developed in 1969. This process consists of a stirred polymer bed into which liquid propylene and catalyst are fed to the bottom. An activator is fed to the top of the reactor. The gas phase reaction is maintained by keeping a quantity of high molecular weight polymer in the reactor. A variety of catalysts have been used including δ-$TiCl_3$ 0.33 $AlCl_3$ activated by $AlEt_2Cl$ and a variety of high activity catalysts such as $MgCl_2$/donor/$TiCl_4$ activated by a $AlEt_3$/donor system. This process has been operated by Rheinische Olefinwerke at Wesseling in West Germany, by ICI and USI (Norchem) and El Paso has used its own version for some time. Himont uses similar technology that it commercialized with Mitsui Petrochemical (Tait, 1989).

Liquid phase reactors

Liquid phase reactors are usually of either slurry type or solution.

The slurry process is a widely used process for production of polypropylene and copolymers where the reactor is filled with a poor solvent for the polymer, like heptane or pentamethylheptane, and the solid catalyst is dispersed in the liquid phase. The polymer then grows around the catalyst forming small particles. Typical conditions are 50-75°C and 10 atm. The catalyst is removed using alcohol and the polymer is separated from the diluent by centrifugation and dried. The atactic polypropylene is soluble in the diluent and must be extracted so that the diluent can be recycled. This process is quite flexible allowing for a variety of random and block propylene ethylene copolymers.

In 1984 the slurry process accounted for 50% of US capacity but by 1988 only accounted for less than 20%. Now liquid phase, bulk polymerization and gas phase reactors predominate (Leaversuch, 1988). Low cost slurry processes for polyethylene

production have also been developed with the ability to produce polymers with a variety of densities, melt flow indexes and molecular weight distributions. See figure 7 for a pictorial representation of the slurry process.

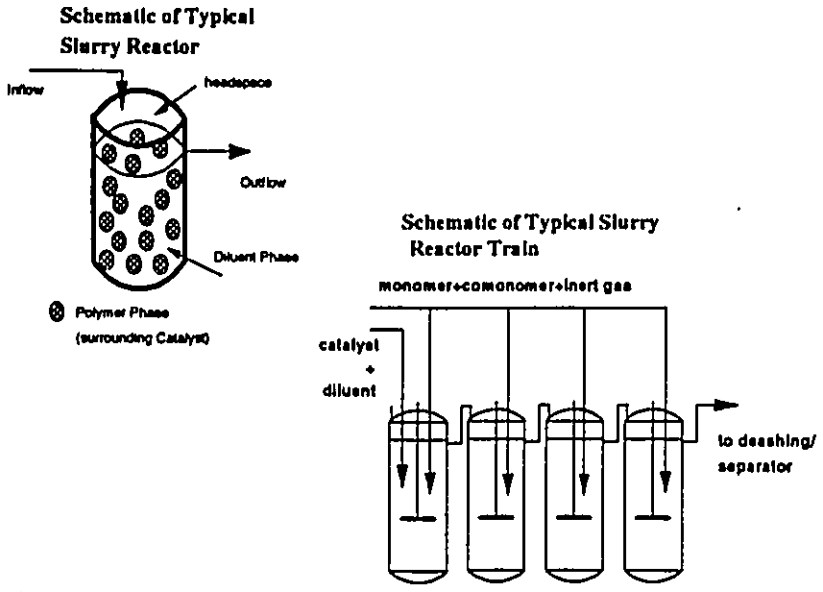

Figure 7 Schematic of Slurry Process

The polymer in the solution processes is not necessarily in solution but may be in a molten state. Du Pont developed a process for the production of HDPE that operates at 200°C and 70 atm. Eastman Kodak has operated a solution process for polypropylene using modified first generation catalysts.

NORSOLOR- ORKEM (France) Company operates a high pressure (600-800 bars) high temperature (200-300°C) CSTR type reactor to make LLDPE. Reaction takes place in super critical phase, the polymer being soluble in the monomer mixture. The outlet is pelletized directly and no solvents are used (Villermaux et al. 1989).

1.3 Overview of reactive processing of polyolefins

Reactive processing is the method where by free radical initiators and possibly other additives are added to the extruder. The polymer is melted and mixed and the chemical reaction allowed to occur. Typical reaction temperatures are from 150 to 300°C. Since the residence times of the extruders are short, from a one to 20 minutes, the reaction must be fast enough to be completed in this time. One of the simplest processes is controlled rheology polypropylene, where polypropylene and a peroxide initiator are

extruded and the molecular weight of the polymer is reduced making the polypropylene easier to process. Branching and crosslinking of polyethylene can be accomplished in the same manner. Grafting processes, like maleation of polypropylene or polyethylene, are performed by adding maleic anhydride along with the peroxide and the polymer. In general when we desire to produce a particular product by one of the scission, branching or grafting processes, the polymer undergoes the other two reactions as well. Reaction conditions, like temperature, screw speed, peroxide levels and addition points, must be adjusted to emphasize the desired reaction.

1.4 Objectives of this thesis

This thesis considers the synthesis and chemical modification of polyolefins. The methodology for this study, is to use the tool of the mathematical model. In developing the mathematical model, one is forced to systematically ask the important questions, and then answer the questions by searching the literature or performing the appropriate experiments. Moreover once the model is developed, it can be used to suggest even more informative experiments. At the end of this process, one has gathered the information, and stored it in a convenient, concise form, a computer simulation model. Given this overall method, the objectives to be accomplished are as follows.

a) To develop a mathematical model for copolymerization of olefins (propylene and ethylene) using Ziegler - Natta catalysts, to describe the rate of reaction and the distributions of the molecular weight, copolymer composition, and the stereoregularity.

b) To develop comprehensive mathematical models for the polymerization of ethylene and comonomers in high pressure autoclave and steady state tubular reactors. These models would predict the rate of polymerization, the temperature, compositions, molecular weight averages, short and long chain branching frequencies, gel content and crosslink density.

c) To study and develop mathematical models for the free radical modification of polyolefins in the melt, to account for random scission and crosslinking and to develop algorithms to solve the models. Furthermore we need to develop suitable experimental and analytical techniques to gather data with which to verify this model.

1.5 Outline of the thesis

Given that this thesis has three major objectives, it is appropriate that the thesis has three major parts. After the compulsory introductory remarks, the first part deals with the production of polyethylene and copolymers by high pressure free radical polymerization. The chemical mechanisms of the system are outlined and then applied to model both tubular and autoclave reactors.

The second part deals with the production of polyolefins, both polypropylene and polyethylene, using Ziegler-Natta catalysts. Again the chemistry of the polymerization system is presented. A multiple active site approach is used to predict the rates of polymerization and the broad molecular weight and compositional distributions.

Lastly, the third part deals with the chemical modification of polyolefins in the melt using free radical mechanisms. The chemistry is again presented and used as the basis for models for the modification of the polymer structure. The algorithm for the solution of the model is presented and the model is compared to experimental data gathered for this thesis.

The thesis is brought to a close with concluding remarks.

1.6 Published reports

Much of what is contained in this thesis has been published in the open literature. Since there are several authors for each paper, the work from these papers that has been performed by the other authors will be pointed out in the appropriate sections of the thesis. The relevant papers are:

Free radical polymerization of polyolefins:

R. C. M. Zabisky, W-M. Chan, P. E. Gloor, A. E. Hamielec, "A kinetic model for olefin polymerization in high pressure tubular reactors - A review and update", *Polymer*, **33** 2243-2262 (1992)

W-M. Chan, P. E. Gloor, A. E. Hamielec, "A kinetic model for olefin polymerization in high pressure autoclave reactors" *AIChE J.* **39**, 111-126 (1993)

Ziegler Natta polymerization of polyolefins:

A. B. M. de Carvalho, P. E. Gloor, A. E. Hamielec, "A kinetic mathematical model for heterogeneous Ziegler-Natta copolymerization", *Polymer*, **30** 280-296 (1989)

A. B. M. de Carvalho, P. E. Gloor, A. E. Hamielec, "A kinetic mathematical model for heterogeneous Ziegler-Natta copolymerization Part 2: Stereochemical sequence length distributions", *Polymer*, **31** 1294-1311 (1990)

Chemical modification of polyolefins:

A. E. Hamielec, P. E. Gloor, S. Zhu, Y. Tang "Chemical modification of polyolefins in extruders: chain scission, long chain branching, crosslinking and grafting. *Compalloy 90* Second international congress on compatabilizers and reactive polymer alloying, New Orleans, March 7-9 (1990)

A. E. Hamielec, P. E. Gloor, S. Zhu "Chemical modification of high molecular weight polymers in extruders: experimentation and computer modelling the kinetics of chain scission, long chain branching, crosslinking and grafting. *Compalloy 91* Third international congress on compatabilizers and reactive polymer alloying, New Orleans, January 30 - February 1 (1991)

A. E. Hamielec, P. E. Gloor, S. Zhu "Kinetics of free radical modification of polyolefins in extruders - chain scission, crosslinking and grafting" *Can. J. Chem. Eng.* **69** 611-618 (1991)

Triacca, V. J., Gloor, P. E., Zhu, S., Hrymak, A. N., Hamielec, A. E. "Free radical degradation of polypropylene: Random chain scission", in press *Polym. Eng. Sci.* (1993)

Gloor, P. E., Tang, Y., Kostanska, A. E., Hamielec, A. E., "Chemcial modification of polyolefins by free radical mechansims - A modelling and experimental study of simultaneous random scission, branching and crosslinking, submitted to *Polymer* (1993)

1.7 The contributions of this thesis

The major contributions of this thesis are:

- a more comprehensive model for high pressure copolymerization of ethylene in steady state tubular reactors, including, a more complete description of the oxygen initiation phenomena, scission of back bone radical centers and including the effects of the pulse valve.
- a model for high pressure copolymerization of ethylene in dynamic vessel reactors including the effects of the mixing, heterogeneous reaction conditions and gel formation.

- a model for Ziegler-Natta copolymerization of polyolefins using a multiple active site approach to describe the broad copolymer and molecular weight distributions.
- a numerical solution to the equation for simultaneous scission and crosslinking of polyolefins in the melt by free radical methods. A methodology for gathering the appropriate data is developed and the model is fit to this data.

1.8 References

Beasley, J. K., (1989) "Polymerization at High Pressure" p. 273-282, vol. 3, *Comprehensive Polymer Science*, Allen, G., Bevington, J. C., Eds. Pergamon Press, Oxford.

Birnkraut, W. H., Braun, G., Falbe, J., (1981) "Ultrahigh Molecular Weight Polyethylene-Processing and Properties.", p. 79-88, *Commodity and engineering Plastics, J. Appl. Poly. Sci.: Applied Polym. Symp. 36.*, N. Platzer (ed.), Wiley & sons. New York.

Cossee, P., *J. Catalysis* **3** 99 (1964)

Elias, H. G., "Mega Molecules", Springer-Verlag, Berlin (1989)

Fawcett, E. W., Gibson, R. O., Perrin, M. W., Paton, J. G., Williams, E.G., (1937) *Brit. Patent 471590* (1937) ICI invs.; Chem. Abstr. 32, 13626 (1938)

Floyd, S., Heiskanen, T., Ray, W. H., (1988) "Solid Catalyzed Olefin Polymerization" *Chem. Eng. Prog.* November pp. 56-62

Floyd S., Heiskanen, T., Mann, G. E., Ray, W. H., (1987) *J. Appl. Polym. Sci.*, **33**, p. 1021

Gupta, S. K., (1987) *Current Science*, **56**, No. 19, 979-984.

Hamielec, L. A., Vlachopoulos, J., (1983) "Influence of Long Chain Branching on Extrudate Swell of Low Density Polyethylenes", *J. Appl. Polym. Sci.*, **28**, 2389-2392

Leaversuch, R. D. (1988), "Resin-making Revolution That Will make Polypropylene the Polymer Star of the 1990s is Well Under Way", *Modern Plastics*, November, pp. 38-44

McAuley, K. B., MacGregor, J. F., Hamielec, A. E., (1990) "A Kinetic Model for Industrial Gas Phase Ethylene Copolymerization" *AIChE J.* **36** (6), 837.

Reid, R. C., Prausnitz, J. M., Polling, B. E., "The properties of gases and liquids" 4th ed. McGraw Hill (1986) p. 381

Schulz, H., (1981) "Twenty-Five Years of Ziegler High Density Polyethylene - History and Outlook", p. 61-65, *ComCommodity and Engineering Plastics, J. Appl. Poly. Sci.: Applied Polym. Symp. 36.*, N. Platzer (ed.), Wiley & sons. New York.

Short, J. N., (1983) *MMI Press Symp. Ser.*, **4**, 651.

Smoluk, G. R., (1989) "Performance Rich UHMWPE is Becoming Easier to Process", *Modern Plastics*, 68-71, May

Talt, P. J. T., (1989) "Monoalkene Polymerization: Ziegler-Natta and Transition Metal Catalysts" p. 1-25, vol. 4, *Comprehensive Polymer Science*, Allen, G., Bevington, J. C., Eds. Pergamon Press, Oxford.

Villermaux, J., Lorenzini, P., Bertrand, P., Greffe, J, L., (1989) "Modelling of Polymerization of Ethylene by Ziegler-Natta Catalysts", In *Polymer Reaction Engineering*, K-H. Reichert, W. Geiseler eds, p. 350 VCH Publ. Weinheim FRG

Yi, K., Pacala, L., (1988) "Linear Low Density Polyethylene: Markets- The First Decade and Beyond", *ANTEC '88* SPE Conf. Proc. 46th Annual Technical Review, Atlanta April 18-21, 1366-1370

Zucchini, U., Cecchin, G., (1983) *Adv. Polym. Sci.* **51** p. 101

Chapter 2 Production of polyethylene and copolymers by free radical polymerization

Low density polyethylene and copolymers are thermoplastics which are used in a large variety of applications. They are produced, at high pressure, in either autoclave type or tubular reactors by free radical polymerization. Figure 8 shows the typical process for high pressure polymerization of ethylene. Ethylene and the initiators are pressurized and fed to the reactor. Residence times in the reactor are of the order of 30 to 60 seconds, and the single pass conversion is usually less than 25 percent. Thus the unreacted ethylene is cooled, flashed off and recycled.

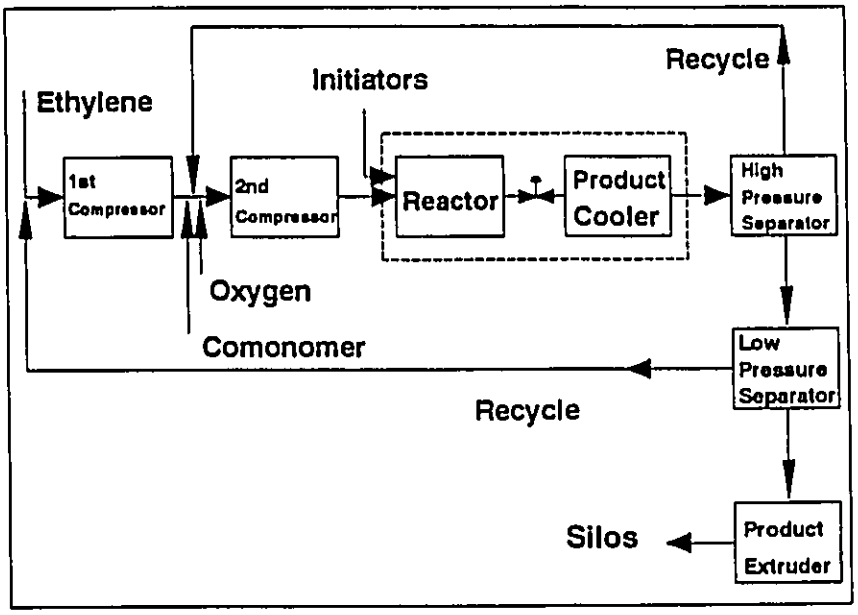

Figure 8 The process for synthesis of high pressure polyethylene and copolymers

The tubular reactors (figure 9) can be over 1000 meters long (coiled) but are only a few centimeters in diameter. Pressurized (2500 to 3500 atm) ethylene and initiators are fed at the front, and at other locations along the tube at a rate to give a residence time of less than one minute. Feed temperatures can be as low as 40 to 50 °C while reaction temperatures approach 300°C. Some cooling is provided by jackets and by cold monomer feed, but a large temperature rise is associated with the reaction. Initiator flows and cooling rates are set to give the desired temperature profiles, conversions and molecular weights. Modifiers are also added to adjust the molecular properties of the polymer.

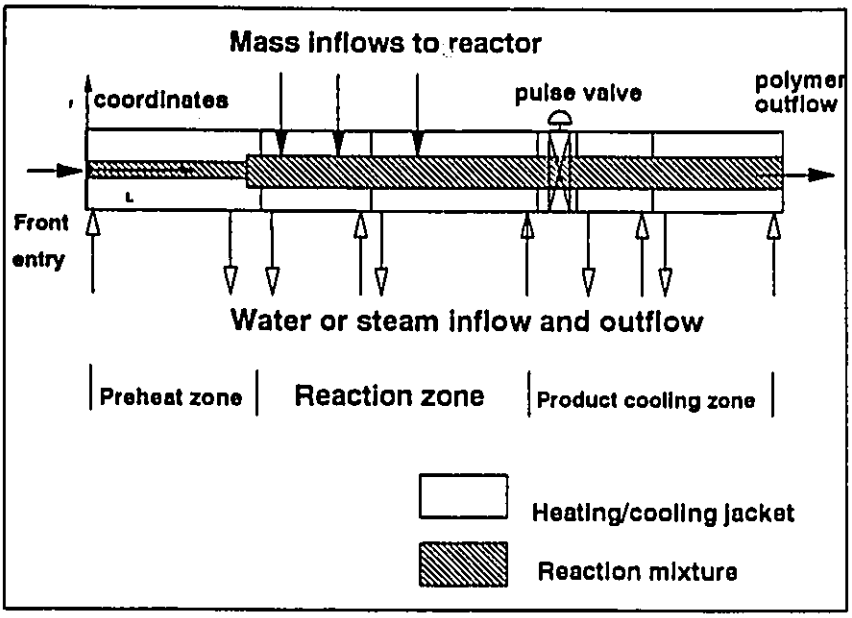

Figure 9 Schematic of tubular reactor with multiple feed points

The vessel type reactors (figure 10) typically operate at lower temperatures and pressures than do tubular reactors and they behave more like a continuous stirred tank reactor (CSTR). The autoclave reactors may be eight to 10 meters tall and have a length to diameter ratio of between four and 20. Mixing is provided by a shaft running down the center of the vessel with several (up to 40 or so) impeller blades of different types. Heat transfer through the walls is limited, so that the reactor is essentially adiabatic with the only cooling provided by the inflow of cold monomer. The inflow of initiator at several points down the reactor vessel provides control of the temperature which may vary down the length of the reactor.

This section develops mathematical models for the production of low density polyethylene and copolymers in both types of high pressure reactors. The mechanism and kinetics of this free radical copolymerization is outlined below and by Zabisky et al. (1992). We shall outline the important features of the tubular and autoclave models and present some simulation results in the form of sensitivity studies and comparisons with the performance of industrial reactors.

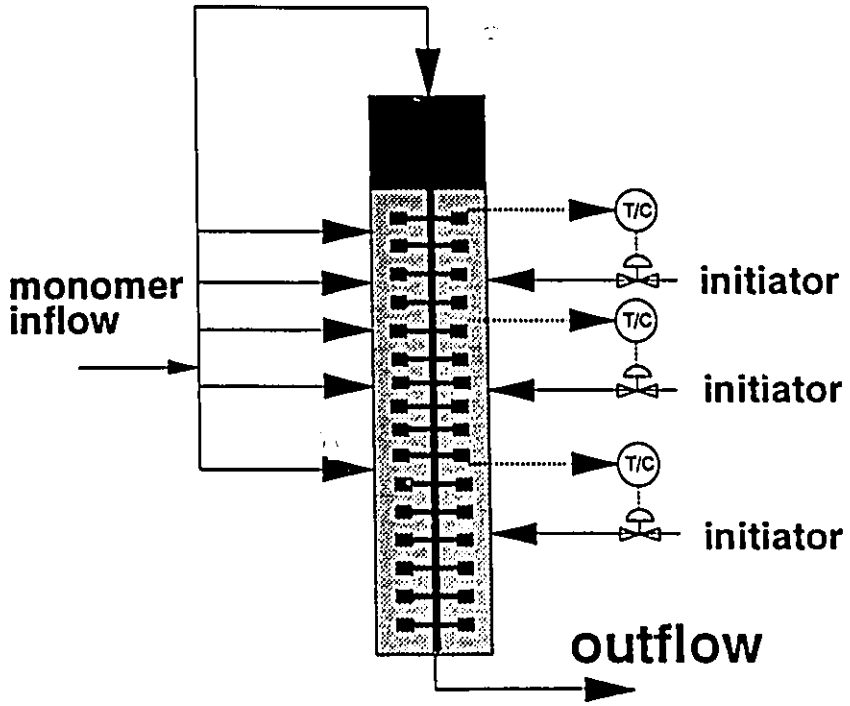

Figure 10. Schematic of a Typical Autoclave Reactor. T/C denotes a temperature controller that manipulates the initiator flow.

2.1 Reaction kinetics for copolymerization

This model attempts to account for the important elementary reactions that are likely to occur in the high pressure reactor assuming the terminal model for copolymerization is valid (penultimate effects are neglected). The reactions to be considered are presented below. The analysis is simplified without any loss of rigor by using pseudo kinetic rate constants (Hamielec and MacGregor 1983, Tobita and Hamielec 1988) . Finally, the model parameter estimation was based on the use of valid literature and plant data. Of note is the fact that the values for the kinetic rate constants, reported in the literature, seem to vary over a wide range (Gupta 1987). If one just considers the rate of polymerization, the ratio $kp/kt^{1/2}$ is important. Figure 11 shows this ratio as reported by several authors. The range over which it varies is quite apparent, although to be fair, it must be pointed out that these values arise from different measurement techniques and modes of initiation. The ratio $kp/kt^{1/2}$ is expected to increase with pressure because of the larger activation volume for k_p than for k_t.

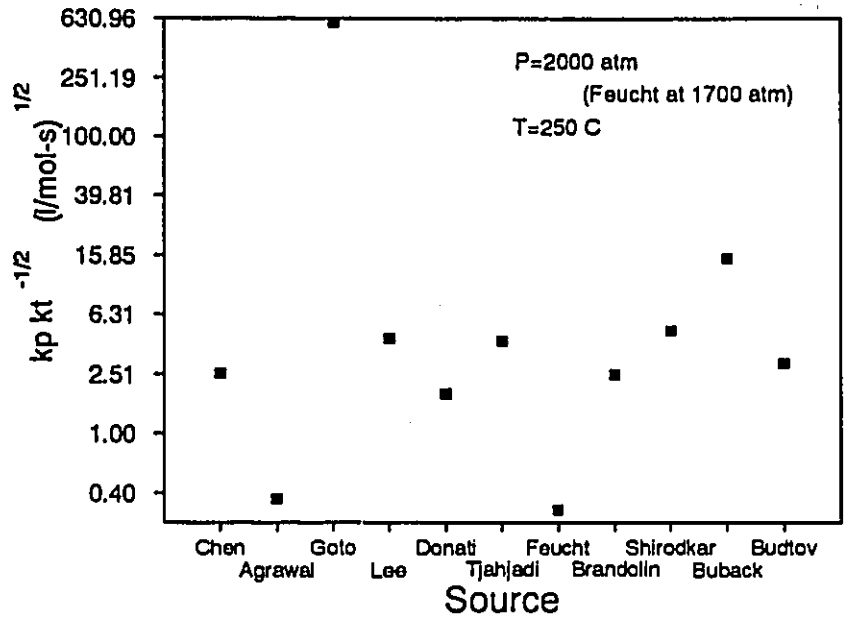

Figure 11 A sampling of the rate parameters for ethylene polymerization, from various sources.

2.1.1 The elementary reactions

The appropriate reactions considered are listed below. The terminal model is assumed to be adequate to describe this kind of polymerization, i.e., the rates of reaction depend only upon the monomer unit on which the radical center is located and thus penultimate effects are ignored. The reactions include initiation, propagation, bimolecular termination, transfer to small molecules and polymer, backbiting, β-scission, reactions with terminal double bonds, and explosive decomposition of monomer and polymer.

Initiation

i) The decomposition of peroxide initiator, I, to form free radicals, R

$$I \xrightarrow{kd} n \cdot R$$

where n is the number of radicals formed per initiator molecule, usually two. It is assumed that each radical formed has the same reactivity. This is true for symmetrical peroxides.

ii) Oxygen initiation of ethylene polymerization was first reported by Fawcett et al. (1938), and has been used commercially in both tubular and vessel type reactors. It is well known that oxygen also acts as an inhibitor in free radical polymerizations at lower temperatures. Ehrlich and Pittilo (1960) studied the O_2 effect and found definite pressure and temperature boundaries between the inhibition and the initiation regimes. On the other hand Gierth (1970) found a gradual transition from one regime to the other. Certainly these phenomena are quite complex. Oxygen may react with radicals or monomer to form polymeric peroxides. These peroxides may then decompose to initiate the polymerization (Marano 1979). Several authors, including Thies (1971), have tried to model O_2 initiation by assuming the overall second order reaction occurs

$$O_2 + M \xrightarrow{k_{d_{O_2}}} 2R$$

neglecting the inhibition reactions, with moderate success. In tubular reactor *simulations*, the tendency is to predict a sharp temperature peak, at the end of each reaction zone, as the oxygen burns out. In industrial practice, a rounded peak is observed for oxygen initiation. Hoiiar and Ehrlich (1983) attempted to produce a rounded peak by incorporating a thermal self initiation reaction for ethylene (Buback 1980). Even so the peak was not rounded but sharp with a more gradual temperature drop, due to this self initiation. They found that the oxygen must behave as two separate initiators, one fast and one much slower. In the present work it was found that a first order oxygen initiation rate does not adequately explain both the initial temperature rise and the rounding off at the peak. We agree that the oxygen acts as two separate initiators, one fast (responsible for the heat kick for the initial temperature rise) and one slower (responsible for the rounded peak). For these reasons it was decided that initiation by oxygen must be examined more closely.

Tatsukami et al. (1980) have studied the oxygen initiation of ethylene and postulated the additional reaction

$$R + O_2 \xrightarrow{kr} XO_2$$

deactivated products and peroxides

where XO_2 represents the products of the inhibition reaction that are peroxides, and X denotes some possibly polymeric end group. These reactions account for the initiation and the inhibition effects of oxygen, but not for the slow initiation at high temperatures responsible for the rounded peak. To explain this, Brandolin et al. (1988) observed that the initiation rate was of order 1.1 with respect to oxygen. In this study, it was decided to try a less empirical method whereby some of the peroxides formed by the inhibition reaction can decompose to further initiate the reaction. Thus oxygen initiation can be modelled with the additional reaction:

$$XO_2 \xrightarrow{kd_p} 2R$$

slow initiation

iii) As mentioned previously, monomer may also thermally combine to form a radical type i. Although this reaction is thought to be very minor for ethylene at moderate temperatures (Marano 1972), it may be significant at higher temperatures, causing reactor runaways (Hollar and Ehrlich 1983). Buback (1980) found this reaction to be third order in ethylene. Since the actual mechanism for this reaction is unknown, it will be used as an overall third order reaction.

$$3M_i \xrightarrow{kth} R_i$$

Propagation

Propagation of monomer type i with radicals of length r with radical centre on monomer type j

$$R_j(r) + M_i \xrightarrow{kp_{ji}} R_i(r+1)$$

Termination

Bimolecular termination reactions between two radicals to form one or two *dead* polymer chains.

By combination

$$R_i(r) + R_j(s) \xrightarrow{ktc_{ji}} P(r+s)$$

or by disproportionation

$$R_i(r) + R_j(s) \xrightarrow{ktd_{ji}} P^{=}(r) + P(s)$$

or

$$P^{=}(s) + P(r)$$

The disproportionation reaction forms a *dead* chain with a terminal double bond, denoted by the superscript =.

Chain Transfer reactions

(i) *Transfer to monomer.* Transfer of reactivity from radical type j to a monomer type i to form a monomer transfer radical and a *dead* polymer chain

$$R_j(r) + M_i \xrightarrow{kfm_{ji}} R_i^{\cdot}(1) + P(r)$$

The transfer radical with propagation will have a terminal double bond and this radical will eventually become polymer with a terminal double bond after termination or chain transfer.

(ii) *Transfer to chain transfer agent, modifier or solvent.* Transfer of reactivity from radical type j to chain transfer agent, TSH, to form a *dead* polymer chain and the transfer radical, TS*.

$$R_j(r) + TSH \xrightarrow{kfts_j} TS^{*} + P(r)$$

It is assumed that, TS*, has the same or greater reactivity as polymer radicals towards monomer addition. The chain transfer agent will thus not affect the rate of polymerization when bimolecular termination is chemically controlled, but can reduce the polymerization rate when termination is diffusion controlled and chain length dependent by reducing the size of the macromolecules.

β-scission of terminal radicals

Terminal radicals may undergo β-scission (Nicolas 1958, Ehrlich and Mortimer 1970) at the high temperatures of polymerization forming a *dead* polymer chain and a radical of unit length.

$$R_j(r) \xrightarrow{k_\beta} P_{i\ or\ j}(r-1) + R_j(1)$$

It is assumed that this will not affect the rate of polymerization, but of course would reduce the molecular weight of the product.

Reactions with internal (backbone) radical centers

An internal radical center is a radical located on a backbone carbon atom and are formed by three reactions types: (i) transfer to polymer, (ii) reactions with terminal double bonds and (iii) backbiting. These internal radical centers can, in theory, undergo all of the reactions that chain end radicals do. Propagation leads to branches, the type (whether long or short) depending upon the radical formation mechanism. Reaction types i and ii lead to long chain branches, and backbiting leads to short chain branches. In addition, these internal radicals could undergo a β-scission reaction to form two smaller chains, one a macroradical and the other a dead polymer chain.

Transfer to polymer leading to long chain branching (LCB)

This reaction involves the transfer of reactivity from radical type j to an i type monomer unit in a *dead* polymer chain to form a radical with the active center somewhere along the chain. In the presence of monomer, propagation leads to long chain branching.

$$R_j(r) + P_i(s) \xrightarrow{kfp_{ji}} R'_i(s) + P(r)$$

and then propagation

$$R'_i(s) + M_j \xrightarrow{kp_{ij}} R_j(s+1) \quad (LCB)$$

where R' denotes an internal radical. One can express this two step reaction as a single overall reaction where K_{LCB} is an overall reaction rate constant as explained in the appendix to this chapter.

$$R_j(r) + P_i(s) \xrightarrow{K_{LCB}} R(s)_{(branched)} + P(r)$$

Backbiting leading to short chain branching (SCB)

For the formation of short chain branches via backbiting, the radical activity is transferred to a site along the same chain and this site may propagate leaving a short chain branch. Three, 4 and 5 membered rings are favoured giving methyl, ethyl and butyl branches.

$$R_j(r) \xrightarrow{kb_{ji}} R_i'(r)$$

and then propagation

$$R_i'(r) + M_j \xrightarrow[SCB]{kp_{ij}} R_j(r+1)$$

As with long chain branching, this two step reaction can be expressed as a single overall reaction:

$$R(r) \xrightarrow{K_{SCB}} R(r)_{(branched)}$$

β-scission at internal radical centres

In addition to the propagation reactions, internal radicals may undergo β-scission to form two smaller radical and *dead* polymer chains, one with a terminal double bond.

$$R_j'(r) \xrightarrow{k'\beta_j} P^{\cdot}(s) + R_{j\ or\ i}(r-s)$$

or

$$P^{\cdot}(r-s) + R_{j\ or\ i}(s)$$

This reaction is also a two step reaction, whereby the first step is the attack of a *dead* polymer chain by a radical, forming an internal radical, the second step being the scission reaction. One can write this as an overall reaction of the form when the radial centres on the backbone are very unstable.

$$R_j(q) + P(r) \xrightarrow{K_\beta} P^{\cdot}(s) + R_{i\ or\ j}(r-s) + P(q)$$

or

$$P^{\cdot}(r-s) + R_{i\ or\ j}(s) + P(q)$$

Terminal double bond reactions

The reactions of termination by disproportionation, β-scission, and transfer to monomer produce chain ends that have double bonds. These double bonds might react with radicals, via a propagation type reaction, producing internal radicals that can propagate to form long chain branches.

$$P_j^{\cdot}(r) + R_i(s) \xrightarrow{kdb_{ji}} R'_j(r+s)$$

Explosive decomposition

The thermal decomposition of monomer and polymer at high temperatures to form a variety of lower molecular weight products

$$M_j \xrightarrow{kdcm_j} \textit{Carbon + hydrogen etc.}$$

$$P(r) \xrightarrow{kdcp} \textit{Carbon + hydrogen etc.}$$

A reactor runaway usually results in a huge pressure increase due to the rapid evolution of small molecules via these decomposition reactions.

2.2 The pseudo kinetic rate constants

One can simplify the mathematical treatment for a copolymerization by using pseudo kinetic rate constants (Hamielec and MacGregor 1983). These rate constants are the rate constants for each elementary reaction weighted by the fraction of monomer or radical type in the reactor. Instead of writing down all the reactions between all monomer or radical types, we can formulate the equations in terms of the total monomer or radical concentrations.

First we must calculate some fractions based upon the composition of the reactor contents, and the kinetic constants. The reactivity ratios for propagation are defined as

$$r_1 = \frac{kp_{11}}{kp_{12}}$$

$$r_2 = \frac{kp_{22}}{kp_{21}}$$

where kp_{ij} is the elementary propagation rate constant for adding monomer type j to polymer radical of type i. The mole fraction of each monomer type in the reaction mixture is given by

$$f_1 = \frac{M_1}{M}$$

$$f_2 = 1 - f_1$$

M_1 and M are moles of monomer of type 1 and the total moles of monomer, respectively. The mole fraction of monomer type 1 chemically bound in the accumulated polymer (i.e., the copolymer composition) is given by:

Accumulated Copolymer Composition:

$$\overline{F_1} = \frac{\Psi_1}{\Psi_1 + \Psi_2}$$

$$\overline{F_2} = 1 - \overline{F_1}$$

where Ψ_1 is moles of monomer 1 bound in accumulated copolymer chains and Ψ_1, and Ψ_2 can be found using a mass balance.

Instantaneous Copolymer Composition:

$$F_1 = \frac{(r_1 - 1)f_1^2 + f_1}{(r_1 + r_2 - 2)f_1^2 + 2(1 - r_2)f_1 + r_2}$$

The mole fraction of polymer radicals of type 1 is given by

$$\phi_1 = \frac{kp_{21}f_1}{kp_{21}f_1 + kp_{12}f_2}$$

$$\phi_2 = 1 - \phi_1$$

This assumes that the long chain approximation is valid. The following pseudo kinetic rate constants are used in modelling

Thermal initiation of monomer:

$$kth = kth_1 f_1^3 + kth_2 f_2^3$$

Propagation:

$$kp = kp_{11}\phi_1 f_1 + kp_{21}\phi_2 f_1 + kp_{12}\phi_1 f_2 + kp_{22}\phi_2 f_2$$

Transfer to monomer:

$$kfm = kfm_{11}\phi_1 f_1 + kfm_{21}\phi_2 f_1 + kfm_{12}\phi_1 f_2 + kfm_{22}\phi_2 f_2$$

Transfer to chain transfer agent (or solvent):

$$kfts = kfts_1\phi_1 + kfts_2\phi_2$$

Termination by disproportionation:

$$ktd = ktd_{11}\phi_1\phi_1 + 2.ktd_{12}\phi_1\phi_2 + ktd_{22}\phi_2\phi_2$$

Termination by combination:

$$ktc = ktc_{11}\phi_1\phi_1 + 2 \cdot ktc_{12}\phi_1\phi_2 + ktc_{22}\phi_2\phi_2$$

and the overall bimolecular termination rate constant:

$$kt = ktc + ktd$$

Decomposition reactions for monomer and polymer:

$$kdcm = kdcm_1 f_1 + kdcm_2 f_2$$

$$kdcp = kdcp_1\overline{F_1} + kdcp_2\overline{F_2}$$

Transfer to polymer:

$$kfp = kfp_{11}\overline{F_1}\phi_1 + kfp_{21}\overline{F_1}\phi_2 + kfp_{12}\overline{F_2}\phi_1 + kfp_{22}\overline{F_2}\phi_2$$

β-scission of terminal radicals:

$$k_\beta = k_{\beta_1}\phi_1 + k_{\beta_2}\phi_2$$

β-scission of internal radicals:

$$k'_\beta = k'_{\beta_1}\overline{F_1} + k'_{\beta_2}\overline{F_2}$$

Backbiting:

$$k_b = k_{b_{11}}\phi_1 F_1 + k_{b_{12}}\phi_1 F_2 + k_{b_{21}}\phi_2 F_1 + k_{b_{22}}\phi_2 F_2$$

Notice that for backbiting, the instantaneous copolymer composition is used.

It should be noted that the use of pseudo kinetic rate constants for reactions including polymer is not strictly correct, since the composition of the chains will vary with monomer conversion. The use of $\overline{F_i}$ is an attempt to correct for compositional drift, however for large extents of compositional drift the errors can be significant. Recently Xie and Hamielec (1992) have quantified the error associated with the pseudo kinetic rate constant approach for branching systems, and have found that the error increases with composition drift, monomer conversion and branching frequency. Since in our case, the conversion is relatively low, and the comonomer composition is small, the composition drift is virtually insignificant (especially for ethylene - vinyl acetate (Beasley 1989) where $r_1 \approx r_2 \approx 1$). The use of pseudo kinetic rate constants should be a valid approximation for the branching reactions while being exact for the remaining, propagation, termination, and transfer reactions (Tobita and Hamielec 1988). Xie and Hamielec (1992) have shown how to completely eliminate the error in M_w by correctly including the transfer reactions in the calculation of the radical fractions.

2.3 A note on collaboration

Thanks to Mr. W-M Chan, Mr. R. C. M. Zabisky and A. B. M. de Carvalho for their assistance in technical details of the industrial processes. Mr. Chan also derived the moment closure formula assuming log normal distribution and was responsible for collecting the industrial data. Mr. P. R. Bellotti performed the *PFLASH* calculations and developed the simplified thermodynamic correlation for the autoclave reactor model.

2.4 Application to high pressure tubular reactors

2.4.1 Introduction

This section concentrates on the production of LDPE and copolymers in tubular reactors with the objective to develop a mechanistic model to describe the important chemical and physical phenomena that occur in this type of polyethylene reactor. There have been several tubular reactor models presented in the literature (as will be described at the appropriate points throughout this work and in table 1), many with shortcomings, lacking comparisons with experimental or industrial data or only for homopolymerization. Many of these models neglect the effects of the pulse valve and the product cooler. This thesis endeavors to present a more comprehensive model and give actual comparisons with industrial data to support the theory.

Table 1 Summary of some recent attempts at modelling LDPE tubular reactors

Author	Reactions Included	Parameters from	Comments
AGRAWAL & HAN (1975)	• PEROXIDE INITIATION • TERMINATION BY COMBINATION • TRANSFER TO MONOMER, POLYMER & TRANSFER AGENT • β –SCISSION	FROM LITERATURE DATA (AGRAWAL 1974)	•STUDIED AXIAL MIXING
CHEN ET AL. (1976)	• PEROXIDE INITIATION • TERMINATION BY COMBINATION • TRANSFER TO POLYMER • β –SCISSION	RATE :EHRLICH & MORTIMER (1970) MWD: TO GIVE REASONABLE VALUES	• SUGGEST NEGLECT AXIAL MIXING • LET REACTION MIXTURE PROPERTIES VARY WITH REACTOR LENGTH •SCISSION OR TRANSFER NECESSARY TO OBTAIN REASONABLE MWD

HAN & LIU (1977)	• PEROXIDE INITIATION • TERMINATION BY COMBINATION • TRANSFER TO MONOMER, POLYMER & TRANSFER AGENT • β –SCISSION	AGRAWAL & HAN (1975)	• MULTIPLE INJECTIONS OF MONOMER & INITIATOR
LEE & MARANO (1979)	• PEROXIDE INITIATION • TERMINATION BY COMBINATION & DISPROPORTIONATION • TRANSFER TO MONOMER, POLYMER & TRANSFER AGENT	SZABO & LUFT (1969), EHRLICH & MORTIMER (1970) ASSUMED ACTIVATION VOLUMES	•DID NOT USE SSH FOR RADICALS • USED MODEL FOR SENSITIVITY STUDY & TO SHOW TRENDS
GOTO ET AL. (1981)	• PEROXIDE INITIATION • TERMINATION • TRANSFER TO MONOMER, POLYMER & TRANSFER AGENT • β –SCISSION OF SEC RADICAL • β –SCISSION OF TERT RADICAL • BACK BITING	• FROM EXPERIMENT IN A VESSEL REACTOR • TERMINATION RATE BY ASSUMING SEGMENTAL DIFFUSION	• EXTENSIVE COMPARISON WITH EXPERIMENTAL DATA
BUDTOV ET AL. (1982)	• OXYGEN INITIATION • TERMINATION BY DISPROPORTIONATION • TRANSFER TO MONOMER, POLYMER & TRANSFER AGENT (PROPANE)	• FROM EXPERIMENT IN A TUBE & SYMCOX & EHRLICH (1962)	• USED OXYGEN INITIATION (1^{ST} ORDER W. R. T.. OXYGEN)
DONATI ET AL (1982)	• PEROXIDE INITIATION • OXYGEN INITIATION • TERMINATION BY COMBINATION & DISPROPORTIONATION		• NO MOLECULAR WEIGHT CALCULATIONS • PULSE VALVE EFFECT ON AXIAL MIXING NEGLIGIBLE, BASED ON FLUID DYNAMIC MEASUREMENTS

HOLLAR & EHRLICH (1983)	• PEROXIDE INITIATION • OXYGEN INITIATION • THERMAL SELF INITIATION • TERMINATION • β –SCISSION	CHEN ET AL. (1976), TAKAHASHI & EHRLICH (1982)	• INCLUDED THERMAL SELF INITIATION OF ETHYLENE • CONCLUDED THAT OXYGEN BEHAVES AS A FAST & A SLOW INITIATOR
YOON & RHEE (1985)	• PEROXIDE INITIATION • TERMINATION • TRANSFER TO MONOMER & POLYMER	• CHEN ET AL. (1976) • LEE & MARANO (1979)	• STUDIED AXIAL MIXING & CONCLUDED IT MAY BE NEGLECTED • STUDIED SSH FOR RADICALS & CONCLUDED IT IS A VALID ASSUMPTION • STUDIED OPTIMAL TEMPERATURE PROFILES
MAVRIDIS & KIPARRISSIDES (1985)	• PEROXIDE INITIATION • TERMINATION BY COMBINATION & DISPROPORTIONATION • TRANSFER TO MONOMER, POLYMER & TRANSFER AGENT • β –SCISSION	LEE & MARANO (1979)	• TESTED SSH FOR RADICAL CONCENTRATION & CONCLUDED IT IS A VALID ASSUMPTION • INCLUDED MOMENTUM BALANCE TO CALCULATE PRESSURE • PERFORMED SENSITIVITY STUDY TO OPTIMIZE PERFORMANCE • MULTIPLE INITIATORS
SHIRODKAR & TSIEN (1986)	• PEROXIDE INITIATION • TERMINATION BY COMBINATION & DISPROPORTIONATION • TRANSFER TO MONOMER, POLYMER & TRANSFER AGENT • β –SCISSION • BACKBITING	PLANT DATA	• TWO REACTION ZONES WITH MULTIPLE INITIATOR & MONOMER FEEDS

GUPTA ET AL. (1987)	• PEROXIDE INITIATION • TERMINATION • TRANSFER TO POLYMER & TRANSFER AGENT • β –SCISSION OF SEC RADICAL & TERT RADICAL • BACKBITING	CHEN ET AL. (1976), GOTO ET AL. (1981)	• CONCLUDE THAT SSH FOR RADICAL CONCENTRATIONS VALID • MULTIPLE INITIATOR & MONOMER FEEDS
TJAHJADI ET AL. (1987)	• PEROXIDE INITIATION • TERMINATION BY COMBINATION	• LAURENCE & POTTIGER (1985)	• SENSITIVITY ANALYSIS PERFORMED
BRANDOLIN ET AL. (1988)	• OXYGEN INITIATION • TERMINATION BY COMBINATION • TRANSFER TO POLYMER & TRANSFER AGENT • β –SCISSION	• RATE PARAMETERS FROM REACTOR TEMPERATURE PROFILE • MOLECULAR WEIGHT PARAMETERS TO MATCH MEASURED MOLECULAR PROPERTIES	• OXYGEN INITIATION MODELED AS N^{th} ORDER REACTION (W. R. T. OXYGEN) N=1.1
VERROS ET AL. (1992)	• PEROXIDE INITIATION • CHAIN INITIATION REACTIONS • TRANSFER TO MONOMER, MODIFIER & POLYMER • TERMINATION BY COMBINATION & DISPROPORTIONATION • BACK BITING β –SCISSION OF TERTIARY & SECONDARY RADICALS	GOTO ET AL. (1981) & GROUPS OF KINETIC RATE CONSTANTS SET EQUAL FOR ETHYLENE & VINYL ACETATE	• DETERMINED WHAT GROUPS OF REACTION RATE CONSTANTS CAN BE INDEPENDENTLY ESTIMATED FROM EXPERIMENTAL DATA.

KALYON ET AL (1992)	• PE HOMOPOLYMER • OXYGEN INITIATION MODELLED AS FIRST ORDER REACTION IN OXYGEN & ZEROTH ORDER FOR MONOMER. • TRANSFER TO MODIFIER & POLYMER • BACKBITING β –SCISSION OF TERTIARY & SECONDARY RADICALS	• ESTIMATED KINETIC VALUES FROM INDUSTRIAL DATA. • NO BRANCHING CORRECTION FOR MW MEASURED BY GPC	• REPORTED INDEPENDENT VALUES FOR KP & KT • PRESENTED RHEOLOGICAL DATA FOR POLYMER PRODUCED UNDER DIFFERENT REACTION CONDITIONS
THIS WORK & ZABISKY ET AL. (1992)	• COPOLYMERIZATION • PEROXIDE INITIATION • OXYGEN INITIATION • OXYGEN RETARDATION & RE-INITIATION • THERMAL SELF INITIATION • TERMINATION BY COMBINATION & DISPROPORTIONATION • TRANSFER TO MONOMER, POLYMER & TRANSFER AGENT • β –SCISSION OF TERMINAL RADICALS • β –SCISSION OF BACKBONE RADICALS • BACKBITING	• INDUSTRIAL REACTOR TEMPERATURE PROFILE & FINAL CONVERSION • MEASURED MOLECULAR WEIGHTS • REASONABLE BRANCHING FREQUENCIES	• ALLOWS FOR COPOLYMERIZATION • ACCOUNTS FOR PULSE VALVE PRESSURE VARIATION • OXYGEN INITIATION, RETARDATION & RE-INITIATION • MULTIPLE INITIATORS • MULTIPLE FEED POINTS

The mathematical model to describe steady state high pressure tubular reactors is developed below. This model is based upon the kinetic mechanisms for the copolymerization (presented above), and upon a knowledge of the reactor flow and temperature characteristics. The model is then used as the basis for a computer program (*TUBULAR*) to simulate the steady state production of LDPE and copolymers in tubular reactors. This computer model predicts the temperature, pressure and fractional

conversion profiles along the reactor as well as the final product quality. The properties of interest are the copolymer composition, molecular weight averages, branching frequencies, melt viscosity and polymer density. The computer simulation should then be useful to develop new products and improved methods of making existing products. Safety calculations can easily be performed using the simulation model. By incorporating the kinetics of free radical copolymerization into the model, we can simulate a multitude of new copolymers to determine, at least as a first estimate, the ideal proportions of each monomer in the feed to yield the desired copolymer product.

This project endeavors to build upon these existing models, and correctly incorporate other physical and chemical phenomena that were neglected by others. Some of the new considerations presented by this work, are

- A more detailed study of the β-scission phenomena including scission of backbone radicals.
- the pulse valve is incorporated to allow for pressure fluctuations
- the product cooling section is included
- a more complete description of the cooling jackets is included.
- oxygen initiation is modelled in more detail to account for initiation, retardation, and re initiation.
- a multiple feed, multiple reaction zone reactor is modelled and the kinetic and heat transfer parameters, although proprietary, are estimated from temperature and conversion data collected from an industrial reactor producing polyethylene and polyethylene vinyl acetate copolymers using both oxygen and peroxide initiation.

2.4.2 Kinetic model development

The mathematical model to describe the polymerization is presented in this section. The model includes mass, momentum and energy balances for a steady state tubular reactor. We assume that the tubular reactor and the cooling jackets experience plug flow, i.e., there are no radial temperature or concentration gradients in the tube or jackets, and no axial mixing. The validity of these assumptions depends upon the L/D ratio, the fluid properties and the Reynolds number. Since the Reynolds number for these reactor is usually greater than 10,000 (Chen, et al. 1976), and the L/D ratios are very

large, these assumptions should be valid. Fluid mechanical studies (Donati et al. 1982) seem to suggest that the axial mixing effect is of minor importance and Yoon and Rhee (1985) confirm this.

We also assume that the reaction mixture is homogeneous. There may be a polymer rich phase precipitating very near the tube wall, where it is cooler. The reaction rates will be much different there, but we are neglecting this since resins produced in tubular reactors do not show the grainy film appearance, a typical characteristic of two phase reaction polymer obtained in autoclave reactors. With these assumptions, the model should give reasonable predictions of the polymer quality, temperature and fractional conversion profiles along the reactor. Relaxing these assumptions would lead to greater model complexity with possibly a small increase in accuracy.

The model is written using axial distance, L, as the independent variable. The resulting ordinary differential equations will be solved in this form by integrating along the reactor length. We will consider mass balances on each species in the reactor, energy balances on the reactor and jacket contents, and a momentum balance to account for the pressure drop in the reactor. Special considerations are made for the pulse valve. The chemical reactions considered are presented in the previous section. Terminal double bond and explosive decomposition reactions are neglected. One can simplify the mathematical equations for a copolymerization by using pseudo kinetic rate constants.

Mass balances on species

In order to find the rate of polymerization we must perform a mass balance on each chemical species including, oxygen, initiator, monomers, radicals chain transfer agents and monomer units bound as polymer. If we consider a *plug* of fluid flowing down the reactor with some velocity, we can write an equation of the form

accumulation in the plug = net generation by reaction

This results in ordinary differential equations with axial distance being the independent variable. These equations can be solved from the front feed of the reactor to the first feed point. Then new initial conditions are found by including the new feeds, and the equations are then solved to the next feed point. This procedure is continued until the exit is reached.

The long chain approximation is made for monomer and the stationary state hypothesis is made for all radical species. Radical formation is by decomposition of peroxide, by oxygen initiation, and by thermal initiation. Oxygen retardation and re-initiation are also included.

The details of the balances are presented in a later section.

Energy balances

The temperature profile along the reactor is an important calculation. The rate of polymerization can double for every 10°C rise in temperature, and thus if the temperature profile is incorrect, the other predictions will certainly be inaccurate. We must also calculate the temperature profile for safety considerations. Energy balances are performed on a plug of the reaction mixture and on a plug of the jacket contents. Heat transfer across the reactor wall is considered and the temperature of the reactor and the jacket is calculated

accumulation of energy in the plug in the reactor=
net generation by reaction
- net energy transferred to jacket

accumulation of energy in the plug in the jacket =
net energy transferred to jacket from the reactor

Again, this results in ordinary differential equations with axial distance being the independent variable. These equations can be solved from the front feed of the reactor to the first feed point or the end of the first jacket section. The new temperature is calculated by assuming instantaneous mixing of the fresh feed and the reaction mixture. An enthalpy balance is performed at the feed point to obtain the new initial conditions. The equations are then solved to the next feed point or jacket section. This procedure is continued until the exit is reached. The temperature of the cooling medium must be specified at the up stream entrance or exit points of each cooling jacket section. For sections of the jacket where the flow is counter current to the flow of reactants, the outflowing temperature must be specified. The down stream temperature is then calculated from the energy balances.

The heat capacity of each stream is assumed to be the sum of the heat capacities of the pure components and we are neglecting heats of mixing and solution. The heat transfer coefficients are calculated by obtaining film heat transfer coefficients

that take into account the properties of the reaction mixture (Chen et al. 1976) and by fitting the wall heat transfer coefficient to match the reactor and jacket temperatures.

The details of the balances are presented in a later section.

Reactor pressure effects

The reactor pressure affects both the rates of reaction and the thermodynamic properties of the reaction mixture. The reactor pressure decreases along the reactor length to the pulse valve, where a larger pressure drop is experienced. Furthermore, the pulse valve is periodically opened and closed, creating pressure waves, to help reduce reactor fouling. All of these effects must be reasonably modelled.

Pressure profiles

Since the rate of reaction depends upon the reactor pressure, it is important that we adequately model the pressure profile down the reactor length. One method is to write a differential equation for the pressure drop for turbulent flow down a tube. This gives (Donati et al. 1982, Kiparissides and Mavridis 1985) from the definition of the Fanning friction factor for turbulent flow.

$$\frac{dP}{dL} = -\frac{f_f \cdot \rho \cdot u^2}{g_c \cdot r}$$

where

ρ	fluid density
r	inner radius of reactor
u	linear velocity of fluid
g_c	the gravitational constant used to convert kgm (kilograms mass) to kgf (kilograms force)
P	reactor pressure.
f_f	the Fanning friction factor

The Fanning friction factor for turbulent flow, under these reactor conditions is probably in the range $0.01 > f_f > 0.0791 \cdot Re^{-1/4}$ (Brandolin et al. 1988). The solution of this equation should give a reasonable pressure profile down the reactor to the pulse valve. Reynolds numbers calculated using the model developed in this thesis show that the flow is fully turbulent.

Pulse valve effects

In this section we are interested in the effect of the valve pulsing and thus, varying the reactor pressure range and the reaction mixture flow rate. This pulsing causes the reaction mixture to heat up and cool down, due to the change in: (a) reaction rates as the pressure changes; (b) flow rates causing variation in residence times; (c) heat transfer coefficients as the velocity changes; and (d) heat transfer coefficients as the fouling is allowed to accumulate, or is removed from the reactor wall. This pulse valve may also cause axial mixing, but for the reasons discussed previously, we are neglecting this. We are also modelling this as a steady state flow reactor, even though the reaction mixture is slightly increasing and decreasing in linear velocity. The optimum case would be to model unsteady flow, accounting for axial mixing. Unfortunately this would involve solving a set of partial differential equations (in time and reactor length), and we may find that the approximations we have made here, give a simpler, but nonetheless adequate model.

Reactor fouling has not been studied for this type of reactor. Since we have no theoretical basis to model the fouling of the tubular reactor, we have neglected this. Furthermore Donati et al. (1982) found in a pilot scale reactor, that the sinusoidal pulsing of the reactor had no significant effect on mixing, heat transfer coefficient and pressure reduction probably due to the low frequency (2 to 10 sec per pulse) of pulsation, as compared to the much higher frequencies of turbulent motion (approximately 10^3 times greater). A large amount of axial mixing (denoted by a small Peclet Number) over a significant length of reactor would be required to strip a reactor of any polymer film fouling the walls. Agrawal and Han (1975) found that a Peclet number near 100 is needed for significant axial mixing. On the other hand Chen et al. (1976) found that the Peclet number is more probably in the order of 10^{14} for a tubular reactor. For these reasons, we feel that we are still justified in neglecting axial mixing (although we did not measure the Peclet number in this study), and in neglecting any fouling on the reactor walls, because the axial mixing that would be present, due to the pulse valve, is not sufficient to strip the walls of any fouling.

Under usual operation, the pulse valve is quickly opened every T_{pulse} seconds, allowing a decrease in reactor entry pressure of ΔP (kgf/cm^2) and slowly closed over T_{close} seconds until the pressure returns to the set point. We assume that the valve is instantaneously opened and linearly closed with time. Since we have not yet developed any realistic model on how the pressure and mass flow rates change with valve position, we assume that the flow increases linearly, and the pressure decreases linearly with valve position as it is opened. The pressure change is a process variable, controlled by the operator, and the flow rate change may be in the order of 20 to 50% (Donati et al. 1982). We also assume that the pressure reduction due to the pulse valve, ΔP, is the same over the entire length of the reactor (up to the pulse valve). Thus the pressure profile down the reactor, P_o, is calculated as in the previous section, and periodic perturbations due to pulsing are superimposed upon this profile. A representation of the pressure profile is shown in figure 12

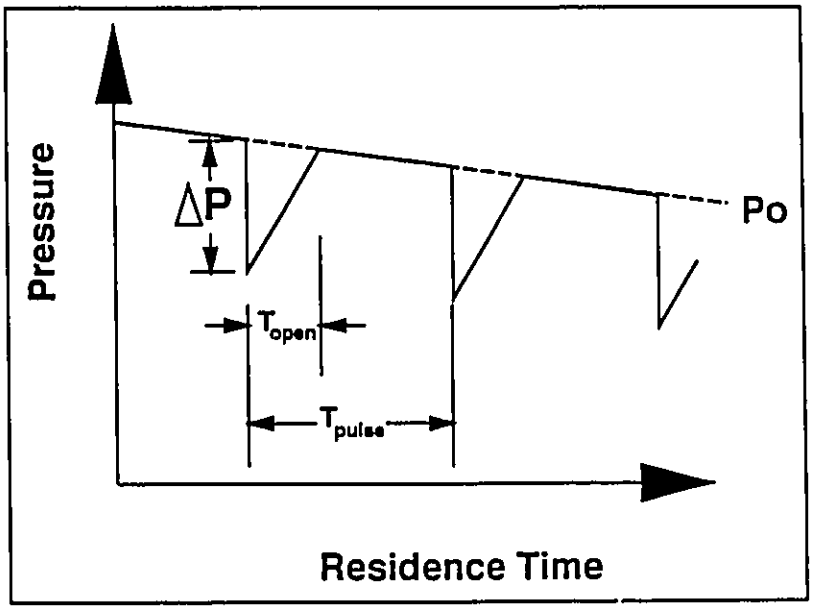

Figure 12 Description of effect of pulse valve on reactor pressure profile

Pressure drop across the pulse valve

The pulse valve causes a large pressure drop from the reactor to the product cooler sections. This pressure drop can change the rate of any residual reactions and

the temperature of the reaction mixture. The pressure drop is probably most simply modelled, in the absence of actual pressure data, as a constant value. This would appear as a discontinuity in the pressure profile down the reactor.

The effect of the pulse valve, can be considered to be a throttling phenomenon. This is a pressure drop at constant enthalpy, assuming that the heat losses to the surroundings are negligible. This is more familiarly known as Joule-Thomson expansion (for example see Smith and Van Ness 1975). The Joule-Thomson coefficient, η_{JT}, is defined as

$$\eta_{JT} = \left(\frac{\partial T}{\partial P}\right)_H$$

This coefficient is a function of temperature, pressure and solution composition. In the absence of thermodynamic data, for the mixture under these conditions, we assume that it is a constant and gives

$$\eta_{JT} = \frac{T_2 - T_1}{P_2 - P_1}$$

So given the pressure drop, and the expansion coefficient, one can estimate the temperature change over the pulse valve. η_{JT} is probably also a function of the valve type, and fluid properties. This analysis may be oversimplified and a more detailed description could be used incorporating the two phase flow after the pulse valve. However since we have very little information about the flow past this valve, we shall use the simpler model.

Molecular weight considerations

A precise knowledge of polymer properties is of great importance, as more and more specialties are required for specific industrial applications. In order to predict the physical properties of a resin, it is indispensable to know the molecular properties of the polymer. For this reason, molecular properties such as molecular weight distribution and branching frequencies are very meaningful calculations for the model. From the industrial point of view, a reliable copolymerization model is capable of appraising synthesis conditions, as well as allowing studies on new copolymers prior to

industrial tests. Thus, new polymer grades could be developed more easily, and the existing ones may be optimized in order to supply consistently high quality resins to customers.

Several attempts to model the molecular weight and branching frequencies have been made, in addition to the necessary initiation, propagation and termination reactions, some have included transfer to polymer and backbiting, but others have neglected either or both termination by combination and β-scission. Additionally, other authors only consider the β-scission of terminal radicals. The β-scission of internal radicals reaction could also cleave long chains into two smaller macromolecules, thus preferentially reducing the molecular weight of the longer chains and narrowing the distribution.

With respect to high pressure polyethylene reactors, a brief discussion of some of the past molecular weight modelling attempts, for homopolymerization, is in order. Saidel and Katz (1967, 1968) considered transfer to solvent and termination by combination and disproportionation but neglected the β-scission, transfer to polymer and backbiting reactions. They then used the method of moments to derive equations for the number and weight average molecular weights. When the stationary state hypothesis for radicals was not used, they found that the moment equations were not closed, i.e., the lower moments were functions of the higher moments. In order to close the equations, a technique presented by Hulburt and Katz (1964) was used. This technique assumes that the molecular weight distribution can be represented as a truncated (after the first term) series of Laguerre polynomials by using a gamma distribution weighting function chosen, so that the coefficients of the second and third terms are zero. It should be noted that this is still an empirical correlation for the higher moments as a function of the lower ones. This correlation may not be valid for many cases and quite possibly not for the polymer produced in this process (Zabisky et al 1992 and later sections).

Mullikin and Mortimer (1970, 1972) used a probabilistic approach to find the molecular weight averages under steady state conditions, including long chain branching, but excluding termination by combination, backbiting and β-scission. Small (1972, 1973) used the same kinetic scheme as Mullikin & Mortimer and the method of generating functions to find the molecular weight averages and the moments of the branching distribution. Jackson et al. (1973) considered transfer to chain transfer agent, termination by disproportionation, termination by combination and transfer to polymer, but neglected backbiting and β-scission.

Agrawal and Han (1975) included termination by combination, transfer to polymer, transfer to monomer and transfer to modifier but neglected backbiting and β-scission. Chen et al. (1976) used the method of moments and the closure technique of Hulburt and Katz. The reaction scheme included termination by combination, transfer to polymer and β-scission of terminal radicals. Han and Liu (1977) used this same kinetic mechanism.

Lee and Marano (1979) used rate constants from Szabo et al. (1969) and Ehrlich and Mortimer (1970) and included transfer to monomer and modifier. Termination was by disproportionation and combination, and backbiting and transfer to polymer to produce branches was also included. The β-scission reaction was modelled for the breakup of the chains at tertiary carbon atoms in the back bone, and the β-scission rate constant would apparently include the fraction of radicals that are on tertiary carbon atoms. In actual fact, they neglected β-scission because they claim that most of the chains are made by either termination or transfer to modifier and because of uncertainty in the rate constant for the β-scission reaction.

Yamamoto and Sugimoto (1979) used the model of Mullikin and Mortimer to estimate the long chain branching rate constant from their polymerization data. They include β-scission of terminal radicals and neglected termination by combination.

The model of Goto et al. (1981) is based upon the probabilistic model suggested by Mullikin and Mortimer but they included the backbiting reaction to produce short chain branches as well as transfer to solvents monomers and β-scission. Hollar and Ehrlich (1983) added thermal initiation to the model of as Chen et al. (1976). Kiparissides and Mavridis (1985a, 1985b) included termination by combination and disproportionation, transfer to monomer, polymer and solvent, and β-scission of terminal radicals but neglected backbiting. They then used the method of moments to find the number and weight average molecular weights, using the Hulburt and Katz (1964) closure method when the stationary state hypothesis was not used for the radical concentration. Gupta (1985, 1987) used the same kinetics as Goto (1981).

Yoon and Rhee (1985) included only transfer to monomer, transfer to polymer and termination by combination. Shirodkar and Tsien (1986) considered transfer to monomer, solvent and polymer, backbiting, and termination by both combination and disproportionation, but neglected β-scission. Postelnicescu and Dumitrescu (1987) considered termination by combination and disproportionation, transfer to monomer and transfer to chain transfer agent, but neglected transfer to polymer, backbiting

and β-scission. Tjahajadi et al. (1987) considered only termination by combination, neglecting all other reactions. Brandolin et al. (1988) included termination by combination, transfer to polymer and solvent, and β-scission of terminal radicals.

What follows is our attempt to model the molecular weight and branching development for a more comprehensive set of reactions, including binary copolymerization. Firstly, balances for the radicals and polymer chains of length r are given and then the method of moments is used to find the molecular weight averages and the branching frequencies. The derivation of the molecular weight moments, using this method, is as follows. Notice that we have used pseudo rate constants to convert the copolymerization equations into simpler homopolymer equations.

Moments of the molecular weight distribution

For such a complex system, it is not possible without excessive computational effort to predict the entire molecular weight distribution. The method of moments, affords a relatively simple method to calculate the important leading averages. The moments of the molecular weight distribution are found by writing balances on the radical and polymer molecules of chain length r, multiplying each term by the appropriate power of r, and summing them from r=1 to ∞. The moments of the dead polymer radical size distribution are defined by

$$Y_i = \sum_{r=1}^{\infty} r^i R(r)$$

and the moments of the polymer size distribution are defined by

$$Q_i = \sum_{r=2}^{\infty} r^i P(r)$$

The moments are found by performing mass balances on species of length r and then multiplying the equation by the desired power of r and summing. Details of the process are given in a later section.

The radical centers can either be at the chain end, or on the backbone of the chain (internal radicals). It is assumed that the concentration of polymeric radicals with two or more radical centres is negligible. We assume that all internal radicals promptly undergo either propagation (forming long or short chain branches) or

β-scission, i.e., the transfer to polymer reaction responsible for the production of the internal radical is the rate limiting step. This is equivalent to assuming that the concentration of backbone radicals is near zero. We therefore neglect tetrafunctional branching and the possibility of crosslinking due to termination by combination of internal radials.

The stationary state hypothesis (SSH) for the radical moments is used. Mavridis and Kiparissides (1985a,b) and Yoon and Rhee (1985) found little difference in the solution to the MWD when the SSH assumption is relaxed. Moreover, in our simulations, when the SSH was relaxed the results were not significantly changed. The assumption makes the ODE's much easier to solve, as they become less stiff.

Mass balances can be performed to find the dead polymer moments. The average chain lengths are then given by:

Number average

$$\overline{r}_n = \frac{Q_1 + Y_1}{Q_0 + Y_0} \approx \frac{Q_1}{Q_0}$$

Weight average

$$\overline{r}_w = \frac{Q_2 + Y_2}{Q_1 + Y_1} \approx \frac{Q_2}{Q_1}$$

z-average

$$\overline{r}_z = \frac{Q_3 + Y_3}{Q_2 + Y_2} \approx \frac{Q_3}{Q_2}$$

Since $Q_i \gg Y_i$.

The problem of closure

When β-scission of the internal radicals is accounted for in the model the moment equations for the lower moments are functions of higher moments, therefore, the system is not "closed" when this reaction is significant. If we include this reaction we must find a suitable a closure technique that will adequately predict the higher moments as a function of the lower ones. Two possible choices have

been selected for a closure technique as described below, and these were evaluated by simulation, and comparing predicted with actual measured molecular weight averages.

Several authors have used the closure technique of Hulburt and Katz (1964), although this method may not be completely suitable for polyethylene produced in a high pressure tubular reactor (Zabisky et al. 1992). Nevertheless, this technique will be evaluated as a possible closure method. The closure equation is:

$$Q_3 = \frac{Q_2}{Q_1 Q_0}(2Q_2Q_0 - Q_1^2)$$

Molecular weight distributions produced in tubular reactors are often close to being Log Normal. For this reason, a log normal distribution is used to derive expressions for the higher moments as a function of the lower moments (see later section for the derivation), and the result is:

$$Q_3 = Q_0\left(\frac{Q_2}{Q_1}\right)^3$$

Comparison with actual data

Experimental molecular weight data for LDPE, produced in a tubular reactor, were provided by Polioleflnas, and are shown in the table 2. It should be noted that the molecular averages were measured by gel permeation chromatography, but no corrections were made for branching. Thus the higher molecular weight averages may be somewhat underestimated, M_w and M_z in particular. The magnitude of the error is unknown but could be checked by comparing the GPC results to an absolute method like high temperature low angle light scattering.

If Q_0 is set to unity, one can calculate the higher moments from the molecular weight data, since $\overline{M_n} = mQ_1/Q_0$, $\overline{M_w} = mQ_2/Q_1$, and $\overline{M_z} = mQ_3/Q_2$ (m is the molecular weight of monomer). One can therefore calculate the third moment (and thus M_z) as given by the Hulburt and Katz (H-K) and log-Normal (L-N) methods and compare the results with those presented above. These are shown in figure 13.

Table 2 Molecular weight data from tubular reactor (Triunfo, Brazil)

Resin	$\overline{M_n}$	$\overline{M_w}$	$\overline{M_z}$
Resin A	25900	222000	705000
Resin B (sample 1)	15800	88300	273000
Resin B (sample 2)	16700	97800	312000
Resin C	21300	148000	445000
Resin D	20500	135000	398000
Resin E (sample 1)	17800	95800	307000
Resin E (sample 2)	17800	99300	330000
Resin E (sample 3)	18900	98500	284000

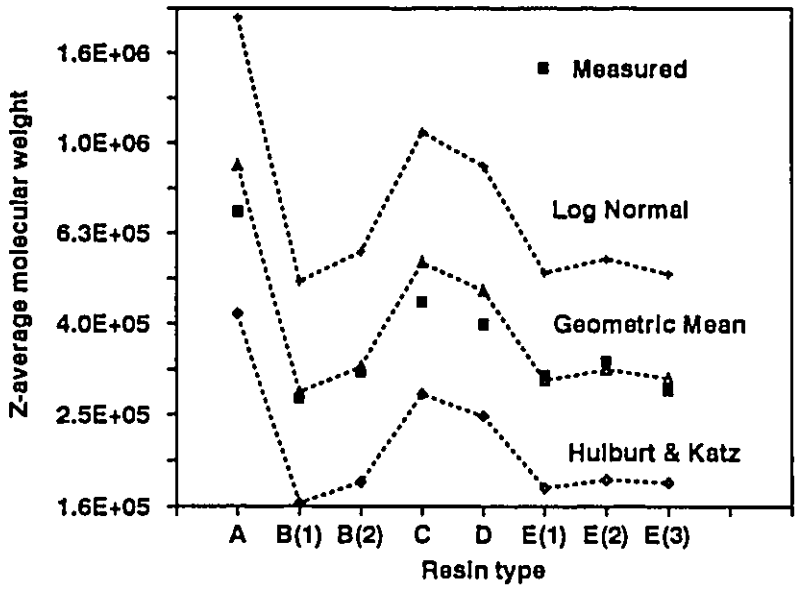

Figure 13 Correlating plant molecular weight data with closure techniques

We can see that the L-N method greatly over predicts the Q_3 value, whereas the H-K method under predicts it. The geometric average of the two methods is in good agreement with plant reactor data.

$$Q_{3_{geometric}} = \sqrt{Q_{3_{H-K}} \cdot Q_{3_{L-N}}}$$

Recommendations for closure

On the basis of these tests, the method of choice appears to be the geometric mean of the Hulburt & Katz method and the Log-Normal method. It should be emphasized that the method that fits the actual plant data best (in this case, the geometric mean) should be used for simulations. Closure methods should not be arbitrarily chosen without validation with real data. Moreover the closure methods are not generally valid, for example they may differ for tubular and autoclave reactors.

Branching frequencies

The short and long chain branching can have an important effect on polymer properties. The more short chain branches incorporated along the polymer chain, the lower will be the polymer density, while long chain branches affect the rheological properties. The branching frequencies can be calculated by mass balance on the total number of long (LCB) and short branches (SCB). The number of short and long chain branches per polymer molecule is calculated as follow:

$$\overline{S_n} = \frac{SCB}{Q_0}$$

$$\overline{L_n} = \frac{LCB}{Q_0}$$

The number of short and long chain branches per 1000 carbon atoms is given by (assuming two backbone carbon atoms per monomer unit)

$$\lambda_s = \left(\frac{SCB}{Q_1}\right) \cdot 500$$

$$\lambda_L = \left(\frac{LCB}{Q_1}\right) \cdot 500$$

Solution of the mathematical model

The model is comprised of a system of coupled ordinary differential equations. These equations may become stiff during the nearly adiabatic temperature rise. To solve these equations, we have used a package called *LSODE* (Hindmarsh 1980, 1983) that uses either a non-stiff (Adams) or stiff (Gear) method with variable step size and interpolating polynomial order.

2.4.3 Simulations

Some typical conversion, temperature, molecular weight and branching frequency profiles are presented in figures 14, 15, 16, and 17. These profiles were generated using the simulation program *TUBULAR* presented in this report and are simply to show standard trends in a multiple feed, multiple reaction zone tubular reactor. The inflow points of monomer, modifier and initiator are shown in these figures. Relative temperature is the reactor temperature over the temperature of the feed monomer. Conversion is presented as the mass of polymer divided by the mass of monomer and polymer.

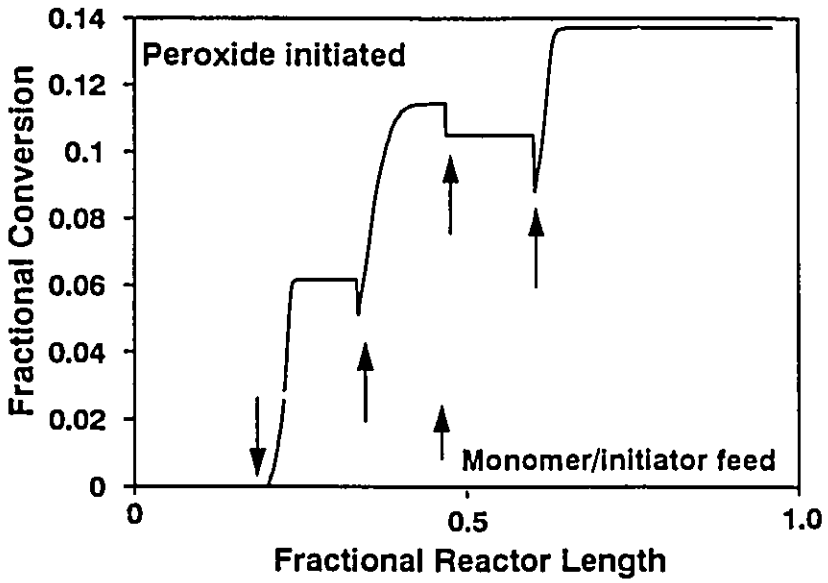

Figure 14 Typical Conversion Profile: Peroxide Initiated Homopolymer

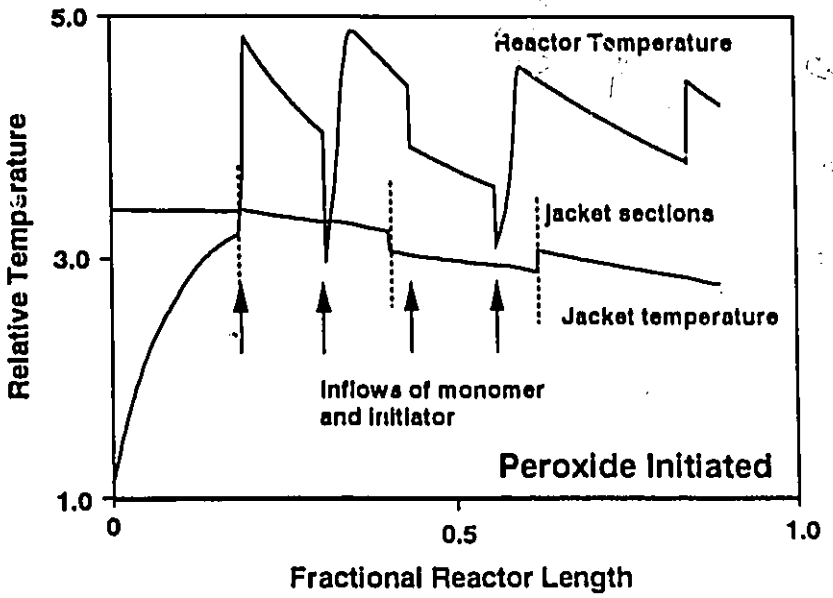

Figure 15 Typical Reactor Temperature Profile for Peroxide Initiated Homopolymer

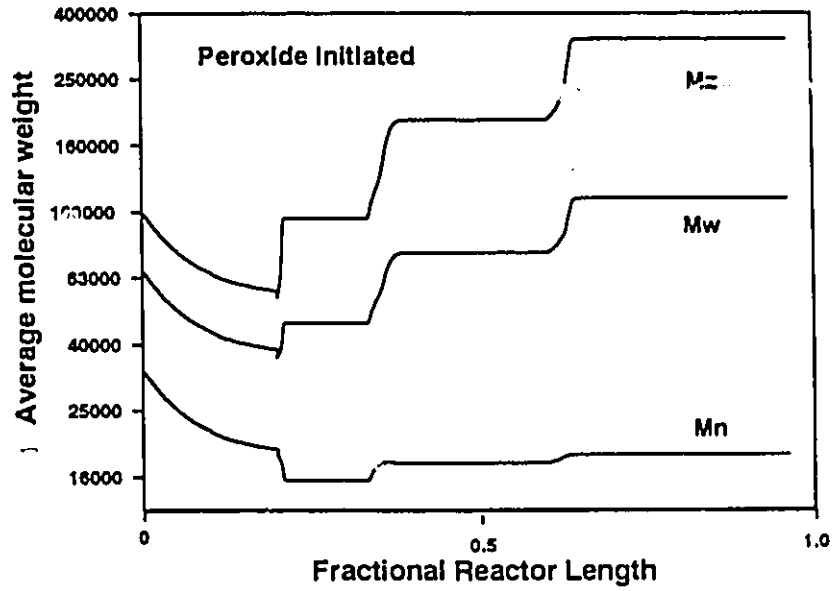

Figure 16 Typical Molecular Weight Average Profile: Peroxide Initiated Homopolymer

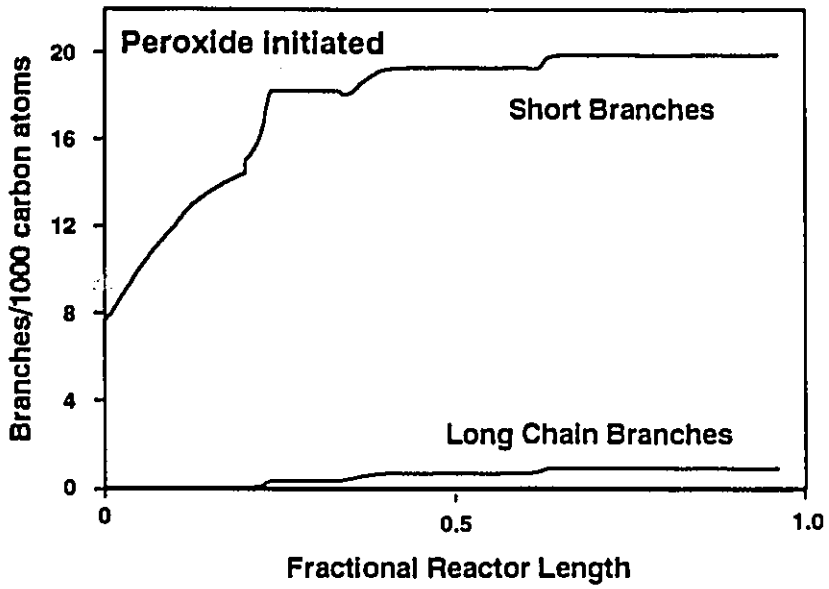

Figure 17 Typical Branching Frequency Profile: Peroxide Initiated Homopolymer

In order to evaluate the validity of the model developed, simulations for both homopolymerization and copolymerization were carried out to compare the model predictions with actual plant data. Since literature values for the kinetic rate constants seem to vary over a wide range (Gupta 1987), we chose to fit the parameters to industrial data. For this reason the values of the rate constants used, must remain proprietary. The results are shown in figures below.

Figures 18 and 19 show the reactor and jacket temperature (Tj) profiles, as well as monomer conversion along the reactor for homopolymerization of ethylene using oxygen as initiator, while figures 20 and 21 employ liquid peroxides instead. Figures 22 and 23 provide the same plots for copolymerization of ethylene and vinyl acetate. For copolymer, the conversion is the total mass conversion of monomer. Notice that in all cases, the model predictions fit the plant data reasonably well, suggesting that the model proposed has the necessary structure and fundamental basis to simulate the industrial reactor. However, efforts still have to be made in the sense of improving parameter estimates of the model, with respect to the molecular properties, and work is currently being done by Polioletinas by measuring molecular properties, and fitting the model parameters.

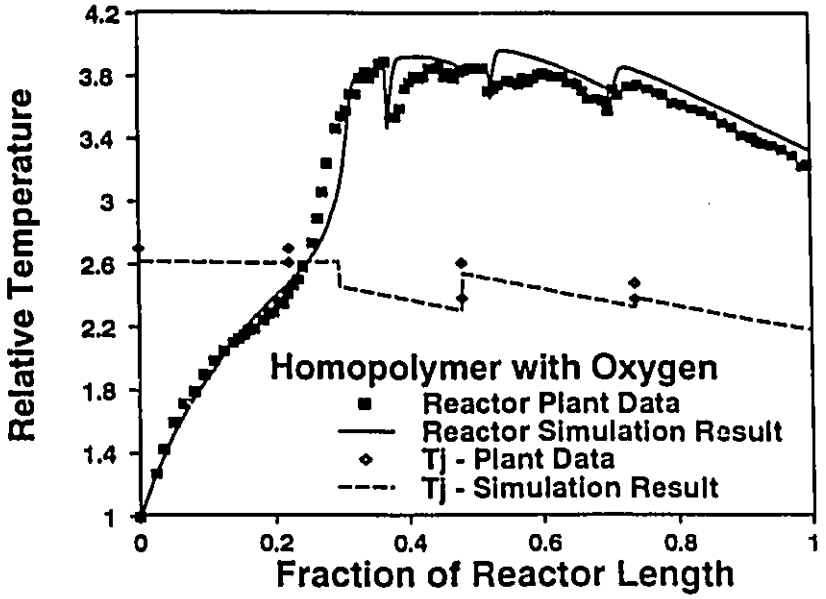

Figure 18 Temperature Profile: Oxygen Initiated Homopolymer

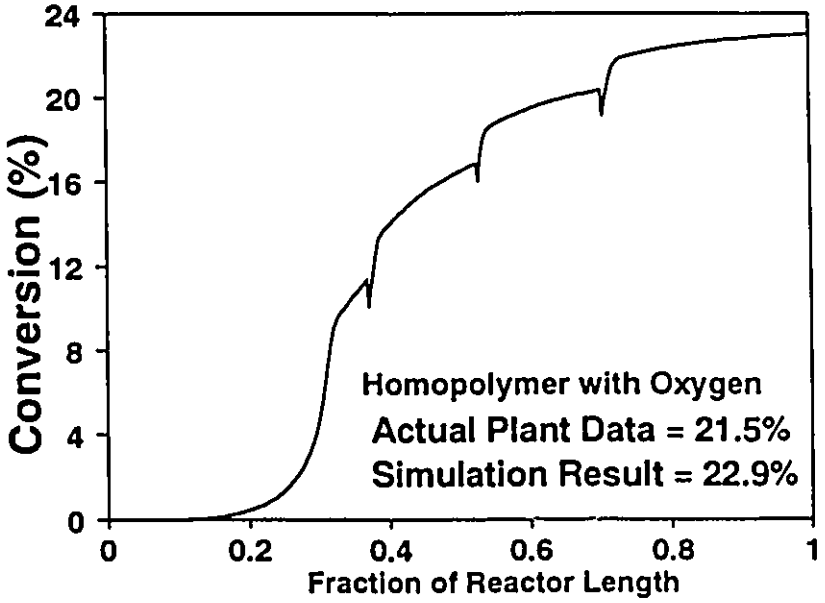

Figure 19 Conversion Profile: Oxygen Initiated Homopolymer

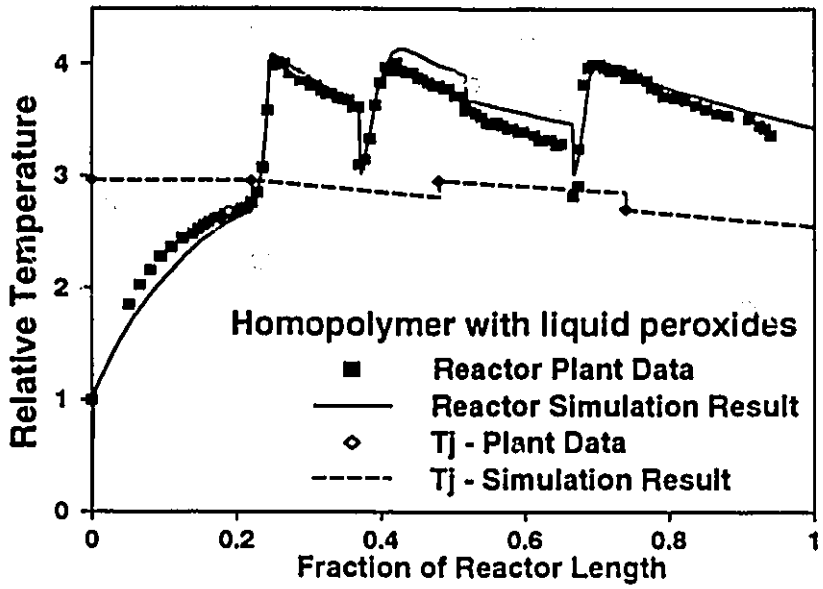

Figure 20 Reactor Temperature Profile: Peroxide Initiated Homopolymer

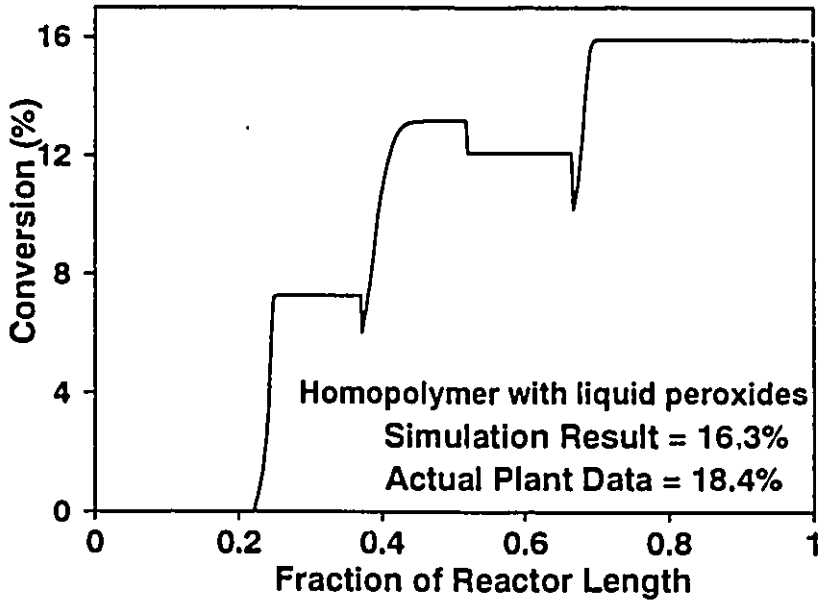

Figure 21 Conversion Profile: Peroxide Initiated Homopolymer

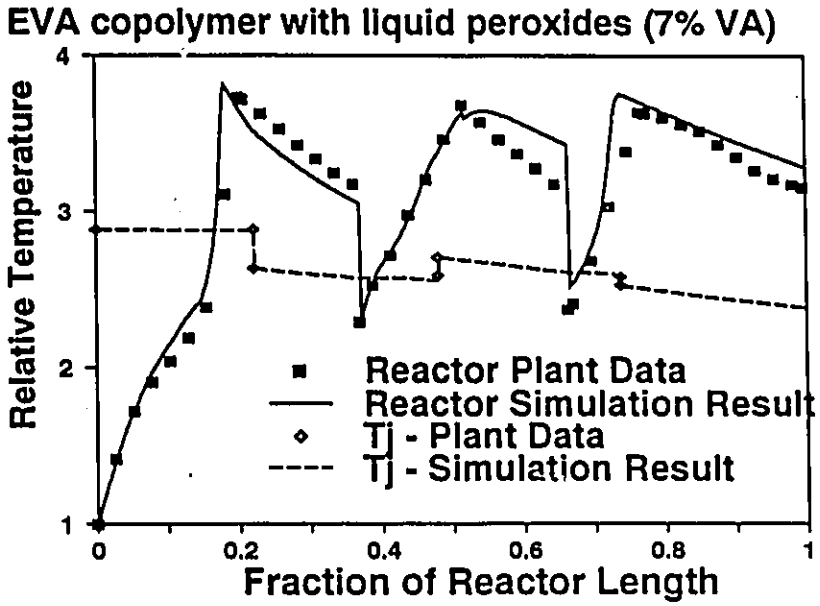

Figure 22 Reactor Temperature Profile: Peroxide Initiated Copolymer

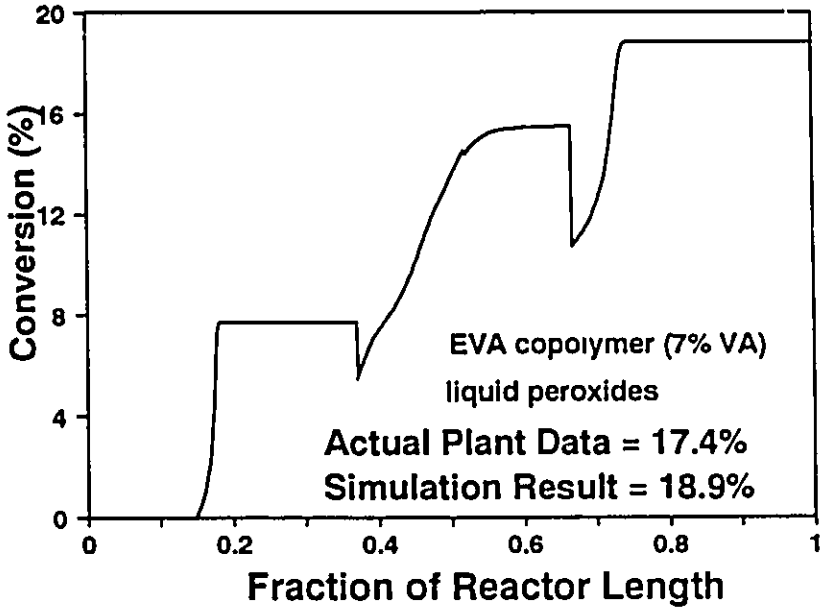

Figure 23 Conversion Profile: Peroxide Initiated Copolymer

2.4.4 Conclusions for tubular reactor model

A more general kinetic model than is available in the open literature has been developed for free radical, high pressure copolymerization in a commercial tubular type

reactor with multiple feeding points. The model accounts for reactions which are frequently neglected by other authors like: thermal initiation of monomer, backbiting, β- scission, and decomposition reactions. In order to represent realistically the polymerization process, the effect of pulse valve and product cooler was also incorporated in the model. In order to have a better understanding of how reactor operation policies affect the polymer microstructure, (and in turn the polymer properties) the model was extended to predict both the molecular weight averages, and the average frequency of long and short chain branching. A new approach for moment closure to evaluate molecular weight averages has also been presented. Simulation results generated from the model were compared with plant data, and have shown encouraging prospects for industrial application.

2.5 Application to high pressure autoclave reactors

2.5.1 Introduction

The mechanism and kinetics of this free radical copolymerization is outlined above and by Zabisky et al. (1992). However, there are several complications which make the modeling of autoclave type reactors highly challenging, namely: a) non-ideal mixing, b) the presence of unstable steady states, c) the existence of reactions in two phases and d) the possibility of gel formation due to crosslinking reactions. In order to develop a comprehensive model capable of predicting the actual plant operating conditions as well as the polymer properties, one must address all of these items without making the model too complex to be readily solved. Attempts have been made to model this type of reactor (Georgakis and Marini, 1982; Marini and Georgakis, 1984), but herein attempts will be made to produce a more comprehensive model to describe not only the rates of reaction, but also the molecular properties of the material formed. Our objective is to create a mathematical structure to account for the rate of polymerization and to describe the molecular weights, compositions, branching frequencies and gel content of the polymer formed. This model includes thermodynamic and kinetic considerations for a heterogeneous reaction mixture and includes a mixing model to account for the flow pattern within the reactor. The model is put together to create a dynamic simulation of commercial autoclave reactors including multiple feed points and temperature controllers.

In this section we shall outline the important features of this model and present some simulation results in the form of sensitivity studies and comparisons with an industrial reactor.

2.5.2 The mixing model

The mixing pattern in an autoclave type reactor tends to be of a recirculating nature. The effect of mixing on reactor performance is very important, especially since an imperfectly mixed vessel requires more initiator per unit of polymer produced than does a more perfectly mixed vessel under the same conditions (Georgakis and Marini, 1982). The initiator tends to decompose near the feed points, and not in the bulk of the reactor, thus not promoting as much polymerization as if the initiator was uniformly distributed throughout the reaction mixture. The presence of temperature gradients down the reactor also reveal imperfect mixing.

Donati et al. (1981) studied a cold mock up of an industrial scale reactor, a CSTR with a single impeller. They found the flow in this compartment tended to be downward near the wall, with back flow in the centre. They modelled this flow pattern as two annuli divided into several CSTR's with axial flow and radial mixing between the two annuli. The regions near the impeller and the bottom of the tank were modelled as CSTR's with no radial gradients. Georgakis and Marini (1982) modelled this same reactor as three CSTR's in series with recycle to each one. They used two small volumes near the initiator feed points and then a larger volume element for most of the reaction. These models which appear to be adequate for a single compartment, at least with respect to initiator consumption, are based upon measurements of the velocities in the actual reactor and therefore should be quite realistic. However these models were proposed only for a single compartment between the stirrer blade and the bottom. The present model must account for the entire vessel.

The proposed mixing model

Consider the autoclave reactor represented by N_v volume elements, each of them consisting of a CSTR segment followed by a plug flow segment to account for steep temperature gradients from one volume element to the next. In the plug flow segment, to avoid solving partial differential equations, we have approximated the whole section by N_p equal volume CSTR's in series. To account for recirculation we allow recycle from the CSTR segment of each element to the CSTR segment of the element above. Figure 24 shows the multiple reaction volume scheme.

We can set the volume of each element, V_j. Moreover, for each volume element we define the volume fraction of the CSTR segment to the total volume of element j as.

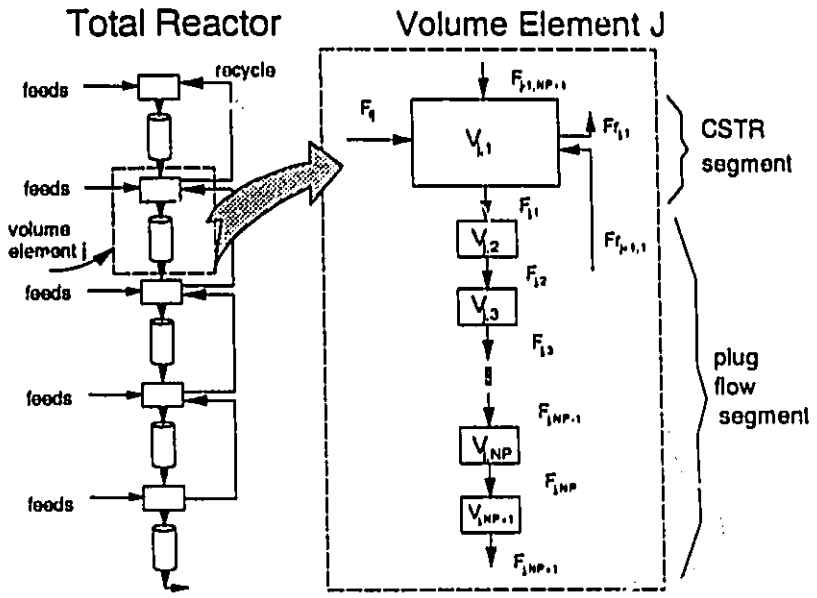

Figure 24. Schematic of proposed mixing model for total reactor, and a blow up for a specific volume element j showing how the plug flow segment is approximated by several small CSTRs.

$$\theta_j = \frac{V_{j,1}}{V_j}$$

and thus θ_j is a parameter to be estimated for each volume element j. The larger θ_j the more the mixing in the element approaches ideal CSTR. The volume of each small CSTR in the plug flow segment is given by

$$V_{j,L} = \frac{V_j(1-\theta_j)}{N_p} \qquad L = 2,3,\ldots,N_p+1$$

The recycle is specified by a recycle ratio, q_j, defined as the volumetric flow rate in the recycle stream divided by the sum of volumetric feed rates to all elements. Thus the parameters which define the mixing model are: a) the number of volume elements (N_v), b) the volume fraction of each element that is the CSTR segment (θ_j), c) the number of smaller CSTR's in the plug flow segment (N_p), and d) the recycle rate for each element, except top element (q_j). Reasonable estimates of these parameters can be obtained from knowledge of the reaction temperature profile, initiator flow rates and stirrer geometry.

2.5.3 The unstable steady state

It has been found (Georgakis and Marini, 1982; Marini and Georgakis, 1984 and this work) that by using a steady state model, one cannot solve both the mass and energy balances for reasonable operating conditions. Considering a single adiabatic CSTR, the monomer conversion given by the steady state energy balance and by the monomer mass balance can be plotted against reaction temperature (Figure 25). There is a steady state near the region where the industrial reactor normally operates, denoted by point ***A***. Here both the mass and the energy balance equations are satisfied. If we attempt to operate at a point on the mass balance line to the right of point ***A*** then the heat generated by the reaction will cause the temperature to rise. On the other hand, if we start at a point on the left hand side of ***A***, the system will cool down until no polymerization occurs. Thus point ***A*** is an unstable steady state. One can use a dynamic simulation and include temperature controller equations to maintain the operating point at the desired steady state.

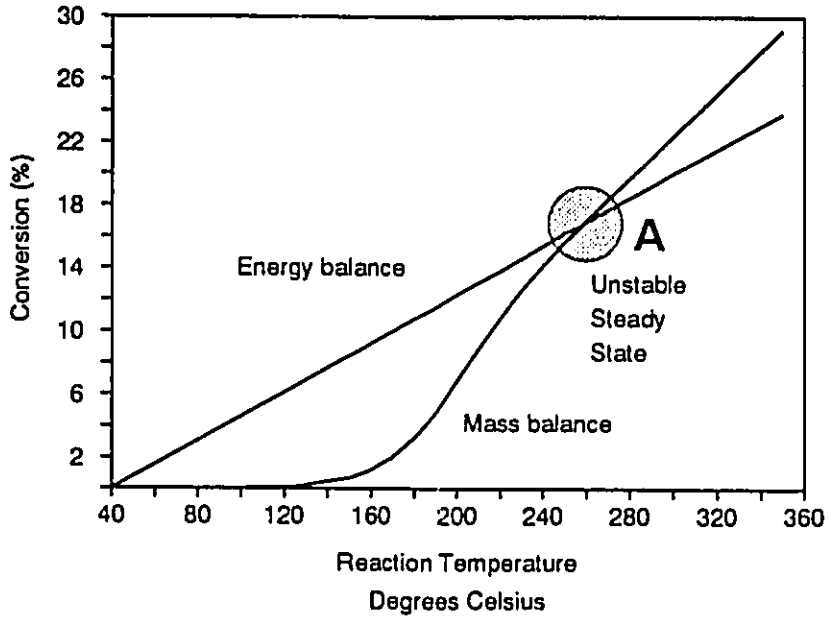

Figure 25. Steady state operating lines for a vessel reactor based upon the mass balance and the energy balance. A single well mixed volume. Feed temperature 40C. Ethylene homopolymerization

2.5.4 A thermodynamic correlation for polymer-monomer phase compositions

Under certain conditions, the polymer may precipitate out from the monomer, forming monomer and polymer rich phases. The polymerization then occurs as a heterogeneous reaction. Reactions with dead polymer, like branching and ultimately gel formation reactions, are accentuated in the polymer rich phase. It has been reported that the polymer produced under heterogeneous conditions differs significantly from the polymer manufactured under homogeneous conditions, the former providing a better balance of mechanical and optical properties (Bogdanovic and Srdanovic, 1986). It is thus vital to quantify the polymer-monomer compositions in each phase during the polymerization. The boundary between homogeneous and heterogeneous reaction conditions is a function of pressure, temperature, and polymer structure.

In order to quantify the monomer and polymer compositions in each phase of the reaction mixture, a joint project was undertaken by Polioletinas and the group of Prausnitz at the University of California, Berkeley, to model the phase equilibrium problem in polymeric systems using the continuous thermodynamics approach and a cubic equation of state (Sako et al. 1989). This resulted in the creation of a software package entitled *PFLASH* (1988). *PFLASH* calculates the weight fraction of polymer in each phase as a function of temperature, pressure and molecular weight. For ethylene - polyethylene, this model predicts an insignificant amount of polymer dissolved in the monomer rich phase under the normal range of operating conditions, so we need only concern ourselves with the monomer concentration in the polymer rich phase.

Due to the relatively large computation time required to run the complex thermodynamic model (*PFLASH*), a much simpler correlation was developed by fitting the output generated by *PFLASH*. Simulations were performed using *PFLASH* following an orthogonal factorial design and multiple linear regression was used to calculate the eight coefficients (Box et al. 1978). All coefficients were significant at the 95% confidence level.

$$W_1 = 0.24548 - 0.05777X_1 - 0.078337X_2 + 0.0048718X_3 - 0.027386X_1X_2 +$$

$$+ 0.0032556X_1X_3 + 0.003281X_2X_3 + 0.0029964X_1X_2X_3$$

where W_1 is the weight fraction of polymer in the polymer rich phase, and X_1, X_2, X_3 are all normalized variables defined as:

$$X_1 = \frac{T(K) - 498.2}{65} \qquad X_2 = \frac{P(Kgf/cm^2) - 1400}{200} \qquad X_3 = \frac{\overline{M}_w - 100000}{35000}$$

This correlation is only valid when all the normalized variables fall within the range of [-1,+1]. Due to our lack of data for the ethylene- vinyl acetate - polymer phase relationships under these conditions, this correlation is only strictly valid for ethylene and polyethylene. The presence of the small amounts of a comonomer, like vinyl acetate, has not been accounted for and this may introduce some error of uncertain magnitude. Figure 26 shows the sensitivity of W_i to temperature, pressure and weight average molecular weight and figure 27 shows the fit for the simplified correlation to the *PFLASH* calculations.

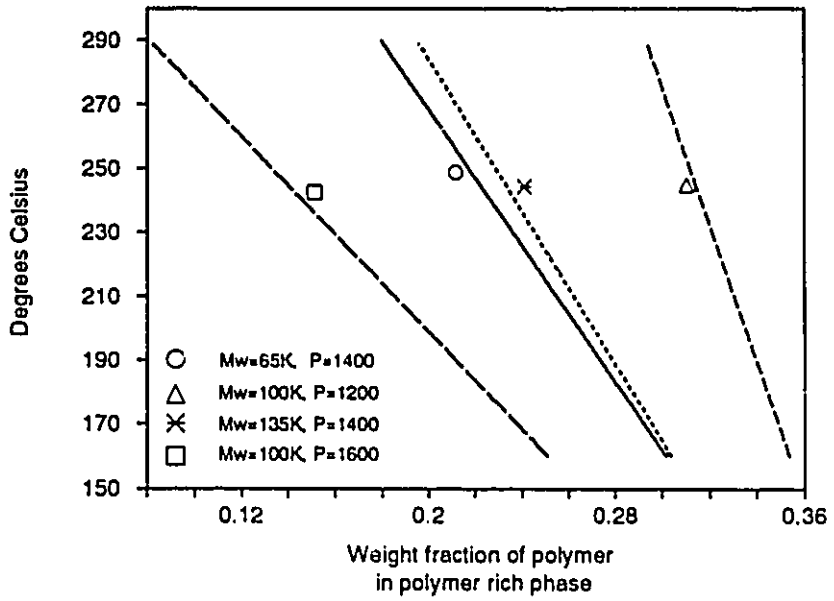

Figure 26. The phase diagram for ethylene - polyethylene from the simplified correlation.

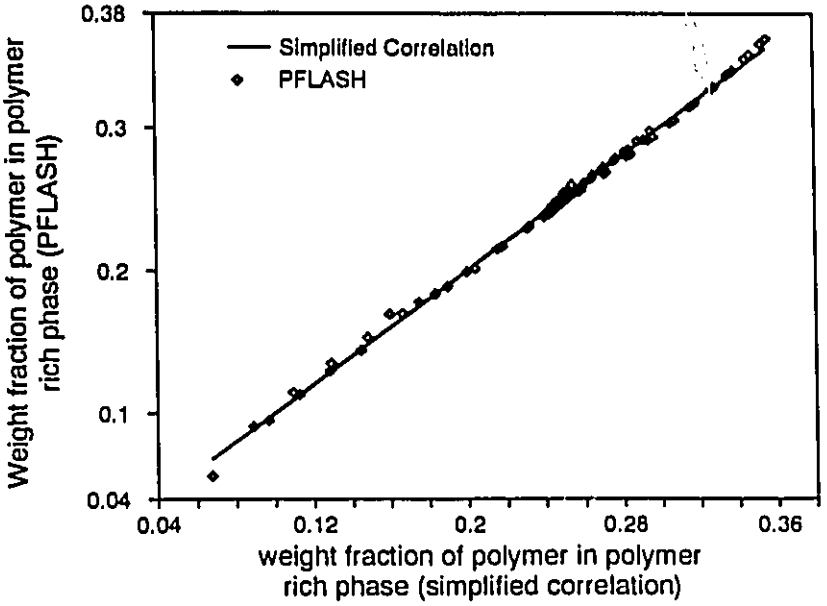

Figure 27. Comparison of the PFLASH predictions and the predictions from the simplified correlation.

2.5.5 Gel formation

Gel is the insoluble polymer network that can be formed under certain reaction conditions, and greatly affects final product properties. By definition, the onset of gelation occurs when the weight average molecular weight ($\overline{M}_w$) goes to infinity. Gel formation is caused by the branching reactions between radicals and dead polymer including transfer to polymer followed by termination by combination, and reactions with terminal double bonds in polymer chains. When the polymer concentration in the polymer rich phase becomes very high, branching reactions and eventual gelation are accentuated. The gel, once formed, acts like a sponge rapidly consuming sol polymer molecules and radicals. One can identify the following reactions as responsible for gel growth: a) addition of monomer to gel radicals by propagation, b) termination by combination of sol radicals with gel radicals c) reaction of sol radicals with terminal double bonds in gel, and d) reaction of gel radicals with terminal double bonds in sol.

In our system, the double bonds on polymer chain ends are produced by β-scission, transfer to monomer, and termination by disproportionation reactions. To account for the reactions with double bonds, one must keep track of all polymer chains with and without double bonds, thus significantly complicating the molecular weight

calculations. However our simulation shows that adequate branching frequencies can be obtained by simply including transfer to polymer reactions. Therefore, as with the tubular reactor model, we shall ignore reactions with terminal double bonds to reduce the complexity of the problem and accept that our model may be deficient in this regard.

2.5.6 Model development

The polymerization reaction mechanisms considered

In this work, the following elementary reactions (table 3) are included from the set presented above and by Zabisky et al. (1992). Initiation is by thermal decomposition of an organic peroxide initiator. The modifier acts as a chain transfer agent, but may also be incorporated into the chain in small amounts to contribute to the short chain branching. The first subscript in the rate constants refers to the type of radical center, and the second describes the monomer type. R' represents a backbone radical center. $R^{=}$, $P^{=}$ denotes a radical or a polymer with a terminal double bond.

As with the tubular reactor model we shall neglect reactions with terminal double bonds and explosive decomposition. Moreover we have neglected the scission of internal radicals since it only complicates the model, and seems not to greatly influence the predicted molecular weights. The lower reaction temperatures should also favour the omission of this scission reaction.

Table 3. The kinetic scheme.

I	$\xrightarrow{k_d}$	$2 \cdot R$	initiation
$R_j(r) + M_i$	$\xrightarrow{kp_{ji}}$	$R_i(r+1)$	propagation
$R_j(r) + M_i$	$\xrightarrow{kfm_{ji}}$	$R_i^{\bullet}(1) + P(r)$	transfer to monomer
$R_j(r) + TSH$	$\xrightarrow{kfs_j}$	$TS^{\bullet} + P(r)$	transfer to modifier
$R_j(r) + TSH$	$\xrightarrow{kps_j}$	$R(r+1)_{short\ branched}$	Modifier incorporated in the chain
$R_j(r) + P_i(s)$	$\xrightarrow{kfp_{ji}}$	$R'_i(s) + P(r)$	transfer to polymer (long chain branching)
$R_j(r)$	$\xrightarrow{kb_{ji}}$	$R'_i(r)$	backbiting (short chain branching)
$R_j(r)$	$\xrightarrow{k_\beta}$	$P^{\bullet}(r-1) + R_j(1)$	β-scission of terminal radicals
$R_i(r) + R_j(s)$	$\xrightarrow{ktc_{ij}}$	$P(r+s)$	termination by combination
$R_i(r) + R_j(s)$	$\xrightarrow{ktd_{ij}}$	$P^{\bullet}(r) + P(s)$	termination by disproportionation

The pseudo kinetic rate constants

One can simplify the mathematical equations for a copolymerization by using pseudo kinetic rate constants as outlined above and by Hamielec et al. (1987) and Zabisky et al. (1992). Instead of writing down all the reactions between all monomer or radical types, we can formulate the equations in terms of the total monomer or radical concentrations. Our mass and energy balances then appear as homopolymer equations but are valid for copolymerizations.

The overall balances

Given the mixing model, one can construct the mathematical model by writing the mass and energy balances for a single volume segment (recalling that a volume element is composed of 1 main CSTR segment and 1 plug flow section approximated by a variable number of CSTR's referred to as plug flow segments). The

resulting set of differential equations, for all volume segments, must usually be solved simultaneously because of the recycle. The mass balance for a species in a volume segment will, in general, have the form:

accumulation in volume segment= ***outflow from previous segment***
+ feed to segment
+ recycle from next element
- outflow to next segment
- recycle to previous element
+ net generation by reaction

For the plug flow segments there will not be any feed, or recycles. We must perform population balances on monomer and comonomer, moles of each monomer bound as polymer, initiators, radicals and modifier. The stationary state hypothesis is used for all radical species. The details of the mass balance equations are given in the appendix to this chapter.

Two phase kinetics

We need to determine the rate of reactions. Since the concentrations of each species may be different in each phase we must consider the contribution of reaction in each phase to the overall rate of reaction. The following assumptions are adopted for the two phase kinetics.

a) Thermodynamic equilibrium. The amount of polymer in the monomer rich phase is negligible. The monomer-polymer compositions in the polymer rich phase are determined by the simplified correlation.

b) In calculating the volume fraction of each phase, the volumes are considered to be additive.

c) The ratio of vinyl acetate to ethylene monomer concentrations will be identical in both the monomer and polymer rich phases.

e) The kinetic rate constant values are the same in both phases.

f) Initiator, modifier and radical concentrations in each phase can be described by partition coefficients. The radical partition coefficient value is equal to the square root of the initiator partition coefficient.

The details of the equations for the volume fractions of each phase, the mass balances for each species and the rates of reaction in each phase are given in the appendix to this chapter.

The molecular weight equations

The molecular weight equations, using the method of moments, are as outlined by Hamielec et al. (1987), and Tobita and Hamielec (1989a), with some modifications for polymerization in two phases. The leading moments for radical and polymer chain length distribution for each phase are explained in the appendix to this chapter. The pseudo kinetic rate constant method can be used with the pseudo kinetic rate constants calculated in the appropriate manner (Xie and Hamielec 1992). Since at the gel point, the weight average molecular weight goes to infinity we need to carry out the molecular weight moment analysis under two distinct domains, namely pregel and postgel regions. In the post gel region, only the molecular weight averages of the sol are calculated. After the gel point, the polymer moment equations are not closed. The i^{th} moment depends on the $(i+1)^{th}$. For this reason, we must use a closure technique in order to calculate the higher moments as a function of the lower ones. The transfer to polymer rate is a function of the higher moments. In the pregel region the transfer to polymer reaction, assuming the stationary state hypothesis for radicals, causes no net change in the number of radicals. Thus for the second moment, these terms cancel out and the moment equations are closed. However in the post gel region, this reaction causes radical centers to move between the sol and the gel phases and thus we can no longer cancel out these terms, and the moment equations are not closed. We have selected the method of Hulburt and Katz (1964) although the validity of this method should be checked by comparison with actual data (Zabisky et al 1992). If molecular weight data are available, the closure equation then should be obtained by fitting a correlation to this data in order to get more accurate results. We should note that obtaining accurate molecular weight averages (M_n, M_w M_z) is not a trivial task for branched polymers and copolymers.

$$[Q_3] = \frac{[Q_2]}{[Q_1][Q_0]}(2[Q_2][Q_0] - [Q_1]^2)$$

Balances are made on short and long chain branches, to determine the branching frequencies. Since the concentration of polymer in the monomer rich phase is negligible, reactions with dead polymer are only considered in the polymer rich phase.

The mass of gel is calculated and is assumed to reside only in the polymer rich phase. At the gel point, the mass of gel must be given some positive, non zero value, however, it is unclear just what this initial value should be. Tobita and Hamielec (1989a) defined a possible initial condition based upon conversion and crosslink density, but the condition is still somewhat arbitrary. Moreover, the gel growth equation does not appear to be very sensitive to the value chosen, therefore for simplicity, we have arbitrarily set the initial gel fraction to a small value (about 10^{-2} or 10^{-3}). The gel point is defined as the point where the weight average molecular weight becomes infinite. For practical purposes, we can not calculate infinite molecular weights, so we must arbitrarily state a maximum molecular weight that is effectively infinite. It is fortunate that at the gel point, the weight average molecular weight grows very rapidly with increasing crosslink density, so that the practical gel point is not sensitive to the maximum molecular weight value chosen. Alternatively, one could specify a large polydispersity (M_w/M_n) which would appear as a scaled maximum molecular weight.

Details of all these equations are given in the appendix to this chapter.

The energy balances

Calculation of the temperature profile along the reactor length and the initiator flow rates requires an energy balance on the reactor contents that accounts for the inflows, out flows, recycles and the reactions. The reactor is assumed to be adiabatic, the only cooling is supplied by cold monomer feed. Heat generation is from the propagation reaction only. The energy balance equation is given in the appendix to this chapter.

The temperature controller equations

The autoclave reactor temperature is controlled by manipulating the initiator feed. The controller is of a continuous proportional - integral - derivative type.

$$F_I = F_{I_{SS}} + K_p(T_{set} - T) + \frac{K_p}{\tau_I}\int_0^t (T_{set} - T)dt + K_p\tau_D\frac{d(T_{set} - T)}{dt}$$

F_I is the initiator flow rate. The subscript ss denotes steady state (or initial value) of the initiator flow. T_{set} is the set point temperature, T is the measured temperature and the parameters K_p , τ_I and τ_D are the proportional gain, integral and derivative time constants respectively. Temperature is controlled in the CSTR segments only and the initiator flow does not necessarily enter the element that is being controlled. For example the temperature at the bottom of the reactor may be controlled by manipulating an initiator flow entering at the mid point of the reactor length.

2.5.7 The solution of the mathematical model

The dynamic mathematical model derived above is comprised of a large set of ordinary differential equations, with its size dependent on the number of volume elements chosen. Recycle causes the ODE's to be coupled. A computer program entitled *DynAuto* was developed to represent the model. *DynAuto* uses the ODE solver *LSODE* (Hindmarsh, 1980, 1983) that uses either a non-stiff or stiff (Gear) method. The model was written in FORTRAN and the simulations were performed using a IBM-PS/2 model 70 (20 MHz) with math coprocessor.

2.5.8 Simulation and results

Some example simulations were performed to show the sensitivity of the mixing and model parameters and to compare with results from a commercial reactor. Simulations using a single volume element and with two elements were considered to study all the mixing parameters. The start-up and grade change simulation and the gel formation simulations used a single volume element with no plug flow segments. The reactor configuration and operating conditions chosen were (except as noted in the text for specific simulations):

a) single volume element

- reaction temperature of 258°C
- about 21% conversion
- pressure of 1440 kg/cm^2
- residence time of 37.6 seconds
- monomer feed temperature of 40°C

- using about 0.5 g/s Trigonox-B (di-tert-butyl peroxide) initiator. The initiator concentration is assumed to be equal in both the monomer rich and the polymer rich phases. The initiator decomposition rate constant was given by

$$kd = 8.843x10^{12}\exp\left(-\frac{15715.0}{T}-\frac{0.15811P}{T}\right)$$

(s^{-1}). T is temperature in degrees Kelvin, P is pressure in kg/cm^2.

b) Two volume elements. The top element comprises approximately 45% of the total reactor volume.

- reaction temperature of 258°C in the top element and 285°C in the second element
- approximately 85% of the monomer feed is to the top element.
- other conditions as above.

The kinetic parameters used for these simulations are given in table 4 The propagation, termination and beta-scission rate constants and the activation energy for the transfer to polymer rate constant are as reported by Brandolin et al. (1988). The transfer to polymer rate constant reported by Brandolin et al. (1988) gave rise to a very large degree of long chain branching, and thus was adjusted downward to give a more reasonable result for branching frequency and weight average molecular weight. The transfer to polymer rate constant was later manipulated for the sensitivity analysis with respect to gel growth. The backbiting rate constant was selected to give the short chain branching frequency reported in table 5.

Table 4. Kinetic parameters used for example simulations except as noted in the text.

Reaction	Frequency factor	Activation Energy (cal/mol)
propagation (cm^3/mol-s)	1.0×10^{9}	5245.0
termination (cm^3/mol-s) ϕ_{tc}=0.5	3.0×10^{11}	3950.0
back biting (s^{-1})	3.27×10^{5}	5245.0
β scission (s^{-1})	7.3×10^{6}	11320.0
transfer to polymer (cm^3/mol-s)	2.0×10^{8}	9500.0

Table 5. Reasonable molecular weights and branching frequencies used to determine transfer to polymer and back biting rate constants for the example simulations.

Quantity	Value	Units
Number average molecular weight	16,000.	g/mol
Weight average molecular weight	82,000.	g/mol
Short chain branching frequency	21.8	branches per 1000 carbon atoms
Long chain branching frequency	0.48	branches per 1000 carbon atoms

Sensitivity analysis of the mixing Parameters

Let us consider the sensitivity of the model predictions (steady state) to the mixing parameters, first for a single volume element, and then for two volume elements.

Single volume element

For a single volume element, there are two mixing parameters to be studied, a) the volume fraction of the CSTR component to the total volume of the element (θ_j) and b) the number of plug flow segments in the volume element (N_p). The plots below show how the number of segments affects temperatures, initiator consumption, and molecular weight averages of the polymer produced. Figure 28 shows how the addition of the segments allows the gradual increase of segment temperatures, avoiding a sudden temperature rise from one volume element to the next. The outlet temperature from the reactor is nearly equal in all cases, but a

smoother profile is generated by having more segments. Figure 29 presents the effect of the number of segments on initiator consumption, defined as the mass of initiator required to produce a certain amount of polymer. The initiator level is manipulated by the controller in order to maintain the temperature at the set point. More initiator is required as the number of segments increases, especially for θ_j = 0.7. This is in agreement with the observation that perfect mixing tends to consume less initiator than does poor mixing (van der Molen et al. 1982). Mixing becomes more segregated as the number of segments increases and as θ_j increases.

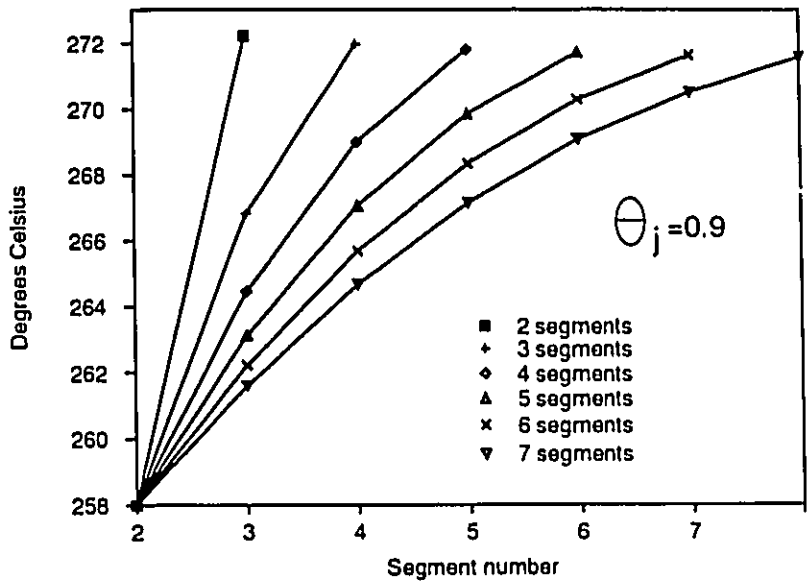

Figure 28. A study of the effect of the number of segments on reaction temperatures in a single volume element. The first segment is the CSTR segment and accounts for θ_j of the element volume.

The effects of N_p and θ_j on the number average molecular weights are shown in figure 30. The number average molecular weight is highest for a single CSTR with no plug flow segments, and decreases as θ_j increases. Increasing the number of segments increases the number average molecular weight. The molecular weight averages are determined by the competition between propagation reaction and all other transfer (including transfer to polymer) and termination reactions. The relative rates of these reactions will change with temperature. The number average molecular weight decreases with increasing temperature, because the radical generation rate is higher, producing more polymer chains. In the single CSTR case all the polymer is produced at 258°C. When we have one plug flow segment, θ_j of the reaction volume

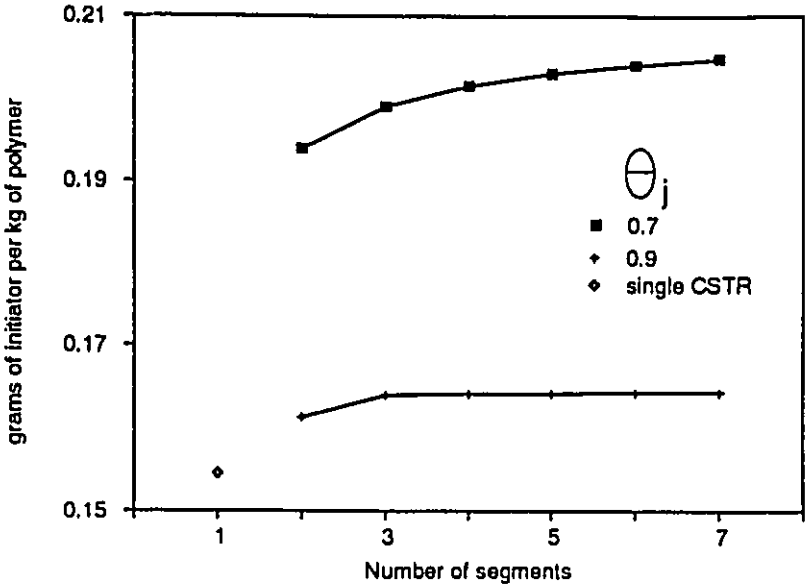

Figure 29. The effect of the number of segments on initiator consumption for a single volume element. Initiator consumption is grams of initiator consumed per kilogram of polymer produced. The single CSTR has no plug flow segments and $\theta_j=1$.

is at 258°C but the remainder of the volume is at about 272°C, thus some of the polymer produced has a lower molecular weight. As the number of segments increases we have polymer produced at several intermediate temperatures between 258 and 272°C and thus the overall molecular weight increases.

The transfer to polymer has a higher activation energy than does propagation, and thus higher temperatures promote branching., Branching causes the molecular weight distribution to be broader as quantified by the polydispersity ($\overline{M}_w/\overline{M}_n$). Figure 31 shows the polydispersity decreasing with increasing numbers of segments, and with increasing θ_j. This can be explained by the same argument as for the molecular weight averages.

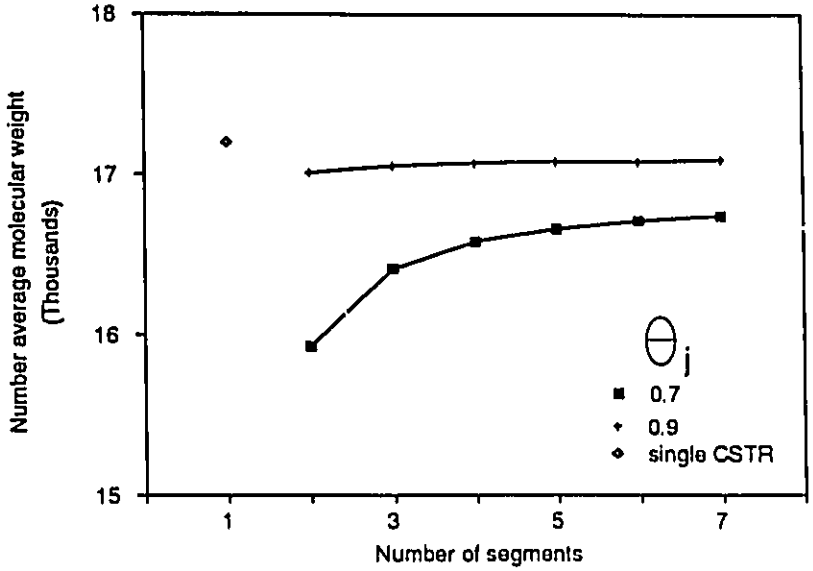

Figure 30. The effect of the number of segments on the number average molecular weight, for a single volume element.

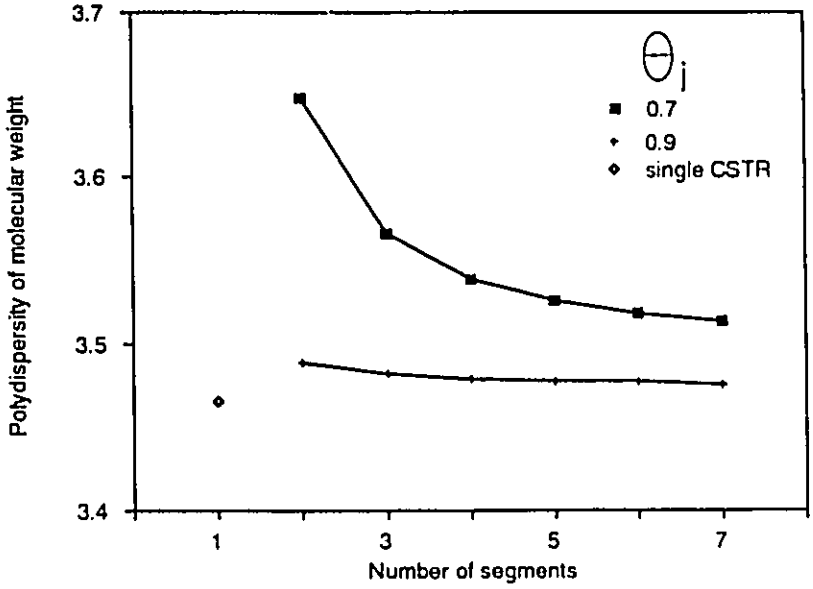

Figure 31. The effect of the number of segments on the polydispersity of the molecular weight averages, for a single volume element.

Two volume elements

For multiple volume elements, there is an additional mixing parameter, the recycle ratio, to be studied. For convenience, we use only two volume elements to analyze the effect of the recycle ratio on temperatures, initiator consumption and number and weight average molecular weights. We shall study the first element, and hold the second element temperature constant by manipulating the initiator flow to that element.

Figure 32 shows the effect of recycle ratio (q_j) on segment temperatures. As the recycle increases the temperature profiles become flatter. Increasing q_j reduces the single pass residence time and increases the mixing and in the limit the element behaves as a single CSTR as demonstrated by the nearly flat temperature profile at higher recycles. The $\theta_j = 0.7$, q_j=1 gives a nice smooth temperature rise to the second volume element.

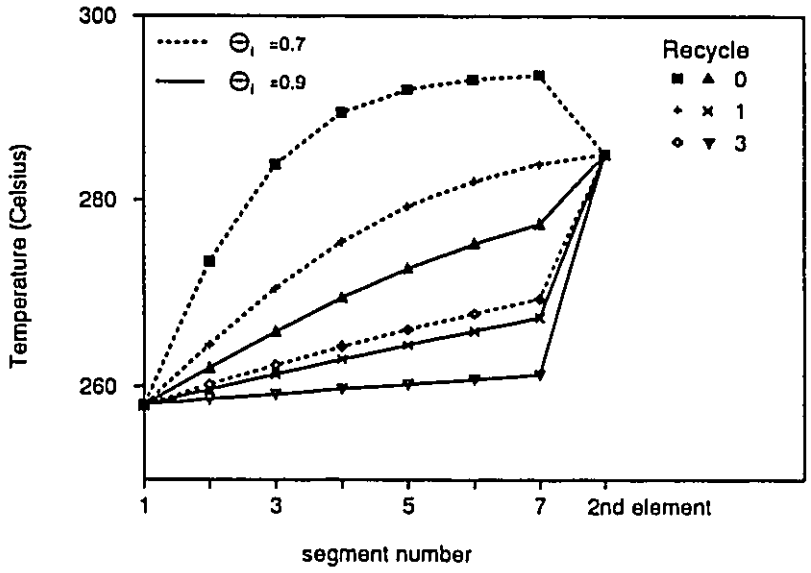

Figure 32. A study of the mixing parameters for a two volume element system showing the effect of recycle ratio, number of segments, and CSTR volume fraction on temperatures in the first element. The second element temperature is held constant at 285°C.

We have observed for the single volume element that the initiator consumption decreased with increasing mixing. Figure 33 shows that increasing the

mixing, now by increasing the recycle, has a similar effect. The number of segments has a much smaller influence on initiator consumption than does the recycle rate or θ_j and the recycle swamps out the other variables at about q_i=4 or 5.

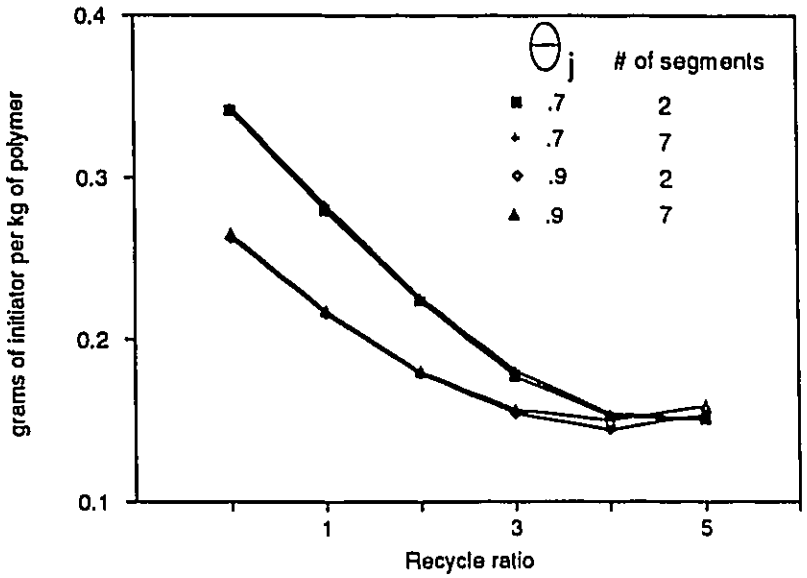

Figure 33. A study of the mixing parameters for a two volume element system showing the effects of recycle ratio, number of segments, and CSTR volume fraction on initiator consumption.

The recycle influences the temperature profile and the monomer and initiator concentrations, which in turn affect the molecular weight averages. Figure 34 shows the relationship between number average molecular weight and recycle ratio. All curves collapse onto approximately the same line at recycle ratio near three indicating that beyond this point, N_p and θ_j have negligible effects on the number average molecular weight when compared to the effect of recycle. The number average molecular weight (for the $\theta_j = 0.7$, 2 segment case) passes through a maximum with increasing recycle. This can be explained by examining the initiator concentration in each volume segment for this case. The initiator concentration decreases with increasing recycle, in the CSTR segment of the first volume element (Figure 35). Since the number average molecular weight will grow smaller with elevated initiator concentrations, increasing the recycle increases the molecular weight of the polymer produced in this segment. However, at the same time, the initiator concentration, in the second element increases causing a reduction of the

molecular weight of the polymer produced in this segment. The molecular weight of the final product is a mixture of the polymers produced in both segments, and thus M_n passes through a maximum because of the two competing effects.

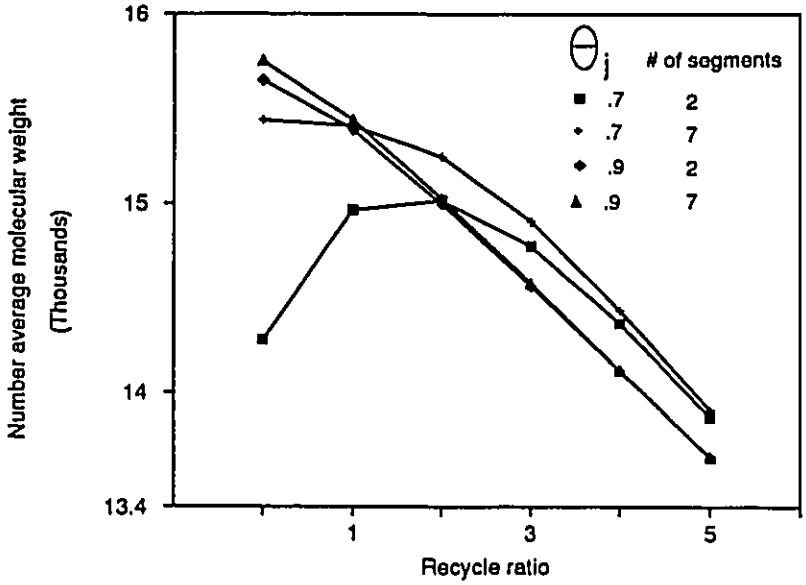

Figure 34. A study of the mixing parameters for a two volume element system showing the effects of recycle ratio, number of segments, and CSTR volume fraction on number average molecular weight of the polymer produced.

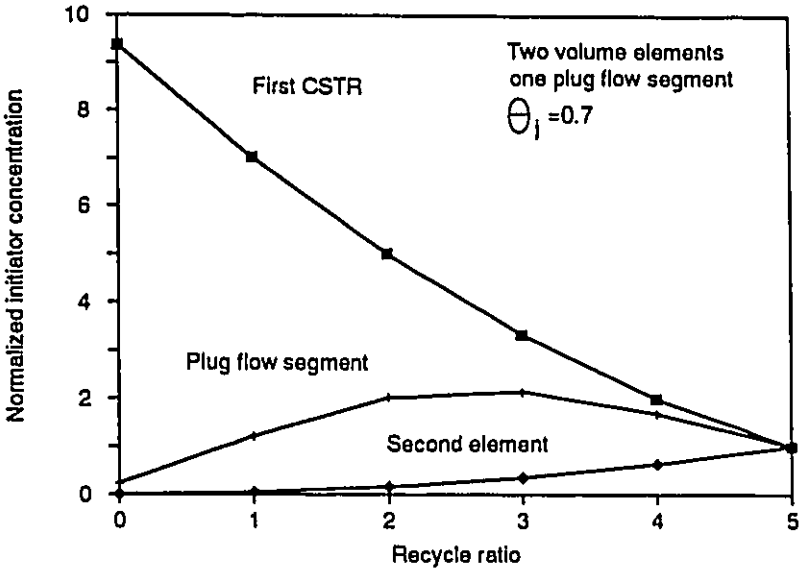

Figure 35. The effect of the recycle ratio on the initiator concentration in each segment for two volume elements. One plug flow segment in the first element, $\theta_j = 0.7$. The concentrations for each segment are normalized by division by the segment concentration at a recycle ratio of five.

Start up and grade changes

During plant operation, the procedure used to switch from one polymer grade to another is critical because it often leads to off specification material produced during the transition period. Knowledge of dynamic responses of the process variables is essential to promote appropriate control actions and grade transition policies. The dynamic response of a single volume element (1 segment) at start-up and for one grade change is shown in figure 36. The initial conditions are that the reactor is full of pure ethylene at 255°C. A grade change is implemented near 10 residence times by changing the set point temperature to 250°C. The responses are normalized by dividing each individual response by its final value so that they may be plotted on the same axes for comparison. Notice that the temperature, and conversion of monomer reach steady state quickly, as influenced by the controller. However, the molecular properties, especially the weight average molecular weight, take much longer to reach the steady state. The short chain branching frequency does not change with the change in temperature since we have specified that the activation energy for backbiting is the same as that for propagation.

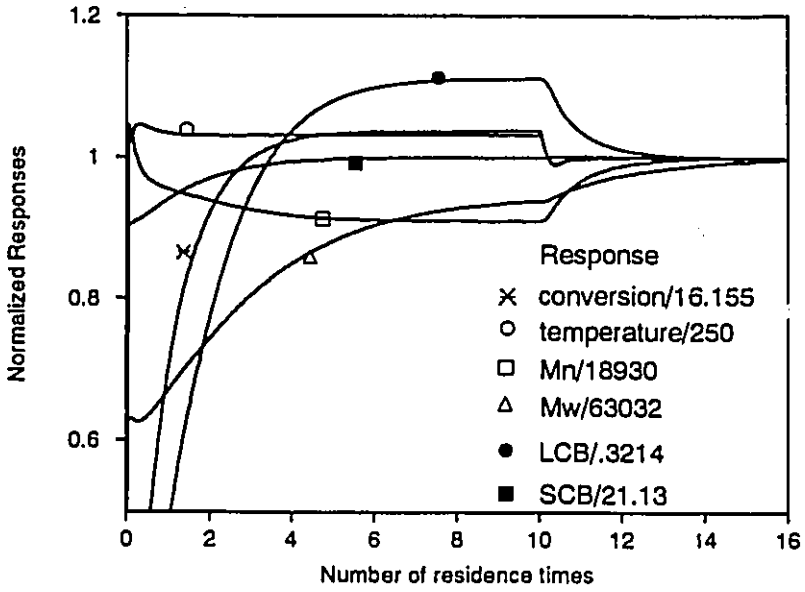

Figure 36. The dynamic response of a single CSTR during start up from pure ethylene, initially at 255 °C. The reactor set point is changed to 250°C after about 10 residence times to simulate a grade change.

Gel formation

It has been reported (Cozewith et al. 1979) that under some circumstances a steady state can not be reached in a continuous flow stirred tank reactor for crosslinking systems. However the molecular weight equations that they use describe the entire polymer population before the gel point. They observe that there are cases where the steady state cannot be reached without the higher molecular weight moments going to infinity, indicating the gel point. Our work agrees with this, however we have also included the equations to describe the sol polymer and the gel fraction after the gel point and a steady state can be reached after the gel point. All of the sol molecular weight moments remain finite. In fact the polydispersity actually decreases after the gel point, since the gel preferentially consumes the longer chains.

Two important kinetic parameters influencing the mass of gel in the reactor, are the transfer to polymer rate constant (k_{fp}) and the fraction of termination by combination, ϕ_{tc}. Figure 37 shows the influence of transfer to polymer and termination by combination rate constants on the steady state gel fraction, for the levels specified in table 6. As transfer to polymer, and the fraction of termination by combination

increase, the steady state gel fraction also increases. If termination is all by disproportionation, then no gel should be formed even in the presence of transfer to polymer reactions (Tobita and Hamielec 1989b).

Table 6. Levels of the kinetic parameters used for the gel study.

Variable	Level		
	-1	0	1
k_{tp}/k_p	1.09×10^{-2}	1.45×10^{-2}	1.82×10^{-2}
ϕ_{tc}	0.5	0.75	1.0

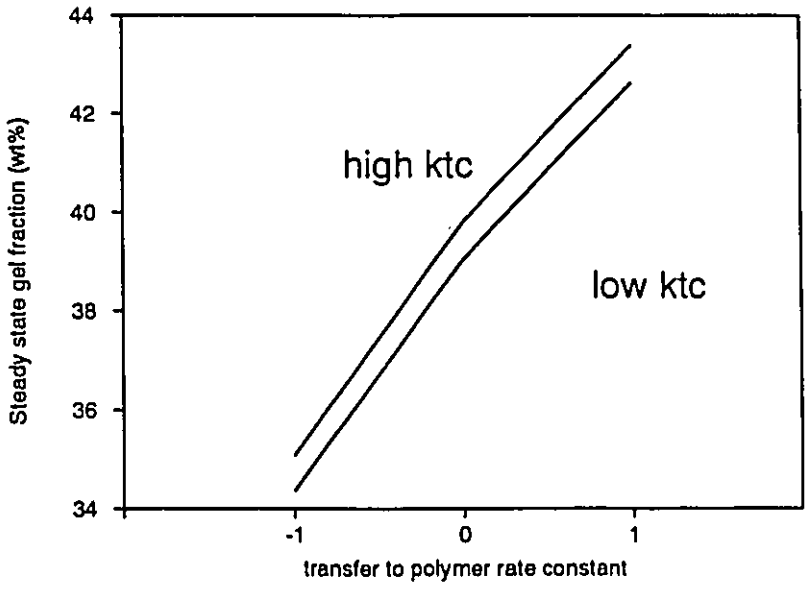

Figure 37. The gel fraction at steady state as a function of termination by combination and transfer to polymer rate. Single CSTR. Temperature fixed at 258°C.

In order to study the gel formation dynamics, a transient was induced from a steady state gel fraction value of near 50% and the response monitored for two different k_{fp} and ϕ_{ic} values. This initial gel level is quite high, but was chosen to better illustrate the behavior. The energy balance equations were not solved, but the initiator flow and the temperature were fixed to isolate the molecular weight behavior from the dynamic temperature response. The results are shown in figure 38. The gel levels may oscillate before steady state is reached and the transients are larger and longer lived if the parameters influencing the rate of gel formation (k_{fp} and ϕ_{ic}) are lower. The molecular weight averages and the gel fractions are also correlated. The rate of gel growth increases as the molecular weight averages increase, since larger molecules are added to the gel for each termination by combination reaction. However, gel preferentially consumes larger molecules, because it is more probable to encounter a radical center in a large chain than on a small one. Thus an increase in molecular weight causes gel to grow faster, then the growing gel consumes the larger chains, reducing the molecular weight averages. Finally, clumps of gel are allowed to flow out of the reactor, reducing the gel fraction, and hence providing the opportunity for the molecular weight to grow again. This cycle is presented in figure 39. The molecular weight averages, especially the number average, lead the gel fraction. Larger and longer lived oscillations were observed at lower values of k_{tp} and ϕ_{ic}. Lower values of these parameters cause lower gel growth rates, and thus the molecular weight averages are allowed to grow to much larger values. When the molecular weight averages are high, the gel growth rate becomes quite large, and a huge oscillation is started quickly driving the gel level up and the molecular weights down. At higher values of k_{tp} and ϕ_{ic} the gel growth is faster and the high molecular weight averages are avoided. The oscillation in gel fraction still needs to be verified by experiment.

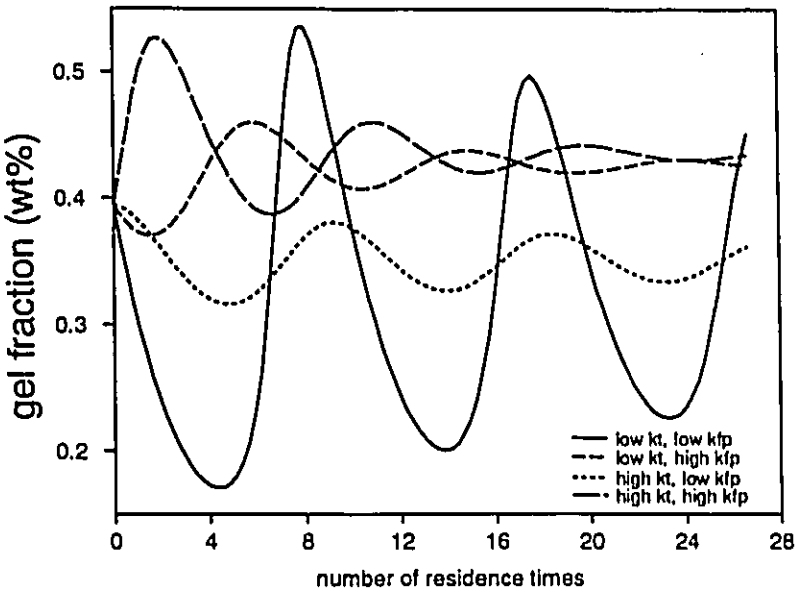

Figure 38. The effects of termination by combination and transfer to polymer rates on the transient gel levels. Single CSTR. Temperature fixed at 258°C.

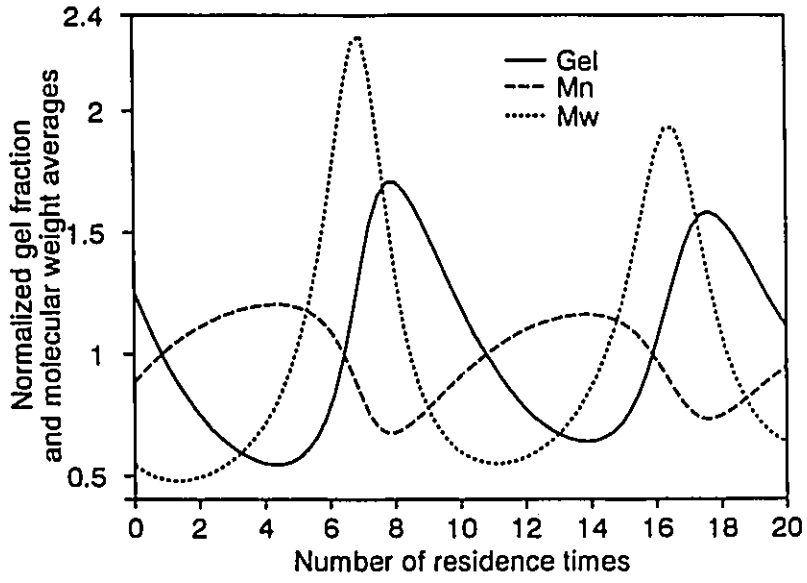

Figure 39. The dynamic relationship between the sol molecular weight averages and the gel fraction. Single CSTR. Temperature fixed at 258°C.

A second case, reactor start up, was simulated. The reactor was initially full of pure ethylene at 258 °C and then the monomer and initiator flows were started and the reaction allowed to come to steady state. In this case high values of k_{fp} and ϕ_{lc} were selected to promote gel formation. Figure 40 shows the molecular weight averages and the gel fraction behavior with time. In the pregel region the molecular weights shown apply to all the polymer but in the post gel region the molecular weight averages only describe the sol polymer. Initially there is no gel in the reactor and the molecular weight averages grow and the polydispersity increases. When the gel point is reached, (as indicated in our simulation by a polydispersity greater than about 20) the gel slowly begins to grow, and the molecular weight averages continue to increase. However, after a brief time, the gel fraction quickly grows and the molecular weight averages and the polydispersity of the sol polymer sharply decrease. The system gradually oscillates to a steady state after about 40 residence times.

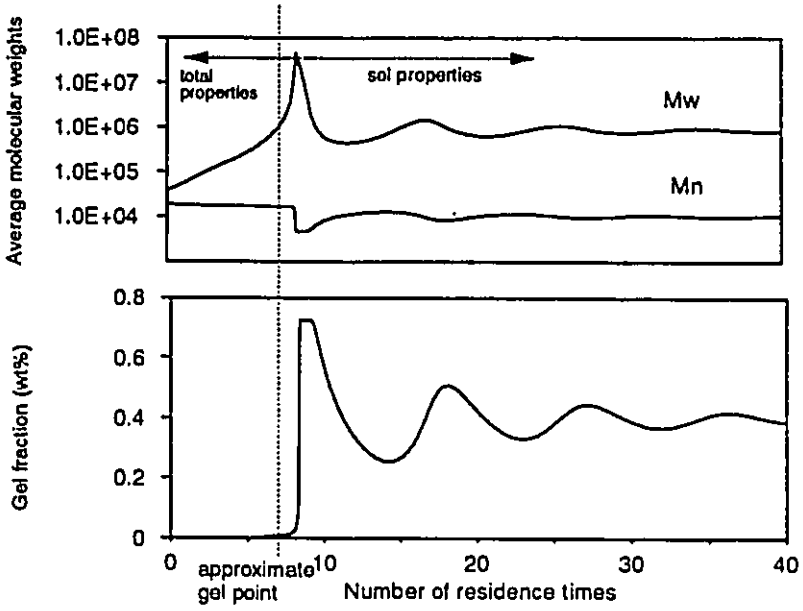

Figure 40. The dynamic behavior of the molecular weight averages and the gel fraction in both the pregel and the post gel region. Start-up from a reactor full of pure ethylene at 258°C. High values of the transfer to polymer and termination by combination rate constants were used.

We have studied the influence of the kinetic parameters k_{fp} and ϕ_{fr} by setting them to arbitrary values. It should be pointed out that these values will be influenced by temperature and pressure and thus are functions of the operating conditions. Moreover the presence and the concentration of the polymer rich phase is also a function of temperature and pressure, and must also influence gel formation. Increasing the temperature and the pressure decreases the weight fraction of polymer in the polymer rich phase and thus should also decrease the tendency to form gel polymer.

Comparisons with industrial data

Actual industrial production recipes were used for simulation to test part of the model by comparing the observed steady-state values with those predicted from the model for monomer conversion, copolymer composition, initiator flow rates and temperature profile along the reactor. Unfortunately measurements of molecular weight, branching frequencies or gel fractions were not available and thus comparisons with these quantities were not possible. Therefore this section only tests the mixing model the parts of the model related to the rate of polymerization and heat generation rates.

The set of model parameters used for the previous simulations did not completely represent the industrial data so a new set were fit to the data. However these kinetic parameters and the process information used to run the model must remain proprietary. The initiator decomposition rate constants used were as reported by the initiator suppliers. The rate constants for propagation and termination were chosen to fit all the polymerization rate data. The rate constants for transfer to modifier, β scission, and transfer to polymer were not needed to describe these observations, since we have no molecular weight data. The mixing parameters (number of elements, and recycles) were chosen to match the temperature profiles and initiator flows for specific recipes. Table 7 summarizes the results obtained for both ethylene homopolymer and ethylene-vinyl acetate copolymer.

The results obtained from the model are quite good in comparison with the actual plant data. The largest relative error of the predicted values was less than thirteen percent for initiator flow rate, and all model responses are within the measurement error of the data collected.

Table 7. Comparison between industrial plant data and the model predictions.

Response	Resin 1 (Homopolymer)			Resin 2 (Copolymer)		
	Predict	Observe	Error (%)	Predict	Observe	Error (%)
Normalized Temperature						
Level 9 (top)	0.9908	0.9923	-0.15	0.726	0.726	0
Level 8	0.9908	0.9923	-0.15	0.726	0.726	0
Level 7	0.9935	0.9923	0.12	0.726	0.726	0
Level 6	0.9935	0.9923	0.12	0.726	0.726	0
Level 5	1	0.9923	0.78	0.836	0.827	1.09
Level 4	1	1	0	0.937	0.907	3.31
Level 3	1	1	0	0.977	0.968	0.93
Level 2	1	1	0	0.996	0.992	0.40
Level 1 (bottom)	1	1	0	0.996	1	-0.40
Total Initiator flow rate (g/s)	0.54	0.55	-1.82	3.20	2.84	12.68
Total Conversion	0.178	0.169	5.33	0.164	0.153	7.19
Comonomer Composition (wt% monomer 2)	-	-	-	4.0	4.2	-4.76

2.5.9 Conclusions for autoclave model

We have endeavored to construct a comprehensive model to describe the high pressure homo and copolymerization of ethylene in autoclave type reactors. This model accounts for the important chemical reactions, the mixing pattern in the vessel, and the two-phase kinetics. It also incorporates the mass and energy balances on the vessel, as well as the temperature controller equations. The model predicts polymer properties such as composition, molecular weight, branching frequencies and gel content.

The model was fit to both homopolymer and copolymer recipes for initiator flow rates and temperature profiles. The fit was quite adequate for steady state conditions. No dynamic data are currently available to test the transient behavior. More data are needed to verify the model predictions for the molecular properties.

To our knowledge, no one has previously presented predictions of gel content for this flow system. The gel content shows oscillations in the transients, but steady state values may be reached which are insensitive to the initial conditions.

2.6 References

Agrawal, S. C., Han, C. D., *AIChE J.*(1975), **21**, No. 3, 449-465.

Agrawal, S. C., Ph.D. Thesis, Polytechnic Institute of New York, Brooklyn. (1974)

Beasley, J. K., "Polymerization at High Pressure", p. 273-282. vol. 3 Comprehensive Polymer Science, Allen G., Bevington, J. C. Eds., Pergamon Press, Oxford. (1989)

Bird, R. B., Stewart, W. E., Lightfoot, E. N., "Transport Phenomena", John Wiley & Sons, New York (1960) p. 186.

Bogdanovic, V., Srdanovic, J., "Differences Between Low Density Polyethylenes Synthesised at Homogeneous and Heterogeneous Reacting Conditions", *J. Appl. Polym. Sci.*, **31**, 1143-1145 (1986)

Box, G. E. P., Hunter, W. G., Hunter, J. S. "Statistics for Experimenters" Wiley, New York, (1978) p. 323

Brandolin, A., Capiati, N. J., Farber, J. N., Vales, E. M. "Mathematical Model for High-Pressure Tubular Reactor for Ethylene Polymerization" *Ind. Eng. Chem. Res.* **27** 784-790 (1988)

Buback, M., *Makromol. Chem.*,(1980), **181**, 373-382.

Budtov, V. P., Polyakov, Z. N., Gutin, B. L., Belayayev, V. M., and Ponomereva, Ye. L. *Polymer Science USSR*, (1982) **24**, no. 6. 1367-1374

Carr, N. L., Parent, J. D., Peck, R. E, *Chem. Eng. Progr. Symposium Ser.* (1955), **51**, No. 6, 91.

Chen, C. H, Vermeychuk, J. G., Howell, J. A., Ehrlich, P., *AIChE J.*, (1976), **22**, No. 3, 463.

Cogswell, F. N, "Polymer Melt Rheology", John Wiley & Sons. New York, (1981), p. 153

Cozewith, C., Graessley, W. W., Ver Strate, G., "Polymer Crosslinking in Continuous Flow Stirred Reactors", *Chem. Eng. Sci.* **34** 245-248 (1979)

Donati, G., Gramondo, M., Langianni, E., Marini, L., "Low Density Polyethylene in Vessel Reactors" *Ing. Chim. Ital.*, **17**, 88-96 (1981)

Donati, G., Marini, L., Marziano, G., Mazzateri, C., Sampitano, M., Langianni, E., *Proc. 7th Int. Symp. Chem. React. Eng.* (1982), Boston, p. 579.

Ehrlich, P., Mortimer, G. A., *Adv. Polymer. Sci.*,(1970) **1**, 386

Ehrlich, P., Pittilo. R. N. J. *Polym. Sci. Vol.*(1960), **43**, 389-412.

Elermann, K. *Modellmassige Deutung der Warmeleitfahigkeit Von Hochpolymeren, K., Koll. Z.*, (1965), **201**, 3.

Fawcett, E. W., Gibson, R. O., Perrin, M. W., Paton, J. G., Williams, E.G., *Brit. 471590* (1937) ICI invs.; *Chem. Abstr.* **32**, 13626 (1938)

Feucht, P., Tilger, B., Luft, G., *Chem. Eng. Sci.* (1985) **40** no. 10, 1935-1942

Foster, G. N., MacRury, T. B., Hamielec, A. E., "Characterization of Polymers with Long Chain Branching - Development of the Molecular Weight and Branching Distribution (MWBD) Method", in Liquid Chromatography of Polymers and Related materials II. Cazes, J., and Delamare, X. (Eds.), Marcel Dekker. (1980)

Georgakis, C., Marini, L., "The Effect of Mixing on Steady-State and Stability Characteristics of Low Density Polyethylene Vessel Reactors" *ACS Symp. Ser.*, **196**, Chemical Reaction Engineering, Boston, 591-602, (1982)

Gierth, V. V, *Die Angewandte Makromol. Chemie.* (1970), **12**, 9-23.

Goto, S., Yamamoto, K., Furui, S., Sugimoto, M., *J. Appl. Polym. Sci.*, (1981), **36**, 21.

Gupta, S. K., *Current Science*, (1987), **56**, No. 19.

Gupta, S. K., Kumar, A., Krishnamurthy, M. V. G.,*Poly. Sci. Eng.* (1985), **25**, No. 1.

Hamielec, A. E., Gloor, P. E., Zhu, S., Tang, Y, *COMPALLOY '90*, Proceedings of 2nd International Congress on Compatibilizers, and Reactive Polymer Alloying, Schotland, New Orleans, March 7-9 (1990).

Hamielec, A. E., MacGregor, J, F., Penlidis, A., "Multicomponent Free-Radical Polymerization in Batch, Semi-Batch and Continuous Reactors", *Makromol. Chem. Macromol. Symp.*, **10/11**, 521-570 (1987)

Hamielec, A. E., MacGregor, J. F., Polymer Reaction Engineering, Eds., K. H. Reichert, W. Geiseler, Hanser Publishers, pp. 21, New York. (1983),

Han, C. D., Liu, T-J., *Kwahak Konghak*, (1977), **15**, No. 4, 249-257.

Hindmarsh, A. C., "LSODE and LSODI, Two New Initial Value Ordinary Differential Equation Solvers", *ACM-Signum Newsletter*, (1980), **15**, No. 4, 10-11.

Hindmarsh, A. C., "ODEPAC, A Systematized Collection of ODE Solvers", Scientific Computing, S. Stepleman et al. (eds.), North-Holland, Amsterdam, (1983) (Volume 1 of IMACS Transactions on Scientific Computation) pp. 55-64

Hollar, W., Ehrlich P., *Chem. Eng. Comm.*, (1983), **24**, 57.

Hulburt, H. M., Katz, S., "Some Problems in Particle Technology, A Statistical Mechanical Formulation", *Chem. Eng. Sci.*, **19**, 555-574, (1964)

Jackson, R.A., Small, P. A., Whiteley, K. S., *J. Polym. Sci., Polymer Chem. Ed.* (1973), **11**, 1781-1809.

Kalyon, D. M., Chiou, Y. N., Kovenklioglu, S., Bouaffar, A., *Polym. Eng. Sci.*, in press (1992)

Katz, S, Saidel, G. M., *AIChE Journal*, (1967), **13**, No. 2 319-326

Kiparissides, C., Mavridis, H., "Mathematical Modelling and Sensitivity Analysis of High Pressure Polyethylene Reactors" in Chemical Reactor Design and Technology, H. de Lasa (ed.) NATO ASI Series E: Applied Sciences, No. 110. (1985)

Laurence, R. L., Pottiger, M. T., (1985) Private communication with Tjahjadi, et al.

Lee, K. H., Marano, J. P. Jr. *ACS Symposium Series*, (1979) **104**, 221-251

Marano, J. P., " Process Technology - Polyethylene" in Polymer Reaction Engineering -- An Intensive Short Course on Polymer Production Technology, School of Chemical Technology, University of New South Wales, Sydney, Australia. (1979) Section 3 p. 7

Marini, L., Georgakis, C., "Low Density Polyethylene Vessel Reactors" *AIChE J.*, 30, 401-415 (1984)

Mavridis, H., Kiparissides, C. *Pol. Proc. Eng.* (1985) **3** 263-290

Mullikin, R. V., Mortimer, G. A., *J. Macromol. Sci. -Chem.*, (1972), **A6 (7)**, 1301-1310

Mullikin, R. V., Mortimer, G. A., *J. Macromol. Sci. -Chem.* (1970), **A4 (7)**, 1495-1505.

Nicolas, L., *J. Chim. Phys.* (1958) **55** 177-196

PFLASH documentation, "Continuous Thermodynamics and Phase Equilibria in Polymeric Systems" Poliolefinas software. (1988)

Posteinicescu, P., Dumitrescu, A.M.,*Materiale Plastice*, (1987), **24**, No. 2.

Saidel, G. M, Katz, S., *J. Polym. Sci., Part A-2*, (1968), **6**, 1149-1160.

Sako, T., Wu, A., Prausnitz, J. M., "A Cubic Equation of State for High Pressure Phase Equilibria of Mixtures Containing Polymers and Volatile Fluids" *J. Appl. Polym. Sci.* **38**, 1839-1858 (1989)

Shirodkar, P. P., Tsien, G. O., *Chem. Eng. Sci.*, (1986), **41**, No. 4, 1031-1038.

Small, P. A., *Polymer*, (1973), **14**, 524-525.

Small, P. A., *Polymer*, (1972), **13**, 536-540.

Smith, J. M., Van Ness, H. C., "Introduction to Chemical Engineering Thermodynamics", third ed. McGraw-Hill, New York (1975), p. 462.

Symcox, R. O., Ehrlich, P., *J. Am. Chem. Soc.* (1962) **84** 531

Szabo, J., Luft, G., Steiner, R., *Chemie-Ing. - Techn.*, (1969) **41**, 1007

Takahashi, T., Ehrlich, P. *Macromolecules* (1982) **15** 714-719

Tatsukami, Y., Takahashi, T., Yoshioka, H., *Makromol. Chem.*, (1980), **181**, 1108-1115.

Thies, J. W., Doctoral Thesis, Technical University at Darmstadt, Germany (1971).

Tjahjadi, M., Gupta, S. K., Morbidelli, M., Varma, A., *Chem. Eng. Sci.*, (1987), **42**, 2385-2394.

Tobita, H., Hamielec, A. E., "Crosslinking Kinetics in Free Radical Copolymerization" *Polymer Reaction Engineering*, 3rd International Workshop on Polymer Reaction Engineering, VCH Publishers, N. Y. pp. 43-83 (1989b)

Tobita, H., Hamielec, A. E., "Modelling of Network Formation in Free Radical Polymerization, *Macromolecules*, **22**, 3098-3105 (1989a)

Tobita, H., Hamielec, A. E., *Makromol. Chem., Macromol. Symp.* (1988), **20/21**, 501-543

Tzoganakis, C., Vlachopoulos, J., Hamielec, A. E., *Intern. Polymer Processing* (1988), **III** 141-150.

van der Molen, T., Keonen, A., Oosterwijk, H., van der Bend, H., "Light-Off Temperature and Consumption of 16 Initiators in LDPE Production" *Ing. Chim. Ital.* **18** 7-15, (1982)

Verros, G., Papadakis, M., Kiparissides, C. "Mathematical modeling of high pressure tubular LDPE copolymerization reactors", *Polym. Reac. Eng.* in press (1992)

Xie, T. Y., Hamielec, A. E. "Modelling free radical copolymerization kinetics- evaluation of the pseudo kinetic rate constant method Part II: molecular weight calculations for copolymers with long chain branching" *Makromol. Chem. Theory Simulations*, accepted (1992)

Yamamoto, K., Sugimoto, M., *J. Macromol. Sci-Chem.*, (1979), **A13 (8)**, 1067-1080.

Yoon, B., J., Rhee, H. - K., *Chem. Eng. Commun.*, (1985), **24**, 253-265.

Zabisky, R. C. M., Chan, W. M., Gloor, P. E., Hamielec, A. E., A Kinetic Model for Olefin Polymerization in High - Pressure Tubular Reactors: A Review and Update" *Polymer* **33**, 2243-2262 (1992)

2.7 Appendix for free radical polymerization

2.7.1 Appendix for tubular reactor model

Details of the kinetic model development

The model includes mass, momentum and energy balances for a tubular reactor. We assume that the tubular reactor and the cooling jackets experience plug flow, i.e., there are no radial temperature or concentration gradients in the tube or jackets, and no axial mixing. We also assume that the reaction mixture is homogeneous.

The model is written using axial distance, L, as the independent variable. The equations are solved in this form by integrating along the reactor length. We will consider mass balances on each species in the reactor, heat transfer from the reaction mixture to the cooling jacket and molecular weights development is addressed last.

Mass balances on species

In order to find the rate of polymerization we must perform a mass balance on initiator species i,

$$\frac{dI_i}{dL} = -Ac \cdot kd_i[I_i]$$

$$(moles/cm)$$

$$Ac = \pi \cdot r^2$$

$[I_i]$ is the moles of initiator i divided by the volumetric flow rate. The rate of radical formation from initiator will be

$$RI_{initiator} = \sum_i (n_i \cdot f_i \cdot kd_i[I_i])$$

where n_i is the number of radicals produced by one initiator molecule decomposing (usually two), and f_i is the initiator efficiency.

The rate of radical production by thermal initiation of the monomer is

$$RI_{thermal} = k_{th} \cdot [M]^3$$

For polyethylene production, the thermal initiation of the monomer may not be important, since initiation rates by peroxides are usually much larger. However, it is included in order to provide analysis on runaway synthesis conditions in the reactor. The form of the rate expression for thermal initiation is from Buback[6] who studied the thermal polymerization of pure ethylene. He found that the activation energy for this reaction was quite large, about 53 kcal/mol, and therefore this reaction may not become significant (if at all) until high temperatures. The contribution of the comonomer to thermal initiation is not known.

Oxygen can both initiate and inhibit free radical polymerization. Thus, the mass balances for O_2 and RO_2 are:

$$\frac{dO_2}{dL} = -Ac\left(kd_{O_2}[O_2][M] + kr[O_2][Y_0]\right)$$

$(moles/cm)$

$$\frac{dRO_2}{dL} = Ac(kr[O_2][Y_0] - kd_p[RO_2])$$

$(moles/cm)$

and the net rate of initiation by oxygen and decomposing peroxides formed from oxygen will be

$$RI_{oxygen} = 2kd_{O_2}[O_2][M] + 2kd_p[RO_2]$$

where [M] is the total monomer concentration and $[RO_2]$ is the concentration of peroxides that form from the inhibition reaction by oxygen. $[Y_0]$ is the total radical concentration or equivalently the zeroth moment of the polymer radical distribution. The total rate of initiation will be given by

$$RI = RI_{initiator} + RI_{thermal} + RI_{oxygen}$$

The rate of monomer consumption, for each monomer type (assuming long chain approximation), is given by

$$\frac{dM_i}{dL} = -Ac(kp_{ii}\phi_i[Y_0][M_i] + kp_{ji}\phi_j[Y_0][M_i])$$

$(moles/cm)$

The moles of monomer 1 and 2 bound as polymer can be calculated using

$$\frac{d\Psi_i}{dL} = Ac \cdot (kp_{ii} \cdot \phi_i \cdot [Y_0][M_i] + kp_{ji} \cdot \phi_j \cdot [Y_0][M_i] - kdcp_i \cdot [\Psi_i])$$

$(moles/cm)$

We also need a balance on the moles of chain transfer agent (modifier or solvent) in the reactor

$$\frac{dTSH}{dL} = -Ac \cdot kfts[TSH][Y_0]$$

Energy balance equations

The energy balance on the reactor contents, considering heat flow from the jacket to the reactor results in:

$$\frac{dT}{dL} = \left(\frac{\overline{\Delta H}}{W \cdot Cp}\right) \cdot \left(\frac{d\Psi_1}{dL} + \frac{d\Psi_2}{dL}\right) + \left(\frac{U \cdot 2 \cdot \pi \cdot r}{W \cdot Cp}\right)(T_j - T)$$

where

C_p heat capacity of reaction mixture;

$\overline{\Delta H}$ average heat of polymerization (energy released/mole monomer reacted), defined, for convenience, as a positive number;

r internal radius of reactor;

T reactor temperature at length L;

T_j jacket temperature at length L;

L length along the reactor;

U overall heat transfer coefficient;

W mass flow of reaction mixture along the reactor.

The overall heat transfer coefficient, U , can be calculated by

$$\frac{1}{U} = \frac{1}{h_i} + \frac{1}{h_w}$$

where

h_i heat transfer coefficient for film between reactor contents and reactor wall;

h_w heat transfer coefficient from the jacket contents and through the jacket wall. This quantity must either be measured or estimated from the heat transfer data, for each heating / cooling zone.

The first term is the resistance to heat transfer from the film inside the reactor, the second term is the resistance to heat transfer from the water/steam mixture to the film inside the reactor.

We can use the approach taken by Chen et al. (1976) where the heat transfer coefficient for the wall is set to a constant for each heating/cooling zone. The thermal conductivity of polyethylene reaction mixture (cal/[cm.s.K]) is given by Eiermann (1965)

$$K = \frac{5.0 \times 10^{-4} W_m + 3.5 \times 10^{-4} W_p}{(W_m + W_p)}$$

where W_m and W_p are masses of monomer and polymer (grams).

The viscosity of the monomer (poise) in the reactor is given by Carr, et al., (1955)

$$\eta_o = 1.98 \times 10^{-4} + \frac{1.15 \times 10^2}{T^2} \qquad (T \text{ in } ^\circ C)$$

and the relative viscosity

$$\log_{10}(\eta_r) = 0.0313 \frac{(Q_1)^{2/3}}{(Q_0)^{1/2}}$$

$$= 0.0313 (r_n)^{1/2} (Q_1)^{1/6}$$

where $$\eta_r = \frac{\text{solution viscosity}}{\text{solvent viscosity}}$$

and Q_0 and Q_1 are the zeroth and the first moments of the polymer chain length distribution, W(r).

The solution viscosity (assuming that monomer is the solvent) is calculated by

$$\eta_s = \eta_r \cdot \eta_o$$

The Reynolds number is

$$R_e = \frac{2 \cdot W}{\pi \cdot r \cdot \eta_s}$$

The Prandtl number is given by

$$P_r = \frac{Cp \cdot \eta_s}{K}$$

The Nusselt number is given by

$$N_u = 0.026 \cdot R_e^{0.8} \cdot P_r^{0.33} \qquad (R_e > 10,000)$$

$$N_u = 0.166(R_e^{2/3} - 125) \cdot P_r^{0.33} \cdot \left[1 + \left(\frac{2 \cdot r}{L}\right)^{2/3}\right]$$

$(R_e < 10,000)$

The inside heat transfer coefficient is given by

$$h_i = \frac{K \cdot N_u}{2 \cdot r}$$

The heat capacity of the reaction mixture is assumed to be the sum of the heat capacities of the pure components and we are neglecting heats of mixing and solution.

Moments of the molecular weight distribution

The moments of the molecular weight distribution are found by writing balances on the radical and polymer molecules of chain length r, multiplying each term by the appropriate power of r, and summing them from r=1 to ∞.

The moments of the polymer radical size distribution are defined by

$$Y_i = \sum_{r=1}^{\infty} r^i R(r)$$

and the moments of the polymer size distribution are defined by

$$Q_i = \sum_{r=2}^{\infty} r^i P(r)$$

The radical centers can either be at the chain end, or on the backbone of the chain (internal radicals). We assume that all internal radicals promptly undergo either propagation (forming branches) or β-scission. We therefore neglect tetrafunctional branching and the possibility of crosslinking due to termination by combination of internal radicals.

To find the polymeric radical moments we must write a balance on radicals of unit length.

$$\frac{1}{Ac}\frac{dR(1)}{dL} = RI - kr[R(1)][O_2]$$
$$- kp[R(1)][M]$$
$$- (ktc + ktd)[Y_0][R(1)]$$
$$+ (\tau + k_h)([Y_0] - [R(1)])$$
$$- K_{LCH}[R(1)][Q_1]$$
$$- K_h[R(1)][Q_1]$$

where

$$\tau = kfm[M] + kfts[TSH]$$

And then for length r ($r \geq 2$),

$$\frac{1}{Ac}\frac{dR(r)}{dL} = kp[M][R(r-1)] - kp[M][R(r)]$$
$$- (ktc + ktd)[R(r)][Y_0] - (\tau + k_h)[R(r)]$$
$$- K_{LCH}[R(r)][Q_1] + K_{LCH}[Y_0]r[P(r)]$$
$$- K_h[R(r)][Q_1] + K_h[Y_0]\sum_{s=r+1}^{\infty}[P(s)]$$
$$- kr[R(r)][O_2]$$

The radical moment equations are represented by:

$$\frac{dY_i}{dL} = \frac{dR(1)}{dL} + \sum_{r=2}^{\infty} r^i \frac{dR(r)}{dL}$$

After substitution of radical balances in the expression above, and noting that

$$Q_i \gg Q_{i-1} \gg Q_{i-2} \cdots$$
$$Y_i \gg Y_{i-1} \gg Y_{i-2} \cdots$$
$$Q_i \gg Y_i$$

we obtain:

$$\frac{1}{Ac}\frac{dY_0}{dL} = RI - kr[Y_0][O_2] - (ktc + ktd)[Y_0]^2$$

$$\frac{1}{Ac}\frac{dY_1}{dL} = RI - kr[Y_1][O_2] - (ktc + ktd)[Y_1][Y_0]$$
$$+ kp[M][Y_0] - (\tau + k_\beta)[Y_1]$$
$$+ K_{LCH}([Y_0][Q_2] - [Y_1][Q_1])$$
$$+ \frac{1}{2}K_\beta[Y_0][Q_2] - K_\beta[Q_1][Y_1]$$

$$\frac{1}{Ac}\frac{dY_2}{dL} = RI - kr[Y_2][O_2] - (ktc + ktd)[Y_2][Y_0]$$
$$+ 2kp[M][Y_1] - (\tau + k_\beta)[Y_2]$$
$$+ K_{LCH}([Y_0][Q_3] - [Y_2][Q_1])$$
$$+ \frac{1}{3}K_\beta[Y_0][Q_3] - K_\beta[Q_1][Y_2]$$

$$\frac{1}{Ac}\frac{dY_3}{dL} = RI - kr[Y_3][O_2] - (ktc + ktd)[Y_3][Y_0]$$
$$+ 3kp[M][Y_2] - (\tau + k_\beta)[Y_3]$$
$$+ K_{LCH}([Y_0][Q_4] - [Y_3][Q_1])$$
$$+ \frac{1}{4}K_\beta[Y_0][Q_4] - K_\beta[Q_1][Y_3]$$

The stationary state hypothesis (SSH) for the radical moments is used to give algebraic equations from ordinary differential equations.

$$[Y_0] = \frac{\sqrt{(kr[O_2])^2 + 4(ktc + ktd)RI} - kr[O_2]}{2(ktc + ktd)}$$

$$[Y_1] = \frac{RI + kp[M][Y_0] + K_{LCH}[Y_0][Q_2] + \frac{1}{2}K_\beta[Y_0][Q_2]}{kr[O_2] + (ktc + ktd)[Y_0] + (\tau + k_\beta) + K_{LCH}[Q_1] + K_\beta[Q_1]}$$

$$[Y_2] = \frac{RI + 2 \cdot kp[M][Y_1] + K_{LCB}[Y_0][Q_3] + \frac{1}{3}K_\beta[Y_0][Q_3]}{kr[O_2] + (ktc + ktd)[Y_0] + (\tau + k_\beta) + K_{LCB}[Q_1] + K_\beta[Q_1]}$$

$$[Y_3] = \frac{RI + 3kp[M][Y_2] + K_{LCB}[Y_0][Q_4] + \frac{1}{4}K_\beta[Y_0][Q_4]}{kr[O_2] + (ktc + ktd)[Y_0] + (\tau + k_\beta) + K_{LCB}[Q_1] + K_\beta[Q_1]}$$

The dead polymer moments can be found by performing a balance on polymer chains of length r

$$\begin{aligned}\frac{1}{Ac}\frac{dP(r)}{dL} = & ktd[R(r)][Y_0] \\ & + \frac{1}{2}ktc\sum_{s=1}^{r-1}[R(r-s)][R(s)] \\ & + kr[O_2][R(r)] \\ & + K_{LCB}[R(r)][Q_1] \\ & - K_{LCB}[Y_0]r[P(r)] \\ & + (\tau + k_\beta)[R(r)] - K_\beta[Y_0]r[P(r)] \\ & + K_\beta[Y_0]\sum_{s=r+1}^{\infty}[P(s)] \\ & + K_\beta[Q_1][R(r)]\end{aligned}$$

Multiplying this equation by the appropriate power of r and then summing, we get the following moments of the polymer size distribution:

$$\begin{aligned}\frac{1}{Ac}\frac{dQ_0}{dL} = & ktd[Y_0]^2 + \frac{1}{2}ktc[Y_0]^2 \\ & + kr[O_2][Y_0] + (\tau + k_\beta)[Y_0] + K_\beta[Y_0][Q_1]\end{aligned}$$

$$\frac{1}{Ac}\frac{dQ_1}{dL} = ktd[Y_0][Y_1] + ktc[Y_1][Y_0] + kr[Q_2][Y_1] + (\tau + k_\beta)[Y_1] + K_{LCB}([Q_1][Y_1] - [Y_0][Q_2]) + K_\mu[Q_1][Y_1] - \frac{1}{2}K_\mu[Y_0][Q_2]$$

using long chain approximation

$$\cong kp[M][Y_0]$$

$$\frac{1}{Ac}\frac{dQ_2}{dL} = ktd[Y_0][Y_2] + ktc([Y_0][Y_2] + [Y_1]^2) + kr[Q_2][Y_2] + (\tau + k_\beta)[Y_2] + K_{LCB}([Q_1][Y_2] - [Y_0][Q_3]) + K_\mu[Q_1][Y_2] - \frac{2}{3}K_\mu[Y_0][Q_3]$$

$$\frac{1}{Ac}\frac{dQ_3}{dL} = ktd[Y_0][Y_3] + ktc([Y_0][Y_3] + 3[Y_1][Y_2]) + kr[Q_2][Y_3] + (\tau + k_\beta)[Y_3] + K_{LCB}([Q_1][Y_3] - [Y_0][Q_4]) + K_\mu[Q_1][Y_3] - \frac{3}{4}K_\mu[Y_0][Q_4]$$

The number and weight average chain lengths are given by:

Number average

$$\overline{r_n} = \frac{Q_1 + Y_1}{Q_0 + Y_0} \cong \frac{Q_1}{Q_0}$$

$$\overline{r_w} = \frac{Q_2 + Y_2}{Q_1 + Y_1} \cong \frac{Q_2}{Q_1}$$

$$\frac{}{r_2} = \frac{Q_3 + Y_3}{Q_2 + Y_2} \approx \frac{Q_3}{Q_2}$$

Since $Q_i \gg Y_i$.

Notice that if we include the scission of internal radical centers, the equations are not closed and a closure method must be used for their solution.

Overall reaction rate constants involving internal radicals

We have written the internal radical β-scission, long and short chain branching rates as overall reactions, even though they are two step reactions. The first step being some sort of transfer to polymer (either by a radical attacking a polymer chain, or by backbiting), and the second step being either scission or propagation which forms branches. The internal radicals can also be consumed by transfer to monomer or to chain transfer agent and, although much less likely, by termination. Internal radicals are shielded by the coiled chain, and surrounded by monomer. For termination to occur, a growing macroradical must penetrate the coiled chain and approach the radical center before the radical center has a chance to propagate. With the large amount of monomer present the concentration of backbone radicals is likely to be too small for significant backbone radical - radical termination. It should be noted that this reaction is very important during polymer degradation in an extruder, where there is no monomer present and significant crosslinking can occur.

Let's consider two types of internal radicals, one formed by transfer to polymer, and one formed by backbiting. The former leads to a long chain branch and the latter to a short chain branch. A balance on these two types of internal radicals of chain length r gives:

long chain branch radicals

$$\frac{1}{Ac}\frac{dR'_L(r)}{dL} = kfp \cdot r \cdot [P(r)][Y_0] - (kp[M] + k'_\beta + \tau)[R'_L(r)]$$

short chain branch radicals

$$\frac{1}{Ac}\frac{dR'_s(r)}{dL} = kb[R(r)] - (kp[M] + k'_\beta + \tau)[R'_s(r)]$$

Making the stationary state hypothesis for these internal radicals, expressions for the concentrations of these internal radicals follow:

$$[R'_L(r)] = \left(\frac{kfp}{kp[M] + k'_\beta + \tau}\right) \cdot r \cdot [P(r)][Y_0]$$

$$[R'_s(r)] = \left(\frac{kb}{kp[M] + k'_\beta + \tau}\right)[R^*(r)]$$

and the total concentrations

$$[R'_L] = \left(\frac{kfp}{kp[M] + k'_\beta + \tau}\right)[Q_1][Y_0]$$

$$[R'_s] = \left(\frac{kb}{kp[M] + k'_\beta + \tau}\right)[Y_0]$$

Considering the generation of long chain branches, we realize that

$$\frac{1}{Ac}\frac{dLCB}{dL} = kp[M][R'_L]$$

$$= kp[M]\left(\frac{kfp}{kp[M] + k'_\beta + \tau}\right)[Q_1][Y_0]$$

$$= K_{LCB}[Q_1][Y_0]$$

and for short chain branches

$$\frac{1}{Ac}\frac{dSCB}{dL} = kp[M][R'_s]$$

$$= kp[M]\left(\frac{kb}{kp[M] + k'_\beta + \tau}\right)[Y_0]$$

$$= K_{SCB}[Y_0]$$

where

$$K_{LCB} = kp[M]\left(\frac{kfp}{k'_\beta + kp[M] + \tau}\right)$$

and

$$K_{scB} = kp[M]\left(\frac{kb}{k'_\beta + kp[M] + \tau}\right)$$

The rate of β-scission of internal radicals is given by

$$\frac{1}{Ac}\frac{d\beta}{dL} = k'_\beta[R'_i]$$

$$= k'_\beta\left(\frac{kfp}{k'_\beta + kp[M] + \tau}\right)[Q_1][Y_0]$$

$$= K'_\beta[Q_1][Y_0]$$

where β is the moles of internal radicals undergoing β-scission per time (moles/s) and

$$K_\beta = k'_\beta\left(\frac{kfp}{k'_\beta + kp[M] + \tau}\right)$$

This neglects the contribution to the internal radical concentration made by backbiting. Backbiting tends to give internal radical centres two or three units from the end of the chain, and not uniformly along the chain. This is quite possibly (Ehrlich and Mortimer 1970, Nicolas 1958) the mechanism for β-scission of terminal radicals described above. Since we have already accounted for this effect, we shall neglect the contribution to the internal radicals produced by backbiting.

It is not clear whether β-scission of internal radicals has an appreciable effect on the molecular weight during polyethylene synthesis. Under industrial conditions, transfer to modifier may produce many more *dead* polymer chains than does β-scission. Only comparison of the model predictions with industrial data can provide clarification of the importance of the β-scission reaction.

We have written all of these two step reactions as overall reactions, with a sort of grouped rate constant for each overall reaction. One last note is that we have written these equations considering a homopolymer; for the copolymer case pseudo rate constants should be adopted.

Branching frequencies

The short and long chain branching can have an important effect on polymer properties. The more short chain branches incorporated along the polymer

chain, the lower will be the polymer density, while long chain branches affect the rheological properties. The short chain branches are produced by the backbiting reaction, therefore, the rate of short chain branching is

$$\frac{1}{Ac}\frac{dSCB}{dL} = K_{SCB}[Y_0]$$

Long chain branches are produced by the transfer to polymer and terminal double bond reactions. As stated before, we have neglected the terminal double bond reactions, thus, the total number of long chain branches produced (LCB) is given by:

$$\frac{1}{Ac}\frac{dLCB}{dL} = K_{LCB}[Y_0][Q_1]$$

The number of short and long chain branches per polymer molecule is calculated as follow:

$$\overline{S_n} = \frac{SCB}{Q_0}$$

$$\overline{L_n} = \frac{LCB}{Q_0}$$

The number of short and long chain branches per 1000 carbon atoms is given by (assuming two backbone carbon atoms per monomer unit)

$$\lambda_S = \left(\frac{SCB}{Q_1}\right) \cdot 500$$

$$\lambda_L = \left(\frac{LCB}{Q_1}\right) \cdot 500$$

The expressions derived above permit one to calculate the branching frequencies. Consequently, it will be possible to control some of the polymer physical properties (such as density) and rheological properties (such as melt flow) through variation in operating conditions of the reactor

A test of the moment closure techniques in branching systems.

It is becoming apparent that modeling of polymer molecular properties for polymerization systems where polymer produced is not inert are becoming more and more important. Such systems involve branching and crosslinking to form a gel, peroxide attack in reactive extrusion, condensation reactions with multi- functional monomers and so on. In the more classical mathematical modeling of the molecular weights of the chains, as in free radical polymerization for example, the radicals grow to a certain length and are terminated by some mechanism, forming dead polymer chains. These chains are inert to further reaction. The production rate of these chains is only a function of the concentration of chains of smaller length. For these systems one can readily calculate the entire chain length distribution using the method of instantaneous molecular weight distribution. Several systems of current interest now involve the case where radicals can attack this polymer to produce new radical centers at points along the backbone of the chain. This can cause scission or produce long chain branching, or if termination by combination is significant, crosslinks leading to gel formation. Now the production rate of chains of a certain length now depends upon of the concentration of chains of all lengths, including those chains longer than the chain length of interest. This means that in theory, in the first case one only needs to account for chains shorter than some maximum chain length, whereas in the later case, one must account for all chains from length unity to infinity (or the longest chain present).

One method of calculating the chain length averages is the method of moments. In this technique, the leading moments of the chain length distribution are calculated. If we define the moments of the distribution to be:

$$Q_n = \sum_{r=0}^{\infty} r^n P(r) + \sum_{r=0}^{\infty} r^n R(r)$$

the n^{th} moment

and the averages are:

$$\overline{r_n} = \frac{Q_1}{Q_0} \qquad \text{number average}$$

$$\overline{r_w} = \frac{Q_2}{Q_1} \qquad \text{weight average}$$

$$\overline{r_z} = \frac{Q_3}{Q_2} \qquad \text{z average}$$

In this special case the moments of the distribution all depend upon the lower moments, i.e.,

$$Q_n = f(Q_n, Q_{n-1}, Q_{n-2}, \cdots, Q_0)$$

In general this need not be the case and we could have the case where

$$Q_n = f(Q_\infty \cdots Q_{n+2}, Q_{n+1}, Q_n, Q_{n-1}, Q_{n-2}, \cdots, Q_0)$$

This means that one may have to calculate an infinite number of moments, certainly an impossible task. This is the closure problem.

A solution to this closure problem is to find an effective empirical equation to evaluate the higher moments as a function of the lower ones. One such method that has been used by several authors was derived by Hulburt and Katz (1964) based upon fitting the distribution by the first term of a Laguerre Series. The closure formula is of the form;

$$Q_3 = \frac{Q_2}{Q_1 Q_0}(2Q_2Q_0 - Q_1^2)$$

This short appendix is to evaluate the usefulness of the Hulburt Katz closure technique and compare it to the Log normal technique presented in Zabisky et al (1992) where

$$Q_3 = \left(\frac{Q_2}{Q_1}\right)^3 Q_0$$

To this end we shall derive the leading moments of the molecular weight distribution for a simple free radical reaction system, which is closed, and compare the results calculated by the moment equations and by the closure technique.

The kinetic example

Consider the simple polymerization mechanism.

decomposition of initiator

$$I \xrightarrow{k_d} 2R(1)$$

propagation

$$R(r)+M \xrightarrow{k_p} R(r+1)$$

transfer to monomer

$$R(r)+M \xrightarrow{k_{fm}} P(r)+R(1)$$

termination by disproportionation

$$R(r)+R(s) \xrightarrow{k_{td}} P(r)+P(s)$$

termination by combination

$$R(r)+R(s) \xrightarrow{k_{tc}} P(r+s)$$

One can also consider radical transfer to polymer, and propagation with internal or pendant double bonds, the branching reactions.

transfer to polymer

$$R(s)+P(r) \xrightarrow{k_{fp}} P(s)+R(r)$$

propagation with internal (or pendant) double bond

$$R(r)+P(s) \xrightarrow{k_p} R(r+s)$$

where

I is an initiator molecule.

M is a monomer molecule

$R(r)$ is a radical of length r.

$P(s)$ is a dead polymer chain of length s.

This kinetic mechanism can be used and expressions found for the molecular weight moments defined as

polymeric radical moments

$$Y_n = \sum_{r=0}^{\infty} r^n R(r)$$

dead polymer moments

$$X_n = \sum_{r=0}^{\infty} r^n P(r)$$

total macromolecule moments

$$Q_n = Y_n + X_n$$

One can use the stationary state hypothesis for the radical moments and assume that $Y_n \ll X_n$ such that $Q_n \approx X_n$. One can write an expression for the moments of the polymer distribution, when transfer to polymer, and propagation with internal double bonds are important. These equations were derived by Tobita and Hamielec (1988):

$$\frac{1}{V}\frac{d(VQ_0)}{dx} = [M_o]\left(\tau' + \frac{\beta}{2} - C_{pl}^{\bullet}\right)$$

$$\frac{1}{V}\frac{d(VQ_1)}{dx} = [M_o]$$

$$\frac{1}{V}\frac{d(VQ_2)}{dx} = [M_o]\left(\frac{2(1+C_{p2}^{\bullet})(1+C_{p2}+C_{p2}^{\bullet})}{\tau'+\beta+C_{pl}} + \beta\frac{(1+C_{p2}+C_{p2}^{\bullet})^2}{(\tau'+\beta+C_{pl})^2}\right)$$

$$\frac{1}{V}\frac{d(VQ_3)}{dx} = [M_o]\left(1 + 3(1+C_{p2}^{\bullet})\frac{Y_2}{Y_0} + 3(1+C_{p,1}^{\bullet})\frac{Y_1}{Y_0} + 3\beta\frac{Y_1Y_2}{Y_0^2}\right)$$

The radical moments are given by

$$Y_0 = \sqrt{(2fkd[I])/(ktc + ktd)}$$

$$Y_1 = \left(\frac{1+C_{p2}+C_{p2}^{\bullet}}{\tau'+\beta+C_{pl}}\right)Y_0$$

$$Y_2 = \left(\frac{1+C_{p,1}+C_{p,1}^{\bullet}}{\tau'+\beta+C_{pl}} + \frac{2(1+C_{p2}^{\bullet})(1+C_{p2}+C_{p2}^{\bullet})}{(\tau'+\beta+C_{pl})^2}\right)Y_0$$

where

$$\tau' = \frac{ktdY_0}{kp[M]} + \frac{kfm}{kp}$$

$$\beta = \frac{ktcY_0}{kp[M]}$$

and

$$C_{pi} = \frac{kfpQ_i}{kp[M]}$$

$$C_{pi}^{\cdot} = \frac{kp^{\cdot}Q_i}{kp[M]}$$

The total number of tri-functional branch points, as generated by transfer to polymer, is given as

$$\frac{1}{V}\frac{d(Q_0B_{N3})}{dx} = [M_o]C_{pi}$$

B_{N3} is the number of tri-functional branch points per polymer molecule.

Where we define conversion as

$$x = \frac{M_0 - M}{M_0}$$

where M_0 is the initial monomer concentration. We can write

$$\frac{dx}{dt} = kpY_0(1-x)$$

One can solve these differential equations above (using the package *LSODE*) from x=0 to x=1 to give us the moments of the molecular weight distribution. Since we have a mathematically closed set of equations, we can calculate M_z and compare it to the value given by the closure techniques. For this test the temperature was isothermal, transfer to monomer was neglected and termination was all by disproportionation. When transfer to polymer is considered, and termination is by combination, the polymer tends to form a gel as indicated by Q_2 growing to infinity. Furthermore propagation with internal double bonds tends to form a gel. Gel formation was avoided in this study by neglecting termination by combination, and propagation with internal double bond reactions.

We shall assume a constant reaction volume of one liter. The parameter values were adjusted to give polymer properties similar to those measured for low density polyethylene (Foster et al. 1980) and thus

$$kp = 26.2$$

$$kd = 4.3x10^{-2}$$

$$ktd = 12.6$$

$$ktc = 0$$

$$kfm = 0$$

$$kfp/kp = 2.0x10^{-2}$$

M_0= 10 and $I_0 = 0.01xM_0$ mol/liter (and constant). The maximum conversion was 25%. This gave the chain properties

$$M_n = 20900$$

$$M_w = 146000$$

$$M_z = 377000$$

$$\lambda_{LCB} = 1.51$$

It should be noted that the polydispersity of LDPE is not totally due to the long chain branching (as in this example), but also to the widely varying temperature and initiator levels experienced in a tubular reactor. The effect of the transfer to polymer rate on the error between M_z and M_z calculated using the closure methods is shown in figure 41. The branching frequency, λ_w, is presented as the number average number of branches per 1000 carbon atoms. The error is calculated as

$$Error(\%) = 100 \cdot \frac{Mz_{(closure)} - Mz_{(actual)}}{Mz_{(actual)}}$$

One can see that the Log normal method greatly over predicts the M_z values for all branching frequencies but especially at higher branching frequencies. The Hulburt and Katz method gives very good results at low branching frequencies but tends to under predict the M_z value at higher branching frequencies. The geometric mean error is, for the most part, less than that for either the Log normal or the H-K method but has comparable absolute error as that of the H-K method at the higher branching frequencies.

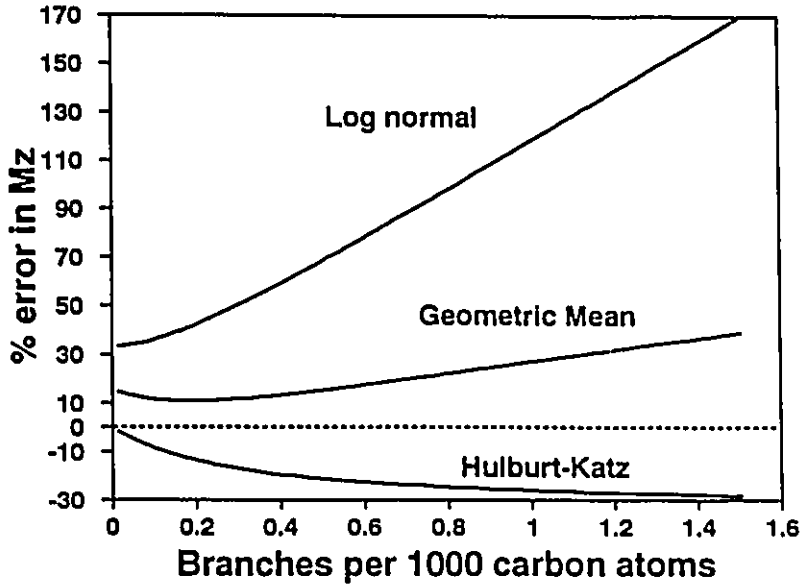

Figure 41 The effect of branching frequency on the error in M_z.

Conclusions for moment closure techniques

The closure technique of Hulburt and Katz seems to be adequate for narrow unbranched distributions but as the distribution broadens the error increases. The technique does not perform as well where there is significant branching, at least by transfer to polymer. In our example here we tried to simulate polymer properties near that measured for HP-LDPE and found the error to be quite significant. Nevertheless for this example the Hulburt and Katz method is superior to the Log normal method. In polyethylene production at temperatures near 300°C β-scission may be important, and would tend to narrow the distribution possibly helping to keep the error in the Hulburt and Katz method within tolerable limits. One must be cautious when choosing a closure technique, since the adequacy of the technique must depend a great deal on the shape of the molecular weight distribution, and on how it changes with conversion.

Nomenclature for tubular reactor model

Subscripts and superscripts

1, 2 pertain to monomer type 1 (and 2) or monomer type 1 (and 2) repeat units.

s, L	pertain to short and long chain branches
'	denotes internal radical.
=	denotes terminal double bond
-	bar denotes accumulated properties

General

A_c	cross sectional area of tubular reactor of constant cylindrical cross section.
C_p	heat capacity of reaction mixture
$\overline{\Delta H}$	average heat of polymerization
f	initiator efficiency
f_f	Fanning friction factor
f_1	comonomer composition, the mole fraction of monomer 1.
F_1	instantaneous copolymer composition, the instantaneous mole fraction of monomer type 1 units in the chain.
$\overline{F_1}$	accumulated copolymer composition, the accumulated mole fraction of monomer type 1 units in the chain
g_c	gravitational constant used to convert $kg_{(mass)}$ to $kg_{(force)}$
h_i	heat transfer coefficient for film between reactor contents and reactor wall
h_w	heat transfer coefficient from the jacket contents and through the jacket wall
k	rate constant in appropriate units for the order of reaction.
L	axial coordinate of the reactor
LCB	the number of long chain branches in the reaction volume
$\overline{L_n}$	the number of long chain branches per polymer molecule
M_i	molar flow rate of monomer type i
m	molecular weight of monomer

n	the number of radicals formed per peroxide molecule
P	reactor pressure
$\overline{M_n}$	number average molecular weight
$\overline{M_w}$	weight average molecular weight
$\overline{M_z}$	z average molecular weight
$\overline{r_n}$	number average chain length
$\overline{r_w}$	weight average chain length
$\overline{r_z}$	z average chain length
$P(r)$	polymer molecule of chain length r
$P^{=}(r)$	polymer molecule of chain length r with a terminal double bond.
Q_i	the i^{th} moment of the polymer molecular weight distribution
r	reactor inner radius
RI	rate of initiation
$R(r)$	radicals of chain length r
$R'(r)$	internal radical of length r
SCB	the number of short chain branches in the reaction volume
$\overline{S_n}$	the number of short chain branches per polymer molecule
t	time
T	reactor temperature at length L
T_j	jacket temperature at length L
u	linear velocity
U	overall heat transfer coefficient
V	volumetric flow rate of reaction mixture
W	mass flow rate of the reaction mixture
W_p, W_m	mass of polymer and monomer
$[X]$	concentration of any species X
Y_i	the i^{th} moment of the total radical molecular weight distribution

Greek letters

ϕ_1	fraction of radical centers that are on monomer type 1 units.
ρ	solution density
η_{JT}	Joule-Thomson coefficient
η_o	monomer viscosity
η_r	relative viscosity
η_s	solution viscosity
Ψ_i	moles of monomer i bound as polymer
λ_L	the number of long chain branches per 1000 carbon atoms
λ_S	the number of short chain branches per 1000 carbon atoms
τ	a grouping of kinetic parameters and concentrations related to the transfer to small molecule reactions.

Rate constants

kb	backbiting reaction
k'_β	β-scission reaction of an internal radical
k_β	β-scission reaction of a terminal radical
kd	initiator decomposition reaction
kdb	terminal double bond reaction
$kdcm$	decomposition of monomer reaction
$kdcp$	decomposition of polymer reaction
kd_{O_2}	oxygen initiation reaction
kdp	slow initiation reaction
kfm	transfer to monomer reaction
kfp	transfer to polymer reaction
$kfts$	transfer to chain transfer agent (CTA) reaction
K_β	overall β-scission reaction for internal radicals

K_{LCB}	overall long chain branches reaction
K_{SCB}	overall short chain branches reaction
kp_{ji}	propagation reaction
kr	inhibition reaction for oxygen
ktc_{ji}	termination by combination reaction
ktd_{ji}	termination by disproportionation reaction
kth	thermal initiation reaction

2.7.2 Appendix for autoclave model

Mass and energy balance equations for autoclave reactor

Given the mixing model, one can construct the mathematical model by writing the mass and energy balances for a single volume segment The mass balance for a species in a volume segment will, in general, have the form :

accumulation in volume segment= outflow from previous segment
+ feed to segment
+ recycle from next element
- outflow to next segment
- recycle to previous element
+ net generation by reaction

Mathematically, for any species X_k

$$\frac{dX_{k,(j,L)}}{dt} = F^{r_k}_{j,L-1} + F^{r_k}_{f,(j,L)} + F^{r_k}_{r,(j+1,L)} - F^{r_k}_{j,L} - F^{r_k}_{r,(j,L)} + r^{r_k}_{j,L} V_{j,L}$$

where

X_k moles of species x_k

F^{r_k} molar flow rate of species x_k

$F^{r_k}_r$ molar recycle flow rate of species x_k

r^{r_k} rate of reaction to generate species x_k

j refers to the volume element, and L refers to the volume segment. Note that from our mixing model:

$$F_{j,1} = F_{j-1,N_p+1}$$

$$F_{f,(j,1)} = F_{f_j}$$

For the plug flow segments (L > 1) there is no feed or recycle

$$F_{f,(j,L)} = F_{r,(j,L)} = 0$$

It is also true that in a CSTR, the following relation holds:

$$F_{j,L}^{T_k} = [X_k]_{(j,L)} \frac{V_{out(j,L)}}{V_{j,L}}$$

where V_{ow} is the volumetric outflow rate. Defining the recycle ratio at volume element j as q_j ,

$$q_j = \frac{Q_{r,(j,1)}}{\sum_{k=1}^{N_v} \left(Q_{f_k}^{M_1} + Q_{f_k}^{M_2} \right)}$$

where Q_r is the volumetric recycle flow rate and $Q_{f_k}^{M_1}$ and $Q_{f_k}^{M_2}$ are the volumetric flow rates of monomer 1 and 2 in the f_k stream. The volumetric feed rates of monomer one and 2 are given by

$$Q_{f_k}^{M_1} = \frac{F_{f_k}^{M_1}}{[M_1]_{f_k}}$$

$$Q_{f_k}^{M_2} = \frac{F_{f_k}^{M_2}}{[M_2]_{f_k}}$$

so the recycle flow rate will be given by

$$Q_{r,(j,1)} = q_j \sum_{k=1}^{N_v} \left(\frac{F_{f_k}^{M_1}}{[M_1]_{f_k}} + \frac{F_{f_k}^{M_2}}{[M_2]_{f_k}} \right)$$

The recycle molar flow rate for each species is then given by

$$F_{r,(j,1)}^{T_k} = [X_k]_{j,1} Q_{r,(j,1)}$$

q_j is a parameter to be estimated, and is zero for all plug flow volume segments.

To determine $V_{out(j,L)}$, assume that volumes are additive and the reaction mixture is essentially monomer and polymer

$$V_{out(j,L)} = \sigma_{M_1} m_1 + \sigma_{M_2} m_2 + \sigma_{P_1} m_1 + \sigma_{P_2} m_2$$

where,

$$\sigma_{M_1} = \frac{F_{j,L-1}^{M_1} + F_{f,(j,L)}^{M_1} + Q_{r,(j+1,L)}[M_1]_{j+1,L} - Q_{r,(j,L)}[M_1]_{j,L} + r_{j,L}^{M_1} V_{j,L}}{\rho_{j,L}^{M_1}}$$

$$\sigma_{M_2} = \frac{F_{j,L-1}^{M_2} + F_{f,(j,L)}^{M_2} + Q_{r,(j+1,L)}[M_2]_{j+1,L} - Q_{r,(j,L)}[M_2]_{j,L} + r_{j,L}^{M_2} V_{j,L}}{\rho_{j,L}^{M_2}}$$

$$\sigma_{P_1} = \frac{F_{j,L-1}^{P_1} + Q_{r,(j+1,L)}[P_1]_{j+1,L} - Q_{r,(j,L)}[P_1]_{j,L} + r_{j,L}^{P_1} V_{j,L}}{\rho_{j,L}^{P}}$$

$$\sigma_{P_2} = \frac{F_{j,L-1}^{P_2} + Q_{r,(j+1,L)}[P_2]_{j+1,L} - Q_{r,(j,L)}[P_2]_{j,L} + r_{j,L}^{P_2} V_{j,L}}{\rho_{j,L}^{P}}$$

and

m_1 = molecular weight of monomer type 1 (g/mol)

m_2 = molecular weight of monomer type 2 (g/mol)

ρ^{M_1} = density of monomer 1 (g/cm^3)

ρ^{M_2} = density of monomer 2 (g/cm^3)

ρ^{P} = density of polymer (g/cm^3)

The rates of reactions $r_{j,L}^{M_1}$, $r_{j,L}^{M_2}$, $r_{j,L}^{P_1}$ and $r_{j,L}^{P_2}$ will be derived in the next section.

We can solve the set of ODE for $X_{k,(j,L)}$ of the form,

$$V_{j,L} \quad \frac{d[X_k]_{j,L}}{dt} = F_{j,L-1}^{r_k} + F_{f,(j,L)}^{r_k} + Q_{r,(j+1,L)}[X_k]_{j+1,L} - (Q_{r,(j,L)} + V_{out(j,L)})[X_k]_{j,L} + r_{j,L}^{r_k} V_{j,L}$$

Depending upon the segment type, there may or may not be fresh feeds or recycles. For simplicity, we are adopting the following nomenclature in our subsequent model development.

$$(inflow - outflow)_{j,L}^{r_k} = F_{j,L-1}^{r_k} + F_{f,(j,L)}^{r_k} + Q_{r,(j+1,L)}[X_k]_{j+1,L} - (Q_{r,(j,L)} + V_{out(j,L)})[X_k]_{j,L}$$

Two phase kinetics

Let Φ_m be the ratio of the mass of monomer to the mass of polymer, both in the polymer rich phase. This quantity can be calculated from:

$$\Phi_m = \frac{1}{W_t} - 1$$

where W_t is the mass fraction of polymer in the polymer rich phase given by equation 3. Defining W_p as the mass of polymer in the polymer rich phase, one can evaluate the volume of the polymer rich phase (swollen with monomer) as:

$$V_p = \left(\frac{m_1 f_1}{\rho_1} + \frac{m_2 f_2}{\rho_2}\right)\left(\frac{W_p \Phi_m}{m_1 f_1 + m_2 f_2}\right) + \frac{W_p}{\rho_p}$$

$$W_p = m_1 P_1 + m_2 P_2$$

where f_1 and f_2 are mole fractions of monomer 1 and 2; m_1 and m_2 are the molecular weights of monomer 1 and 2; ρ_1, ρ_2 and ρ_p refer to density of monomer 1, monomer 2 and polymer respectively; P_1 and P_2 are monomer 1 units and monomer 2 units bound as polymer. This assumes that the volumes are additive. The monomer rich phase volume is given by:

$$V_m = V_s - V_p$$

where V_s is the volume of the segment.

Now that we have expressions to calculate V_m and V_p, we are now able to derive mass balance equations for each species in an arbitrary volume segment (*J, L*). Firstly, we assume the initiator and the modifier to partition according to:

$$\frac{[I]_m}{[I]_p} = K_I$$

$$\frac{[TSH]_m}{[TSH]_p} = K_{TS}$$

K_I and K_{TS} need not be identical for all initiator or modifier types. In our simulations both K_I and K_{TS} were assumed to be unity. From the mass balances and the partition coefficients, one can calculate the concentration of initiator and modifier in each phase as

$$[I]_p = \frac{[I]_{total} V_s}{K_I V_m + V_p}$$

$$[TSH]_p = \frac{[TSH]_{total} V_s}{K_{TS} V_m + V_p}$$

If the stationary state hypothesis (SSH) is adopted, then one can calculate the radical concentrations in each phase. For the pregel region

$$[R]_m = \left(\frac{2 f k_d [I]_m}{k_t} \right)^{\frac{1}{2}}$$

$$[R]_r = \left(\frac{2 f k_d [I]_p}{k_t} \right)^{\frac{1}{2}}$$

where $k_t = k_{tc} + k_{td}$. In the postgel region, the polymer rich phase is composed of sol plus gel. The monomer rich phase radical concentration is unchanged and the polymer phase radical concentrations are given by these two simultaneous algebraic equations

$$[R]_x = \frac{k_{fp}[M_g][R]_p}{k_{fm}[M]_p + k_{fi} + (k_{tcsx} + k_{tdsx})[R]_p + k_{fp}[Q_1]_p + k_{fts}[TSH]_p}$$

$$0 = (k_{tcss} + k_{tdss})[R]_p^2 + \{k_{fp}[M_g] + (k_{tcsx} + k_{tdsx})[R]_x\}[R]_p - \{2 f k_d [I]_p + k_{fm}[M]_p [R]_x + k_{fts}[TSH]_p [R]_x + k_{fp}[R]_x [Q_1]_p\}$$

where $[M_g]$ denotes the moles of monomer units bound in the gel per unit of volume; $[R]_p$ is the sol radical concentration; $[Q_1]_p$ represents the first polymer moment in the sol; and the subscript '*sg*' in the termination rate constants denote sol-gel. Note that we have assumed that $k_{tcss} = k_{tc}$, and $k_{tdss} = k_{td}$.

A balance on initiator and monomer types 1 and 2 gives

$$V_s \frac{d[I]_{total}}{dt} = (inflow - outflow)_{j,L}^{I} - k_d \{[I]_m V_m + [I]_p V_p\}$$

$$V_s\frac{d[M_1]}{dt}=(inflow-outflow)_{j,L}^{M_1}-k_{p11}\{[M_1]_m\phi_1[R]_mV_m+[M_1]_p\phi_1([R]_p+[R]_x)V_p\}$$
$$-k_{p21}\{[M_1]_m\phi_2[R]_mV_m+[M_1]_p\phi_2([R]_p+[R]_x)V_p\}$$

$$V_s\frac{d[M_2]}{dt}=(inflow-outflow)_{j,L}^{M_2}-k_{p12}\{[M_2]_m\phi_1[R]_mV_m+[M_2]_p\phi_1([R]_p+[R]_x)V_p\}$$
$$-k_{p22}\{[M_2]_m\phi_2[R]_mV_m+[M_2]_p\phi_2([R]_p+[R]_x)V_p\}$$

The concentrations of monomer in the polymer and monomer rich phases are given by:

$$[M_1]_p=\frac{f_1W_p\Phi_m}{V_p(m_1f_1+m_2f_2)}$$

$$[M_2]_p=\frac{f_2W_p\Phi_m}{V_p(m_1f_1+m_2f_2)}$$

$$[M_1]_m=\frac{V_s[M_1]-[M_1]_p[V_p]}{V_m}$$

$$[M_2]_m=\frac{V_s[M_2]-[M_2]_p[V_p]}{V_m}$$

Similar balances can be made to find the moles of each monomer bound as polymer and the modifier in the reactor.

$$V_s\frac{d[P_1]}{dt}=(inflow-outflow)_{j,L}^{P_1}+k_{p11}\{[M_1]_m\phi_1[R]_mV_m+[M_1]_p\phi_1([R]_p+[R]_x)V_p\}$$
$$+k_{p21}\{[M_1]_m\phi_2[R]_mV_m+[M_1]_p\phi_2([R]_p+[R]_x)V_p\}$$

$$V_s\frac{d[P_2]}{dt}=(inflow-outflow)_{j,L}^{P_2}-k_{p12}\{[M_2]_m\phi_1[R]_mV_m+[M_2]_p\phi_1([R]_p+[R]_x)V_p\}$$
$$+k_{p22}\{[M_2]_m\phi_2[R]_mV_m+[M_2]_p\phi_2([R]_p+[R]_x)V_p\}$$

$$V_s\frac{d[TSH]}{dt}=(inflow-outflow)_{j,L}^{TSH}-k_{fts}\{[R]_m[TSH]_mV_m+([R]_p+[R]_x)[TSH]_pV_p\}$$
$$-k_{pts}\{[R]_m[TSH]_mV_m+([R]_p+[R]_x)[TSH]_pV_p\}$$

Molecular weight and moment equations

We are using the method of moments to find the molecular weight averages. r_n and r_w are the number and weight average chain lengths and Q_0, Q_1, Q_2 are the leading moments of the molecular weight distribution.

$$r_n = \frac{[Q_1]}{[Q_0]}$$

$$r_w = \frac{[Q_2]}{[Q_1]}$$

The leading moments for radical and polymer chain length distribution for each phase are derived below. By definition, the moments of the dead polymer and macroradical distribution are:

$$[Q_i] = \sum_{r=2}^{\infty} r^i [P(r)]$$

$$[Y_i] = \sum_{r=1}^{\infty} r^i [R(r)]$$

Notice that $[Y_{i+1}] >> [Y_i] >> [Y_{i-1}]$

$[Q_{i+1}] >> [Q_i] >> [Q_{i-1}]$

$[Q_i] >> [Y_i]$

and advantage is taken of these inequalities to simplify the expressions whenever possible. One can also neglect the term $2fk_d[I]$ where its value is insignificant as compared to other terms.

Firstly consider the pre gel region. The radical moments are given by

$$[Y_0]_m = [R]_m = \left(\frac{2fk_d[I]_m}{k_t}\right)^{0.5}$$

$$[Y_0]_p = [R]_p = \left(\frac{2fk_d[I]_p}{k_t}\right)^{0.5}$$

$$[Y_1]_m = \frac{[Y_0]_m}{\tau_m + \beta_m}$$

$$[Y_1]_p = \frac{(1+C_{p2})[Y_0]_p}{\tau_p + \beta_p + C_{pl}}$$

$$[Y_2]_m = \frac{2[Y_0]_m}{(\tau_m + \beta_m)^2}$$

$$[Y_2]_p = \frac{2[Y_1]_p + C_{p3}[Y_0]_p}{\tau_p + \beta_p + C_{pl}}$$

where

$$\tau_m = \frac{k_{fm}[M]_m + k_{fts}[TSH]_m + k_{fi} + k_{td}[Y_0]_m}{k_p[M]_m}$$

$$\tau_p = \frac{k_{fm}[M]_p + k_{fts}[TSH]_p + k_{fi} + k_{td}[Y_0]_p}{k_p[M]_p}$$

$$\beta_m = \frac{k_{tc}[Y_0]_m}{k_p[M]_m}$$

$$\beta_p = \frac{k_{tc}[Y_0]_p}{k_p[M]_p}$$

$$C_{pi} = \frac{k_{fp}[Q_i]_p}{k_p[M]_p}$$

The polymer moments are given by

$$V_s \frac{d[Q_0]}{dt} = (inflow - outflow)_{j,L}^{Q_0} + \left(\tau_m + \frac{\beta_m}{2}\right) k_p[M]_m [Y_0]_m V_m$$

$$+ \left(\tau_p + \frac{\beta_p}{2}\right) k_p[M]_p [Y_0]_p V_p$$

$$[Q_1] = [P_1] + [P_2]$$

$$V_s \frac{d[Q_2]}{dt} = \left[\frac{2}{\tau_m + \beta_m} + \frac{\beta_m}{(\tau_m + \beta_m)^2}\right] k_p[M]_m [Y_0]_m V_m$$

$$+ \left[\frac{2(1+C_{p2})}{\tau_p + \beta_p + C_{pl}} + \frac{\beta_p (1+C_{p2})^2}{(\tau_p + \beta_p + C_{pl})^2}\right] k_p[M]_p [Y_0]_p V_p$$

$$+ (inflow - outflow)_{j,L}^{Q_2}$$

Since there is no dead polymer in the monomer rich phase, the following relationship holds:

$$[Q_i]_p = [Q_i]\frac{V_s}{V_p}$$

Now consider the post gel region where we can write expressions for the molecular weight of only the sol polymer. Since there is no gel in the monomer rich phase, the postgel radical moments are the same as those in pregel region. However they differ in the polymer rich phase.

$$[Y_0]_p = [R]_p$$

$$[Y_0]_g = [R]_g$$

$$[Y_1]_p = \frac{k_p[M]_p[Y_0]_p + k_{fm}[M]_p[Y_0]_T + k_{fts}[TSH]_p[Y_0]_T + k_{fp}[Y_0]_T[Q_2]_p + k_{fi}[Y_0]_T}{(k_{tcss} + k_{tdss})[Y_0]_p + (k_{tcsg} + k_{tdsg})[Y_0]_g + k_{fm}[M]_p + k_{fts}[TSH]_p + k_{fp}[Q_1]_p + k_{fp}[M_g] + k_{fi}}$$

$$[Y_2]_p = \frac{k_{fm}[M]_p[Y_0]_T + k_{fts}[TSH]_p[Y_0]_T + k_{fi}[Y_0]_T + 2k_p[M]_p[Y_1]_p + k_{fp}[Q_3]_p[Y_0]_T}{k_{fm}[M]_p + k_{fts}[TSH]_p + k_{fi} + k_{fp}[Q_1]_p + k_{fp}[M_g] + (k_{tcss} + k_{tdss})[Y_0]_p + (k_{tcsg} + k_{tdsg})[Y_0]_g}$$

where

$$[Y_0]_T = [Y_0]_g + [Y_0]_p$$

The polymer moments are given by

$$V_s\frac{d[Q_0]}{dt} = (inflow - outflow)_{j,L}^{Q_0} + k_{fm}[M]_m[Y_0]_m V_m + k_{fm}[M]_p[Y_0]_p V_p$$

$$+\frac{1}{2}k_{tr}[Y_0]_m^2 V_m + \frac{1}{2}k_{tcss}[Y_0]_p^2 V_p + k_{td}[Y_0]_m^2 V_m + k_{tdss}[Y_0]_p^2 V_p$$

$$+ k_{tdsg}[Y_0]_p[Y_0]_g V_p - k_{fp}[Y_0]_g[Q_1]_p V_p + k_{fp}[Y_0]_p[M_g]V_p + k_{fi}[Y_0]_m V_m$$

$$+ k_{fi}[Y_0]_p V_p + k_{fts}[TSH]_m[Y_0]_m V_m + k_{fts}[TSH]_p[Y_0]_p V_p$$

$$[Q_1] = [P_1] + [P_2] - [M_g]$$

$$V_s\frac{d[Q_2]}{dt}=(inflow-outflow)_{j,L}^{Q_2}+k_{fm}\{[M]_m[Y_2]_mV_m+[M]_p([Y_0]_g+[Y_0]_p)V_p\}$$
$$+k_{fts}\{[TSH]_m[Y_2]_mV_m+[TSH]_p([Y_0]_g+[Y_0]_p)V_p\}+k_{fi}\{[Y_2]_mV_m$$
$$+([Y_0]_g+[Y_0]_p)V_p\}+2k_p[M]_p[Y_1]_pV_p$$
$$+k_{tc}\left([Y_0]_m[Y_2]_mV_m+[Y_1]_m^2V_m\right)+k_{td}[Y_0]_m[Y_2]_mV_m$$
$$+k_{tcs}[Y_1]_p^2V_p-k_{tcsg}[Y_0]_g[Y_2]_pV_p$$

where the moles of monomer bound as gel is given by

$$V_s\frac{d[M_g]}{dt}=(inflow-outflow)_{j,L}^{M_g}+k_p[M]_p[Y_0]_gV_p+k_{tcsg}[Y_0]_g[Y_1]_pV_p$$
$$-k_{fi}[Y_0]_gV_p$$

In the post gel region the polymer moment equations are not closed. We have selected the closure method of Hulburt and Katz (1964) to express Q_3 as a function of the lower moments.

$$[Q_3]=\frac{[Q_2]}{[Q_1][Q_0]}(2[Q_2][Q_0]-[Q_1]^2)$$

The short chain branching frequency is given by

$$V_s\frac{d[SCB]}{dt}=(inflow-outflow)_{j,L}^{SCB}+k_b[Y_0]_mV_m+k_b[Y_0]_pV_p$$
$$+k_{pts}[Y_0]_m[TSH]_mV_m+k_{pts}[Y_0]_p[TSH]_pV_p$$

We do not consider backbiting by gel radicals, or the consumption of short chain branched sol polymer by the gel. In the pregel region, the long chain branching frequency is given by:

$$V_s\frac{d[LCB]}{dt}=(inflow-outflow)_{j,L}^{LCB}+k_{fp}[Y_0]_p[Q_1]_pV_p$$

In the postgel region, considering branches only in the sol:

$$V_s\frac{d[LCB]}{dt}=(inflow-outflow)_{j,L}^{LCB}+k_{fp}([Y_0]_p+[Y_0]_g)[Q_1]_pV_p$$

This equation neglects the consumption of branches from the sol caused by incorporation of branched polymer into the gel. The number of short and long chain branches per 1000 carbon atoms is given by (assuming two backbone carbon atoms per monomer unit):

$$\lambda_S = 500\frac{[SCB]}{[Q_1]}$$

$$\lambda_L = 500\frac{[LCB]}{[Q_1]}$$

Energy balance

The energy balance, for any reaction volume, assuming no losses to the surroundings is given by

$$\frac{dH}{dt} = (m_1F_1 + m_2F_2)Cp_{feed}(T_{feed} - T_{ref}) + \rho_{in}Q_{in}Cp_{in}(T_{in} - T_{ref})$$

$$+ \rho_{r,in}Q_{r,in}Cp_{r,in}(T_{r,in} - T_{ref}) - \rho(Q_{r,out} + Q_{out})Cp(T - T_{ref}) - \Delta H_{rxn}R_pV_r$$

(cal/s)

where $\Delta H/(m_1Cp) = 1300°C$.

Notation for autoclave model

Cp	The heat capacity of mixture (cal/g-°C)
C_{pi}	dimensionless group for molecular weight calculations related to transfer to polymer
f	initiator efficiency
f_1, f_2	monomer composition (mole fraction of monomer 1 and monomer 2)
F_1, F_2	instantaneous copolymer compositions (mole fraction of monomer 1 and monomer 2 bound as polymer)
$\overline{F_1}, \overline{F_2}$	accumulated copolymer compositions (mole fraction of monomer 1 and monomer 2 bound as polymer)

F	molar flow rate (mol/s)
F_I	molar initiator flow rate (mol/s)
F_r	molar recycle flow rate (mol/s)
H	the change in enthalpy of the reactor contents from the reference conditions (cal)
ΔH	heat of polymerization (cal/mole)
I	initiator species
k_b	rate constant for backbiting reaction (s^{-1})
k_d	rate constant for initiator decomposition reaction (s^{-1})
k_{fm}	rate constant for transfer to monomer reaction (cm^3/mol-s)
k_{fp}	rate constant for transfer to polymer reaction (cm^3/mol-s)
k_{fs}	rate constant for transfer to modifier reaction (cm^3/mol-s)
k_p	rate constant for propagation reaction (cm^3/mol-s)
k_{ps}	rate constant for modifier incorporation reaction (cm^3/mol-s)
k_{tc}	rate constant for termination by combination reaction (cm^3/mol-s)
k_{tcsg}	rate constant for termination by combination reaction between one sol radical and one gel radical (cm^3/mol-s)
k_{tcss}	rate constant for termination by combination reaction between two sol radicals (cm^3/mol-s)
k_{td}	rate constant for termination by disproportionation reaction (cm^3/mol-s)
k_{tdsg}	rate constant for termination by disproportionation reaction between one sol radical and one gel radical (cm^3/mol-s)

k_{ulss}	rate constant for termination by disproportionation reaction between two sol radicals (cm^3/mol-s)
K_I	partition coefficient for initiator (mol/cm^3 in monomer rich phase : mol/cm^3 in polymer rich phase)
K_p	proportional gain for the controller (g/s-°C)
K_{TS}	partition coefficient for modifier (mol/cm^3 in monomer rich phase : mol/cm^3 in polymer rich phase)
LCB	moles of long chain branches
m_1, m_2	molecular weight of monomers (g/mol)
M	monomer species
M_g	moles of monomer units bound as gel polymer
N_p	number of plug flow segments in a volume element
N_v	number of volume elements in the reactor
P_1, P_2	moles of monomer units bound in the polymer
Q	volumetric flow rate (cm^3/s)
Q_i	the i^{th} moment of the polymer distribution (mol/cm^3)
Q_r	volumetric recycle flow rate (cm^3/s)
R	radical species
q_j	recycle ratio at volume element j
r_1, r_2	reactivity ratios
r, R_p	rate of reaction (mol/cm^3-s)
r_n	number average chain length
r_w	weight average chain length

SCB	moles of short chain branches
TSH	modifier
T_{set}	set point temperature (°C)
V_j	volume of a single volume element (cm^3)
$V_{j,L}, V_s$	volume of a segment (cm^3)
V_m	volume of the monomer rich phase (cm^3)
V_{out}	volumetric outflow rate from a segment (cm^3/s)
V_p	volume of the polymer rich phase (cm^3)
V_T	total volume of the reactor (cm^3)
W_p	mass of polymer in the polymer rich phase (g)
W_t	weight fraction of polymer in the polymer rich phase
X_1, X_2, X_3	normalized variables for temperature, pressure and weight average molecular weight respectively (dimensionless)
$[X_k]$	concentration of species X_k (mol/cm^3)
Y_i	the i^{th} moment of the radical distribution (mol/cm^3)

Greek symbols

β, τ	:	dimensionless group for molecular weight calculations
τ_I	:	integral time constant for the controller (s)
τ_D	:	derivative time constant for the controller (s)
ϕ_1, ϕ_2	:	mole fraction of polymer radicals
Φ_m	:	ratio of the mass of monomer in polymer rich phase to the mass of polymer in the polymer rich phase
ϕ_{tc}	:	fraction of total termination by combination

θ_j : volume fraction of the CSTR component to the total volume element J

ρ : density (g/cm^3)

λ_L : number of long chain branches per 1000 carbon atoms

λ_s : number of short chain branches per 1000 carbon atoms

Subscripts

g : related to gel polymer

m : related to monomer rich phase

p : related to polymer rich phase

r : related to recycle

TS : related to modifier

1,2 : related to monomer 1 and 2

Chapter 3 Production of polyolefins and copolymers by Ziegler-Natta polymerization

3.1 Introduction

Ever since their discovery, the heterogeneous isospecific catalysts based on $TiCl_3$ and organometallic compounds have caused not only major industrial innovations, but also a great deal of scientific effort in order to better understand the fundamentals involved in this field. This research has covered a wide spectrum of subjects including polymerization kinetics and chemistry, catalyst synthesis, as well as the characterization of both homopolymers and copolymers. These attempts have resulted in several new developments, especially with regards to catalyst synthesis. For instance, the production of supported catalysts based on $TiCl_4$ and $MgCl_4$ has induced the appearance of new technologies such as gas phase and bulk processes which are now replacing the old slurry processes. Unfortunately, much of the scientific information generated during the development of creating such processes is maintained in secrecy by the companies which have performed the studies. Even so, a large number of papers have been published, as well as some relevant books and theses.

Despite all of this research, many aspects related to the polymerization of olefins using heterogeneous Ziegler-Natta catalysts remain poorly understood and even matters of some controversy. One of the most important sources of controversy is the reason for the broad molecular weight distribution (molecular weight distribution) and for the compositional inhomogeneity of copolymers even if prepared at constant monomer composition. Presently, there are two main theories which try to explain these observed phenomena, namely, the presence of either a distribution of activities for the catalyst sites or diffusional effects limiting the transport of reactants. The former assumes the existence of multiple catalyst sites of different activities, whereas the latter proposes the encapsulation of the catalyst particles by the semicrystalline polymer creating a diffusional barrier for monomer transport.

According to the first point of view, the different types of sites have different propagation, decay and possibly transfer rates to account for both the broad molecular weight distribution and the copolymer composition inhomogeneity. As for the second hypothesis, two consequences could occur: i) the efficiency of the catalyst will drop as the catalyst particles become more and more encapsulated, and ii) active sites at

different radial positions in the particle will have different levels of monomer available to them. Furthermore, different monomers will have different diffusion rates, resulting in the production of a spectrum of chain lengths and compositions.

3.1.1 Literature review

Boor (1979) recognized that the reasons for the wide molecular weight distribution in polymers prepared using Ziegler-Natta catalysts were not well understood and presented five proposals covering both chemical and physical points of view. One of these was the existence of a multiple site distribution related to the propagation rate constants as had been proposed by Grieveson (1965), whereas two others took into account diffusional limitations created by the encapsulation of the reactive sites by the growing polymer chains. In fact, many experimental results have been interpreted either by using a distribution of site activities (Barbe et al. 1983, Begley 1966, Berger and Grieveson 1965, Bohlm 1978 1981, Burfield 1983, Chien et al. 1976 1982 1985, Cozewith and Ver Strate 1971, Doi et al. 1983, Gordon and Roe 1961, Kashiwa and Yoshitake 1984, Keii et al. 1982 1984, Martineau et al. 1983, Mussa 1959, Roe 1961, Sergev et al. 1984, Zakharov et al. 1984) or by using the diffusional limitation approach (Baker et al. 1973, Brockmeier and Rogan 1976, Bukatov et al. 1982, Buls and Higgins 1970, Crabtree et al. 1973, McGreavy and Rawlings 1976, Schindler 1963, Schmeal and Street 1972, Singh and Merril 1971 Ross 1984a,b, Meyer 1977, Nagel et al. 1980, Taylor et al. 1982 1983).

Kissin (1985) has pointed out that even for low monomer conversions, when diffusional effects should be minimized, it has been experimentally observed that the copolymer composition is not homogeneous even for polymer produced at constant monomer composition.

A large number of physical models have been proposed in order to explain the wide molecular weight distribution and the copolymer compositional inhomogeneity. Some of these have been described mathematically and applied for simulation purposes (Brockmeier and Rogan 1976, Schmeal and Street 1972, Singh and Merril 1971, Taylor et al. 1982 1983, Galvan 1986, Bosworth 1983). Models have been developed in order to take into account the wide distribution of rate constants. Some attempts consider a small number (around 2) of different sites (Galvan 1986) . The reasons for such a small number of sites seems to be that the added complexity of using more sites may limit the model's use for simulation purposes, and the estimation of the large number of kinetic parameters may be prohibitive. Bosworth (1983) has made an attempt to use statistical distributions (Normal and Log-Normal) for the propagation

rate constants and has concluded that the variance for the distributions must be very large to explain the observed polydispersity. Bosworth considered this large variance to be improbable. Both authors use a model that included diffusional aspects and a few types of active sites.

3.1.2 Why a multiple active site model?

We believe that the existence of a distribution for the rate constant values with respect to the catalyst sites constitutes the most probable hypothesis for explaining the broad molecular weight, copolymer composition and stereoregularity distributions based upon the following reasons.

a) Kissin (1985) states that fractions, separated based upon solubility, of homopolymer produced by heterogeneous Ziegler-Natta catalysts have a characteristic stereoregularity (as measured by melting points, NMR and IR) and is not just a mixture of purely isotactic and atactic polymer. This suggests that there is a continuous distribution of values for the stereo-reactivity ratios s^L, s^D. Where

$$s^D = \frac{k^{DD}}{k^{DL}}$$

$$s^L = \frac{k^{LL}}{k^{LD}}$$

DD and LL represent the two possibilities for isotactic linking between monomers and DL and LD represent the two possible syndiotactic linkings. Diffusional limitation models can not account for this distribution of chains with regard to stereo regularity, but a multiple site model, each type of sites having its characteristic s^D, s^L values, naturally accounts for this phenomenon.

b) Usami et al. (1986) have separated fractions of linear low density polyethylene using temperature-rising elution fractionation (TREF). Their TREF curve had two distinct peaks, representing distinct copolymer compositions. The reactivity ratios, as measured by carbon-13 NMR, were different for each peak. They concluded that each peak was produced by a different kind of active site.

Based upon this evidence we believe that a valid model must include multiple site types for the Ziegler-Natta polymerization of olefins. Under certain conditions it may be necessary to include diffusional limitations for the reactions. This could be added later as necessary (Soares 1992).

3.1.3 A note on collaboration

This modelling was done in collaboration with Bruno de Carvalho and led to the publications de Carvalho et al. (1989a, 1990). de Carvalho's knowledge of the commercial processes was invaluable. A proprietary extension of this project was applied to Polibrasil's[1] polypropylene - ethylene production plant and much of his time was devoted to this proprietary segment (de Carvalho et al. 1989b). Large portions of the mathematical model were derived together, relying a great deal on my, and certainly Dr. Hamielec's, past modelling experience and de Carvalho's background on the chemistry of Ziegler-Natta polymerizations. de Carvalho also derived many of the expressions for the stereo- chemical sequence length distributions presented in de Carvalho et al. (1990), and thus these results are not presented in this thesis.

3.2 Reaction mechanism

The polymerization reactions occur on several reactive site types on the catalyst particle. In general, each type or site (i.e. site of type j) will have different reaction rates associated with it. The reactions listed below correspond to production of j type sites and propagation, transfer, and deactivation reactions on these. It is assumed that a terminal model is appropriate to model these reactions and thus penultimate effects are ignored.

3.2.1 Initiation

We shall define any active site with a monomer molecule or growing polymer chain on it as a propagation site (N(r,j) for r=1,2,3...). Any active site without a monomer molecule or growing chain is an initiation site ($N(0,j), N_H(0,j), N_R(0,j)$). The number of active sites is the sum of the propagation sites and the initiation sites. A potential site (N*(j)) is a site that may react via a formation reaction to form an active site. The total number of sites may be proportional to the total surface area of the catalyst particles.

---

1 Polibrasil (Camaçari, Bahia) was known as Polipropileno S/A at that time.

The formation of type j propagation sites can be written as two reactions. Firstly a potential site on the catalyst particle and the co-catalyst react to form an initiation site, N(0,j). This site can then react with monomer i to produce a propagation site, $N_i(1,j)$, of unit length. The relative rates of these two reactions determine the extent of the acceleration stage in the polymerization (Kissin 1985). The reactions may be written as

$$N^*(j) + co - catalyst \xrightarrow{kf(j)} N(0,j)$$

This initiation site can then react with monomer type 1 or monomer type 2 to form a propagation site of type 1 or 2.

$$N(0,j) + M_1 \xrightarrow{ki_1(j)} N_1(1,j)$$

$$N(0,j) + M_2 \xrightarrow{ki_2(j)} N_2(1,j)$$

The initiation sites $N_H(0,j), N_R(0,j)$ are formed by transfer to hydrogen, spontaneous transfer and transfer to organometallics as explained below.

3.2.2 Propagation

The propagation sites support growing polymer chains. These chains grow by the addition of either monomer type 1 or type 2 to the chain at the point were the chain is attached to the catalyst site. The chain itself can end in either a monomer type 1 or type 2 group. Thus there are four propagation reactions. Reactions between a chain r units long ending in a monomer type i group and a monomer type k molecule (i=1,2 and k=1,2).

$$N_i(r,j) + M_k \xrightarrow{kp_{ik}(j)} N_k(r+1,j)$$

If one assumes a terminal type model then the propagation rate constants are not functions of the penultimate monomer type, but only functions of temperature and site type.

3.2.3 Transfer

As well as undergoing propagation reactions these sites can be involved in transfer reactions. These reactions involve the substitution of a small molecule on the active site, displacing the polymer chain. This chain becomes a dead polymer chain of length r, Q(r), and is no longer involved in the polymerization (is permanently dead). The active site with the small molecule attached can then undergo propagation reactions or initiation reactions to produce propagation sites. Thus one catalyst site can produce many polymer chains during the reaction.

Transfer to hydrogen

Reactions can occur between a chain r units long ending in a monomer type i group and a hydrogen molecule to form an initiation site with a hydrogen on it and a dead polymer chain of length r.

$$N_i(r,j) + H_2 \xrightarrow{kfh_i(j)} N_{II}(0,j) + Q(r)$$

This site can then undergo an initiation reaction with monomer type i to become a growing polymer chain. This probably is the most important transfer reaction for processes that use hydrogen to control molecular weight.

$$N_{II}(0,j) + M_i \xrightarrow{kh_i(j)} N_i(1,j)$$

Transfer to monomer

Reactions can occur between a chain r units long ending in a monomer type i group and a monomer type k molecule to form a site with a monomer k (i.e. a polymer chain of length 1) on it and a dead polymer chain of length r ending with a terminal double bond. This reaction can be expressed as

$$N_i(r,j) + M_k \xrightarrow{kfm_{ik}(j)} N_k(1,j) + Q(r)$$

This site can then undergo propagation to form a long polymer chain.

Transfer to organometallics

Reactions can occur between a chain r units long ending in a monomer type I group and a organometallic molecule left over from the catalyst formation reactions.

$$N_i(r,j) + AR_x \xrightarrow{kfr_i(j)} N_R(0,j) + Q(r)$$

The dead polymer chain has an end group of type AR_{x-1}. This initiation site can then undergo an initiation type reaction with monomer type I to become a growing polymer chain.

$$N_R(0,j) + M_i \xrightarrow{kr_i(j)} N_i(1,j)$$

Spontaneous transfer

The propagation site may be able to spontaneously lose its polymer chain forming a site with a hydrogen on it and a dead polymer chain with a terminal double bond.

$$N_i(r,j) \xrightarrow{kfs_i(j)} N_H(0,j) + Q(r)$$

This site can undergo initiation reactions with monomer to become a growing chain as for transfer to hydrogen. It could be possible for the double bonds created by this

reaction to insert into a catalyst site and propagate thus creating a branched polymer chain. However we feel that in systems where hydrogen is added this reaction will probably be insignificant.

3.2.4 Deactivation

It has been shown (Kissin 1985) that for some polymerizations the rate of reaction will decrease with time. This suggests a catalyst deactivation reaction of unstable centres. It has been found (Keii 1972 1975, Tsvetkova et al. 1969, Spitz et al. 1984, Wu et al. 1982) that the rate of deactivation does not depend upon either the amount or type of monomer present. Thus the rate of deactivation can be considered to be independent of the polymerization process. The deactivation reaction is probably a complex series of reactions but one may be able to approximate it with a first order reaction of the form

$$N(r,j) \xrightarrow{kd(j)} N_d(j) + Q(r) \qquad (r \geq 0)$$

The deactivation reaction forms a dead polymer chain and a dead catalyst site. The rate of decay does not continue until all the catalyst sites are dead. It appears to level off after 1 or 2 hours (Kissin 1985). This suggests that not all j sites have the same stability, and for some site types, kd(j) will be zero.

3.3 Model development

Given the reactions, and the multiple site concept described above, one can derive a model for heterogeneous Ziegler-Natta copolymerization. The following few paragraphs give a brief overview of the approach taken with the details given in the next few sections.

The reaction mechanisms are general, applying to any process, so it should be possible to adapt the model to gas phase (e.g. UNIPOL) or to liquid phase (e.g. slurry), by taking into account the physics and thermodynamics of the system to determine the appropriate concentrations etc. In fact this has been done for UNIPOL (McAuley et al. 1990) and for slurry (de Carvalho et al 1989b). If catalyst break up is important, it will be a function of the physical properties of the catalyst (porosity, support strength etc.) and it must be modelled as well but this is beyond the scope of the work presented here.

The model is a set of mass balances on the important species, and will give a collection of algebraic and ordinary differential equations. We shall assume a perfectly mixed dynamic vessel allowing for both inflow and outflow, and write the equations accordingly, in this way several reactor types are accounted for. For instance a steady state reactor model is given by simply setting the time derivatives to zero and solving the resulting set of algebraic equations.

The rates of each reaction will be written in terms of the concentrations available at the reaction site. It is assumed that the concentrations are the same for all sites, and that these concentrations will be determined by the reactor type. For instance, for a gas phase process one must account for the concentrations in the gas phase, the polymer phase and on the catalyst surface, for a slurry process one must also account for the concentrations in the diluent phase. This partitioning can be modelled using available thermodynamic relationships, if equilibrium can be assumed. Some suggestions are presented in the next section for slurry reactors and for UNIPOL by McAuley et al. (1990)

The equations are written for copolymerization, and pseudo kinetic rate constants (Hamielec and MacGregor 1983) are defined for each site type, to reduce them to simpler homopolymerization equations. In this manner one could also easily extend the model to three or more monomer types.

A balance on the numbers of each site type can be made by accounting for the rates of initiation, deactivation, transfer and inflow and outflow. The rate of polymerization (monomer consumption) is determined by summing the monomer consumption rate on all site types. The copolymer composition produced by each site, can be calculated by performing a mass balance on the moles of each monomer type converted to polymer by that site. Given the distribution of site types, one can find a distribution of compositions. Notice that this gives a single, but different, copolymer composition for each site type, in general each site type will produce a distribution (although it may be narrow) simply due to statistical broadening for short chains. We are assuming that this distribution is much narrower than the overall distribution and thus neglect this statistical broadening. Statistical broadening of compositon can be accounted for, in fact McAuley et al. (1990) used Stockmayer's bivariate distribution (composition and molecular weight) to give a distribution of compositions for each site type.

It is also possible, to derive expressions for the sequence length distribution of the copolymer made on each site type, and thereby the overall sequence length distribution (de Carvalho et al. 1990) of the copolymer product.

The copolymer molecular weights can be calculated in two ways, the first a more general method, gives the average molecular weights for each site type, and thereby the overall averages for the polymer product, and a second method, giving the entire molecular weight distribution. The first, more general method, uses the method of moments, for both the live and the dead polymer species. A balance on polymer of chain length r, for both the living and the dead polymer populations, is made for each site type. Polymer grows by propagation, and is terminated by transfer to hydrogen monomer, or some other small molecule, or spontaneously. Given these balances, it is possible to derive equations for the moments of the living and the dead polymer populations, and thus the overall averages for the polymer product. The second method assumes that the living polymer concentration is much smaller than that of the dead polymer population, and that the inflow and outflow of sites is much smaller than the generation and consumption of site types by initiation, and transfer. Given these assumptions it is possible to derive an expression for the instantaneous chain length distribution produced on a catalyst site type. The overall distribution for the polymer product can be found by averaging over all site types. In this manner the molecular weight distribution can be found, as well as the averages. It can be shown that the polydispersity of the polymer formed under steady state conditions, or instantaneously, is a function only of the overall mean propagation rate constant, and the variance of the propagation rate constant over all site types. The instantaneous molecular weight distribution on each site type has a polydispersity of two and it is the most probable distribution.

In order to specify an active site type distribution, one must be able to assign propagation rate constants for each site type. There does not appear to be any way to define the active site type distribution *a priori*, but only via experimentation. One can arbitrarily define an active site type distribution for simulation purposes. On the other hand a systematic method (but by no means the only method) to select an active site distribution this is to assume that the frequency factor for each site type is the same, and that the activation energies are Normally distributed. In this manner one must only specify the number of site types, one frequency factor, and a mean and a variance for the activation energies. Broad kp distributions can be achieved in this manner, because it approximates a log normal distribution for kp. The number of site types chosen may be

arbitrary, but experimentation may reveal the number of site types. For instance, if two narrow specific molecular weight (or compositional) peaks are observed, one may choose two site types. Alternatively if one were using TREF to measure data with which to estimate the kinetic parameters, it might be appropriate to chose one site type for each TREF fraction. The mean propagation rate must be chosen to give the observed production rate of polymer, and the variance chosen to give the desired polydispersity.

If TREF fractions are obtained, and the molecular weight (by GPC for example) and copolymer compositions (and possibly sequence length distributions by NMR) of each fraction are determined, one could assign an active site type to each fraction. Then based upon the composition and the molecular weights found for the fractions determine a set of reactivity ratios and propagation and transfer rate constants.

One can also define a set of stereo addition rate constants (analogous to copolymer propagation rate constants for binary copolymerization) for each site type. Thus for each type one can identify a parameter S(j) specifying the stereoregulating power of a site type where S(j) is the ratio of isotactic placements over syndiotactic placements. A difficulty arises when one tries to determine the value of S for each j type, since there are no good methods to precisely measure the stereoregularity distribution.

3.3.1 Formation of initiation and propagation sites

The rate of formation of active sites will be given by

$$\left(\begin{array}{c}\text{Rate of formation}\\ \text{of type j active sites}\end{array}\right) = kf(j)\cdot[N^*(j)]\cdot[Co-Cat]\cdot V \qquad \left(\frac{moles}{second}\right)$$

If the co-catalyst is added in excess then

$$\left(\begin{array}{c}\text{Rate of formation}\\ \text{of type j active sites}\end{array}\right) = kf(j)\cdot[N^*(j)]\cdot V \qquad \left(\frac{moles}{second}\right)$$

where [X] denotes concentration of species X. The concentrations of sites are in moles per litre in the reactor, and all other concentrations of reactant species are moles adsorbed per unit of catalyst surface, multiplied by the total catalyst surface area per litre of reaction mixture. In this way all concentrations have units of moles per litre of reaction mixture, i.e.

$$\frac{moles}{area}\cdot\frac{area}{litre}=\frac{moles}{litre}$$

It is assumed that the concentrations of reactants available to each site are independent of the site type and location. It may be that concentrations vary spacially but this is neglected.

In the same manner one could define the concentration of sites as the moles of sites per unit catalyst surface area, multiplied by the total catalyst surface area per unit volume in the reactor. This gives the same result as saying moles of sites per unit volume. In a slurry reactor the volume of the reaction mixture is the volume of the diluent phase, since there are no catalyst sites in the head space of the reactor.

[N*(j)] is the concentration (moles/litre) of potential sites of type j in the reactor, and V is the reaction volume in liters. The units of the second order rate constants are in (litres/mole-second). The deactivation rate constant is assumed not to be a function of the chain composition or molecular weight growing on the site or what type of monomer molecule resides on the site, but only a function of the site type.

The rate of deactivation of active sites will be given by

$$\begin{pmatrix}\text{Rate of deactivation}\\ \text{of type j active sites}\end{pmatrix}=kd(j)\cdot[N_T(j)]\cdot V \qquad \left(\frac{moles}{second}\right)$$

Remember that the deactivation rate constant, kd(j), will be zero for some values of j.

Since transfer and propagation reactions do not change the total number of active sites one obtains a balance on the total number of type j active sites in the reactor as

$$\frac{dN_T(j)}{dt}=kf(j)\cdot[N^*(j)]\cdot V-kd(j)\cdot[N_T(j)]\cdot V$$

$$+N_T(j)_{in}-N_T(j)_{out} \qquad \left(\frac{moles}{second}\right)$$

where

$$N_T(j)=\sum_{r=1}^{\infty}N(r,j)+N_H(0,j)+N_R(0,j)+N(0,j)$$

Notice that $kd(j)$ depends only on j, i.e., it has been assumed to be equal for every kind of site which constitutes $N_T(j)$.

The inflow $(N_T(j)_{in})$ and outflow $(N_T(j)_{out})$ will be determined by the type of process is being used, i.e. batch, semibatch, or continuous.

A balance on the total number of active sites where the number of active sites can be written in terms of moles in the reactor (e.g. $[N(r,j)] \cdot V = N(r,j)$), is given by,

$$\frac{dN_T}{dt} = \overline{kf} \cdot N^*_T - \overline{kd} N_T + N_{T\,in} - N_{T\,out}$$

where

$$\sum_{j=1}^{\infty} N_T(j) = N_T$$

$$\overline{kf} = \sum_{j=1}^{\infty} (kf(j) \cdot \gamma(j))$$

$$\overline{kd} = \sum_{j=1}^{\infty} (kd(j) \cdot \gamma(j))$$

and the fraction of the total active sites that are of type j is given by

$$\gamma(j) = \frac{N(j)}{N_T}$$

The total number of potential sites is N^*_T

One must also perform mass balances on the number of initiation sites in the reactor.

$$\frac{dN_H(0,j)}{dt} = kfh(j) \cdot [H_2] \cdot Y_0(j) + kfs(j) \cdot Y_0(j) - kh(j) \cdot N_H(0,j) \cdot [M] - kd(j) \cdot N_H(0,j) + N_H(0,j)_{in} - N_H(0,j)_{out}$$

$$\frac{dN_R(0,j)}{dt} = kfr(j) \cdot [A] \cdot Y_0(j) - kr(j) \cdot N_R(0,j) \cdot [M] - kd(j) \cdot N_R(0,j) + N_R(0,j)_{in} - N_R(0,j)_{out}$$

$$\frac{dN(0,j)}{dt} = kf(j) \cdot N^*(j) - ki(j) \cdot N(0,j) \cdot [M] - kd(j) \cdot N(0,j) + N(0,j)_{in} - N(0,j)_{out}$$

where $Y_0(j)$ is the zeroth moment of the live polymer distribution on type j sites, or equivalently the moles of j type propagation sites in the reactor. $[A]$ is the concentration of organometallic. The rate constants kfh(j), kfr(j), kfs(j), kh(j), ki(j) and kr(j) are pseudo rate constants that take into account the copolymer and comonomer composition and all the elementary reactions.
I.e.

$$kfr(j) = \phi_1(j) \cdot kfr_1(j) + \phi_2(j) \cdot kfr_2(j)$$

$$kfh(j) = \phi_1(j) \cdot kfh_1(j) + \phi_2(j) \cdot kfh_2(j)$$

$$kfs(j) = \phi_1(j) \cdot kfr_1(j) + \phi_2(j) \cdot kfs_2(j)$$

$$kr(j) = f_1 \cdot kr_1(j) + f_2 \cdot kr_2(j)$$

$$kh(j) = f_1 \cdot kh_1(j) + f_2 \cdot kh_2(j)$$

$$ki(j) = f_1 \cdot ki_1(j) + f_2 \cdot ki_2(j)$$

and $\phi_1(j)$ is the fraction of j type sites that have a growing chain ending with a monomer 1 type unit and accounts for the copolymer composition. f_1 is the mole fraction of the monomer adsorbed onto the catalyst surface that is monomer type 1.

3.3.2 Rate of polymerization

The rate of polymerization can be found from the rate of monomer consumption. The total rate of monomer consumption is given by propagation, transfer and initiation reactions. If one uses the long chain approximation then the consumption of monomer by transfer and initiation reactions is neglected. The rate of polymerization of monomer type 1 is:

$$Rp_1 = \sum_{j=1}^{\infty} (k_{11}(j) \cdot N_1(j) + k_{21}(j) \cdot N_2(j))[M_1] \qquad \left(\frac{moles}{second}\right)$$

where $[M_1]$ is the concentration of monomer on the surface of the catalyst and $N_i(j)$ is the moles of j type sites having a growing chain with monomer of type i at the active site. The rate of polymerization of monomer 2 is given by

$$Rp_2 = \sum_{j=1}^{\infty} (k_{22}(j) \cdot N_2(j) + k_{12}(j) \cdot N_1(j))[M_2] \qquad \left(\frac{moles}{second}\right)$$

The rate of change of moles of total monomer in the reactor is given by

$$\frac{dM}{dt} = \sum_{j=1}^{\infty} -(kp(j)\cdot[M]\cdot N(j)) + M_{in} - M_{out} \qquad \left(\frac{moles}{second}\right)$$

where M is the total moles of monomer, $[M]=[M_1]+[M_2]$ is the concentration of total monomer at the surface of the catalyst, and $N(j)=N_1(j)+N_2(j)$ is the total moles of propagation sites of type j. The pseudo propagation rate constant is given by

$$kp(j) = k_{11}(j)\cdot\phi_1(j)\cdot f_1 + k_{12}(j)\cdot\phi_1(j)\cdot f_2 + k_{21}(j)\cdot\phi_2(j)\cdot f_1 + k_{22}(j)\cdot\phi_2(j)\cdot f_2$$

If one defines the fraction of propagation sites that are of type j then

$$\eta(j) = \frac{N(j)}{N_p}$$

where N_p is the total number of propagation sites.

$$N_p = \sum_{r=1}^{\infty}\sum_{j=1}^{\infty} N(r,j)$$

$$= \sum_{j=1}^{\infty}(N_T(j) - (N_R(0,j) + N_H(0,j) + N(0,j)))$$

$$= \sum_{j=1}^{\infty} Y_0(j)$$

Then the mean propagation rate constant will be given by

$$\overline{kp} = \sum_{j=1}^{\infty} kp(j)\cdot\eta(j)$$

and the rate of polymerization will be given by

$$Rp = \overline{kp}\cdot[M]\cdot N_p \qquad \left(\frac{moles}{second}\right)$$

The instantaneous weight fraction of polymer made by each j site will be given by

$$W(j) = \frac{(m_1 \cdot F_{1inst}(j) + m_2 \cdot (1 - F_{1inst}(j))) \cdot kp(j)N(j)}{\sum_{j=1}^{\infty}(m_1 \cdot F_{1inst}(j) + m_2 \cdot (1 - F_{1inst}(j))) \cdot kp(j) \cdot N(j)}$$

where m_1 and m_2 are molecular weights of monomer 1 and 2 and F_{1inst} is the instantaneous copolymer composition (mole fraction of monomer 1 type units in polymer).

3.3.3 Copolymer composition

The total moles of monomer type 1 bound as polymer (both living and dead) in the reactor is given by the solution to

$$\frac{dP_1}{dt} = \sum_{j=1}^{\infty}((k_{11}(j) \cdot f_1 \cdot \phi_1(j) + k_{21}(j) \cdot \phi_2(j) \cdot f_1)N(j) \cdot [M])$$

$$+ P_{1in} - P_{1out} \qquad \left(\frac{moles}{second}\right)$$

A similar equation can be written for moles of monomer type 2 bound as polymer in the reactor. The copolymer composition of the polymer in the reactor is then given by

$$F_1 = \frac{P_1}{P_1 + P_2}$$

and the instantaneous copolymer composition of the polymer made on a type j site will be given by

$$F_{1inst}(j) = \frac{(r_1(j) - 1) \cdot f_1^2 + f_1}{(r_1(j) + r_2(j) - 2)f_1^2 + 2(1 - r_2(j))f_1 + r_2(j)}$$

where the reactivity ratios for each type of site are given by

$$r_1(j) = \frac{k_{11}(j)}{k_{12}(j)}$$

$$r_2(j) = \frac{k_{22}(j)}{k_{21}(j)}$$

The fraction of propagation sites that have a monomer type 1 end group on it can be found by using the second long chain approximation,

$$k_{12}(j) \cdot \phi_1(j) \cdot f_2 = k_{21} \cdot \phi_2(j) \cdot f_1$$

and

$$\phi_2(j) = 1 - \phi_1(j)$$

to get

$$\phi_1(j) = \frac{k_{21}(i) \cdot f_1}{k_{21}(j) \cdot f_1 + k_{12}(j) \cdot f_2}$$

3.3.4 Concentrations on the catalyst surface

To this point we have described the polymerization in terms of the concentrations of the species on the surface of the catalyst. Unfortunately one does not know these concentrations but the bulk concentrations or partial pressures of the species in the reactor. For this reason one must consider expressions for the surface concentrations in terms of the bulk concentrations.

Any species in the reactor, except growing polymer chains, can, in theory, exist in four phases. These species may be (i) in the vapour phase in the head space, (ii) dissolved in the diluent phase, (iii) in the swollen polymer phase surrounding a catalyst particle, and of course (iv) on the surface of the catalyst. Each species will have different affinities for each phase. There may be diffusion limitations between any two phases, for example, there may be resistance to diffusion from the vapour phase into the liquid phase (Floyd et al 1986, Kisin 1986), or a diffusion limitation from the diluent phase though a very viscous swollen polymer particle to the catalyst surface. These limitations may depend upon the reactor type, and on the operating conditions.

One can find the equilibrium concentrations of the species in the diluent and the vapour phases by using some equation of state (e.g. the Modified Benedict-Webb-Rubin equation (Orye 1969)) or phase-equilibrium constants (Phase equilibrium 1959) to relate the pressure of the reactor to the composition in the liquid phase.

Alternatively, Henry's law could be used to relate the diluent and polymer phase concentrations to the vapour phase concentrations for ethylene and propylene. Raoult's law could be assumed for the diluent concentration in the vapour phase. Thus the ideal gas law would be assumed for the vapour phase. The amount of swelling of the polymer phase by the diluent could be approximated by the Flory-Huggins equation (Flory 1953).

To relate the surface concentrations to the surrounding concentrations one can use the Langmuir adsorption equation. The assumptions that must be valid to use this equations are (Keii 1972) (i) adsorption of a molecule or atom takes place on an adsorption site, and only one molecule can be accepted by each site, (ii) the surface sites all have identical heats of adsorption, and (iii) there are no energy interactions between the adsorbed molecules. Then the fraction of adsorption sites on the catalyst surface that have a species k molecule adsorbed on them is given by

$$\theta_k = \frac{K_k \cdot C_k}{1 + \sum_i K_i C_i}$$

k can be monomer, comonomer, organometallic, or hydrogen and the summation with respect to i includes all species that compete for adsorption sites on the catalyst surface including species k.

K_i is the adsorption equilibrium constant for species i and is a function of temperature

$$K_i = Ko_i \cdot \exp\left(\frac{E_i}{RT}\right)$$

the activation energy E_i is in the order of 10 kcal per mole (Keii 1972)

C_i is the concentration of species i in the surrounding phase.

The total concentration of species k on the surface is given by

$$[k] = \theta_k \cdot \theta_T \qquad \left(\frac{moles}{volume}\right)$$

θ_T is the total number of adsorption sites on the catalyst surface per unit volume. This value is proportional to the total catalyst surface area divided by the volume of the reaction mixture.

A diatomic molecule like H_2, which is adsorbed in the dissociated form, the term $K_H \cdot C_H$ is replaced by $(K_H \cdot C_H)^{1/2}$. It should be noted that the parameters to relate the concentrations will be grouped with the rate constants for the chemical reactions, and thus if absolute values for the thermodynamic parameters are not found, the simulations should still be valid because the estimated reaction rate constants should compensate for the error.

3.3.5 Molecular weight development

In order for the model to be useful, it must be able to predict the molecular weight of the polymer produced. The development of the molecular weight equations is presented for the general case, and then a simplified development is derived. This simplified set of equations will be applicable under certain operating conditions and gives us a different insight into the factors that affect the molecular weight distribution. The simplified equations are easier to solve.

General development

In general both the molecular weight of the live and dead polymer contribute significantly to the overall molecular weights. For this general case it would be difficult to solve for the molecular weight distribution, but easy to solve for the leading moments of the distribution. In this case one can obtain expressions for the number and weight average molecular weights and for the polydispersity of the distribution.

If one considers a balance on the moles of growing chains of length r on a j type site (for r greater than or equal to 2)

$$\frac{dN(r,j)}{dt} = kp(j)\cdot[M]\cdot N(r-1,j) - kp(j)\cdot[M]\cdot N(r,j)$$
$$- kt(j)\cdot N(r,j) - kfm(j)\cdot[M]\cdot N(r,j) - kd(j)\cdot N(r,j)$$
$$+ N(r,j)_{in} - N(r,j)_{out}$$

where

$$kt(j) = kfs(j) + kfh(j)\cdot[H_2] + kfr(j)\cdot[A]$$

All of the rate constants presented here are pseudo rate constants that take into account the comonomer and copolymer composition.

A balance on propagation site type j of unit length yields

$$\frac{dN(1,j)}{dt} = kfm(j)\cdot[M]\cdot Y_0(j) + kI(j)\cdot[M] - kd(j)\cdot N(1,j) - kt(j)\cdot N(1,j) - kp(j)\cdot[M]\cdot N(1,j) - kfm(j)\cdot[M]\cdot N(1,j) + N(1,j)_{in} - N(1,j)_{out}$$

where

$$kI(j) = kr(j)\cdot N_R(0,j) + kh(j)\cdot N_H(0,j) + ki(j)\cdot N(0,j)$$

and $Y_0(j)$ is the zeroth moment of the live polymer distribution on site type j. The consumption of N(1,j) by transfer to monomer term appears because we have included N(1,j) in the generation of N(1,j) by transfer to monomer (in $Y_0(j)$).

The definition of the nth moment of the live polymer distribution is

$$Y_n(j) = \sum_{r=0}^{\infty} r^n \cdot N(r,j)$$

and notice that N(0,j) (i.e. r=0) is not considered live polymer so the summation may start at r=1 instead of r=0.

To find this moment we must simply multiply the equation for N(r,j) by r^n and sum it from $r = 2 \rightarrow \infty$ then add the equation for N(1,j) to complete the sum from $r = 1 \rightarrow \infty$.

Setting n = 0 and noting that

$$\sum_{r=2}^{\infty} N(r-1,j) = \sum_{r=1}^{\infty} N(r,j) = Y_0(j)$$

one gets

$$\frac{dY_0(j)}{dt} = kl(j)\cdot[M] - kt(j)\cdot Y_0(j) - kd(j)\cdot Y_0(j) + Y_0(j)_{in} - Y_0(j)_{out}$$

Repeating this procedure for n=1 and noting that

$$\sum_{r=2}^{\infty} r\cdot N(r-1,j) = \sum_{r=1}^{\infty} (r+1)\cdot N(r,j) = Y_1(j) + Y_0(j)$$

and that

$$Y_2(j) \gg Y_1(j) \gg Y_0(j)$$

one gets

$$\frac{dY_1(j)}{dt} = kp(j)\cdot[M]\cdot Y_0(j) + kl(j)\cdot[M] - kfm(j)\cdot[M]\cdot Y_1(j) - kt(j)\cdot Y_1(j) - kd(j)\cdot Y_1(j) + Y_1(j)_{in} - Y_1(j)_{out}$$

And repeating this procedure for n=2 and noting that

$$\sum_{r=2}^{\infty} r^2\cdot N(r-1,j) = \sum_{r=1}^{\infty} (r+1)^2\cdot N(r,j) = Y_2(j) + 2Y_1(j) + Y_0(j)$$

one gets

$$\frac{dY_2(j)}{dt} = kp(j)\cdot[M]\cdot 2\cdot Y_1(j) + kl(j)\cdot[M] - kfm(j)\cdot[M]\cdot Y_2(j) - kt(j)\cdot Y_2(j) - kd(j)\cdot Y_2(j) + Y_2(j)_{in} - Y_2(j)_{out}$$

Now one must account for the dead polymer produced by the transfer and deactivation reactions. A balance on dead polymer of chain length r produced by a j type site gives (for r greater than or equal to 2)

$$\frac{dQ(r,j)}{dt} = kt(j)\cdot N(r,j) + kfm(j)\cdot[M]\cdot N(r,j) + kd(j)\cdot N(r,j) + Q(r,j)_{in} - Q(r,j)_{out}$$

Since Q(1,j) is not considered dead polymer Q(1,j)=0.

Let the nth moment of the dead polymer distribution produced by a type j site be given by

$$X_n(j) = \sum_{r=1}^{\infty} r^n Q(r,j)$$

The N(1,j) term must be subtracted since the transfer reactions with N(1,j) do not produce polymer but

$$Y_2(j) \gg Y_1(j) \gg Y_0(j) \gg N(1,j)$$

The moments of the dead polymer distribution produced by site j are given by

$$\frac{dX_0(j)}{dt} = (kt(j) + kfm(j)\cdot[M] + kd(j))\cdot Y_0(j) + X_0(j)_{in} - X_0(j)_{out}$$

$$\frac{dX_1(j)}{dt} = (kt(j) + kfm(j)\cdot[M] + kd(j))\cdot Y_1(j) + X_1(j)_{in} - X_1(j)_{out}$$

$$\frac{dX_2(j)}{dt} = (kt(j) + kfm(j)\cdot[M] + kd(j))\cdot Y_2(j) + X_2(j)_{in} - X_2(j)_{out}$$

Now having the moments of the live and dead polymer distribution one can find the accumulated number and weight average chain lengths of the accumulated polymer product

$$\overline{rn} = \frac{\sum_{j=1}^{\infty}(Y_1(j) + X_1(j))}{\sum_{j=1}^{\infty}(Y_0(j) + X_0(j))}$$

$$\overline{rw} = \frac{\sum_{j=1}^{\infty}(Y_2(j) + X_2(j))}{\sum_{j=1}^{\infty}(Y_1(j) + X_1(j))}$$

and the polydispersity is given by $\overline{rw}/\overline{rn}$.

Simplified analysis

This simplified analysis depends upon making some assumptions about the operating conditions in the reactor. This analysis allows one to find a simple expression for the instantaneous molecular weight distribution and expressions for the number and weight average molecular weights as well as for the polydispersity.

We shall introduce these assumptions at the points where they are needed in the derivation. Firstly, the stationary state hypothesis (SSH) for growing chains of length r will be assumed. This assumption involves the supposition that most of the polymer in the reactor is dead polymer, and the life time of the growing polymer is short with respect to the total polymerization time. This assumption should be valid for cases where the hydrogen concentration in the reactor is high enough for large transfer rates. Secondly, it will be assumed that the inflows and outflows of live polymer chains are negligible. If the concentration of live polymer in the reactor is small then this should

be valid. Furthermore, the deactivation rate will be considered to be negligible. Therefore, the moles of growing chains on type j sites with a chain length of two or greater will be given by:

$$N(r,j) = \frac{kp(j)\cdot[M]\cdot N(r-1,j)}{kp(j)\cdot[M]+kt(j)+kfm(j)\cdot[M]} \qquad (moles)$$

If we let

$$\tau(j) = \frac{kt(j)}{kp(j)\cdot[M]} + \frac{kfm(j)}{kp(j)}$$

$$= \frac{kfs(j)+kfh\cdot[H_2]+kfr(j)[A]}{kp(j)\cdot[M]} + \frac{kfm(j)}{kp(j)}$$

If only transfer to hydrogen is important, this equation becomes:

$$N(r,j) = \left(\frac{1}{1+\tau(j)}\right)\cdot N(r-1,j)$$

$$= \left(\frac{1}{1+\tau(j)}\right)^{(r-1)}\cdot N(1,j)$$

Considering the chains of unit length, the application of both the SSH and the assumption for negligible amount of these species in the stream, as made above, leads to:

$$N(1,j) = \frac{kfm(j)\cdot[M]\cdot Y_0(j)+kt(j)\cdot[M]}{kp(j)\cdot[M]+kt(j)+kfm(j)\cdot[M]}$$

$$= \frac{\left(\frac{kfm(j)}{kp(j)}\right)Y_0(j)+\left(\frac{kt(j)}{kp(j)}\right)}{1+\tau(j)} \qquad (moles)$$

Now, repeating the same procedure for the initiation type sites, one gets:

$$N_H(0,j) = \frac{(kfh(j)+kfs(j))\cdot Y_0(j)}{kh(j)\cdot[M]} \qquad (moles)$$

$$N_R(0,j) = \frac{kfr(j)Y_0(j)}{kr(j)\cdot[M]} \qquad (moles)$$

$$N(0,j) = \frac{kf(j)\cdot N^*(j)}{ki(j)\cdot[M]} \qquad (moles)$$

Substituting these in to the balance for N(1,j) and dividing both top and bottom by kp(j)[M] one gets

$$N(1,j) = \frac{\tau(j) \cdot Y_0(j) + \frac{kf(j) N^*(j)}{kp(j) \cdot [M]}}{1 + \tau(j)}$$

let

$$\beta(j) = \frac{kf(j) \cdot N^*(j)}{kp(j) \cdot [M]}$$

thus

$$N(r,j) = \left(\frac{1}{1+\tau(j)}\right)^r (\beta(j) + \tau(j) \cdot Y_0(j))$$

The instantaneous weight fraction of dead polymer produced on a j type site that is length r is given by

$$Wd(r,j) = \frac{(kfm(j) \cdot [M] + kfh(j)[H_2] + kfr(j)[A] + kfs) N(r,j) \cdot r}{kp(j) \cdot [M] \cdot Y_0(j)}$$

$$= \tau(j) \cdot r \cdot \left(\frac{N(r,j)}{Y_0(j)}\right)$$

$$Wd(r,j) = \left(\frac{1}{1+\tau(j)}\right)^r \cdot r \cdot (\tau(j) \cdot \beta(j) + \tau(j)^2)$$

If we assume that all the active sites are formed before flowing into the reacto then $\beta(j) = 0$ and we define

$$\psi(j) = \frac{1}{1+\tau(j)}$$

then

$$Wd(r,j) = \tau(j)^2 \cdot r \cdot \psi(j)^r$$

We have assumed that both the formation and the deactivation of active sites are negligible during the polymerization. This means that the number of active sites remains constant throughout the polymerization.

The instantaneous weight fraction of polymer produced by a type j site is given by

$$W(j) = \frac{kp(j) \cdot Y_0(j)}{\overline{kp} \cdot N_p}$$

The overall dead polymer instantaneous molecular weight distribution is given by

$$Wd(r) = \sum_{j=1}^{\infty} W(j) \cdot \tau(j)^2 \cdot r \cdot \psi(j)^r$$

$$= \sum_{j=1}^{\infty} \frac{kp(j) \cdot Y_0(j)}{\overline{kp} N_p} \cdot \tau(j)^2 \cdot r \cdot \psi(j)^r$$

The instantaneous weight average chain length is given by

$$rw = \sum_{r=1}^{\infty} (r \cdot Wd(r))$$

$$= \sum_{j=1}^{\infty} \left(W(j) \cdot \tau(j)^2 \cdot \sum_{r=1}^{\infty} r^2 \cdot \psi(j)^r \right)$$

Notice that

$$\sum_{r=1}^{\infty} (r^2 \cdot \psi(j)^{r-1}) = \frac{1 + \psi(j)}{(1 - \psi(j))^3}$$

Then

$$rw = \sum_{j=1}^{\infty} W(j) \cdot \tau(j)^2 \cdot \psi(j) \left(\frac{1 + \psi(j)}{(1 - \psi(j))^3} \right)$$

If $\tau(j) \ll 1$ (as it should be since it is the ratio of transfer reactions to propagation reactions) then

$$\psi(j) \cong 1$$

and

$$1 - \psi(j) = 1 - \left(\frac{1}{1 + \tau(j)} \right) = \frac{\tau(j)}{1 + \tau(j)} \cong \tau(j)$$

then

$$rw = 2 \sum_{j=1}^{\infty} \frac{W(j)}{\tau(j)}$$

replacing W(j) we find that

$$rw = \frac{2}{kp} \sum_{j=1}^{\infty} \frac{kp(j)^2 \cdot \eta(j)}{\lambda(j)}$$

where

$$\lambda(j) = kfm(j) + \frac{kfs(j)}{[M]} + \frac{kfr(j) \cdot [A]}{[M]} + \frac{kfh(j) \cdot [H_2]}{[M]}$$

Thus the instantaneous weight average chain length for the polymer produced by a type j site is given by

$$rw(j) = \frac{2}{\tau(j)}$$

The instantaneous number average chain length is given by

$$rn = \frac{1}{\sum_{r=1}^{\infty} \left(\frac{W(r)}{r} \right)}$$

$$\frac{1}{rn} = \sum_{j=1}^{\infty} \left(W(j) \cdot \tau(j)^2 \sum_{r=1}^{\infty} \psi(j)^r \right)$$

Since

$$\sum_{r=1}^{\infty} \psi(j)^{r-1} = \frac{1}{1 - \psi(j)}$$

Therefore

$$\frac{1}{rn} = \sum_{j=1}^{\infty} \left(W(j) \cdot \tau(j)^2 \cdot \frac{\psi(j)}{1 - \psi(j)} \right)$$

$$= \frac{1}{kp} \cdot \sum_{j=1}^{\infty} \eta(j) \cdot \lambda(j)$$

also notice that the number average molecular weight of the polymer produced by a type j site is given by.

$$rn(j) = \frac{1}{\tau(j)}$$

If we assume that the transfer reactions are not functions of the type of reactive site, then $\lambda(j)$ is not a function of j. It may quite well be valid if the rate of transfer to hydrogen dominates the transfer process. Hydrogen is a small molecule and may therefore have a transfer rate that is independent of the site type. Thus, the instantaneous polydispersity is given by

$$\frac{rw}{rn} = 2\left(1 + \frac{\sigma^2}{\overline{kp}^2}\right)$$

where σ^2 is the variance of the distribution of propagation rate constants.

$$\sigma^2 = \sum_{j=1}^{\infty} \eta(j) \cdot (kp(j) - \overline{kp})^2$$

We have derived an expression for the instantaneous polydispersity that uses only the mean propagation rate constant and the variance of the kp(j)'s. The instantaneous molecular weight distribution for each j site is the most probable (rw(j)/rn(j)=2) and varies from the most probable for the entire polymer produced by ratio of the variance of the kp(j)'s to the mean kp value. Nevertheless, this expression should be seen as an approximation which will only be valid if all the assumptions made during its derivation were fulfilled. As we have pointed out above, the molecular weight distribution for a copolymer produced with heterogeneous Ziegler-Natta catalyst is broad even if the polymerization is carried out under steady state conditions at constant monomer ratio. In that case, this equation is actually not able to predict a broad molecular weight distribution when some of the most common statistical distributions are adopted for the propagation rate constant, $k_p(j)$. For instance, if the propagation rate constant is assumed as exponentially distributed this equation will give a small value (equal to 4) for the polydispersity. In addition, if a normal distribution is assumed, one may have to consider negative values for the rate constant in order to achieve the usual large values for the polydispersity. Consequently, in order to explain the wide molecular weight distribution by using this equation, one must adopt a skewed distribution for the propagation rate constant, such as the log-normal distribution.

To find the accumulated number and weight average molecular weights and polydispersity ($\overline{rn}, \overline{rw}, \overline{rw}/\overline{rn}$) one must find the weighted averages of the instantaneous values (rn, rw, rw/rn) and the inflows and outflows. To find the accumulated weight average chain length we must take a mass weighted average of rw, i.e. we must

weight the instantaneous rw by the mass of polymer that is that rw. Mp is the mass of polymer in the reactor and m is the effective molecular weight per repeat unit. The subscripts 'in' and 'out' denote inflowing and outflowing quantities.

$$\frac{dMp \cdot \overline{rw}}{dt} = \overline{rw}_{in} \cdot Mp_{in} + rw \cdot m \cdot \overline{kp} \cdot N_p \cdot [M] - \overline{rw}_{out} \cdot Mp_{out}$$

$$\frac{dMp}{dt} = Mp_{in} + m \cdot \overline{kp} \cdot N_p \cdot [M] - Mp_{out}$$

and the accumulated weight average molecular weight of the polymer in the reactor is given by the ratio of the solutions to the two equations above, i.e.

$$\overline{rw} = \frac{Mp \cdot \overline{rw}}{Mp}$$

For an ideal CSTR the properties of the outflowing polymer are the accumulated properties in the reactor, i.e. $\overline{rw}_{out} = \overline{rw}$

To find the accumulated number average chain length we must find the number weighted average of rn, i.e. we must weight the instantaneous rn by the number of moles of polymer that is that rn, i.e. $Mp/(m \cdot rn)$.

$$\frac{d}{dt}\left(\frac{Mp}{m \cdot \overline{rn}}\right) = \frac{Mp_{in}}{m \cdot \overline{rn}_{in}} + \frac{\overline{kp} \cdot N_p \cdot [M]}{rn}$$

$$- \frac{Mp_{out}}{m \cdot \overline{rn}_{out}}$$

The number average chain length is then given by dividing the mass of polymer in the reactor by the solution to the above equation, i.e.

$$\overline{rn} = \left(\frac{1}{m}\right) \cdot \left(\frac{Mp}{Mp/(m \cdot \overline{rn})}\right)$$

and the accumulated polydispersity is given by the ratio of the accumulated averages.

The accumulated molecular weight distribution is given by weighting the mass of fraction of polymer of chain length r by the mass of polymer in exactly the same manner as we found the accumulated weight average molecular weight.

$$\frac{dMp \cdot \overline{Wd}(r)}{dt} = \overline{Wd}(r)_{in} \cdot Mp_{in} + \sum_{j=1}^{\infty} (Wd(r,j) \cdot m \cdot kp(j) \cdot Y_0(j) \cdot [M]) - \overline{Wd}(r)_{out} \cdot Mp_{out}$$

and

$$\overline{Wd}(r) = \frac{Mp \cdot \overline{Wd}(r)}{Mp}$$

We now have expressions for the accumulated number and weight average molecular weights. But more importantly we now have a simple expression for the instantaneous molecular weight distribution. From this we can calculate the weight fraction of polymer of any chain length and not just the averages.

3.4 Estimation of parameters

Possibly, the major difficulty associated with a model which takes into account a multiple activity site distribution is the large number of parameters to be estimated. Cozewith and Ver Strate (1971) have shown that if N multiple sites are present, the reactivity ratios estimated from the conventional copolymerization equation (r_1 and r_2) should be seen as average values. Following our nomenclature, these averages can be expressed as:

$$r_i = \frac{\sum_{j=1}^{N} (r_i(j) \cdot k_{ik}(j) \cdot \phi_i(j) \cdot \eta(j))}{\sum_{j=1}^{N} (k_{ik}(j) \cdot \phi_i(j) \cdot \eta(j))}$$

where k, i = 1, 2; $k \neq i$

Analyzing a binary monomer system, Cozewith and Ver Strate (1971) have concluded that the product of these average values falls between the reactivity ratio products of the individual j sites. Moreover, the application of the average $r_1 \cdot r_2$ values and the average copolymer composition to predict the propagation probability underestimate the amount of material in longer sequences.

Many attempts have been made in order to calculate the reactivity ratios for whole insoluble samples of copolymers produced with heterogeneous Ziegler-Natta catalysts. Some of them have used the multiple active site hypothesis because these copolymers failed the first-order Markov process. Carbon-13 NMR has been applied as a powerful technique to calculate reactivity ratios and the chemical composition distribution (Kakugo et al 1982, Ross 1986) Analyzing propylene/ethylene copolymer produced with $TiCl_3$, Kakugo et al. (1982) have interpreted discrepancies for ethylene centered triads, determined with basis on r_i, as though they were caused by at least two different kind of sites. Ross (1984a, 1986) and very recently Cozewith (1987), has discussed Kakugo's data. The former has derived equations for diad and triad distributions with regard to multiple sites, each site having random character. This model fit Doi (1983) and Kakugo's data much better than the first-order Markov approach. Cozewith has analyzed the suitability of three different models (single site, multiple sites with $r_1 \cdot r_2 = 1$, and two-sites also having random character) to fit data generated not only from their work but also by Kakugo (1982), Ray et al. (1977), and Doi (1983). They concluded that multiple catalyst species were present in all cases, in general more than two. According to their estimates, the reactivity ratio products for the individual sites lie between 0.5 and 3.0. Even so, the two-random site model was appropriate for many cases.

As it has been pointed out above, the reactivity ratios calculated with basis on a sample of the whole insoluble copolymer are averages of the individual reactivity ratios. Therefore, in order to determine the individual reactivity ratios it is necessary to perform NMR on each copolymer fraction produced by each j site type.

We shall point out how to estimate the main parameters of the model presented in the previous sections, without assuming any particular character for the j sites.

3.4.1 A conceptual approach

Considering a binary copolymer produced using a heterogeneous Ziegler-Natta catalyst one should identify three main sources of heterogeneity:

a) That which is caused by differing mean chain lengths for each site and leads to the broad molecular weight distribution;

b) That which is caused by differing mean chemical composition for each site and results in the existence of a broad comonomer sequence distribution; and

c) That which is caused by differing mean stereo regularities for each site and brings about the existence of a broad stereo sequence distribution.

The ideal approach would consist of an effective technique which was capable of either separating fractions according to their chemical composition independent of both molecular weight and stereoregularity distributions, or fractionating the copolymer in terms of its stereoregularity independent of molecular weight and chemical composition distributions. If such a procedure were to exist, one could develop the following conceptual model: each fraction obtained by this procedure would be generated by an individual type of site, having as its characteristic parameters the rate constants for formation, initiation, transfer, deactivation, and propagation reactions. Therefore, by analyzing each fraction, one could determine, for each type of site, the main parameters associated with molecular weight, chemical composition and stereoregularity distributions, which are functions of the rate constants.

As this ideal technique does not exist, we will develop a practical approach to estimate, as well as possible, the parameters for the model by using TREF, NMR and GPC techniques, while maintaining the conceptual basis for the existence of individual site types which produce particular fractions.

3.4.2 A practical approach

Attempts have been made to achieve separation based on compositional differences by using fractionation based upon crystallizability, via either isothermal crystallization at successive lower temperatures (Allen et al. 1964, Kamath and Wild 1966) or isothermal dissolution at a series of rising temperatures (Wijga et al. 1960, Nakajima and Fujiwara 1964).

Recently, Wild et al. (1982) have reported an improved temperature-rising elution fractionation (TREF) system capable of fractionating a copolymer according to its chemical composition without being influenced to a great extent by both molecular weight distribution and co-crystallization effects between unlike macromolecule species. Wild used mainly polyethylene and ethylene α-olefin copolymers to develop the analytical technique called TREF so that short branching constituted the main source for copolymer inhomogeneity. At that time Wild suggested the possibility to perform joint TREF and SEC analysis in order to characterize copolymers.

Following Wild's ideas, Nakano and Goto (1981) have developed an automatic cross-fractionation technique which combined both crystallizability and molecular weight fractionation. Nevertheless, Nakano was more concerned with the analytical technique itself than with the copolymer structure interpretation.

Subsequently, Wild et al. (1986) reported the analysis of cross-fractionation data in which fractions obtained by TREF were subjected to SEC measurements. By following such methodology he has obtained tridimensional plots for characterizing not only HP-LDPE but also LLDPE polymers. According to these plots, HP-LDPE has a unimodal bivariate distribution whereas LLDPE is bimodal.

In 1986, Usami et al. reported an attempt to characterize TREF fractions of copolymers (LLDPE) produced with heterogeneous Ziegler-Natta catalysts. Analyzing LLDPE samples from four different continuous processes (gas-phase, bulk, solution, and slurry), he found bimodal TREF distributions for all of them, confirming Wild's observations. As the hypothesis for the existence of a common discontinuous change in monomer concentration in the four processes seemed to be quite improbable, he assumed that the cause for the bimodal distribution should be associated with the existence of at least two site types on the catalyst used each having its characteristic reactivity ratio product. After having obtained six fractions of a sample from the gas-phase process, he observed sharp DSC thermograms for each one, indicating that the TREF performed well. He also obtained three more fractions on the same sample by using only three elution temperatures instead of the previous six. For five of the first six fractions, as well as for the last three, the reactivity ratio products were determined using carbon-13 NMR. In general, the values were different for each fraction, varying from 0.49 to 1.00. He concluded that the two peaks on the TREF curves were caused by two different site types, one having an alternating character ($r_1(1) \cdot r_2(1) = 0.50$ to 0.60) and the other having random character ($r_1(2) \cdot r_2(2) = 1.00$). The molecular weight distribution measurements allowed him to also state that the sites with alternating character produce lower molecular weight polymer whereas the sites with random character give the higher molecular weight polymer.

The methodology of the work described above constitutes the most advanced tool for estimation of the parameters of a multiple site model available at this time. It is a practical attempt to carry out the ideal approach presented above. However, as it will be shown, extensive analysis on TREF fractions are able to estimate directly only those parameters which lead to monomer reaction rates, chemical composition, and molecular weight distribution. The stereoregularity parameters for each kind of site can not be estimated in this manner because four different rate constants for isotactic and syndiotactic addition are included in each rate constant for propagation. Moreover, even though the TREF fractionation is not strongly influenced by molecular weight distribution and co-crystallization between unlike chains, it seems improbable that the

fractionation should be independent of the stereoregularity. Therefore, unless the amount of atactic and stereo-block polymer is negligible, an overlap between chemical and configurational compositions should be expected when performing fractionation based on crystallizability. Otherwise, a previous segregation of the polymer in atactic (that fraction soluble in cold solvent), stereo-block polymer (that fraction soluble in boiling solvent), and isotactic (that insoluble fraction) should be performed before the TREF analysis in order to reduce the effects of stereo-inhomogeneity.

Mathematical treatment

Having obtained a TREF curve by analyzing a copolymer sample produced with constant monomer composition, one can, using a calibration curve, generate a plot between the weight percent of copolymer and the copolymer composition. Then, following our conceptual model, each discretized coordinate on the TREF curve can be seen as a particular point which corresponds to a individual type of site. Evidently, in a practical sense one has to select the significant coordinates through a careful analysis of the TREF pattern and operational conditions. Nevertheless, the TREF curve is not sufficient, by itself, to estimate all the parameters because the copolymer composition equation:

$$F_{k_{inst}}(j) = \frac{\left(r_k(j)\cdot\left(\frac{f_1}{1-f_1}\right)+1\right)}{\left(r_1(j)\cdot\left(\frac{f_1}{1-f_1}\right)+1\right)+\left(r_2(j)\cdot\left(\frac{1-f_1}{f_1}\right)+1\right)}$$

where k = 1, 2, can not be solved for both $r_1(j)$ and $r_2(j)$. Thus, each chosen fraction ought to be subjected to extensive characterization. Each fraction of copolymer taken from the elected TREF coordinates will consist of chains which are constituted by four kinds of diad sequences, namely:

$$d_{ik}(j) \text{ for } M_k \text{ units added to the } N_i(j) \text{ sites.}$$

where i, k = 1, 2. Each of these diad compositions is produced according to its corresponding propagation equation. Therefore, the instantaneous number of diads can be derived from:

$$d_{ik_{inst}}(j) = \frac{k_{ik}(j)\cdot\phi_i(j)\cdot f_k}{k_p(j)}$$

Using both the first and the second long chain approximation, and if the copolymer comes from a steady state process in which not only the monomer composition is constant throughout the copolymerization the four diad composition equations can be reduced to:

$$d_{11}(j) = \frac{r_1(j)\cdot\left(\frac{f_1}{1-f_1}\right)}{\left(r_1(j)\cdot\left(\frac{f_1}{1-f_1}\right)+1\right)+\left(r_2(j)\cdot\left(\frac{1-f_1}{f_1}\right)+1\right)}$$

$$d_{12}(j) = d_{21}(j) = \frac{1}{\left(r_1(j)\cdot\left(\frac{f_1}{1-f_1}\right)+1\right)+\left(r_2(j)\cdot\left(\frac{1-f_1}{f_1}\right)+1\right)}$$

$$d_{22}(j) = \frac{r_2(j)\cdot\left(\frac{1-f_1}{f_1}\right)}{\left(r_1(j)\cdot\left(\frac{f_1}{1-f_1}\right)+1\right)+\left(r_2(j)\cdot\left(\frac{1-f_1}{f_1}\right)+1\right)}$$

Now it follows that:

$$F_k(j) = (d_{ik}(j))_{i=k} + (d_{ik}(j))_{i\neq k}$$

And therefore the reactivity ratios can be expressed as:

$$r_k(j) = \frac{(d_{ik}(j))_{i=k}\cdot(1-f_k)}{(F_k(j)-(d_{ik}(j))_{i=k})\cdot f_k}$$

It should be recognized that both $F_k(j)$ and $d_{ik}(j)$ can be interpreted in terms of probabilities. The former represents the probability of a k monomer addition to any site whereas the latter is the probability of a k monomer addition to an i site, producing a specific ik diad. Note that one can also define the following conditional probabilities from the diads and copolymer composition, for the formation of a new i site from a given k site, as:

$$p_{ik}(j) = \frac{d_{ik}(j)}{F_k(j)}$$

Or, in kinetic terms:

$$p_{ik}(j) = \frac{k_{ik}(j)\cdot\phi_k\cdot f_i}{\sum_{i=1}^{2}(k_{ik}(j)\cdot\phi_k\cdot f_i)}$$

For a given k, these conditional probabilities are such that:

$$\sum_{i=1}^{2} p_{ki}(j) = 1$$

Therefore, the reactivity ratios can be calculated via:

$$r_k(j) = \frac{(p_{(kk)}(j)) \cdot (1 - f_k)}{(p_{(ki)}(j)) \cdot f_k}$$

And by using carbon-13 NMR on each TREF fraction, those conditional probabilities can be determined providing estimation for each j set of reactivity ratios. Furthermore, the main parameters associated with the propagation rate can be estimated from the weight fraction of the copolymer, as follows. The weight of the copolymer sample subjected to TREF is given by:

$$S_w = \sum_{j=1}^{\infty} (m_1 \cdot F_1(j) + m_2 \cdot (1 - F_1(j))) \cdot k_p(j) \cdot \eta(j) \cdot \Delta t$$

where Δt is some small interval of reaction time. Also, the weight of each selected TREF fraction is given by:

$$S_w(j) = (m_1 \cdot F_1(j) + m_2 \cdot (1 - F_1(j))) \cdot k_p(j) \cdot \eta(j) \cdot \Delta t$$

Thus, the weight fraction of copolymer for each j fraction can be split for both k = 1 and k = 2 monomers according to:

$$W_k(j) = F_k(j) \cdot W(j)$$

where:

$$W(j) = \frac{S_w(j)}{S_w}$$

It provides the following pair of equations (k=1,2) for each j fraction:

$$W_k(j) = \left(\frac{m_k \cdot F_k(j) \cdot \eta(j)}{S_w} \right) \cdot (k_{11}(j) \cdot \phi_1(j) \cdot \left(f_1 + \frac{f_2}{r_1(j)} \right) + k_{22}(j) \cdot \phi_2(j) \cdot \left(\frac{f_1}{r_2(j)} + f_2 \right))$$

and from the second long chain approximation, as before

$$\phi_1(j) = \frac{\frac{k_{22}(j)}{r_2(j)} \cdot f_1}{\frac{k_{22}(j)}{r_2(j)} \cdot f_1 + \frac{k_{11}(j)}{r_1(j)} \cdot f_2}$$

$$\phi_2(j) = 1 - \phi_1(j)$$

Therefore, these equations can be solved for the propagation rate parameters, namely:

$$k_{ik}(j) \cdot \eta(j)$$

In order to complete the estimation process, GPC analysis carried out on each TREF fraction provides estimations for $Mn(j)$, and $Mw(j)$. Thus, $\tau(j)$ can also be evaluated, making the determination of the total transfer rate constant possible.

3.5 Simulations

We shall use this model to perform some simple calculations to generate TREF and molecular weight plots. It will be shown that this model is able to predict, even for a copolymer produced under steady state conditions, broad chemical composition and molecular weight distributions. If the model is able to simulate TREF and molecular weight plots then it should be possible to estimate model parameters from actual TREF and molecular weight measurements.

For illustrational purposes we shall arbitrarily choose a distribution for the propagation rate constant, which has mean values roughly corresponding to literature values for the copolymerization of propylene (1) and ethylene (2) with titanium trichloride and aluminum alkyl as active catalyst. However, just what should the distribution look like? Since we know nothing about the actual λ distributions, we can adopt an empirical distribution for the propagation rate constants so as to have the parameters of these distributions as adjustable model parameters. These distributions must be in agreement with experimental evidence, i.e., they ought to be positively skewed. Proceeding in this manner, we can only generate speculative results for the polymer microstructure simulation. Unfortunately, any choice of distribution for $\lambda(j)$ will be completely arbitrary, because there are no reasonable guidelines for the choice of this distribution.

3.5.1 Active Site Distribution

The chosen distribution for the propagation rate constants must be consistent with the experimental evidence available. Kissin (1985) has reported that for propylene

polymerization with $\delta - TiCl_3 + AlEt_2Cl$ at 30 °C, the range for the propagation rate constant is quite wide: 2.0 to 500.0 liter/mol-sec. The average value (about 10.0 liter/mol-sec.) is, however, much smaller than the upper limit. Bohm (1978a) has also reported analogous figures for ethylene polymerization at 85 °C, using a highly active catalyst system, obtained by reacting $Mg(OEt)_2$ with $TiCl_4$. Interpreting GPC data from polymer produced in different stages of polymerization (15 and 7200 seconds), he has concluded that 2% of the active sites have a very high propagation rate constant (greater than 2900 liter/mol-sec.), whereas most of them (68%) have propagation rate constant values near the average value of 80 liter/mol-sec. Therefore, one can say that

$$\bar{k} = \int_{kmin}^{kmax} k \cdot f_d(k) \cdot dk$$

where k is a continuous random variable, having a positively skewed density function, f_d, such that

$$\int_{kmin}^{kmax} f_d(k) \cdot dk = 1$$

It has been shown above that the instantaneous polydispersity of the polymer produced on each j type site must be equal to two. In addition, if the catalyst is stable and the polymerization takes place under steady state conditions, the overall polydispersity can be expressed by

$$\frac{r_w}{r_n} = \frac{2}{\bar{k}^2} \cdot \left(\sum_j \frac{k^2(j) \cdot \eta(j)}{\lambda(j)} \right) \cdot \left(\sum_j \lambda(j) \cdot \eta(j) \right)$$

where

$$\lambda(j) = k(j) \cdot \tau(j)$$

$$= k_{fm}(j) + \frac{k_{fs}(j) + k_{fr}(j) \cdot [A] + k_{fh}(j) \cdot [H_2]}{[M]}$$

is the ratio between the total transfer rate and the monomer concentration. If this ratio is assumed to be independent of j, then the fraction of each site type can be written in terms of the mean and the variance of the k(j) distribution

$$\frac{r_w}{r_n} = 2 \cdot \left(1 + \frac{\sum_j \left(k(j) - \sum_j k(j) \cdot \eta(j) \right)^2 \cdot \eta(j)}{\left(\sum_j k(j) \cdot \eta(j) \right)^2} \right)$$

In the literature two different positively skewed distributions have been adopted, to represent the propagation rate constant distribution, namely the Exponential (Caunt 1966) and the Log-Normal (Bosworth 1983). If we apply the Exponential distribution for the propagation rate constant in this equation, we get a maximum polydispersity of only four, which is much less than the observed polydispersities. The log normal distribution will give much larger polydispersities and thus will be used in this report. It should be noted that a Log-Normal distribution for the propagation rate constant implies that (if the frequency factor is assumed to be constant for all j) the activation energy is normally distributed, because of the Arrhenius expression which relates them. Therefore, each **N(j)** associated with its correspondent **k(j)**, can be evaluated by solving the following relationships

$$N(j) = \int_{k(j-1)}^{k(j+1)} N \cdot f_d(k) \cdot d(k)$$

$$k(j) = \frac{k(j-1) + k(j+1)}{2}$$

$$\int_0^{kmax} f_d(k) \cdot dk = \sum_j \eta(j) = 1$$

$$f_d(k) = \left(\frac{k^{-1}}{(2 \cdot \pi)^{1/2} \cdot \sigma^*} \right) \cdot \exp\left(- \frac{(k^* - \mu^*)^2}{2 \cdot \sigma^{*2}} \right)$$

where $k^* = \ln(k)$ is normally distributed with parameters (mean and variance) μ^* and σ^{*2}, respectively. These parameters are related to the mean and variance of the Log-Normally distributed k variable by means of

$$\mu = \exp\left(\mu^* + \frac{\sigma^{*2}}{2} \right)$$

$$\sigma^2 = \exp(2 \cdot \mu^* + \sigma^{*2}) \cdot (\exp(\sigma^{*2}) - 1)$$

Therefore

$$\frac{r_w}{r_n} = 2 \cdot \exp(\sigma^{*2})$$

Notice that if one lets μ^* and σ^{*2} be the mean and the variance of the Normal activation energy distribution, then this equation can be used to calculate the mean and the variance of the corresponding quasi-Log-Normal distribution for the propagation rate constant by means of

$$\mu_{k(j)} = A \cdot \exp\left(\left(-\frac{\mu_{E(j)}}{R \cdot T}\right) + \frac{\left(\frac{-\sigma_{E(j)}}{R \cdot T}\right)^2}{2}\right)$$

$$\sigma^2_{k(j)} = A^2 \cdot \exp\left(2 \cdot \left(\frac{-\mu_{E(j)}}{R \cdot T}\right) + \left(\frac{-\sigma_{E(j)}}{R \cdot T}\right)^2\right) \cdot \left(\exp\left(\left(\frac{-\sigma_{E(j)}}{R \cdot T}\right)^2\right) - 1\right)$$

where the subscripts **k(j)** and **E(j)** denote, respectively, the rate constant and the activation energy of the j type sites. **A**, **R**, and **T** are the frequency factor, assumed to be independent of j, the gas constant, and the reactor temperature. Furthermore, one can also express the polydispersity in terms of the variance of the Normally distributed activation energies

$$\frac{r_w}{r_n} = 2 \cdot \left(1 + \frac{\sigma^2_{k(j)}}{\mu^2_{k(j)}}\right) = 2 \cdot \exp\left(\left(\frac{-\sigma_{E(j)}}{R \cdot T}\right)^2\right)$$

These equations show that instead of defining a Log-Normal distribution for the propagation rate constant, one can take an easier path by adopting a Normal distribution for the activation energy, obtaining a quasi-Log-Normal distribution for the propagation rate constant. In this case, the standard deviation of the activation energy distribution should be regarded as an adjustable parameter for the model simulation.

3.5.2 Catalyst reactivity profiles

Let us choose the catalyst site distribution to be defined by the parameters given in table 8 using 51 active site types and briefly study the copolymerization of propylene and ethylene using hydrogen as a chain transfer agent. The base case active site distribution yields an activation energy distribution presented in figure 42 and the propagation rate constant profiles are given in figure 43. The distribution for the product of the reactivity ratios is presented in figure 44. Notice that the reactivity ratio product varies over a wide range of values, allowing the formation of copolymer with alternating character as well as copolymer with preponderantly block character. Table 9 shows the concentrations of the reactants for the various simulations.

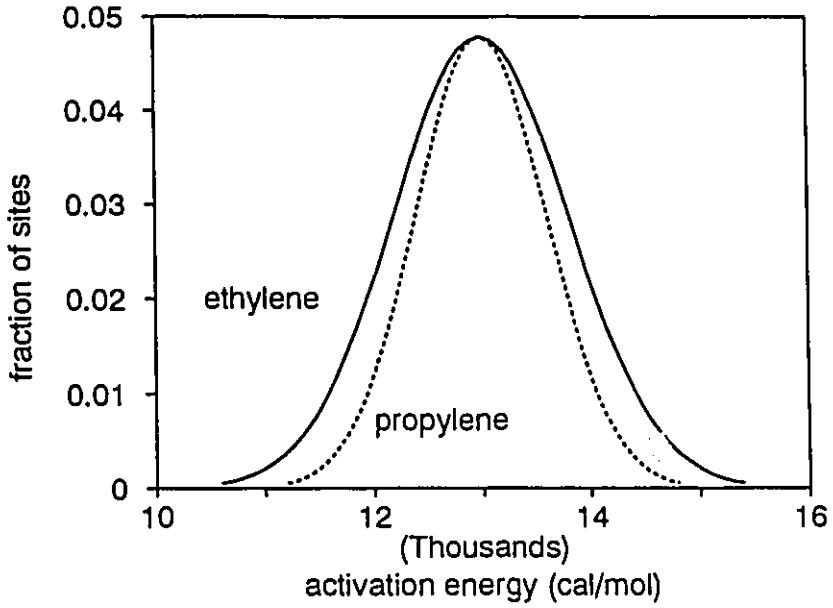

Figure 42. Activation energy profiles for the propylene and ethylene homopolymerization rate constants for the base case distribution.

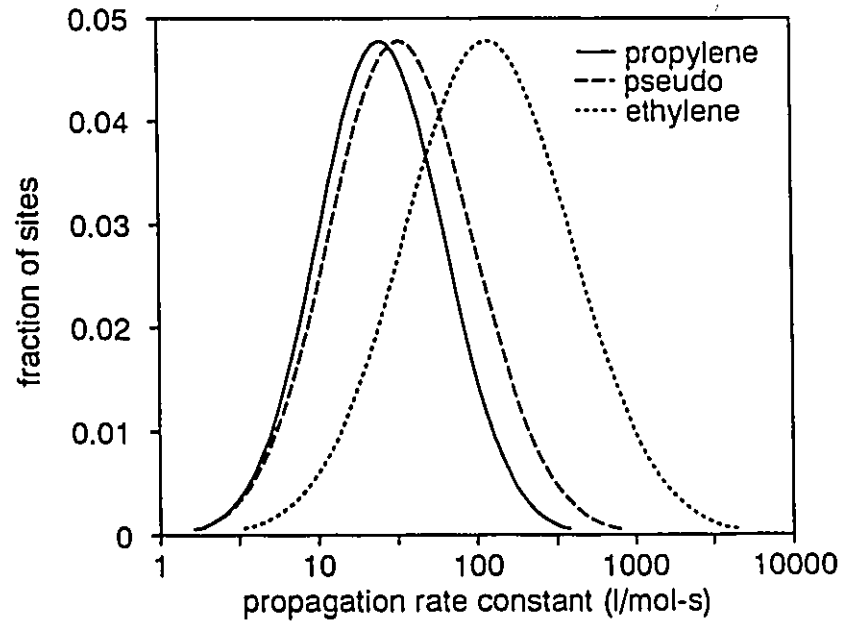

Figure 43. The propagation rate constant distribution for the propylene and ethylene homopolymerization and the pseudo propagation rate for the base case distribution and concentrations.

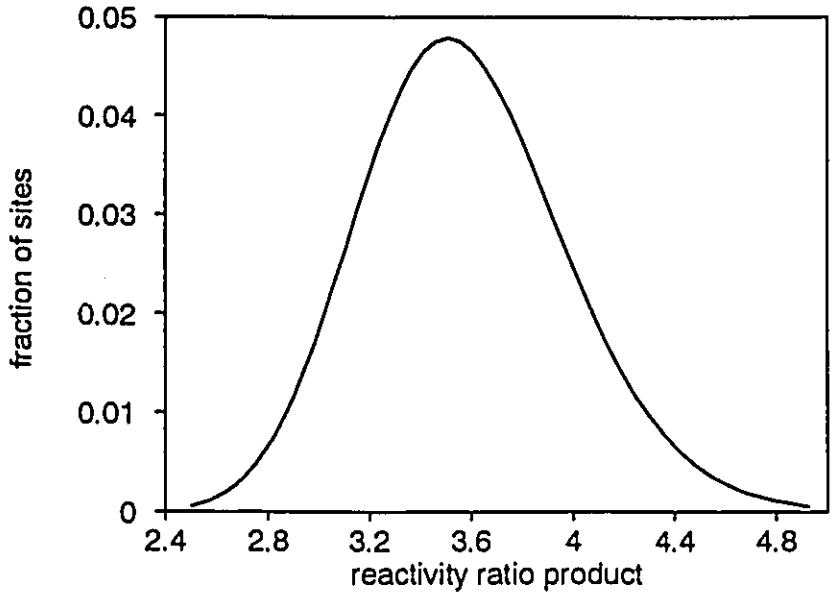

Figure 44. The distribution for the product of the reactivity ratios for the base case distribution.

Table 8 Catalyst site distribution parameters

Reaction	frequency factor (l/mol-s)	activation energy (cal/mol)	standard deviation of activation energy (cal/mol) (narrow, base, wide)
propylene-propylene	8.5×10^9	0.13×10^5	(300, 600, 1200)
ethylene-propylene	5.7×10^9	0.13×10^5	(325, 650, 1300)
propylene-ethylene	17.0×10^9	0.13×10^5	(338, 675, 1350)
ethylene-ethylene	40.0×10^9	0.13×10^5	(400, 800, 1600)
transfer to hydrogen	10.0×10^9	0.13×10^5	0

Table 9 Reactant levels for Ziegler-Natta simulations

Species	low (mol/l)	base case (mol/l)	high (mol/l)
propylene	-	25	-
ethylene	2.25	6.25	10.25
hydrogen	0.001	0.01	0.1

Let us investigate the effect of the width of the distribution on the copolymer and molecular weight distributions by performing simulations using the base case concentrations. We manipulate the width of the active site distribution by using the low and high variances for the activation energies. Figure 45 shows the molecular weight distributions generated using the three distributions. Naturally as the active site distribution gets broader, the molecular weight distribution gets broader. Figure 46 show the copolymer composition distributions, presented as simulated TREF responses. Each propylene unit adds one short branch so polypropylene homopolymer has 500 short branches per 1000 carbon atoms. As these figures demonstrate, the copolymer produced with multiple active site catalysts has a wide chemical composition distribution, even for constant monomer composition. Again as the active site distribution narrows, so does the copolymer composition distribution.

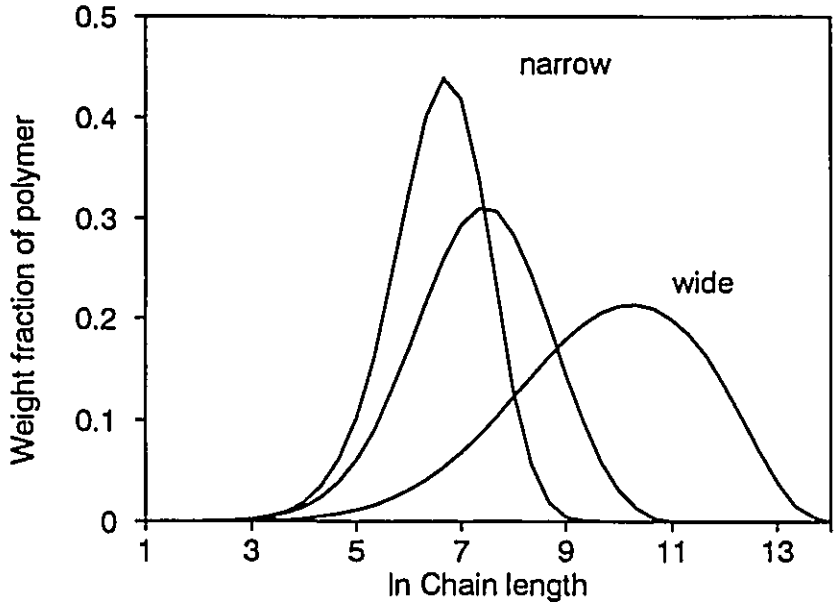

Figure 45. The effect of the active site distribution on the molecular weight distribution using the base case concentrations.

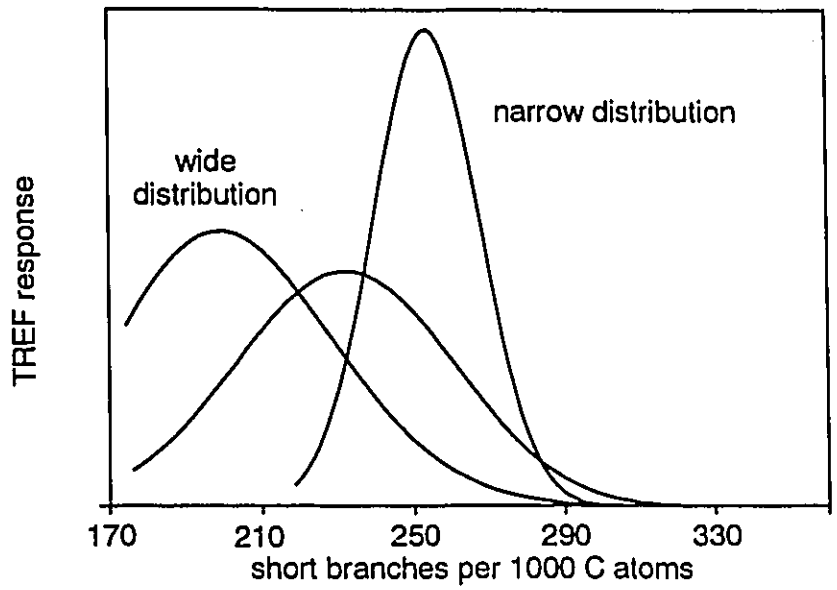

Figure 46. The effect of the active site distribution on the copolymer composition distribution using the base case concentrations.

3.5.3 Reactant concentrations

We can also vary the reactants in the simulation. Hydrogen is added as a chain transfer agent to control the molecular weight. Figure 47 presents the molecular weight distributions for the three hydrogen levels. The hydrogen obviously reduces the molecular weight of the polymer produced, however, for these simulations, where the transfer to hydrogen rate constant is independent of site type, the shape of the distributions remains unchanged. We suggest an experiment where the hydrogen level would be varied and the polydispersity measured. If the polydispersity remains constant then the transfer to hydrogen rate would be a constant for all j for that catalyst type. However hydrogen has been observed to increase the polydispersity for a commercial Stauffer type AA $TiCl_3 \cdot \frac{1}{3}AlCl_3$ with DEAC co-catalyst (Yuan et al. 1982). Therefore the transfer to hydrogen rate constant may differ with site type.

We can also change the level of the comonomer, ethylene, and scrutinize the effect on the copolymer composition distribution presented in figure 48. Two observations are apparent, firstly as more ethylene is added the copolymer composition distributions shift to higher levels of ethylene (lower branching frequencies). Secondly, the distribution gets wider with increasing ethylene content. Remember that we

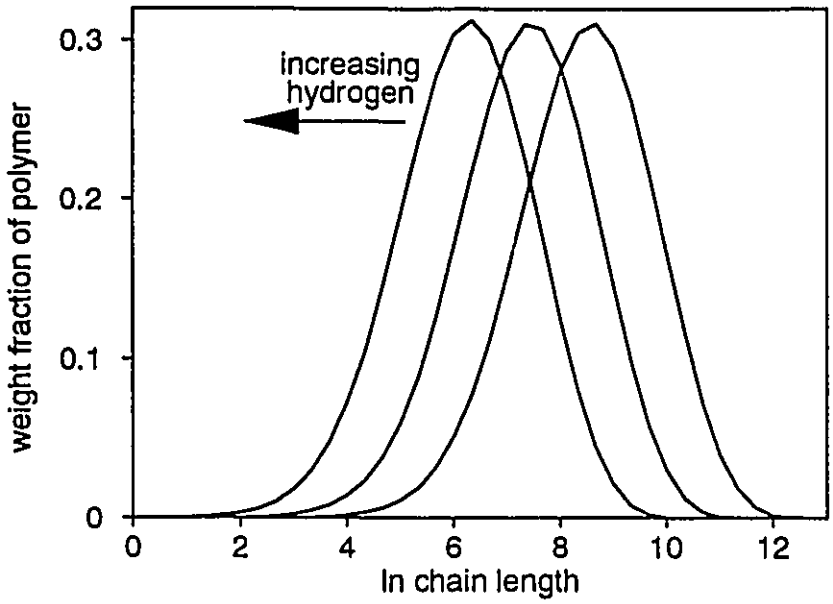

Figure 47. The effect of hydrogen on the molecular weight distribution using the base case active site distribution.

specified a larger activation energy variance for ethylene than for propylene. Therefore we are widening the pseudo propagation rate constant distribution by adding more ethylene.

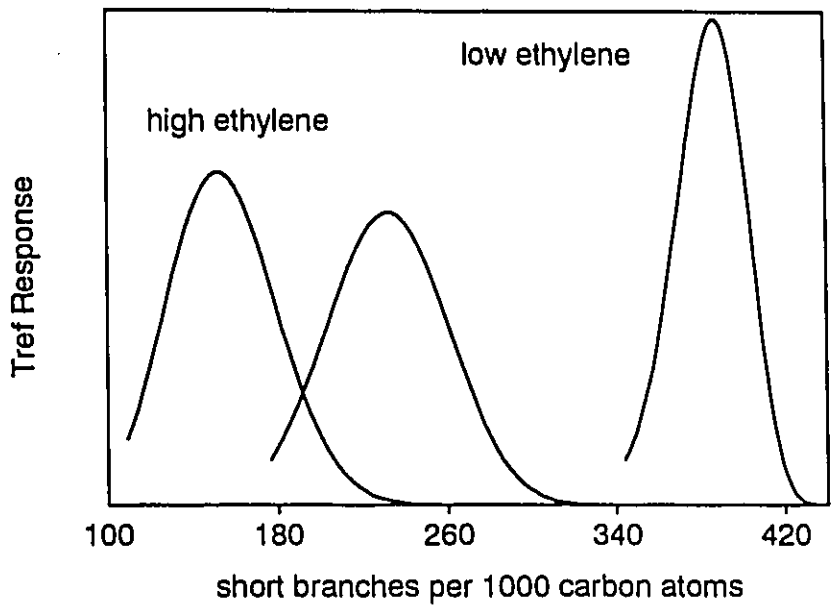

Figure 48. The effect of ethylene on the copolymer composition distribution using the base case active site distribution.

3.6 Conclusions

- A multiple site model is necessary to account for the molecular properties of polymer produced by heterogeneous Ziegler-Natta catalysts. These properties include broad molecular weight, copolymer composition, and stereo-regularity distributions. A kinetic model has been derived, based upon multiple catalyst site types of differing reactivities, for the Ziegler-Natta copolymerization of olefins. The kinetic scheme accounts for the formation, initiation and deactivation of active sites, as well as spontaneous transfer and transfer reactions to hydrogen, monomer and organometallics. The model predicts the rate of polymerization, the copolymer composition and the molecular weight distribution of the polymer produced as well as accounting for the observed broad copolymer composition and molecular weight distributions.
- A generalized molecular weight development has been derived by calculating the leading moments of the live and dead polymer chain length distributions for each type of active site. A simplified method was also proposed, that would be valid under certain operating conditions, and that gives some insight to the factors influencing the molecular weight distribution. From this analysis an

equation for instantaneous molecular weight distribution (not just the leading moments) was found. The instantaneous molecular weight distribution for each site would be the Most Probable Distribution (polydispersity = 2) and the instantaneous polydispersity for the entire amount of polymer produced would deviate from two by the ratio of the variance of the propagation rate constants to the mean propagation rate constant.

- Guidelines are given for the estimation of the model parameters based upon a conceptual approach, according to which, each fraction segregated on the basis of crystallizability can be seen as if it came from a particular type of site. The technique of temperature rising elution fractionation (TREF), is presented as the best available method of separating fractions based on crystallizability. Following this point of view, it is shown that NMR and GPC analysis on selected TREF fraction allows the estimation of the parameters associated with the propagation and transfer rates, the chemical composition, as well as the molecular weight distribution, separately, for each type of site. It is not possible to estimate the stereo-regularity ratios via this technique.

- Some computer simulations were made to demonstrate the ability of the model to predict broad chemical composition and molecular weight distributions. These simulations demonstrate that the multiple active site model explains the polymer inhomogeneity by proposing that the polymer is composed of different fractions, each fraction being produced by a particular type of catalyst site. Composition and molecular weight distributions can be generated that could be compared to polymer subjected to a cross fractionation technique like that of Nakano and Goto (1981) or Wild (1986). This sort of characterization is now underway (Soares 1992)

3.7 References

Allen, G., Booth, C., and Jones, M. N., *Polymer*, **5**, 257 (1964)

Baker, R. T. K., Harries, P. S., White, R. J., and Roper, A. N., *J. Polym. Sci. Lett. Ed.*, **11**, 45 (1973)

Barbe, P. C., Noristi, L., Baruzzi, G., and Marchetti, E., *Makrom. Chem. Rap. Comm.*, **4**, 249, (1983)

Begley, J. W., *J. Polym. Sci.* , **A-1,4**, 319 (1966)

Berger, M. N., and Grieveson, B. M., *Makrom. Chem.*, **83**, 80 (1965)

Bohm, L. L., *Makrom. Chem.*, **182**, 3291 (1981)

Bohm, L. L., *Polymer*, **19**, 544 (1978)

Boor, J., "Ziegler-Natra Catalysts and Polymerizations, Academic Press, 1979

Bosworth, J. D., "The Mathematical Modelling of Gas-Phase Polymerization Reactors", Ph.D. Thesis, Imperial College of Science and Technology, University of London. UK. 1983

Brockmeier, N. F., Rogan, J. B., *AIChE Symp. Ser.*, **72** (160), 28 (1976)

Bukatov, G. D., Shepelev, S. H., Zakharov, V. A., Sergeev, S. A., and Yermakov, Y. I., *Makrom. Chem.* **183**, 2657 (1982)

Buls, V., and Higgins, T. L., *J. Polym. Sci.*:**A-1**, 8, 1025 (1970)

Burfield, D. R., *Makrom. Chem.*, **184**, 1469 (1983)

Caunt, A. D., *J. Polym. Sci.* **C4** 49, (1966)

Chien, J. C. W., Kuo, C. I., and Ang, T., *J. Polym. Sci.: Chem. Ed.*, **23**, 723 (1985)

Chien, J. C. W., Wu J. C., *J. Polym. Sci. Chem. Ed.* **20** 2461 (1982)

Chien, J. C. W. and Hsieh, J. T. T., *J. Polym. Sci.*: Chem. Ed., **14**, 1915 (1976)

Cozewith, C., and Ver Strate, G., *Macromolecules*, **4**, 482 (1971)

Cozewith, C., *Macromolecules* **20**, 1237 (1987)

Crabtree, J. R., Grimsby, F. N., Nummelin, A. J., and Sketchley, J. M., *J. Appl. Polym. Sci.*, **17**, 959 (1973)

de Carvalho, A. B. M., Gloor, P. E., Hamielec, A. E., "A kinetic mathematical model for heterogeneous Ziegler-Natta copolymerization Part 2: Stereochemical sequence length distributions", *Polymer*, **31** 1294-1311 (1990)

de Carvalho, A. B. M., Gloor, P. E., Hamielec, A. E., "A kinetic mathematical model for heterogeneous Ziegler-Natta copolymerization", *Polymer*, **30** 280-296 (1989)

de Carvalho, A. B. M., Gloor, P. E., Hamielec, A. E., "Modelling the Ziegler-Natta copolymerization in slurry type reactor trains" internal report, Polipropileno S. A. Pólo Petroquimico do Nordeste, Rue Hidrogênio, s/n, Camaçari, Bahia, Brazil (1989b)

Doi, Y., Ohnishi, R., and Soga, K., *Makrom. Chem. Rap. Comm.*, **4**, 169 (1983)

Flory, P. J. "Principles of Polymer Chemistry", Cornell University Press, Ithica, N. Y. (1953)

Floyd, S., Hutchinson, R. A., and Ray, W. H., *J. Appl. Polym. Sci.*, **32**, 5451 (1986)

Galvan, R., "Modeling of Heterogeneous Ziegler-Natta (Co)polymerization of α - Olefins", Ph.D. Thesis, University of Minnesota, 1986

Gordon, M., and Roe, R. J., *Polymer*, **2**, 41 (1961)

Grieveson, B. M., *Macromol. Chem.* **84**, 93, (1965)

Hamielec, A. E., MacGregor, J. F., Polymer Reaction Engineering, Eds., K. H. Reichert, W. Geiseler, Hanser Publishers, pp. 21, New York. (1983),

Kakugo M., Naito, Y., Mizunuma, K., and Miyatake, T., *Macromolecules* **15**, 1150, (1982)

Kamath, P., and Wild, L., *Polym. Eng. Sci.*, **6**, 213 (1966)

Kashiwa, N., and Yoshitake, J., *Polymer Bull.*, **12**, 99 (1984)

Keii, T., " Coordination Polymerization" (J. C. W. Chien, ed.), Academic Press, New York, (1975)

Keii, T., " Kinetics of Ziegler-Natta Polymerization", Kodansha, Tokyo, (1972)

Keii, T., Doi, Y., Suzuki, E., Tamura, M., Murata, M., and Soga, K., *Makrom. Chem.*, **185**, 1537 (1984)

Keii, T., Suzuki, E., Tamura, M., Murata, M., and Doi, Y. *Makrom. Chem.*, **183**, 2285 (1982)

Kisin, K. V., Lavrov, V. A., Romanikhin, V. B., and Smirnov, P. A., *J. Appl. Chem.* **59**, 2307 (1986)

Kissin, Y. V., "Isospecific Polymerization of Olefins with Heterogeneous Ziegler-Natta Catalysts", Springer-Verlag, New York, (1985)

Martineau, D., Dumas, P., and Signwalt, P., *Makrom. Chem.*, **184**, 1389 (1983)

McAuley, K. B., MacGregor, J. F., Hamielec, A. E., (1990) "A Kinetic Model for Industrial Gas Phase Ethylene Copolymerization" *AIChE J.* **36** (6), 837.

McGreavy, C., and Rawlings, N., 4th International Symposium on Chemical Reaction Engineering, 1, Heidelberg, 1976

Meyer, H., and Reichert, K. H., *Die Ang. Makrom. Chem.* **57**, 211 (1977)

Mussa, C. I. V., *J. Appl. Polym. Sci.* **1**, 300 (1959)

Nagel, E. J., Kirillov, V. A., Ray, W. H., *I & EC Prod. Res. and Dev.*, **19**, 372 (1980)

Nakajima, A., and Fujiwara, H., *Bull. Chem. Soc. Jpn.*, **37**, 909, (1964)

Nakano, S., and Goto, Y., *J. Appl. Polym. Sci.*, **26**, 4217 (1981)

Orye, R. V., *I&E.C. Proc. Des. Dev.*, **8**, no.4, 579 (1969)

Phase Equilibrium of Light Hydrocarbons (Symposium) [in Russian] Gostoptekhizdat, Moscow (1959)

Ray, G. J., Johnson, P. E., and Knox, J. R., *Macromolecules* **10**, 773 (1977)

Roe, R. J., *Polymer*, **2**, 60 (1961)

Ross, J. F., *J. Macrom. Sci.-Chem.*, **A21**, 453 (1984)a

Ross, J. F., *J. Macrom. Sci.-Chem.*, **A22**, 2255 (1984)b

Ross, J. F., *J. Macromol. Sci. Chem.*, **A23** (12) 1443 (1986)

Schindler A., *J. Polym. Sci.*, **C4**, 81 (1963)

Schmeal, W. R., and Street, J. R., *J. Polym. Sci.: Phys. Ed.*, **10**, 2173 (1972)

Sergev, S. A., Bukatov, G. D., and Zakharov, V. A., *Makrom. Chem.* **185**, 2377 (1984)

Singh, D., and Merrill, R. P., *Macromolecules*, **4**, 599 (1971)

Soares, J. Ph.D. project, McMaster University, Hamilton Ontario Canada (1992)

Spitz, R., Lacombe, J. L., and Guyot, A., *J. Polym. Sci., Polym. Chem. Ed.*, **22**, 2625, (1984)

Taylor, T. W., and Ray. W. H., Paper presented at the 1982 AIChE Annual meeting, Los Angeles, Nov. 1982

Taylor, T. W., Choi, K. Y., Yuan, H., and Ray, W. H., *MMI Symp. Ser.*, **4**(a), 191, Harwood Academic Pub, New York, 1983.

Tsvetkova, V. I., Plusnin, A. N., Bolshakova, R. F., Uvarov, B. A., and Chirkov, N. M., *Vysokomol. Soedin*, **A11**, 1817, (1969)

Usami, T., Gotoh, Y., Takayama, S., *Macromolecules*, **19**, 2722 (1986)

Wijga, P. W. O., van Schooten, J., and Boerma, J., *Makromol. Chem.*, **36**, 115, (1960)

Wild, L., Ryle, T. R., and Knobeloch, D. C., *Polymer Preprints*, **23**, no. 2, 133 (1986)

Wild, L., Ryle, T. R., Knobeloch, D. C., and Peak, I. R., *J. Polym. Sci.: Polym. Phys. Ed.*, **20**, 441 (1982)

Wu, J. C., Kuo, C. I., and Chien, J. C. W., *IUPAC Macromol. Symp.*, Amherst, Massachusetts, 1982, Proceedings.

Yuan, H. G., Taylor, T. W., Choi, K. Y., Ray, W. H, *J. Appl. Polym. Sci.*, **27**, 1691-1706 (1982)

Zakharov, V. A., Makhtarulin, S. I., Poluboyarov, V. A., and Anufrienko, V. F., *Makrom. Chem.* **185**, 1781 (1984)

3.8 Appendix for Ziegler-Natta polymerization

3.8.1 Nomenclature

r	chain length
j	active or potential site type
N*(j)	moles of potential sites of type j. Potential sites are catalysts sites that do not facilitate polymerization, but may react, via formation reactions, to form active sites that do facilitate polymerization
N(r,j), N(j)	moles of propagation sites of type j with growing chain of length r, and total moles of propagation sites of type j
$N(0,j), N_H(0,j), N_R(0,j)$	moles of initiation sites of type j produced by formation, by transfer to hydrogen or spontaneous transfer and by transfer to organometallic.
$N_T(j), N_T$	moles of active sites of type j. (Sum of initiation sites and propagation sites of type j) and total number of active sites.
$N_p(j), N_p$	moles of propagation sites of type j, and total moles of propagation sites.
$N_i(r,j), N_i(j)$	moles of active sites with polymer of chain length r ending in a monomer type i group, and total moles of active sites having a chain ending in a monomer type i group
Q(r,j), Q(j)	moles of dead polymer of chain length r produced by type j sites and moles of dead polymer of all chain lengths produced by type j sites
M_i, M	moles of monomer type i and total monomer
Mp	mass of polymer in the reactor (or inflowing and outflowing if the subscripts 'in' or 'out' are present)
m_1, m_2, m	the molecular weight of monomer 1, 2 and the effective molecular weight per repeat unit.
A	moles of organometallic
H_2	moles of hydrogen

V	reaction volume
t	time
f_i	mole fraction of adsorbed monomer that is type i (monomer composition)
F_i, F_{iinst}	accumulated and instantaneous mole fraction of monomer type i bound as polymer (copolymer composition)
P_i	total moles of monomer type i bound as polymer
Rp	rate of polymerization
W(j)	instantaneous mass fraction of polymer produced by j type sites
Wd(r,j), Wd(r)	the instantaneous weight fraction of dead polymer that is chain length r produced by type j sites, and by all sites
W' and $\dot{W}$	the differential weight fraction of polymer in terms of short chain branching and mole fraction of monomer 1 bound as polymer.
$Y_n(j)$	the n th moment of the live polymer chain length distribution produced by j type sites
$X_n(j)$	the n th moment of the dead polymer chain length distribution produced by j type sites
$\overline{rn}, \overline{rw}$, rn, rw	the accumulated number and weight average chain lengths and the instantaneous number and weight average chain lengths.
[X]	denote concentrations of species X either on the catalyst surface or in the reactor. (moles/litre).
C_i	denote the bulk concentrations of species i in the reactor (moles/litre).
K_i	the equilibrium constant for adsorption of species i on the catalyst surface.
s^D, s^L	stereo reactivity ratios. The ratio of the rate constant for isotactic addition of monomer to syndiotactic addition of monomer
d_{ik}	probability of forming a diad with monomers i and k.

p_{ik}	the conditional probability that a i type monomer adds on to a growing chain given that a k type monomer unit was added immediately before, or equivalently, the probability of adding a monomer type i to a growing chain ending in monomer type k.
$S_w, S_w(j)$	the total sample mass for TREF and the mass of the j fraction.
$\overline{property}$	any quantity that is an accumulated property (as opposed to an instantaneous property)

Greek Letters

$\gamma(j)$	the fraction of the total active sites that are of type j
$\eta(j)$	the fraction of the propagation sites that are type j
$\phi_i(j)$	the fraction of j type sites that have a growing chain ending in a monomer type i unit
$\tau(j)$	the ratio of the transfer rates to the propagation rates for type j sites
$\psi(j)$	a grouping of constants related to $\tau(j)$
$\lambda(j)$	a grouping of transfer constants
σ^2	the variance of the propagation rate constants about the mean propagation rate constant
θ_k	the fraction of adsorption sites on the catalyst surface that are occupied by a k type molecule (k= hydrogen, monomer, organometallic)
θ_T	the total moles of adsorption sites on the catalyst surface per unit volume of reaction mixture (moles/litre).

Subscripts

1,2	pertaining to monomer types 1 and 2
H,R,S h,r,s	pertaining to reactions with hydrogen and organometallic and spontaneous reactions
T	denote total quantities

in, out	denote flows into and out of the reactor
inst	denote an instantaneous value
D, L	denote the stereoregular orientation of the monomer.

Kinetic Rate Constants

Rate constants with (j) denote reactions with type j sites. The subscripts i, k denote monomer types, and if the rate constant has no i, k subscript they are pseudo rate constants that take into account the copolymer and monomer compositions. First order rate constants will have units of reciprocal time, and second order rate constants will have units of litre/moles-time.

$kf(j), kf'(j)$	pertaining to formation of active catalyst sites (type j) from potential sites
$ki(j)$	pertaining to formation of propagation sites from initiation sites (initiation reactions)
$kh(j), kr(j)$	pertaining to formation of propagation sites from initiation sites that have been formed by transfer to a hydrogen or organometallic reactions (initiation reactions)
$k_{ik}(j), kp(j)$	pertaining to propagation reactions
$kfm(j), kfh(j),$ $kfr(j), kfs(j)$	pertaining to transfer to monomer, transfer to hydrogen, transfer to organometallic, and spontaneous transfer reactions
kd (j)	deactivation reactions
$\overline{kp}, \overline{kd},$ $\overline{kf}$	mean propagation, deactivation, and formation reaction rate constants
$k_{ik}^{DL}(j)$	the propagation rate constant for the addition of k type monomer with L configuration to a growing chain ending in an i type monomer in the D configuration on a type j site.

Chapter 4 Chemical modification of polyolefins by free radical mechanisms

4.1 Introduction

Reactive processing now allows the conversion of lower cost commodity polymers, such as polyolefins, to higher priced specialty polymers. Extruders are used because of their low capital costs and high flexibility. Specialty polymers are produced by modifying the molecular weight (either a reduction in the averages and polydispersity as in the case of controlled rheology polypropylene, or a build up of molecular weight, as in the case of polyethylene), or by grafting functional groups onto the polymer backbone. This grafting process can be accompanied by other changes in the structure and properties of the basic polymer (Kwei et al. 1991).

Moreover, with increased awareness of our extravagant lifestyle, and its impact on our environment, recycling of polymers is becoming a hot topic for discussion and research. Different kinds of plastics are difficult to sort and separate, and do not, in general, make blends with good mechanical properties without some sort of compatibilization. Reactive processing offers techniques to make compatible blends or alloys. Reactive processing techniques involve the introduction of an initiator into the polymer melt, which produces free radicals to commence the modification of the molecular structure of the polymer. However these free radicals also initiate a host of reactions that may produce other, less desirable, modifications. In general, scission, grafting, branching and crosslinking may all occur simultaneously. The difficulty is to promote the desired reactions while suppressing the undesired. To date much of the work in reactive processing has been of the *try it and see* approach, and several useful products and techniques have been developed. More fundamental studies are certainly less abundant. These studies may be more difficult, but have greater potential to allow for conceptual leaps than do the more empirical approaches. The optimization process can be facilitated by the use of mathematical models to relate the extent of the reactions, and therefore also the final properties of the polymer, to the processing conditions and the initial polymer properties.

This thesis deals with the development of mathematical models to relate the molecular modifications, scission, branching and crosslinking to process conditions. The models, based upon generally accepted kinetic mechanisms and certain assumptions

about the nature of simultaneous scission and crosslinking, can predict the molecular weight averages, degrees of crosslinking, scission and branching, and the amount of sol and gel.

Numerical algorithms to solve the model equations have been developed. One can specify any arbitrary initial molecular weight distribution, (e.g. as measured by GPC), the free radical initiator concentration, and the kinetic parameters for scission, and termination, and solve for the entire molecular weight distribution, before and after the gel point, as well as the gel fraction and branching frequencies.

The models have unknown parameters which must be estimated by matching the predictions to experiments. In this investigation, experiments were performed with high density polyethylene, polypropylene and peroxides in an extruder and in ampoules. The polymer was analyzed for molecular weight and gel fraction. These results were then used to estimate the model parameters.

Before we proceed with the discussion of the present work, let us quickly scrutinize some of the work that has been presented in the past.

4.2 A note on collaboration

Thanks to Y. Tang for the gel fraction measurements, and A. Kostanska for performing some of the DSC measurements.

4.3 Literature Review

In this section, we review the appropriate literature pertaining to the chemical modification of the polyolefins, emphasizing polyethylene. Firstly we shall discuss the chemistry of the system, the attempts to model the chemical kinetics, and finally the experimental work that has been reported.

4.3.1 The Chemistry

The chemical reactions involved are shown in table 10. In the free radical modification of polymers, we need a source of radicals, and in our case we are using chemical initiators. These may be peroxides or azo-compounds. These initiators decompose at the reaction temperature to produce free radicals. The initiator radicals can then a) transfer their reactivity to a polymer chain by abstracting a hydrogen and producing a backbone radical, b) terminate with another radical, c) react with an

unsaturation in the polymer chain producing an allylic chain end radical (Hulse et al. 1981, Hendra 1987), d) react with an additive (Chodak et al. 1987) or impurity that may present, or e) recombine to form some possibly inert product.

Consider the backbone radical and its formation. Firstly the radical must be sufficiently energetic to abstract a hydrogen. Not all initiator radicals are suitable (Chodak and Lazar 1982, Callais 1990). Secondly the polymer must have an abstractable hydrogen available, and not all hydrogens are equal in this respect. The backbone radical will be either secondary or tertiary depending upon whether a branch is present or not. The radical then has a variety of fates. It can a) undergo β-scission to form a chain end radical and a dead polymer with a terminal double bond, b) terminate by combination with another backbone radical leading to crosslinking and the formation of X branches (tetra functional branches), c) terminate by combination with an chain end radical leading to a Y branch (tri functional branches), c) terminate by disproportionation leading to an unsaturation d) terminate with a primary radical, e) transfer its reactivity to another chain, f) react with an additive (M) or impurity leading to grafting. Polypropylene tends to undergo scission, since most of the backbone radicals formed are tertiary. Polyethylene homopolymer tends to crosslink, but scission has been observed (Kwei 1991), especially if branches are present. Polypropylene can be made to crosslink at high peroxide concentrations (Chodak and Lazar 1982) or by using additives that react with the tertiary radical before it has a chance to undergo scission (Chodak and Lazar 1986). Grafted additives may have radical centres that can terminate by combination with backbone radicals producing crosslinks. Propagation of the additive species is also a possibility, production a homopolymer of species M.

When enough crosslinking has occurred, a three dimensional network of polymer is formed, that is insoluble in even the best solvents for the polymer. This is called *gel*. The remaining linear and branched, but still soluble, polymer is defined as *sol*. The point at which the first gel appears is the *gel point*. On the other hand, if only scission occurs, the molecular weight averages decrease, and the width of the distribution changes, approaching $M_w/M_n = 2$ in the limit.

Terminal radicals, produced either by scission or reaction with terminal unsaturation, can terminate with each other leading to chain extension. If one of the terminal radicals is an allylic, a backbone unsaturation is produced, probably *trans*-vinyl unsaturation (Bremner and Rudin 1990). Scission of radicals at branch points can lead to vinylidene unsaturation (Bremner and Rudin 1990).

Table 10 Chemical reactions for free radical modification of polyolefins.

Decomposition of peroxide to form two radicals

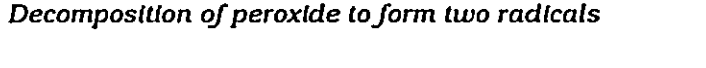

Consumption of peroxide radicals by additive molecule

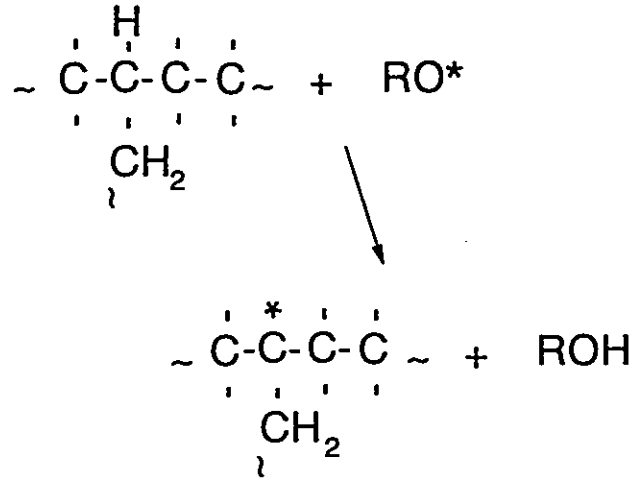

Hydrogen abstraction by peroxide radical, forming tertiary radical. This branch need not be only one carbon long.

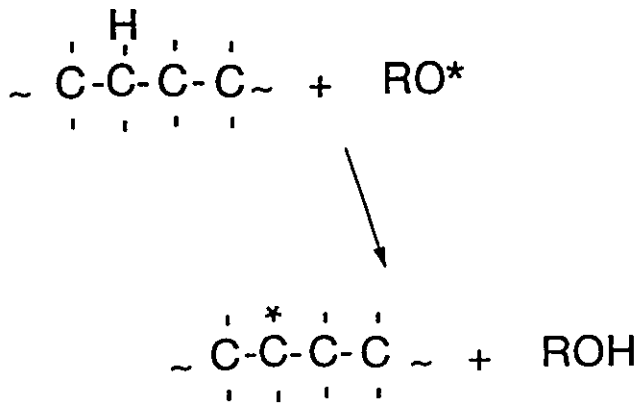

Hydrogen abstraction by peroxide radical, forming secondary radical

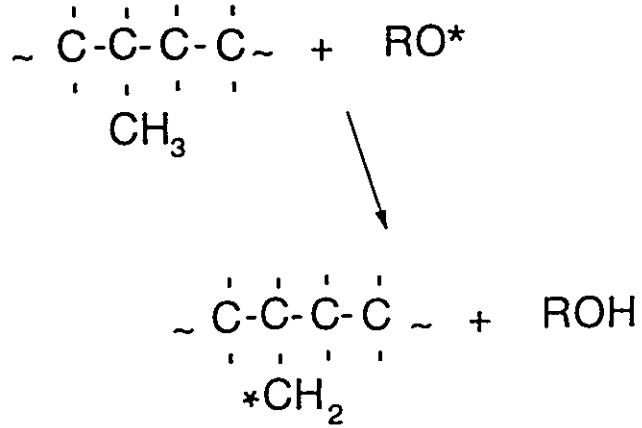

Hydrogen abstraction by peroxide radical, forming primary radical

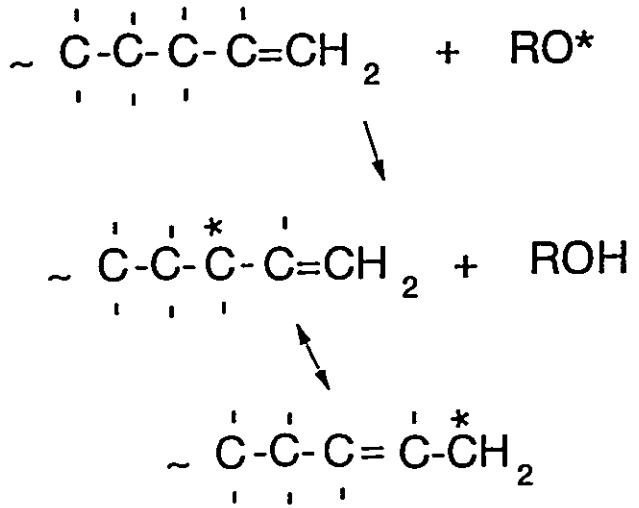

Hydrogen abstraction by peroxide radical at terminal unsaturation forming allylic radical, and its resonance structure.

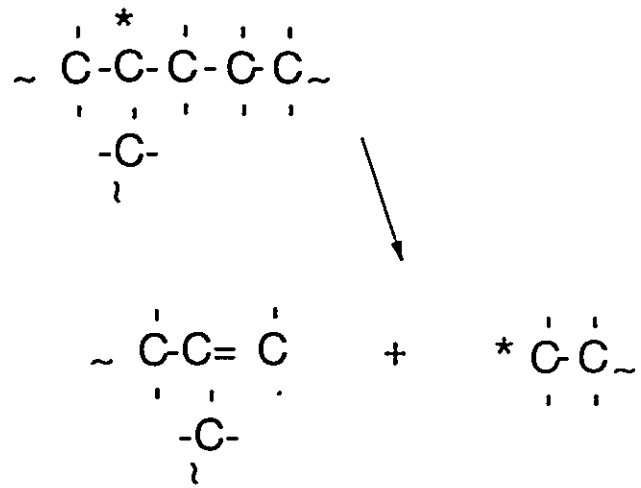

β-scission of tertiary radical

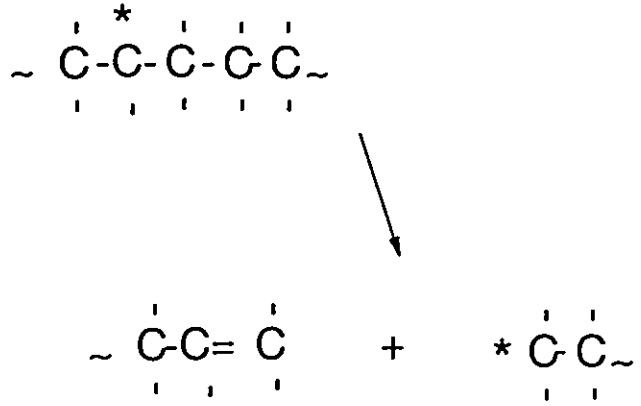

β-scission of secondary radical

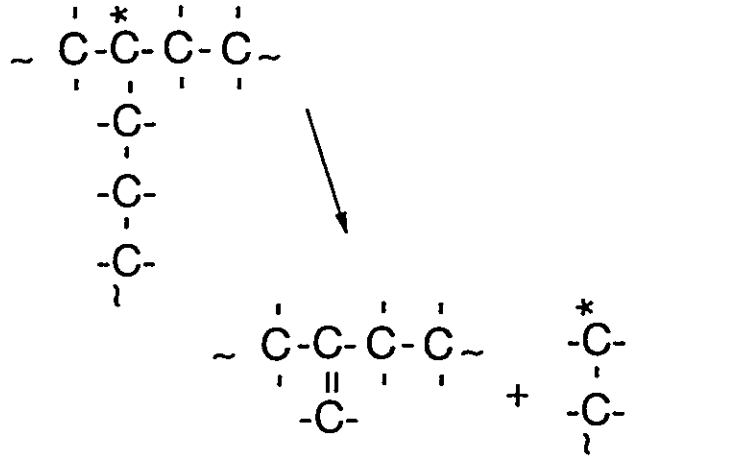

β-scission of long branch forming a vinylidene unsaturation

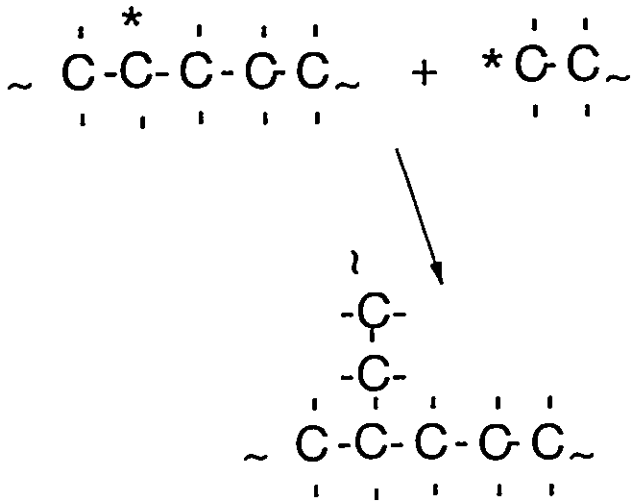

Termination by combination forming a Y branch (tri functional branch)

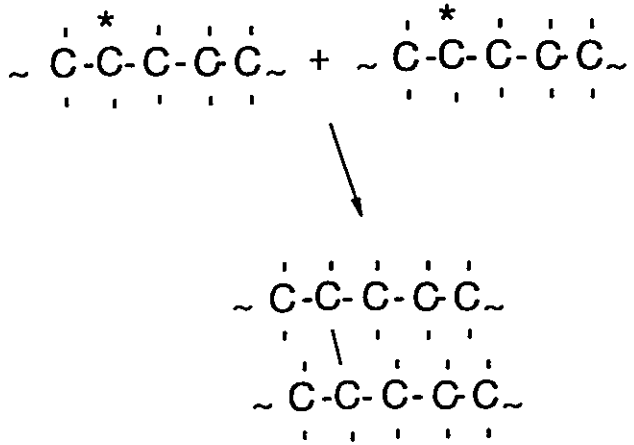

Termination by combination forming an X branch (tetra functional branch).

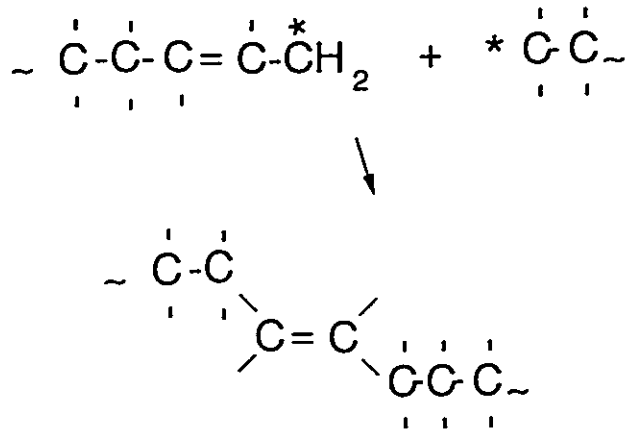

End linking of an allylic radical forming an unsaturation in the backbone

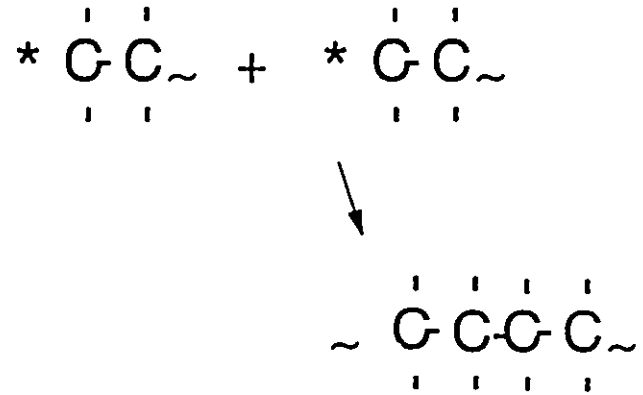

End linking of primary radicals.

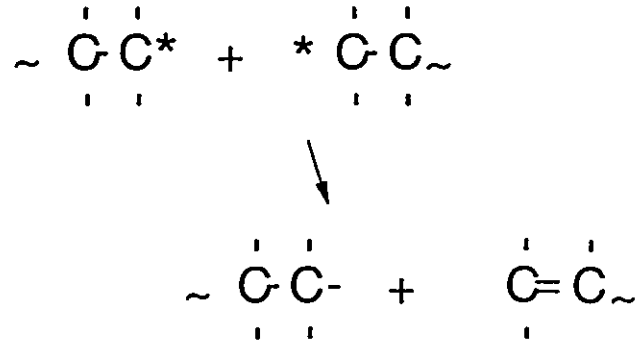

Termination by disproportionation to produce a double bond.

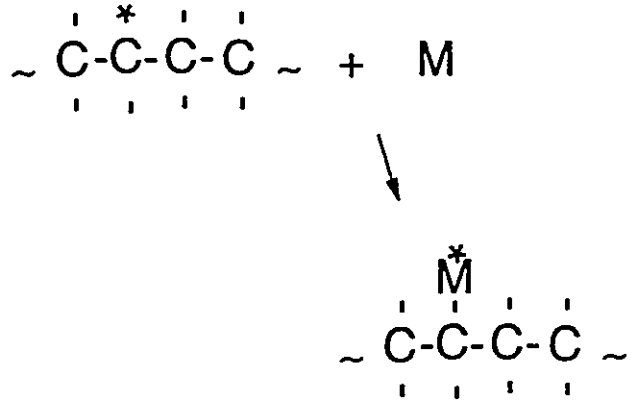

Grafting of a small molecule, M, onto a backbone radical. This new radical could then undergo termination by combination to promote crosslinking, propagate with another M species, terminate with another species (like initiator fragments) or simply be inert.

4.3.2 Mathematical Modelling

Given the set of chemical reactions, it is possible to develop models to calculate the molecular weights of the polymer being produced. The kinetic modelling methodology is to make mass balances on polymer chains of length r as a function of time, and initiator concentrations. Balances are also needed for all the radical species, and using the stationary state hypothesis, algebraic equations result. The number of balance equations on polymer is extremely large (one for each chain length), but it is often possible to a) solve for about 100 different chain lengths to describe the molecular weight distribution, or b) group the mass balances together to yield only the averages. Using these approaches, we can make some assumptions about the system (neglecting some reactions) and develop simpler models for specific cases.

Pure Scission

Lets now consider the case of pure scission, i.e. no crosslinking or grafting. It is possible to postulate that the scission reaction could occur preferentially at the center, at the ends, or randomly along the chain. For the case where the polymer undergoes only random scission, one can derive a model that gives the entire molecular weight distribution as a function of the degree of scission. This was done by Saito (1958, 1972) for the case of irradiated polymers, but is certainly applicable for the case of the chemical modification of polypropylene (Triacca et al. 1993).

$$w(r,p) = \left(w(r,0) + pr \int_r^\infty \left(\frac{(2 + p(s-r))}{s} \right) w(s,0) ds \right) \exp(-pr)$$

where w(r,p) is the weight fraction of polymer of chain length r, at degree of scission p. The degree of scission is the fraction of all repeat units in the backbone of the linear chains that have undergone scission, and will be a function of the number of radicals generated by initiator molecules that have decomposed up to this time and thus there is a relationship between p and reaction time. The initial molecular weight distribution is arbitrary

The model of Suwanda et al. (1988) and Lew et al. (1989) is equivalent to Saito's equation since the same chemical reactions are considered and the derivation follows the same path, but the equation is simply in a different form when employed by these authors.

Ziff and McGrady (1986) removed the assumption that scission is random and consider the balance on polymer of length r as

$$\frac{\partial P(r)}{\partial t} = -P(r)\int_0^r F(y,r-y)dy + 2\int_r^\infty P(y)F(r,y-r)dy$$

where F(r,y) is the rate of fragmentation of a chain of length r at the y^{th} unit. This equation may be solved for arbitrary functions of F(r,y) and reduces to Saito's equation when F(r,y) is equal to a constant.

In addition one could use the method of moments to find the molecular weight averages instead of the whole distribution. This was the approach taken by Tzoganakis et al. (1989) and Hamielec et al. (1990, 1991). The moments of the molecular weight distribution are defined as:

$$Q_i = \sum_{r=0}^{\infty} r^i P(r) = Q_1 \sum_{r=0}^{\infty} r^{(i-1)} w(r)$$

$$= Q_1 \int_0^\infty r^{(i-1)} w(r)dr$$

where Q_i is the i^{th} moment of the molecular weight distribution, r is the chain length, P(r) is the concentration of polymer chains of length r, and w(r) is the weight fraction of polymer having chain length r. The average chain lengths are then given by $r_n = Q_1/Q_0$ and $r_w = Q_2/Q_1$ where r_n and r_w are the number and weight average chain lengths. Using these quantities, one can develop a model for pure random scission of the form.

$$\frac{dQ_0}{dt} = \lambda(Q_1 - 3Q_0)/(Q_1 - Q_0)$$

$$\frac{dQ_2}{dt} = \lambda\left(-\frac{Q_3}{3} + \frac{Q_1}{3} - 2Q_2\right)/(Q_1 - Q_0)$$

where $\lambda = 2 \cdot f \cdot kd \cdot [I]$ depends upon the initiator concentration, [I], efficiency, f, and decomposition rate constant, kd. Since the mass of polymer in the system is constant $dQ_1/dt = 0$. Notice that the balance equation for Q_2 contains a term with Q_3, and thus the moment equations are not *closed*. Lower moments are functions of higher moments. Tzoganakis (1988) and Hamielec (1990) addressed this problem with different empirical closure equations, and this gives rise to the two different models. Tzoganakis (1988) attempted to fit the initial distribution using a closure rule based on Hulburt and Katz (1964)

$$Q_3 = 2Q_2(2Q_2Q_0 - Q_1^2)/(Q_1Q_0)$$

whereas Hamielec et al. (1990) tried to fit the final distribution, assuming it to be the most probable distribution

$$Q_3 = \frac{3Q_2^2}{2Q_1}$$

Zhu (1991) addressed this moment closure problem, in a more general manner showing that the closure rule changes with the degree of scission and depends upon the initial molecular weight distribution.

Another interesting approach is that of Ballauff and Wolf (1981). They define a rate constant for chain scission as k_{ij}. This is the rate constant for the breakage of a chain of length i at the j^{th} unit. And the rate constant for breakage of a molecule of length i, at any point, is simply

$$k_i = \sum_{1}^{i-1} k_{ij}$$

One can then write a balance on chains of length i

$$\frac{dP(i)}{dt} = -\sum_{0}^{i-1} k_{ij}P(i) + (k_{i+1,1} + k_{i+1,i})P(i+1) + \ldots + (k_{r,1} + k_{r,r-1})P(r)$$

where r is the maximum chain length. One now has a set of linear differential equations, one for each i value, and so far nothing has been said about the scission mechanism. The scission mechanism (random, preferring the center, preferring the ends ...) will be contained in the selection of the k_{ij} values, for example for random scission k_{ij}=k. We can rewrite this set of equations in matrix form

$$\frac{d\bar{p}}{dt} = \bar{A}\bar{p}$$

And this can be solved by solving the eigenvalue problem of matrix $\bar{A}$. Notice that $\bar{A}$ is upper triangular so the eigenvalues are simply the diagonal elements. Any initial distribution can be entered.

The major draw back of this method is, probably, the amount of storage space needed for the matrices, since $\bar{A}$ is roughly an rXr matrix (although upper triangular) where r is the maximum chain length needed. In fact in the Ballauff and Wolf (1981) paper they state "...restrictions imposed by computer memory capacity do not permit

one to take all possible rupture sites along the chains into account. The polymer molecule is therefore divided into a certain number of subunits. It has to be checked in each case that the results of the calculation do not depend on the length of the subunits". The power of this method is that a) no assumptions about the type of scission was included, so our assumption of random scission could be relaxed and b) no difficult numerical solution solutions need be used.

Monte Carlo type simulations have also been done by Guaita et al. (1990) to study the effect of non-random scission, to very high degrees of scission.

Pure Random Crosslinking

For the case of pure random crosslinking (transfer to polymer and termination by combination), we can follow the same approach and perform mass balances on polymer of chain length r. Doing so and making the stationary state hypothesis for radicals and assuming that all radicals terminate with the same rate constant, one can find (Saito 1972, Tobita 1990, Hamielec et al. 1991)

$$\frac{dw(r,x)}{dx} = -rw(r,x) + \frac{r}{2}\int_0^r w(s,x)w(r-s,x)ds$$

and now x the degree of crosslinking, i. e. the fraction of all repeat units that have a crosslink. We define a crosslink as a branch point so when two chains are tied together, two crosslinks are needed. The general analytical solution to this equation has not yet been found, and a numerical solution is required. Attempts have been made (Triacca et al. 1991) with moderate success, but a useful numerical solution is presented in this report. It should be noted that one performed only a mass balance on the sol polymer, and thus w(r) will *always* include only the sol. But the reactions with gel polymer are included. Thus $\int_0^\infty w(r)dr$ is the mass fraction of sol and will equal 1 until the gel point and then fall, as the sol is consumed by the gel. In this way the equations show no discontinuity at the gel point.

An alternative approach, again, is to use the method of moments. Since Q_1, the total mass of polymer, is a constant, we can normalize the moments to make them dimensionless by defining $q_n = Q_n/Q_1$. The moment equations, before the gel point when $q_1=1$, become

$$\frac{dq_0}{dx} = -\frac{1}{2}$$

$$\frac{dq_2}{dx} = q_2^2$$

and the average chain lengths become, in terms of the initial chain lengths, r_{n0}, and r_{w0}

$$\frac{1}{r_n} = \frac{1}{r_{n_0}} - x/2$$

$$r_w = \frac{r_{w_0}}{1 - x \cdot r_{w_0}}$$

The gel point has been defined as the point where the weight average molecular weight approaches infinity. Using this definition one can relate the gel point to the degree of crosslinking and the initial molecular weight average to find the *critical degree of crosslinking*, x_c

$$x_c = \frac{1}{r_{w0}}$$

After the gel point, q_1, the mass fraction of sol, is no longer unity, but falls, and the moment equations are not closed. The moments are as follows.

$$\frac{dq_0}{dx} = -q_1\left(1 - \frac{q_1}{2}\right)$$

$$\frac{dq_1}{dx} = -q_2(1 - q_1)$$

$$\frac{dq_2}{dx} = -q_3(1 - q_1) + q_2^2$$

One could use a closure equation, like that of Hulburt and Katz (1964), Hamielec (1990) or another. Flory (1953) developed a statistical expression to relate the sol fraction, q_1 to the degree of crosslinking and the initial molecular weight distribution. (The primary chains in Flory's analysis are part of the initial molecular weight distribution before chemical modification)

$$q_1 = \sum_{r=1}^{\infty} w(r,0)[1-x(1-q_1)]^r$$

Thus we can substitute this expression for q_1 into our differential equation for q_1 and solve for q_2 (Zhu 1991).

Simultaneous random scission and Crosslinking.

Now we must address an even more interesting and difficult problem where both random scission and random crosslinking are important and occur simultaneously. An approach (Saito, 1958, 1972) to solve this problem is to consider modification to occur in two stages, serially, first random scission, followed by random crosslinking. In this manner we can use Saito's scission equation to determine the molecular weight distribution after the desired degree of scission, p. Then we can use the pure random crosslinking equations, on the degraded polymer, to determine the new molecular weight distribution after the desired amount of crosslinking, x. The total degree of modification is z=x+p. If the initial distribution is linear and most probable and the ratio of scission to crosslinking is constant then this approach leads to the Charlesby-Pinner equation (Charlesby and Pinner 1959).

$$s + s^{1/2} = \frac{2}{x \cdot r_{w0}} + \frac{p}{x}$$

where s is the sol fraction. This equation is widely used (with some slight modifications), even for polymer with initial distributions much broader than random for example: Kwei et al. (1991), de Boer and Pennings (1981), Capla and Borsig (1980) and in a host of papers on irradiation of polyethylene. In sol gel measurements, the measured quantity $s+s^{1/2}$ is plotted vs. the reciprocal of the peroxide concentration and a straight line drawn through the points. The intercept (at infinite peroxide level) gives the ratio of scission to crosslinking p/x. It should be noted that since crosslinking is a second order reaction with respect to radical concentration, and scission is first order, the ratio of scission to crosslinking will change with initial peroxide concentration and as the initiator is depleted (see appendix).

There is really no reason why the initial molecular weight distribution needs to be random, because one can use any initial distribution in both the scission and crosslinking equation. The assumption of constant scission to crosslinking ratio can also be relaxed. Numerical solutions are needed since the Charlesby-Pinner equation is no longer valid, but still the two step approach is solvable and the FORTRAN program *2step*

was created in this thesis for this purpose. The real limitations of the Charlesby-Pinner equation lie in the assumptions of a) independent crosslinking and scission (in two steps) b) constant p/x and c) initially linear polymer. There are some other concerns, specifically related to radiation crosslinking that are addressed in Babic and Stannett (1987).

The problem with the two step process is simply, that's not what really happens in real life. The scission and crosslinking occur *simultaneously*, not serially with scission occurring first. In fact, for peroxide induced modification, where the peroxide level will fall with time, one should expect more crosslinking to occur first, and scission later, and thus p/x will not be constant. Higher peroxide levels enhance crosslinking over scission. Moreover, scission will produce terminal radicals and these radicals could combine with backbone radicals to form Y branches. The two step process precludes the formation of Y branches, allowing only X branches. Both Y and X branches are observed in practice (Horii et al. 1990).

Many of the commercial polymers that are chemically modified are not linear (for example low density polyethylene). What chains are produced when these branched molecules undergo scission? This is a key question and the heart of the problem of modelling *simultaneous* scission and crosslinking. Consider a linear chain of length r. (Figure 49) We can count units from one end to find the j^{th} unit. If it undergoes scission at the j^{th} unit the products are two chains, one of length j, and one r-j. We know that we can always make a chain of length j if $r > j$ and it doesn't matter from which end of the chain we start to count, a cut at the j^{th} unit always makes the same products. However now consider a tetra functionally branched chain. We wish to cut it at the j^{th} unit, but how do we find the j^{th} unit? If we start to count from one end, and count units towards the center, what do we do at the branch? Suppose all the arms of the molecule are longer than j units, then we can produce a linear polymer j units long by cutting the j^{th} unit measured from any of the ends, i.e. 4 different ways. If only 3 of the four arms were longer than j, we can only make linear polymer of length j three ways and so on. The possible ways to cut a chain, to produce the desired products, depends upon the structure of the branching, and since we have a vast number of possible configurations for the branched polymer, the problems is extremely complicated. It is even possible to cut a unit, and not change the total number of molecules in the system.

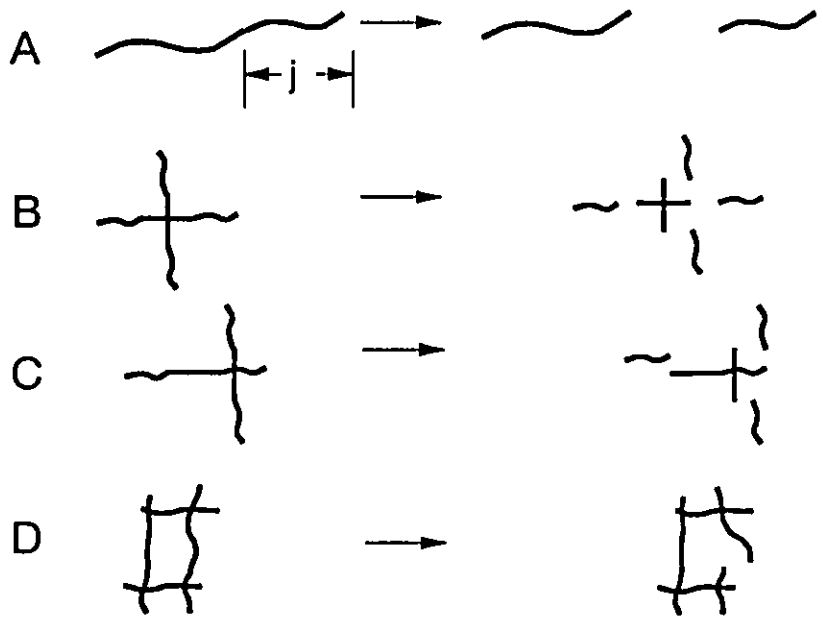

Figure 49. Scission of several branched molecules.
A) a linear molecule, B) the four ways to make linear chains j units long. C) the three ways to make linear chains j units long and D) scission that does not lead to a new polymer molecule.

Zhu (1991) (see also Hamielec et al. 1990) developed a integro differential equation, by extending Saito's work, that accounts for simultaneous random crosslinking, random scission and random grafting, including the production of Y branches.

$$\frac{1}{r}\frac{\partial w(r,z)}{dz} = -w(r,z) + 2\alpha \int_r^\infty \frac{w(s,z)}{s} ds$$

$$+ \frac{\beta_4}{2} \int_0^r [w(s,z) w(r-s,z)] ds$$

$$+ \beta_3 \int_0^r \left[w(s,z) \int_{r-s}^\infty w \frac{(m,z)}{m} dm \right] ds$$

$$+ \frac{\beta_2}{2} \int_0^r \left[\int_s^\infty w \frac{(m,z)}{m} dm \int_{r-s}^\infty w \frac{(m,z)}{m} dm \right] ds$$

where z is the degree of modification and α is a group of kinetic parameters related to scission, β_4, β_3 and β_2 are groups of kinetic parameters related to the formation of X branches, Y branches and end linking respectively. It is assumed that there are two ways to cut a chain to make the desired products. This is exactly correct if the chains are linear. While this is not an ideal assumption, it should be better than assuming the two step model of Saito, since Zhu's model can predict the formation of Y branches whereas Saito's can not.

A statistical approach put forward by Shy and Eichinger (1986) and Gallatsatos and Eichinger (1988) whereby a number (Np) of primary chains are randomly distributed in a cubical box with edge length $L = (MnNp/\rho Nav_p)^{1/3}$ where Mn is the number average molecular weight of the primary chains, Na Avagadro's number, v_p the volume fraction of polymer and ρ the density of polymer. Potential scission and crosslinking sites are generated at random along the main chains, with the ratio of crosslinking to scission set by the parameter s ($3 < s < 15$ for PE). The formation of crosslinks is controlled by varying a capture radius, centered on each of the unreacted crosslinking sites. The closest radical that is within this radius will be allowed to crosslink with the one at the centre of the radius. After all the crosslinks are made, the scission sites are allowed to break. The software keeps track of the structures produced, and the sol and gel fractions. In this way defects, including cycles and dangling ends, can be determined. This model was compared to sol/ gel, swelling and visco-elastic data for irradiated polymer with generally good agreement.

This approach is interesting for a couple of reasons, firstly it allows random scission of branched chains, and secondly it gives information on the structure of the network formed. We can do scission on branched chains, since we are keeping track of all the structures produced in the system. The limitations may be that the crosslinking and scission are still done in a two step serial process (now crosslinking first) and secondly a finite number of chains needs be specified due to computational requirements, although the authors state that this is not a difficulty.

Finally, Demjanenko and Dusek (1980) have considered a complex statistical model from the theory of branching processes based upon the graph model (Gordon 1962, 1966, 1975, 1976), that accounts for scission followed by crosslinking, crosslinking followed by scission and simultaneous random scission and crosslinking.

4.3.3 Experimental and Analytical

Several studies on the chemical crosslinking of polyethylene (and copolymers) have been done. See table 11 for a brief summary of some of the methods and results of the more recent ones. People have studied high density polymers, low density polymers, different molecular weights, different initiators, different temperatures, different reaction times, with and without additives, in extruders, batch mixers, molds, test tubes and thin films. However most of the work, at least one of the following is true:

a) initial polymer is not completely characterized with respect to molecular weight distribution, copolymer composition, branching and level of unsaturation.

b) the reaction temperature is not well defined over the entire reaction period. In extruders and to a lesser extent in batch mixers the temperature is not very well known for the whole polymer sample. For hot pressed molds, test tubes, and thin films the heat up time to reaction temperature may be significant, and is not often reported. Moreover this temperature- time profile may not be reproducible from one experiment to another.

c) the validity of the method of analysis may be suspect, for example, using GPC to measure the molecular weight of branched polymer.

Table 11 Summary of some recent studies of chemically crosslinking polyethylene

Authors	Modification method	Analysis method	Initiator	Polymer	comments
(1991) Kwei et al.	see Schlecht et al. (1988)	GE	DTBP		Adapted CP equation to include time of reaction. Used CP equation to quantify the amount of scission and crosslinking during grafting of hexafluoraoacetone onto PE. (p/x= 0.33 ± 0.1).
(1990) Bremner and Rudin	Thin films (20 to 33 min.)	FTIR, ^{13}C-NMR, GPC-LALLS, DSC	DCP	HDPE	HDPE purified of additives. Long branch formation favoured by higher temperatures. Chain extension reactions due to C=C were favoured by lower temperatures. Trans C=C increase as terminal C=C decrease with increasing DCP. Chain coupling converts terminal C=C to trans C=C. Increasing temperature leads to increased terminal C=C indicating scission. The virgin HDPE had no SCB but did have LCB as measured by NMR. DCP leads to scission of these LCB Crystallinity decreases with increasing DCP.
(1990) Suwanda and Balke	hot press static mixers in SSX press SSX, STM	GPC, DSC, MFI, TREF	L-130,	LLDPE, HDPE	Looked at mixing of initiator at feed port and into the melt using a blue dye. Feed port feed is best since the mixing is poor when fed directly into the melt. TREF of HDPE broadened with increasing initiator due to branching plus molecular weight effects. DSC showed little change in crystallinity. GPC (no branching corrections) showed increase in molecular weight for LLDPE
(1990) Song and Baker	Haake batch type mixer	IR, FTIR, MFI, NMR, SF	L-130, BPO, CHPO, TBHPO, TBPO	LLDPE	Considered grafting on to PE. High temperatures and longer reaction times favoured crosslinking of the polymer over grafting. Peroxides were effective but azo initiators were not. Temperature not constant with time.

(1989) Suwanda and Balke	hot press SSX, static mixer	MFI, DSC, GPC, GE, FTIR	L-101, L-130, DCP, DTBP	LDPE, LLDPE, HDPE	Crosslinking reaction seems slow. Low levels of initiator used in extruder to prevent pressure build up. This should favour chain extension and branching to crosslinking. FTIR suggests C=C in HDPE are consumed. GPC and DSC not sensitive to the small changes.
(1989) Kampouris and Andreopoulos	brabender plasticorder (160°C)	GE, DENSITY TMA	DCP	LDPE, HDPE	Density is reduced with gel (especially for HDPE). Hardness and wear resistance are reduced.
(1987) Kampouris and Andreopoulos	Brabender plasticorder	GE, TENS	BPO	LDPE	For the application of crosslinking during injection molding. Studied effect of initial MFI, density and particle size (pellets and powders) Lower MFI -> higher crosslinking Pellets lead to nonhomogeneous product
(1987, 1984) Peacock	hot press, after mixing initiator and polymer in a hot solution.	FTIR	DCP	LPE	Investigated the effect of terminal C=C present in PE. C=C measured by FTIR. DCP preferentially reacts with C=C to extend the chains before random crosslinking. Used a statistical model to account for pure random crosslinking.
(1987) Chodak et al.	hot press at 170°C	GE	DCP	LDPE	Influence of the additives hydroquinone (HQ), p-benzoquinone (p-BQ) and diallyl phthalate (DAP) were studied. HQ and p-BQ retarded crosslinking by consuming radicals, DAP promoted it.
(1987) Hendra et al.	Hot press (180°C)	GE, SWEL, DSC, RAMAN, FTIR	DCP	LPE	DCP was added to viscous solution of PE and xylene at 100°C. Each chain had a terminal $HC=CH_2$. Until approx. 1/2 of the C=C's are consumed, no crosslinking occurs. MP and crystallinity fall with DCP
(1982) Lem and Han	molded at 170 C and 2000 - 2400 psi.	cone and plate rheometer, GE, GPC	DCP	LDPE, HDPE	Looks at the rheological properties of modified polyethylene. No gel. Trouble to get measurement if gel present. LDPE (not HDPE) has some scission since GPC trace shows some lower molecular weight material than virgin. Viscosity, the 1st normal stress difference, shear thinning, elasticity increase with DCP. It may be possible to make a resin that is less viscous (especially at high shear rates) and more elastic.

(1981) Borsig and Szöcs	pressing and heating (pulse in temperature)	GE	BPO		Studied pressure (300, 600 800 MPa) effect. An activation volume of 9.1 cm^3 mol^{-1} was found at 120°C. Gel grows for over 100 minutes at high pressure but at 0.5 Mpa reaction is complete at very low times. BPO decomposition slows down with increasing pressure. Gel level is decreased with increasing pressure.
(1981) de Boer and Pennings	Comp. Mold at 180 C	IR, GE, SWEL	L-130	UHMWPE	No scission of polymer as calculate by CP equation. Crosslinking not detected by IR, but C=C could be seen.
(1981) Hulse et al.	pressed into pellets and heated in a test tube	IR, GE, VISC, NMR	DCP	Linear PE, C14	Unreacted C14 removed by steam. C28 not volatile. C=C measured by IR. Can get dimerization of C14 across DCP by product but minor. 30% of DCP results in C=C. Both combination and disproportionation important.
(1980) Capla and Borsig	heated in glass tubes at 150°C	SWEL	DCP	PE -PP copolymers	The ratio of scission to crosslinking (from CP equation) depends linearly upon PP content.
(1970) Simunkova et al.	mixed in brabender (117C) and heated in glass tubes	GE	DCP, 14P	LDPE	Identified decomposition rate 14P in LDPE and n-octane (very slow). Found only combination, no disproportionation or scission.
(1989) Mukherjee et al.	SSX (135 to 145 C) into bath at 90°C	drawing SWEL	DCP	LDPE	Tensile properties, percent shrinkage and density were improved with increasing DCP. Percent swelling decreased.

Abbreviations

14P $\alpha-\alpha'$ – bis(tert-butyl peroxy)-p-diisopropylbenzene

BPO benzoyl Peroxide

C=C unsaturations in the chain, or at chain ends.

CHPO cumene hydroperoxide

Cn a lower molecular weight model compound having *n* carbons.

CP Charlesby Pinner equation

DCP Dicumyl Peroxide

DSC Differential scanning calorimeter

DTBP di- t- butyl peroxide

FTIR Fourier transform infrared spectroscopy

GE gel extraction

GPC Gel permeation chromatography

HPDE high density polyethylene

IR infrared spectroscopy

L-101 Lupersol 101 (2,5-dimethyl-2,5-di(t-butylperoxy) hexane)

L-130 Lupersol 130 (2,5-dimethyl-2,5-di(t-butylperoxy) hexyne-3)

LCB long chain branch

LDPE low density polyethylene (from high pressure process and thus possibly having long branches)

LLDPE linear low density polyethylene

LPE linear polyethylene

MFI melt flow index

NMR nuclear magnetic resonance

SCB long chain branch

SF fractionation by solvents

SSX single screw extruder

STM static mixer

SWEL swelling

TBHPO tert-butyl hydroperoxide

TBPO tert -butyl peroxide

TENS tensile strength

TMA thermal mechanical analyzer

UHMWPE ultra high molecular weight polyethylene

VISC viscosity

4.4 Mathematical Modelling

Of the chemical reactions listed in the previous section, let us choose the subset that includes, initiator decomposition, radical attack of back bone hydrogen atoms, scission of the chains and termination by combination (figure 50). We can perform population balances on chains of length r (Zhu 1991) and derive expressions for the molecular weight distribution as a function of degree of modification. The degree of modification can be related to the peroxide concentration and the reaction time. The classical solution to this problem has been to use the two step approach (Saito and Flory). In this work we have developed a numerical solution to the equation developed by Zhu (1991). In the next sections we shall discuss some of the inadequacies of the two step approach, the numerical solution of the Zhu equation, and present some comparisons between the two approaches.

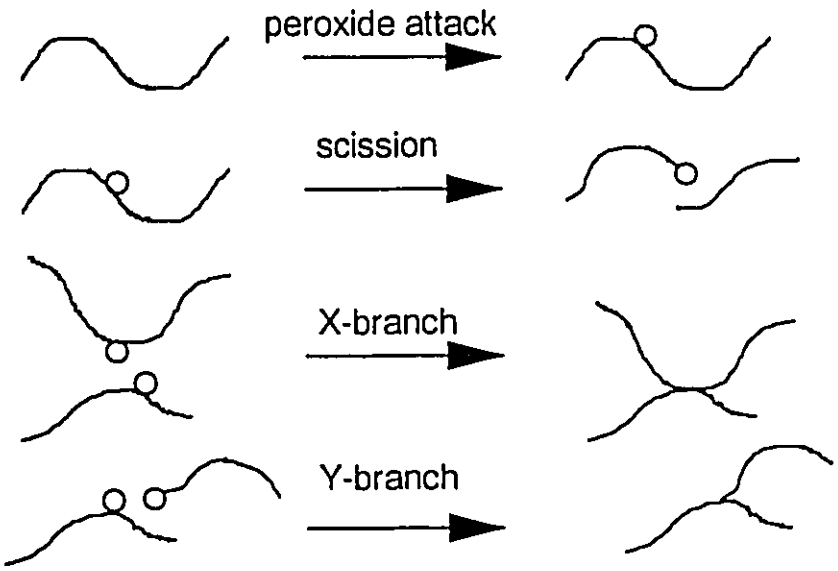

Figure 50. The chemical reactions that modify the polymer molecular structure during simultaneous random scission and crosslinking.

4.4.1 Some discussion of the two step approach.

Software entitled *2step* was developed to use the two step approach to find the gel fraction, and for special cases the molecular weight distribution and the molecular weight averages, for a given initial distribution and peroxide level. This model solves differential equations for the initiator concentration, the degree of scission and

the degree of crosslinking. Then given the degrees of scission and crosslinking, Saito's equation for pure random scission and Flory's equation for pure random crosslinking are used to find the gel fractions. One obtains the entire molecular weight distribution for pure random scission. The averages in the pre gel region predicted. The averages after the gel point can be calculated if we start with the most probable distribution by using equations 43, 44, 47, 48, 49 and 50 in Hamielec et al. (1991).

The Charlesby-Pinner equation has been widely used, for example Kwei et al. (1991), to find the ratio of scission to crosslinking for polyolefins. Let us take a look at how valid this approach is for chemically induced modification. The assumptions of the Charlesby-Pinner equation are a) two step solution is valid for scission and crosslinking, b) initial distribution is the most probable distribution, c) the ratio of scission to crosslinking (p/x) is constant and d) random scission and crosslinking. The Charlesby-Pinner equation is used by plotting $s+\sqrt{s}$ versus the reciprocal of the crosslink density, drawing a straight line through the data, extrapolating to infinite degrees of crosslinking to find the ratio of scission to crosslinking. Figure 51 shows predicted curves for various conditions on a Charlesby-Pinner plot.

Lines 1 and 2 demonstrate the effect of the initial molecular weight distribution. The p/x ratio was held constant at p/x=0.43 (by artificially forcing the initiator concentration to be constant). The quantity $s+\sqrt{s}$ is calculated as the peroxide causes crosslinking. Line 1 is calculated using the most probable distribution as the initial distribution and is a straight line with intercept equal to 0.43 as expected. Line 2 uses a broader distribution with identical Mw. This line is not straight but curved. However the intercept will still be equal to 0.43. Thus fitting a straight line to experimental data, where the initial distribution is not the most probable can be in serious error. A more realistic case is given by lines 3 and 4 where the initiator concentration is allowed to fall with reaction, and the ratio of p/x is not constant. Line 3 uses a most probable distribution and line 4 uses the broader distribution. The final value of p/x was arbitrarily set to be 0.43 by varying the scission and crosslinking parameters. The initial p/x will be smaller. Notice the trend at higher values of crosslink density, the quantity $s+\sqrt{s}$ actually increases with increasing crosslinking. This is because the ratio of p/x is increasing and the calculated gel level *falls*. Lines 1 through 4 all have the same initial peroxide concentration. Lines 5 and 6 are calculated by varying the initial peroxide concentration and calculating the $s+\sqrt{s}$ when all the peroxide is consumed. This is usually how the experiments are performed when experimental Charlesby-Pinner plots are constructed. The ratio of p/x is allowed to vary but the scission and crosslinking parameters are set to

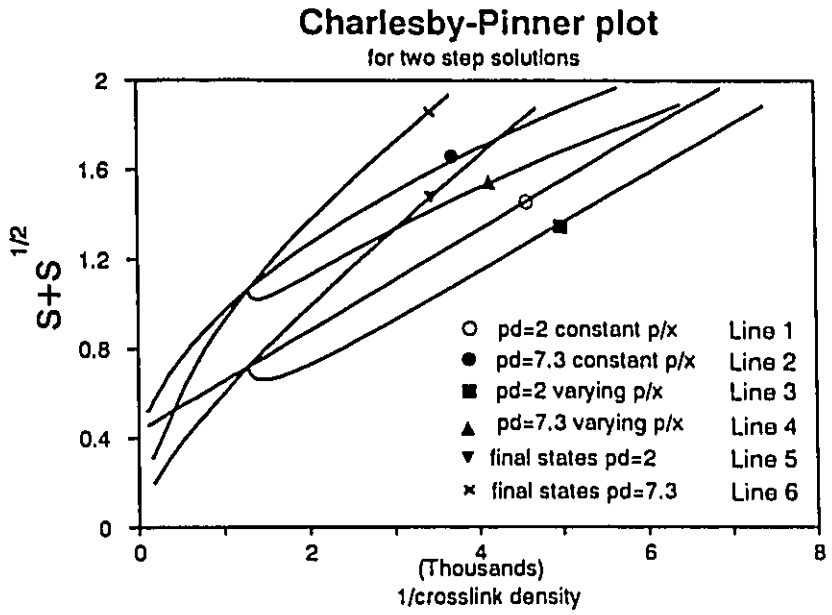

Figure 51. Charlesby- Pinner plots for several two step solutions. 1) most probable initial distribution and p/x constant, 2) broad distribution and p/x constant, 3) most probable distribution and p/x not constant 4) broad distribution and p/x not constant 5) the final values due to different initial peroxide concentrations for most probable distribution, 6) the final values due to different initial peroxide concentrations for a broad initial distribution

the identical values as for lines 3 and 4. Lines 5 and 6 do not follow any of the other lines. The lines are a somewhat closer to linear, except that the intercept is now not equal to 0.43 but will tend to zero as [I]o increases (see appendix). These observations lead one to the conclusion that using Charlesby-Pinner plots to find the ratio of scission to crosslinking, for peroxide induced modifications, is not valid.

The classical approach assumes that the polymer undergoes the entire amount of scission and then the entire amount of crosslinking. An improvement could be to use a two step model were the polymer undergoes a small fraction of the total scission, then a small fraction of the total crosslinking. This slightly modified molecular weight distribution is then subjected to an additional small amount of scission followed by additional crosslinking. This process is continued until the desired amount of scission and

crosslinking is reached (Hrymak 1993). This approach still neglects end linking and the formation of Y branches, and requires a numerical solution for the crosslinking step, but may give better results that the classical two step approach.

4.4.2 Numerical solution of the model equations

We are interested in solving an equation of the form, as derived by Zhu (1991) for simultaneous random scission and crosslinking.

$$\frac{1}{r}\frac{\partial w(r,z)}{dz} = -w(r,z) + 2\alpha \int_r^\infty \frac{w(s,z)}{s} ds$$

$$+ \frac{\beta_4}{2} \int_0^r [w(s,z)w(r-s,z)] ds$$

$$+ \beta_3 \int_0^r \left[w(s,z) \int_{r-s}^\infty w \frac{(m,z)}{m} dm \right] ds$$

$$+ \frac{\beta_2}{2} \int_0^r \left[\int_s^\infty w \frac{(m,z)}{m} dm \int_{r-s}^\infty w \frac{(m,z)}{m} dm \right] ds$$

where z is the degree of modification and α is a group of kinetic parameters related to scission, β_4, β_3 and β_2 are groups of kinetic parameters related to the formation of X branches, Y branches and end linking respectively.

$$\beta_4 = \frac{k_{tc} R_b^2}{k_p R_b + k_{tc} R_b^2 + k_{tc} R_b R_e}$$

$$\beta_3 = \frac{k_{tc} R_b R_e}{k_p R_b + k_{tc} R_b^2 + k_{tc} R_b R_e}$$

$$\beta_2 = \frac{k_{tc} R_e^2}{k_p R_b + k_{tc} R_b^2 + k_{tc} R_b R_e}$$

$$\alpha = \frac{2k_p R_b - k_{tc} R_e^2 - k_{tc} R_e R_b}{2(k_p R_b + k_{tc} R_b^2 + k_{tc} R_b R_e)}$$

R_b and R_e are backbone and chain end radical concentrations, respectively, and are given by using the stationary state hypothesis for all radical species

$$R_b = \frac{k_{fp} Q_1 R_o}{k_p + k_t R_t}$$

$$R_e = \frac{k_p R_b}{k_t R_t}$$

$$R_t = \left(\frac{f k_d [I]}{k_t} \right)^{1/2}$$

$$R_o = \frac{f k_d [I]}{k_{fp} Q_1 + k_t R_t}$$

R_t and R_o are the total radical concentration and concentration of radicals on initiator fragments. Here it is assumed, in α, that there are two ways to cut a chain to make the desired products. However some modifications to this equation yield an equation of the same form, that can be solved using the same algorithm as described here.

Triacca et al. (1991) attempted to solve this equation by selecting several chain lengths (200 or so) and solving the resulting differential equations using the package LSODE (Hindmarsh 1983). The integrals were evaluated using the trapezoid rule. The solution for the pure random crosslinking case was found to about 80% of the way to the gel point before excessive numerical errors and computational time were encountered.

The following is a more efficient algorithm. Firstly the molecular weight distribution was discretized, roughly equally spaced on a natural log of chain length scale. About 50 to 100 nodes are used and each node becomes a differential equation to be solved (see figure 52) with either time or the degree of modification as the independent variable. The equation is transformed using W(r) dr = W'(x) dx where x=ln(r) to improve the accuracy of the solution, especially that of the integrals. The molecular weight distribution is then interpolated using a natural cubic spline. This provides a smooth interpolation, without excessive *waviness* and allows one to solve the integrals in a more efficient manner. These differential equations are then solved using LSODE. Each differential equation has a number of integrals to be solved, let's number them as

(integral 1) $$\int_r^\infty \frac{w(s,z)}{s} ds$$

(Integral 2)

$$\int_0^r [w(s,z)w(r-s,z)]ds$$

(Integral 3)

$$\int_0^r \left[w(s,z) \int_{r-s}^{\infty} w\frac{(m,z)}{m}dm \right] ds$$

(Integral 4)

$$\int_0^r \left[\int_s^{\infty} w\frac{(m,z)}{m}dm \int_{r-s}^{\infty} w\frac{(m,z)}{m}dm \right] ds$$

Integral 1 can be evaluated between the nodes by substitution of the spline coefficients for W(r) and solving the integral analytically. To obtain the entire integral we simply sum up the results between all nodes from r to infinity. Notice that this integral also appears in integrals 3 and 4 and thus are solved in the same manner for these cases. We initially calculate the value of integral 1 at each node, and save these values in an array. We can then obtain the value of the integral at any r value by solving the integral from r to the next nodal value (analytical solution) and adding this to the value of the integral at the next nodal value.

Integrals 2, 3 and 4 are all evaluated over the same region (0 to r) and thus these integrals can be evaluated at the same time. Gaussian quadrature (four integration points) was used to evaluate the integrals between the nodes (or partial regions between the nodes) and then sum up the values for each portion. The differential equations are solved using a predictor-corrector package called LSODE (Hindmarsh 1983)

The sol fraction and the molecular weight averages can be found by integrating over the entire molecular weight distribution. By assuming a cubic for W(x) between the nodes, we can find an analytical solution to these integrals. The sol fraction will be the area under the curve W(x) versus x and will fall below unity when gel is formed. In this way the gel fraction is calculated. Moreover when no gel is formed, the sol fraction will give us an indication of the numerical error.

The number of nodes required to adequately represent the initial distribution was investigated by choosing a most probable distribution, descretizing it using a number of nodes and interpolating with the spline, and then comparing approximately 1000 interpolated values with the actual values. The error decreases with increasing number of nodes indicating that we need at least 25 nodes to adequately approximate the distribution. More than 100 nodes is probably unnecessary (see figure 53). Moreover if

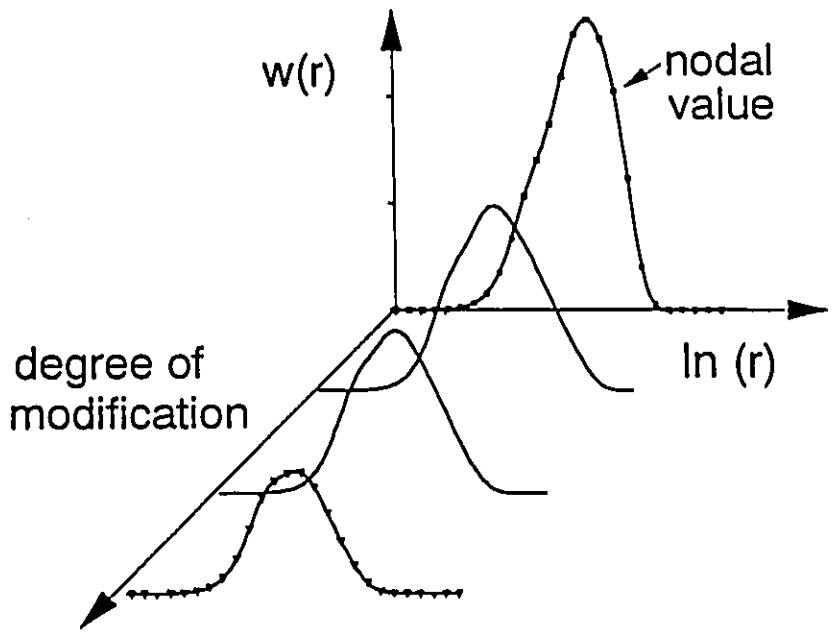

Figure 52. The algorithm. 1) select nodal values on molecular weight distribution to obtain one differential equation for each node, 2) interpolate between the nodes using cubic splines 3) evaluate integrals using gaussian quadrature, or analytically using the spline 4) Solve the differential equations using LSODE

we assume an initial distribution that is most probable, one can derive analytical solutions to integrals 1 to 4 for a specific chain length at zero degree of modification. When three point gaussian quadrature was used, for the interval between the nodes, the error in the integrals was insignificant.

Computer software entitled *SIMULTAN* was created to use this algorithm to calculate the molecular properties for any arbitrary initial molecular weight distribution, initiator concentration, reaction time and temperature. The language is FORTRAN. *SIMULTAN* also can perform the calculations using the two step approach for comparison purposes. The solution requires approximately five minutes for the pure random scission case, and between five and 40 minutes for the pure random crosslinking case on a IBM PS/2-70, 386 machine with math coprocessor operating at 20 Mhz clock speed. Computer time depends upon the required degree of modification and the accuracy requested.

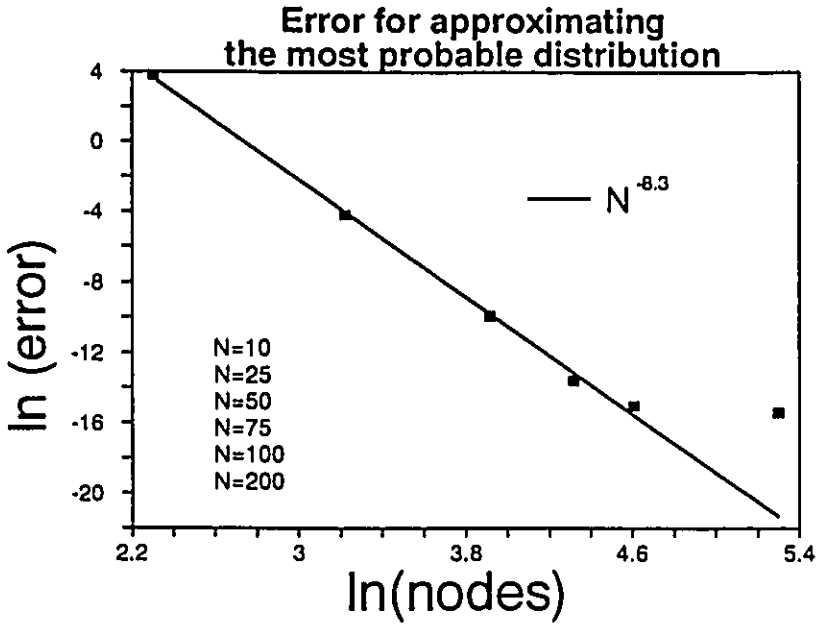

Figure 53. The number of nodes needed to approximate the initial most probable distribution.

4.4.3 Comparisons with classical solutions

Pure random scission

For the case of pure random scission, one only needs to evaluate integral 1 for each differential equation, and thus the solution is quite fast. We started with an arbitrarily broad distribution and calculated the molecular weight distributions and averages for increasing degrees of pure random scission. The molecular weight distributions are presented in figure 54. Increasing scission narrows the molecular weight distribution to approach the most probable. This is a somewhat trivial result, as Saito (1972) has presented an analytical solution for this case, however this exercise provides the opportunity to check part of the numerical solution. The error in the calculation, as indicated by the sol fraction is less than one percent for 100 nodes. Figure 55 compares the molecular weight averages calculated by our numerical solution to that predicted by Saito. The agreement is excellent.

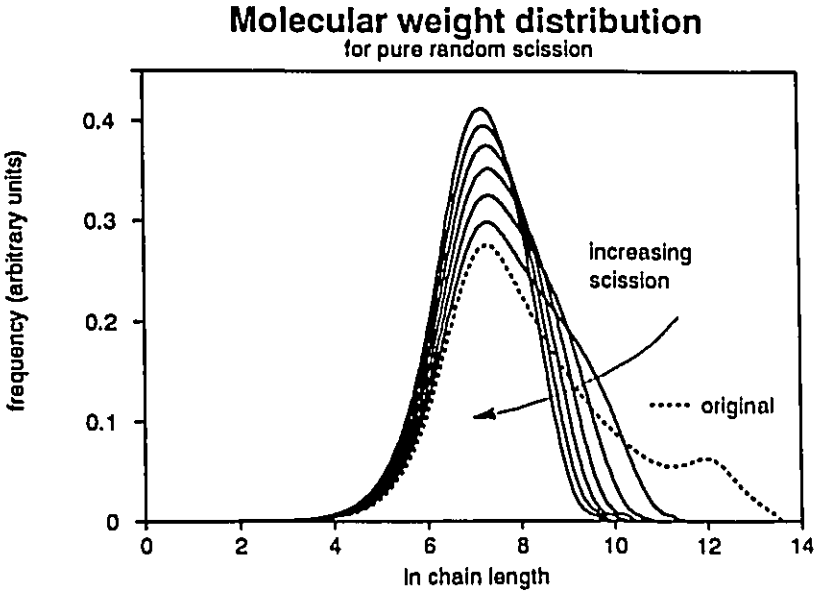

Figure 54. Molecular weight distribution for pure random scission.

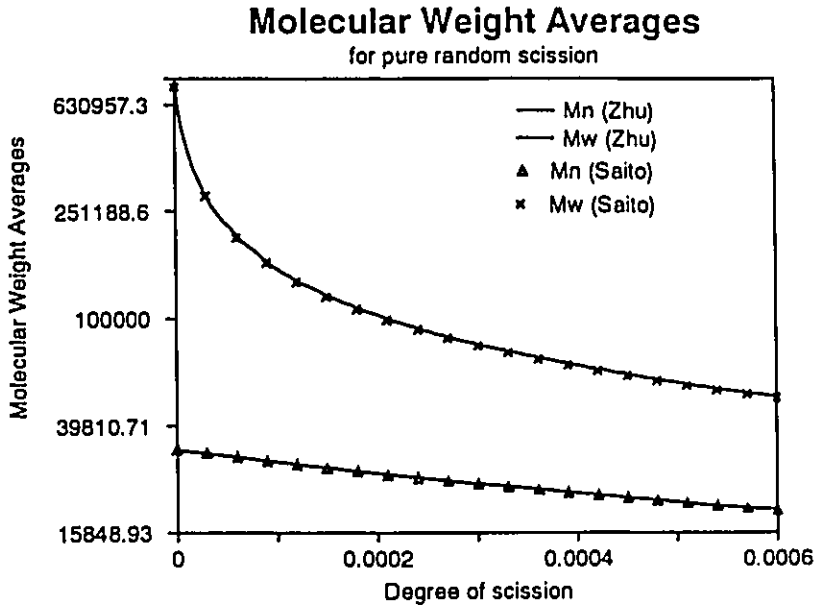

Figure 55. Molecular weight averages for pure random scission.

Pure random crosslinking

Next we test pure random crosslinking using an initial distribution that is most probable. The weight average molecular weight is 250,000. Figure 56 reveals that the molecular weight distribution first broadens as higher molecular weight material is created, until the gel point. After the gel point the molecular weight distribution of the sol narrows as the gel grows by preferentially consuming the higher molecular weight sol material. In the post gel region the molecular weight distribution and the averages describe the sol fraction only, and the area of the peak is equal to the sol fraction.

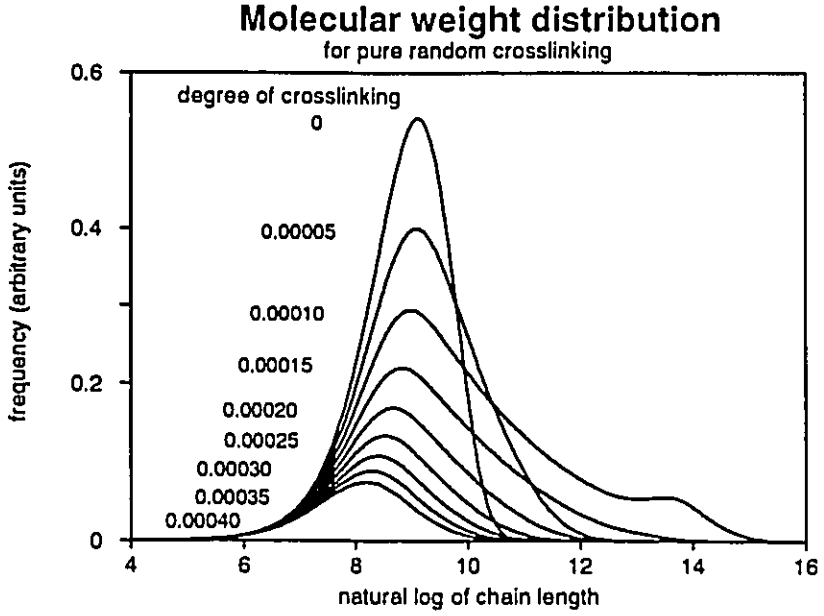

Figure 56. Molecular weight distributions as a function of the crosslink density.

There are two parameters that we use to control the error of the solution, the tolerance for LSODE and the number of nodes. Increasing the number of nodes or reducing the tolerance for LSODE increases the time for the solution of the model. The relative tolerance for LSODE seems to have little effect on the error as long as it is set to be less than about 10^{-3}. Figure 57 shows the gel fraction as a function of the crosslink density for different numbers of nodes. In all cases the gel fraction becomes slightly negative before the gel point and then rises to become greater than zero. Increasing

the number of nodes tends to make the negative deviation sharper and moves the gel point closer to the gel point predicted by Flory. At higher gel fractions all solutions approach the values predicted by Flory.

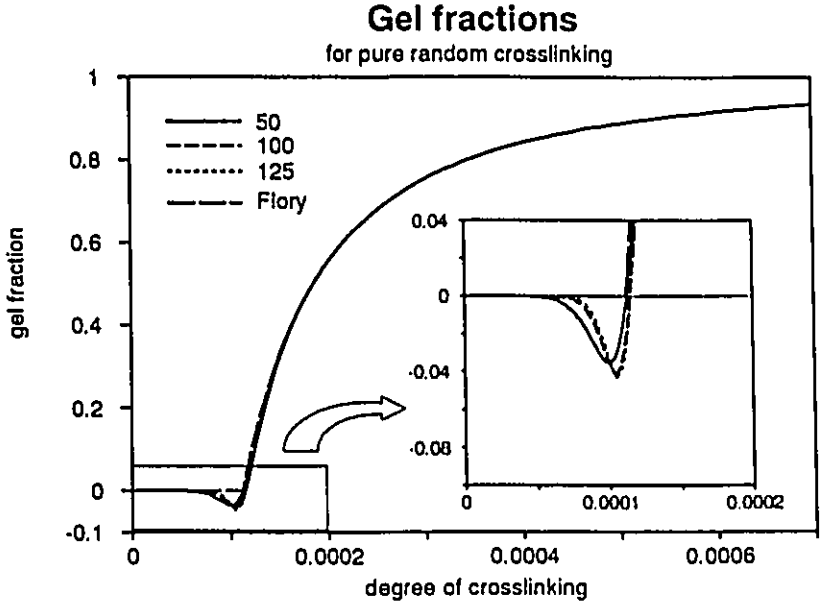

Figure 57. Gel fraction for pure random crosslinking as a function of the crosslink density and the number of nodes.

Since we assumed the most probable distribution for the initial molecular weight distribution, the gel fraction and the molecular weight averages can be calculated from equations 43, 44, 47, 48, 49 and 50 of Hamielec et al. (1991). Figure 58 shows how the weight average molecular weight, as predicted by Flory, grows to infinity at the gel point, and then falls after the gel point. The numerical solution does not go to infinity but shows a smooth transition through the gel point. The peak becomes sharper as the number of nodes is increased. The number average molecular weight follows the same increasing - decreasing trend but remains finite right through the gel point. The number of nodes does not greatly influence the number average. In all regions, except right very near the gel point, the numerical solution and the classical solution are in excellent agreement.

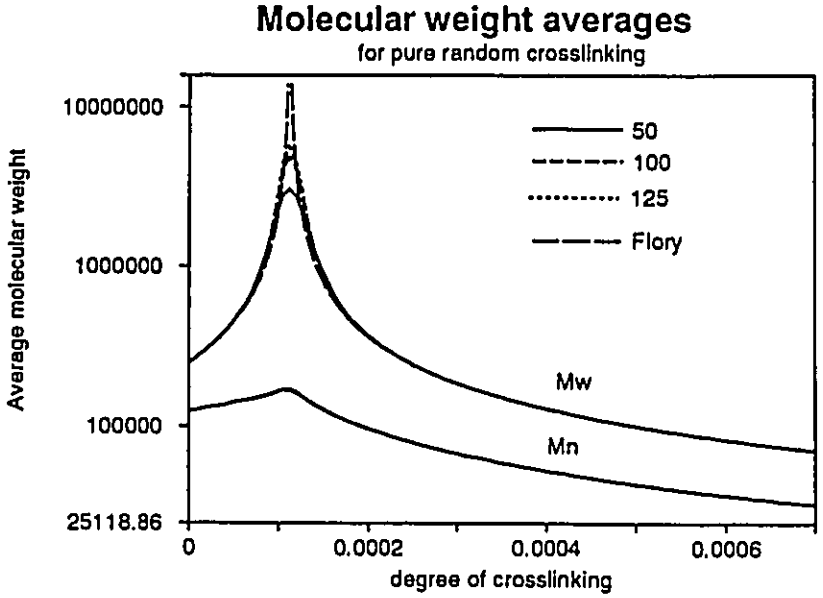

Figure 58. Average molecular weights as a function of crosslink density and the number of nodes.

Simultaneous random scission and crosslinking

The numerical solution to Zhu's equation compares quite well with the classical solutions for pure random scission or pure random crosslinking, however this equation was derived to describe the case of simultaneous random scission and crosslinking. One can consider simultaneous random scission and crosslinking of an initial distribution which is broader than the most probable, using both Zhu's equation and the two step solution. We set the parameters such that we obtain the overall ratio of scission to crosslinking equal to p/x=0.43, and use 75 nodes for the numerical solution. Figure 59 compares the gel fraction predictions. The simultaneous solution predicts that the gel point occurs at lower degrees of crosslinking and gives a higher gel fraction over the entire range. At large degrees of modification the two step solution predicts a reduction in the gel fraction. Zhu's equation shows a continuous rise in gel fraction. The reduction in the gel fraction seems to be an unreasonable consequence of the two step assumption. If one considers the branching frequencies, one can see that there can be a significant contribution to the molecular weight due to Y branches. Figure 60 shows the predicted branching frequencies versus degree of modification. In this case there are more X branches than Y branches, and the rate of branching

appears to change slightly as the initiator decomposes, with the rate of X branching decreasing and the rate of Y branching increasing. Higher initiator concentrations favour X branches over Y branches. The two step model neglects the Y branches, and thus must underestimate the molecular weight build up, and the gel fraction. Zhu's model assumes that the termination rate constant for the production of Y branches is equal to that for the production of X branches. In fact, the termination rate constant for production of Y branches may be larger because of steric difficulties in getting two backbone radicals together to form a X branch.

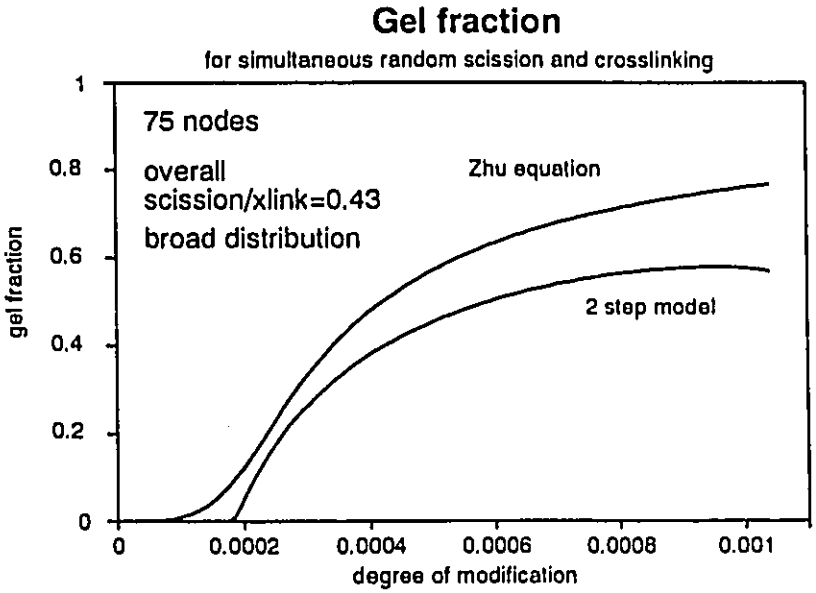

Figure 59. Comparison of the gel fractions predicted for simultaneous random scission and crosslinking using Zhu's equation and the two step solution.

The average molecular weights, in the pre gel region, agree quite well (Figure 61), except at the gel point where the two step solution predicts an infinite weight average molecular weight. Calculation of the two step averages after the gel point for this arbitrarily broad distribution was not done and so no comparison was possible here.

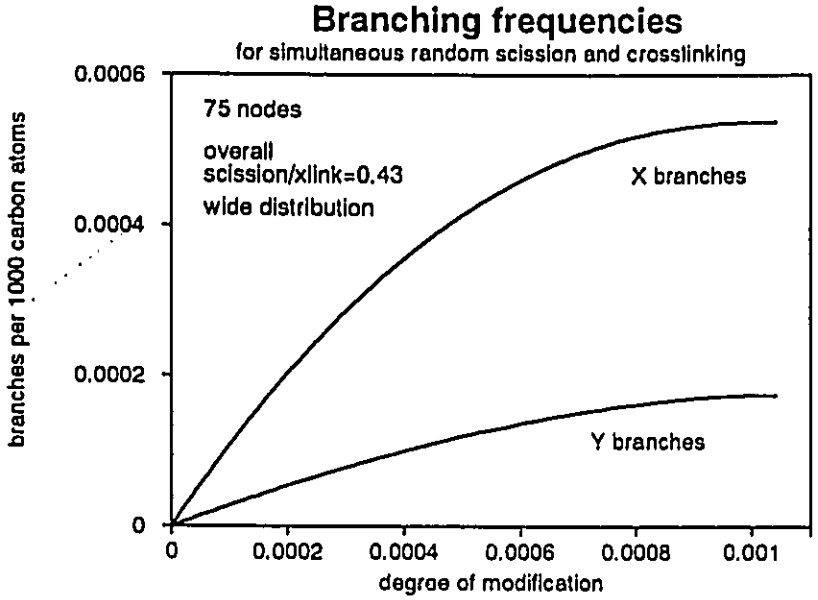

Figure 60. X and Y branching frequencies for scission and crosslinking. Frequencies are as branches per thousand backbone carbon atoms.

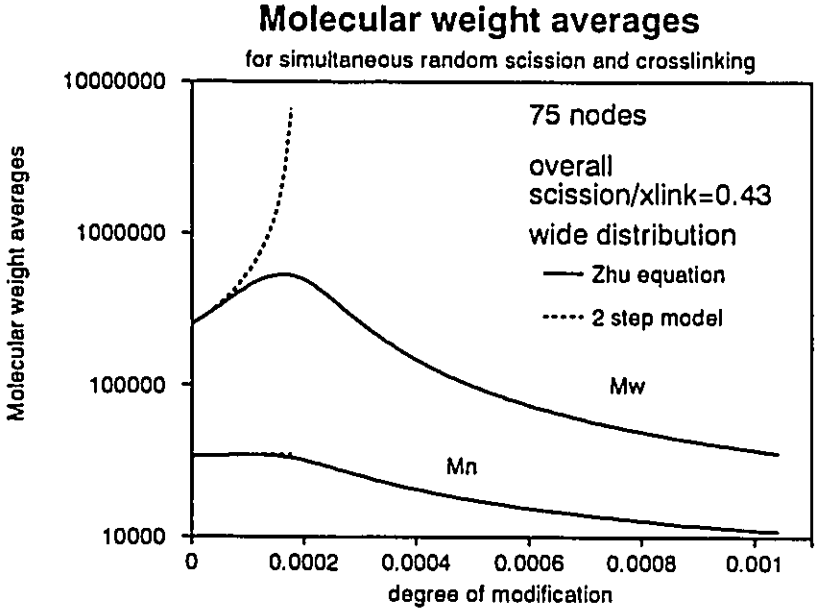

Figure 61. Comparison of the molecular weight averages predicted for simultaneous random scission and crosslinking using Zhu's equation and the two step solution.

Figure 62 shows the results of a calculation for various degrees of modification, and compares the final results to that given by the two step approach. Here, the two step approach is implemented by solving Zhu's equation for pure random scission up to degree p, and then for pure random crosslinking up to degree x. The two step approach seems to overestimate the size of the high molecular weight tail.

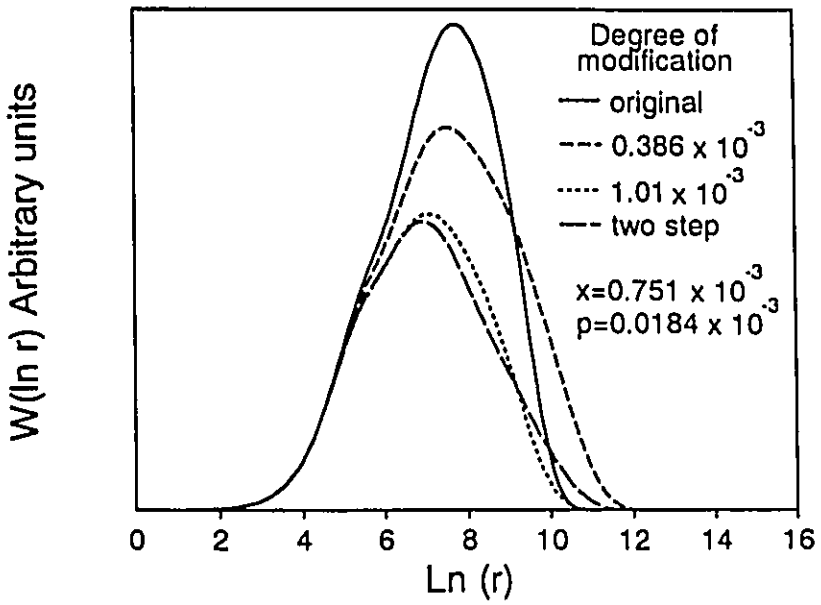

Figure 62. Molecular weight distributions during simultaneous random scission and crosslinking as calculated by solving Zhu's complete equation simultaneously or by solving it in two steps.

In summary one can say:

- the numerical solution to Zhu's equation compares quite well with the classical solutions for pure random scission and crosslinking. There is some disparity between the molecular weight averages near the gel point for pure random crosslinking.
- For simultaneous random scission and crosslinking, Zhu's equation predicts the gel point to occur at lower degrees of modification than does the two step solution. Higher gel fractions are predicted by Zhu's equation at all degrees of modification.
- Unlike the two step model, which predicts a reduction in the gel fraction at higher degrees of modification, Zhu's equation shows a continuous increase.

- The number and weight average molecular weights predicted by both methods, in the pre gel region are quite similar.

4.4.4 Modifications for random scission of branched polymers

The equation for simultaneous random scission and crosslinking, developed by Zhu (1991) assumes that the molecules that undergo scission are linear. This means that each molecule has two ends, and thus there are two possible ways to cut the chain to create a smaller molecules of specified length. To modify a chain of length r to create a chain of length s (s<r), we can cut the chain s units from either end. On the other hand, branched molecules will have more than two ends per molecule and thus the possibilities should increase however the number of possibilities will not equal the number of ends, but will also depend upon the placement of the branch along the backbone. Moreover in some cases, especially for gel, a scission will not create a second molecule. What we need to do is to make some assumptions about the average branching structures, for instance, assume the molecules are linear (Zhu 1992), stars or combs and so on.

Let us make the first step, and assume that all the polymer molecules are stars, and all the branches are of the same length and radiate from the center of the molecule. Based upon the branching frequencies and the degree of scission, we can easily calculate the number of chain ends per molecule.

Each scission adds two ends and increases the number of molecules by one.

Each Y branch formed reduces the number of ends by one, and reduces the number of molecules by one.

Each X branch formed does not change the number of ends, but reduces the number of molecules by one.

Therefore the total number of molecules is given by

$$Q_0 = Q'_0 + (p - (x + y))Q_1$$

where Q'_0 is the initial number of molecules, p is the number of scission reactions and x and y are the number of X branches and Y branches. Q_1 is the first moment of the polymer molecular weight distribution and is constant. The number of ends equals

$$E = 2Q'_0 + (2p - y)Q_1$$

The total number of ends per molecule is then given by E/Q_0. Making this ratio and using the initial number average chain length calculated by $r_{n_0} = Q_1/Q'_0$ we can find that

$$e = \frac{E}{Q_0} = \frac{2 + (2p - y)r_{n0}}{1 + (s - y - x)r_{n0}}$$

Let us consider a star polymer of length r, with four branches of length r/4. If we wish to cut the molecule to create a second molecule of length n we have four cases.

1) n > r : no possibility of creating a molecule of length n

2) n < (r/4) : four possibilities to create a molecule of length n

3) (r-r/4) < n < r : we can cut r-n off of any end to get a molecule n units long, therefore there are four possibilities.

4) (r/4) < n < r-r/4 : no possibilities since we would have to cut off more than r/4 from any end.

For the more general case, we simply replace 4 with the number of ends per molecule, e, and we can still consider the number of possibilities (see figure 63).

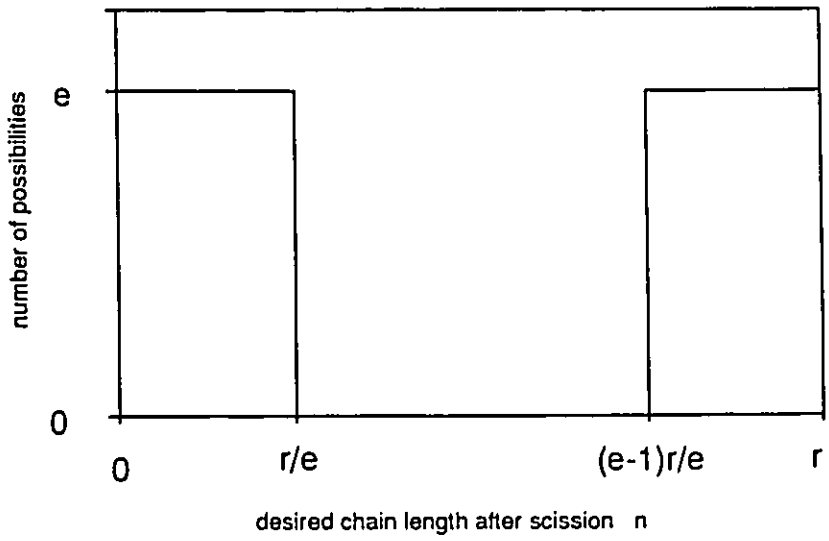

Figure 63. The possibilities for creation of a molecule of length n from a star shaped molecule having r units and e ends.

The term for the production rate of molecules of length n by random scission of is given by the term

$$\alpha \int_n^\infty \phi \frac{W(r)}{r} dr$$

where $\phi = e$ if n < r/e or n > (e-1)r/e and $\phi = 0$ otherwise. Thus we can break this integral up into two integrals

$$\alpha \int_n^\infty \phi \frac{W(r)}{r} dr = e\alpha \int_n^{m(e-1)} \frac{W(r)}{r} dr + e\alpha \int_m^\infty \frac{W(r)}{r} dr$$

Notice that this reduces to the case given by Zhu (1991) if e is equal to two. A simple illustration of the effects can be made if we assume that the molecular weight distribution is the most probable distribution.

$$w(r) = \tau^2 r \exp(-\tau \cdot r)$$

Branched molecules will most likely have a distribution broader than the most probable. We can substitute this expression into the integrals above and solve them analytically. We can also ratio this to the integral assuming linear molecules to determine the relative change in the scission term. This equation then becomes

$$\frac{\text{scission of stars}}{\text{scission of linear molecules}} = \left(\frac{e}{2}\right)\left[1 - \exp\left(\tau n\left(1 - \frac{e}{e-1}\right)\right) + \exp(\tau n(1-e))\right]$$

Figure 64 shows the results of this calculation for several values of $n \cdot \tau$, the relative length of the molecule to be formed by scission, and several average ends per molecule. For small values of $n \cdot \tau$ the ratio is larger than one, and in the limit as $n \cdot \tau$ gets smaller the ratio will equal e/2. This result is expected since when we are making small molecules by scission, nearly all of the branches are longer than the desired molecule, and thus they can all be used. However as $n \cdot \tau$ gets larger the ratio falls below unity, reaches a minimum and then rises to some final value, above unity. Work is currently underway to determine the effect of this modification and others including the comb structures (Giudici 1992).

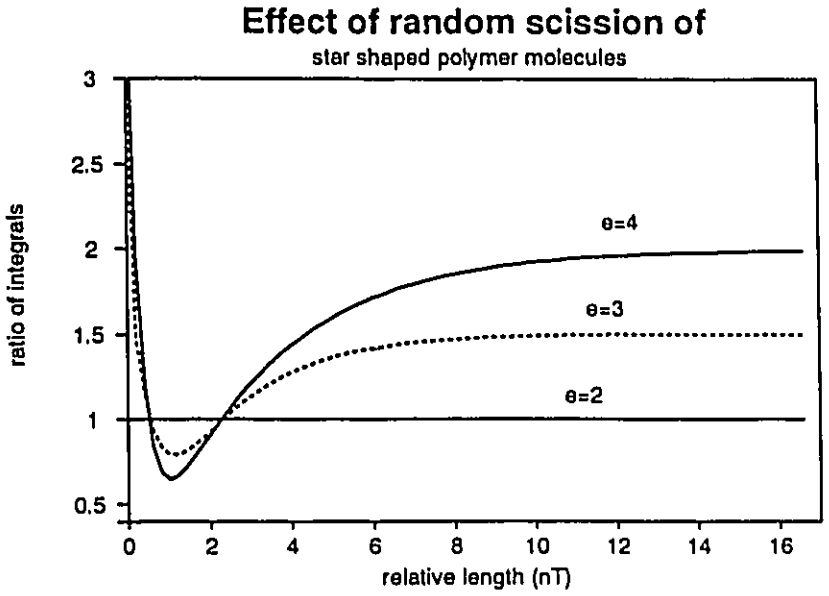

Figure 64. The ratio of the random scission of star molecules to linear molecules as a function of the number of ends per molecule and the relative length of the molecule to be formed by scission ($\tau \cdot n$). The most probable distribution is assumed.

4.5 Experimental

4.5.1 Modification of polyethylene

The polyethylene powder (HDPE) used was Novacor Product W50555-H with average molecular weights (as calculated by GPC) of around Mn= 10000, Mw=180000. The isotactic polypropylene powder used was Shell KY-6100.

The polymer was coated with the peroxides, Lupersol 101 (2,5-dimethyl-2,5 (t -butylperoxy) hexane, Atochem) and Lupersol 130 (2,5-dimethyl-2,5 (t -butylperoxy) hexyne-3, Atochem) (see table 12). This was accomplished by dissolving the desired amount of peroxide in acetone (BHD Inc.) and adding this to the polymer. Additional acetone was added to create a slurry which was well shaken. This slurry was placed in an aluminum pie dish and the acetone allowed to evaporate for at least 48 hours. The sample was stirred occasionally during the evaporation time. The polymer - peroxide mixture was then heated either in the minitruder or in ampoules and the resulting modified polymer analyzed for either gel content or molecular weight.

Table 12. Initiator decomposition rates.

Peroxide type	A - Frequency factor (s^{-1})	E - Activation energy (cal/mol)	Molecular weight	Percent Active
Lupersol 101	8.73×10^{15}	37182.	290.4	92.0%
Lupersol 130	7.88×10^{15}	38127.	286.4	92.5%

kd = A exp (-E/RT). T is temperature in Kelvin, R=1.987 cal/mol-K.
ref: Atochem

Minitruder experiments

Several experiments were performed using a minitruder (Randcastle Inc.) having the following specifications:

- single 1/4 inch screw. 24:1 L/D barrel
- three heated zones with temperature controllers to control within 1 °C
- maximum throughput to approximately 120 g/h at maximum speed of approximately 115 RPM. Controlled by tachometer feedback.

All polymer powders were screened through a 20 mesh sieve to help ensure adequate feeding. The throughput of the minitruder was measured for polypropylene at 200°C and was found to be a linear function of RPM.

$$Q = 0.3669 \quad RPM \qquad (mg/s)$$

The mass of polypropylene contained in the barrel and die was measured using a carbon black tracer at several RPM values and at 200°C and on average was 1.051 g. This allows the calculation of an approximate residence time (see figure 65).

$$\tau = \frac{2.8637x10^{3}}{RPM} \qquad (seconds)$$

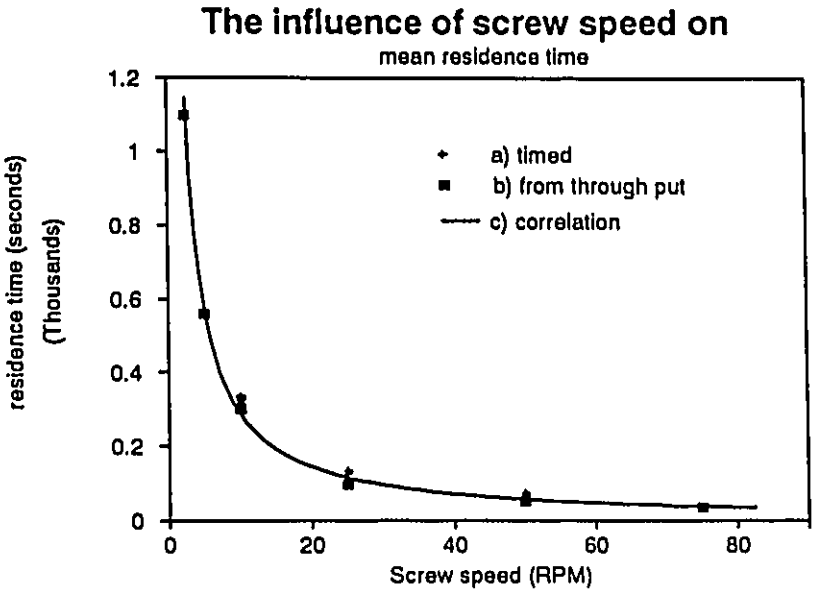

Figure 65. Residence time for minitruder calculated by a) measuring the time for a carbon black plug to pass through the extruder, b) by measuring the mass through put and the mass of polymer in the barrel and c) from the correlation.

Extrusion experiments were then performed at RPM settings to allow at least enough mean residence time for 99% consumption of the peroxide added at the temperature selected using the decomposition rate given by Atochem. The usual experimental conditions used for polyethylene modification are as follows (table 13), extra experiments and replicates were also performed and are highlighted in the discussion section.

Table 13. Usual experimental conditions for polymer modification in minitruder.

Temperature (°C)	Peroxide type	Peroxide level (wt%)	RPM
190	Lupersol 101	0.2 to 0.88	10
200	Lupersol 101	0 to 2	10
200	Lupersol 130	0 to 1.4	10
230	Lupersol 101	0 to 2	30
230	Lupersol 130	0 to 1.4	30

Ampoule experiments

In order to determine the effect of the extruder mixing some reactions with polyethylene were performed in small aluminum ampoules in a heated oil bath. Figure 66 diagrams a typical ampoule. The inside of the ampoules were coated with a silicone mould release compound (Moulders Supply Ltd.) to allow the sample to be removed from the ampoule. The polymer, coated with peroxides as in the minitruder experiments, was placed in the ampoules, and packed tightly to facilitate good contact between the powder particles to obtain a homogeneous polymer/peroxide mixture. The ampoules were closed and suspended in an oil bath at the desired temperature, for the desired time. The samples were then cooled, removed, cut up, and analyzed for gel content.

The approximate center line temperature was measured using a thermocouple and pure polymer (see figure 67). The thermocouple was placed by first melting some polymer in the ampoule, and then drilling a hole down the centre line of the polymer. The thermocouple was then placed in the hole. These profiles showed that the center line reached 99% of the bath temperature after only a few seconds.

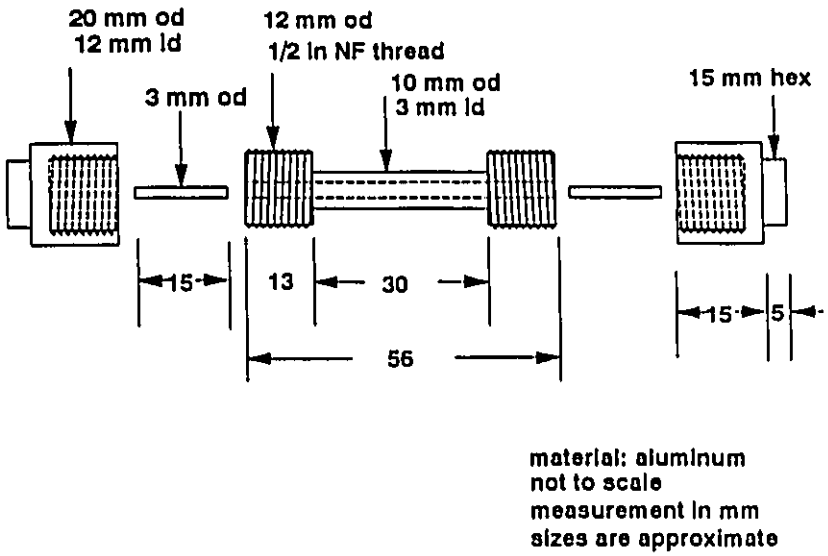

Figure 66. Exploded view of a typical ampoule. Sizes are approximate and may vary slightly from ampoule to ampoule.

The ampoule experiments were performed using Lupersol 130 since this peroxide's crosslinking efficiency showed a small temperature dependence (see discussion section) and the half life was much larger than the heat up time (figure 68).

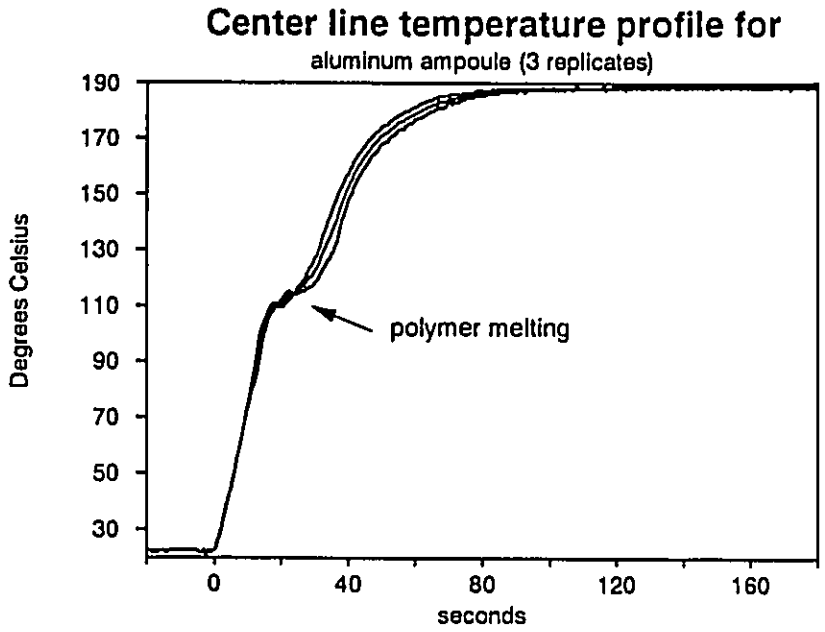

Figure 67. Center line temperature profile for aluminum ampoules.

The ampoule experiments were performed at 200 °C using Lupersol 130 in concentrations of 0.218, 0.88 and 1.37 wt% with replicates at the highest peroxide level.

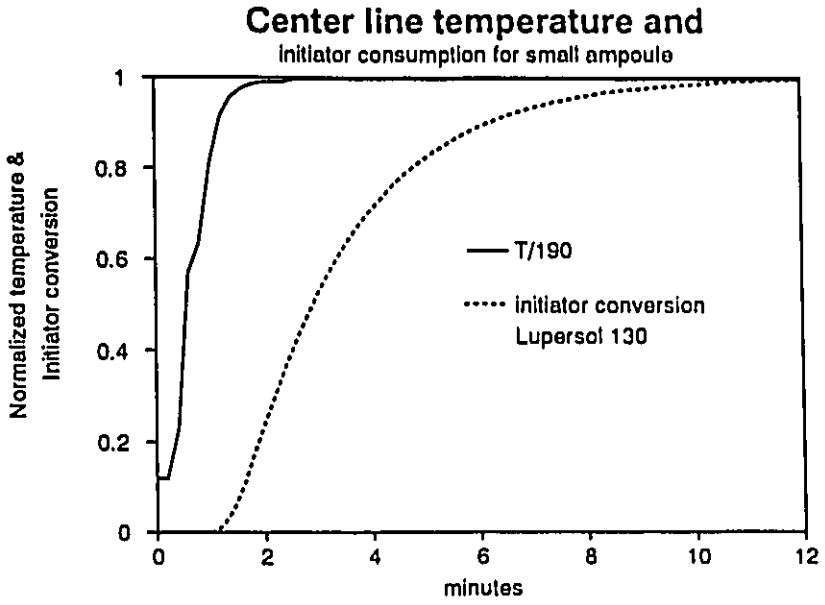

Figure 68. Temperature profile and initiator conversion for Lupersol 130 in aluminum ampoules at 190 °C. Temperature is normalized by division by 190. Initiator conversion is the fraction of the initiator that has decomposed.

4.5.2 Molecular weight measurements

The molecular weights of the linear polymers were measured using a Waters 150-C gel permeation chromatograph. No quantitative molecular weight measurement of branched polymers was performed. Three columns obtained from American Polymer Standards (AM gel 10^6 A- 15 micron, AM gel linear - 15 micron, AM gel 500 A -15 micron and a guard column) were used. 1,2,4- trichlorobenzene (J. T. Baker Chemical Co.) with 2,6, di tert butyl p-cresol (Fisher Scientific) stabilizer added. Column and injector temperatures were 135 °C and the flow rate was 1.0 ml/min. Sensitivity was set to 256 (-256 for polystyrene) and the scale factor to 20. Three hundred microlitres of a 0.1 wt% polymer - TCB solution was injected. The samples were made up using the same TCB as the mobile phase for the GPC. Sixty minutes were allowed for each analysis and 5 minutes allowed between injections.

Narrow polystyrene standards (Tosoh Corporation set D) were used to calibrate the GPC. The Universal calibration using $K= 1.21x10^{-4}$ & $a= 0.7070$ for linear polystyrene (Dawkins 1984), $K=5.260x10^{-4}$ & $a=0.700$ (Wagner 1985) for polyethylene and were used for analysis of polyethylene (HDPE).

The results were then checked against broad polyethylene (American Polymer Standards and Polymer Laboratories). An independent check for the HDPE molecular weight distribution was performed by American Polymer standards and they found the HDPE molecular weights to be (averages of five injections)

Mn= 14,000 (14770, 13180, 13040, 14960, 14340)

Mw= 182,000 (177400, 181200, 180800, 178100, 183400)

Mz= 760,700. (711000, 772900, 777700, 781200, 961900)

The weight average molecular weight agreement is adequate, and the number average molecular weights were some what lower than reported for the standards, possibly due to peak broadening. Since this work is primarily interested in changes in the molecular weights, and not absolute values, the universal calibration, using the constants above was used with no corrections for peak broadening.

The raw chromatograms were then exported from the GPC software as ASCII files, smoothed and the calibration curves used to convert the chromatograms to molecular weight distributions for use in the models.

Because of the errors introduced by the branches, even though they may be approximately corrected for by using viscometry or light scattering (Foster et al. 1980, Shiga and Sato 1987), branched polymer was only qualitatively analyzed using GPC.

4.5.3 Measurement of gel fraction

The gel fraction was determined using ASTM D-2765 with some modifications. The polymer sample to be analyzed was divided into three specimens, each approximately 0.5 g. If needed, the polymer was cut into small pieces. A specimen holder was made of 400 mesh stainless steel cloth as per the ASTM D-2765. The polymer was placed in the specimen holder and they were weighed and suspended in approximately 350 g of boiling (190 °C) decahydronaphthalene (decaline, Aldrich Chemical Co.) for at least 72 hours. It was observed that if the extraction time was less than 48 hours, the results showed unacceptable variance. Moreover, extraction for longer than 72 hours did not significantly change the measurement. Approximately

three grams of Antioxidant 2246 (American Cyanamid) was added to the decaline to avoid oxidative degradation. The sample was then removed, dried at room temperature for 24 hours, and then vacuum dried at 145 to 150°C for 24 hours. The sample and the specimen holder were then re-weighed and the sol fraction calculated based upon the loss of polymer during the extraction process.

The technique was developed by measuring the gel content of polyethylene that was subjected to gamma irradiation for a range of doses.

For some samples, the sol was collected, filtered and dried for further analysis.

4.5.4 NMR measurements

^{13}C NMR was used to in an attempt to quantify the number of X and Y branches in the polymer. However the width of the lines in the spectra obscured the lines due to these branch types. This could have been due to insufficient times for dissolution or measurement (8 hours). It should be noted that the gel will only swell and not dissolve and thus does not give as clear a signal as polymer in solution. The peaks are broader and overlap for swollen gel as compared to polymer in solution

4.5.5 DSC measurements

Differential scanning calorimetry was used (ASTM D3417) to find the heat of transition and the transition temperatures for polymer with different peroxide levels by either melting or crystallizing the polymer. Moreover the DSC was used as a small chemical reactor. The DSC used was a DuPont 910 differential scanning calorimeter with a LNCA II cooling attachment. The polymer, coated with peroxides, was placed in the DSC pan and hermetically sealed. The temperature was increased to the desired reaction temperature (160 or 180 °C) and held for sufficient time to consume 99.9% of the peroxide (Lupersol 101), see figure 69. All heating and cooling rates were 10°C per minute. After the reaction was complete, the ASTM temperature profile was run and the heats of transition and the peak temperatures of transition were recorded. A typical cooling transition peak is shown in figure 70 The baseline was always selected to be a horizontal line as shown in this figure. Using the common nomenclature, the area of this curve is the *heat of crystallization* and the peak temperature is the *crystallization temperature*. The heating peak has a similar shape but with negative heat flow. The area is called the *heat of fusion* and the peak is the *temperature of fusion*.

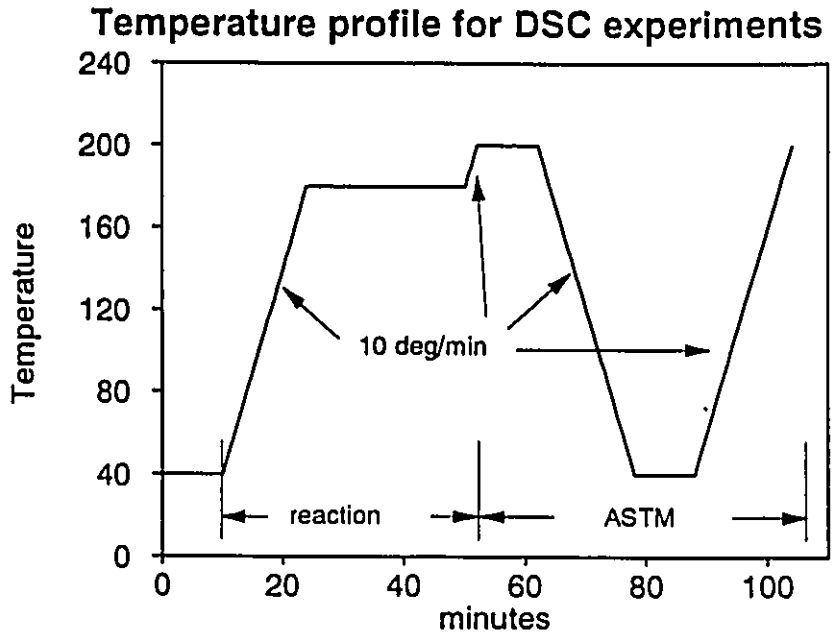

Figure 69. Temperature profile for DSC experiments. Where polymer modified in ampoules was tested, only the ASTM section was used.

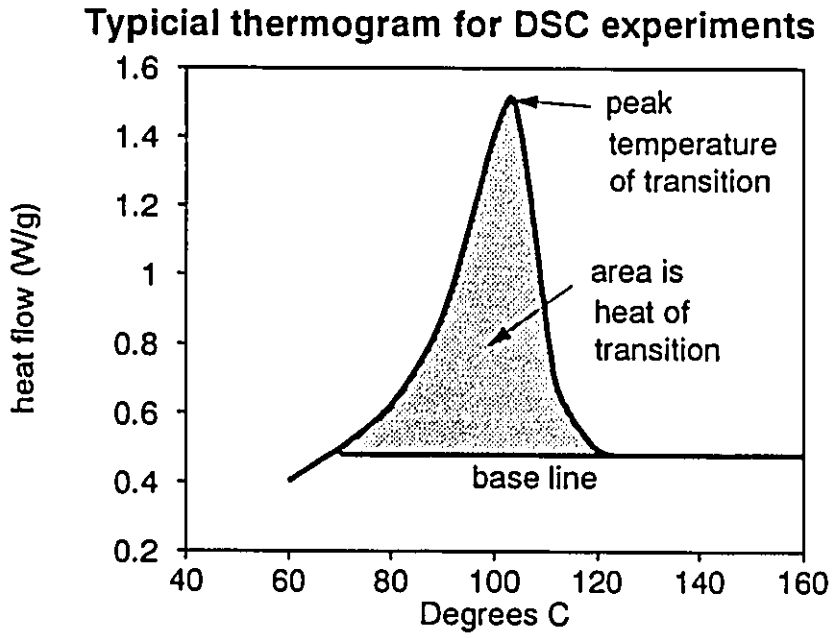

Figure 70. Typical thermal response profile for DSC using the ASTM method.

4.6 Discussion

The experimental results are presented and discussed first on their own and compared to model predictions where applicable.

4.6.1 Differential scanning calorimetry

Several experiments were performed with coated polymer powder at 160 and 180 °C, and with polymer modified in ampoules at 180°C. In all cases the peroxide used was Lupersol 101. Figure 71 shows that the heat of crystallization is reduced with increasing peroxide levels. The heat of crystallization should be proportional to the amount of crystalline polymer formed, and thus the modification is reducing the crystallinity by introducing defects into the polymer molecules, or by reducing the mobility of the molecules to inhibit crystal growth. However the heats of transition for polymer modified at 160 and 180 or in the ampoules are statistically equal, and thus either the polymer is being modified to the same degree for all the temperatures, or the DSC is not sensitive enough to resolve the difference.

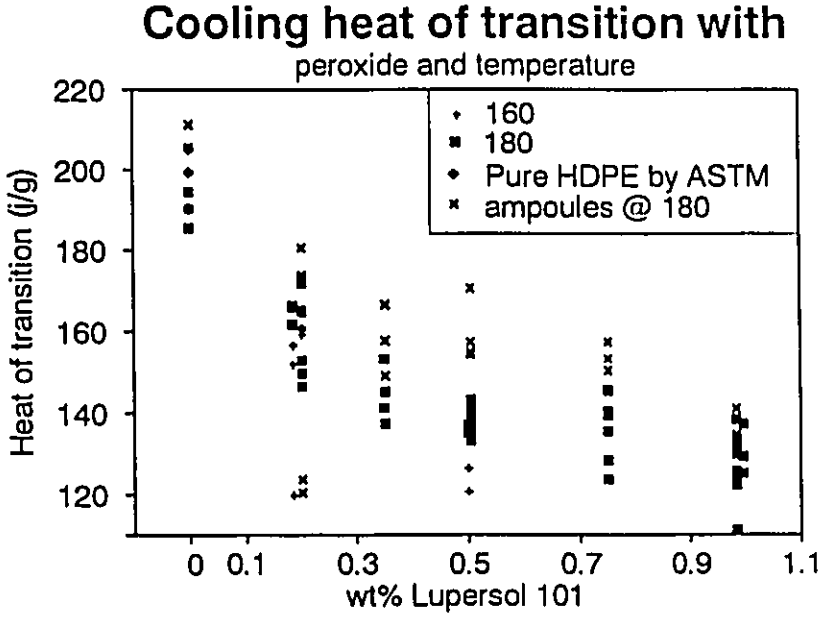

Figure 71 The heat of crystallization as a function of the peroxide level and reaction temperature. This heat was measured by cooling the sample from 200 to 40°C

The peak temperature of transition, as shown in figure 72, also demonstrates a reduction in the transition temperature with an increase in peroxide level. And again no significant difference could be found between polymer modified at 160, 180 °C or in ampoules.

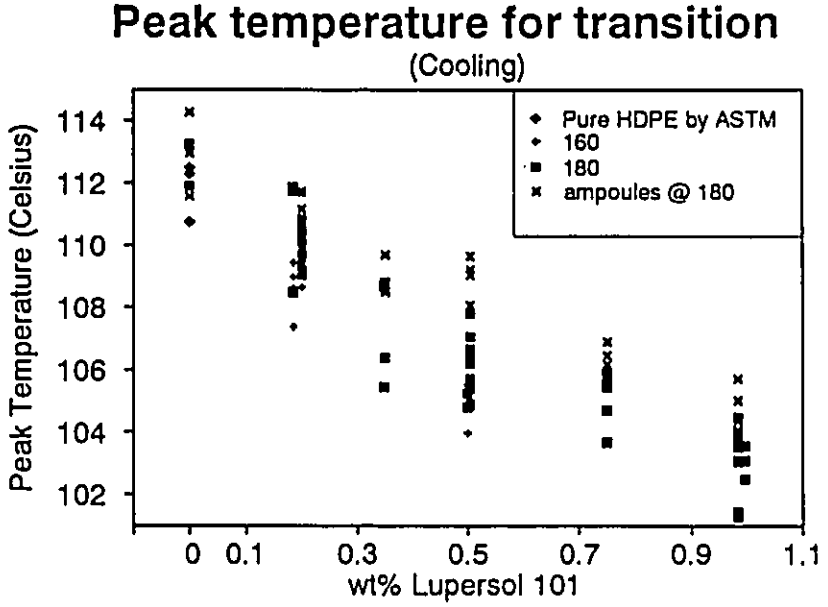

Figure 72 The peak temperature of transition as a function of the peroxide level and reaction temperature. This temperature was measured by cooling the sample from 200 to 40°C

The heat of fusion, and the peak temperature of fusion, as measured by heating the sample from 40 to 200 °C showed the same trend. The heat of fusion was approximately 25% larger than the heat of crystallization, and the peak temperature for fusion was about 20% larger than the temperature of crystallization.

If one can say that the change in the thermal properties, as measured by the DSC, is caused by the degree of modification by the peroxide, it appears that the reaction temperature has no effect on the degree of modification.

4.6.2 Extrusion experiments

Firstly we shall present some overall observations about the minitruder experiments. We were able to extrude the polyethylene even when containing the highest amounts of peroxides used. The electrical current required by the extruder did not appreciably increase with peroxide content. As the peroxide content increased,

the extrudate became rougher, and finally began to form flakes instead of a continuous extrudate. Polymer powder coated with higher amounts of peroxide tended to aggregate near the hopper wall and did not feed as easily into the barrel of the extruder.

Several experiments were performed where polymer was extruded in the absence of peroxide and the gel level measured to determine if there is any modification occurring due to the extruder. The gel levels measured for these conditions was less than three percent (see appendix). The gel level was also measured for virgin, unextruded, polymer powder and found to be, on average, 2.8%. It should be noted that the gel measurement technique is biased slightly to give higher gel levels. It is easier to not extract enough polymer than to extract too much, and thus we expect the measured gel level to be slightly higher than the actual level. For this reason we can accept that gel levels less than three percent actually represent zero gel. Furthermore the simple act of extruding the polymer does not significantly increase the gel level, in the absence of peroxides.

Figures 73, 74 and 75 show the gel fraction vs the amount of Lupersol 101 for experiments performed at 190, 200 and 230 °C respectively. In all cases the gel level increases with increasing peroxide except at the highest peroxide level where it actually decreases. The gel levels appear to be quite similar for that extruded at 190 and 200 °C but somewhat lower for that extruded at 230°C.

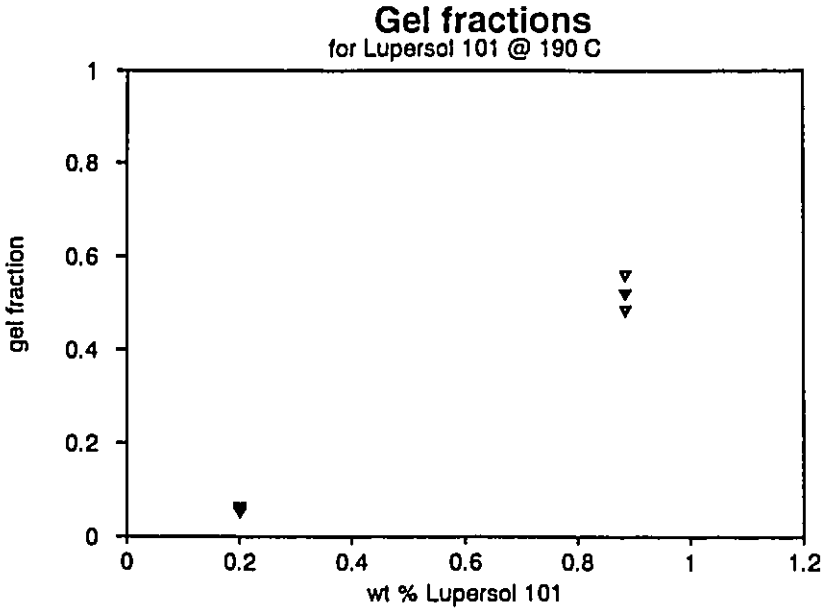

Figure 73. Gel fractions measured for minitruder experiments performed at 190°C using Lupersol 101 initiator.

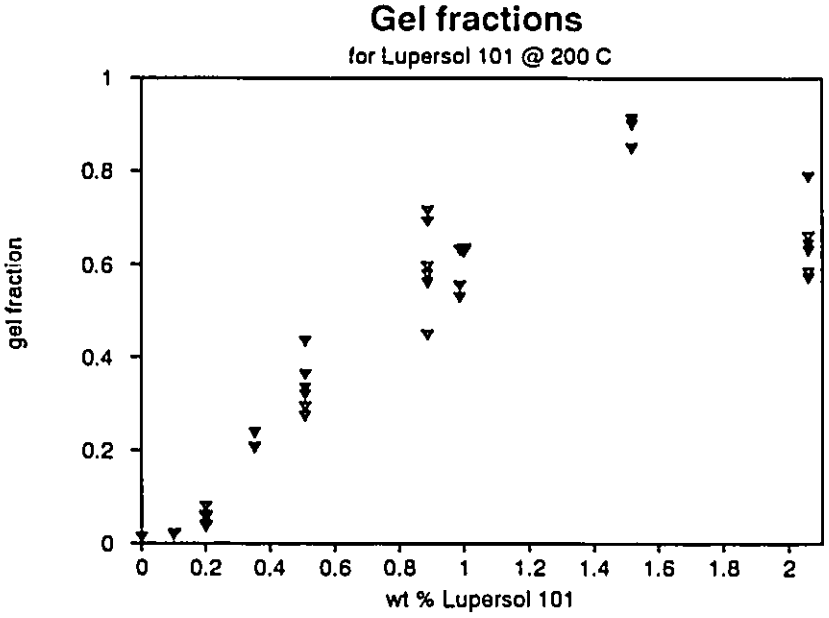

Figure 74. Gel fractions measured for minitruder experiments performed at 200°C using Lupersol 101 initiator.

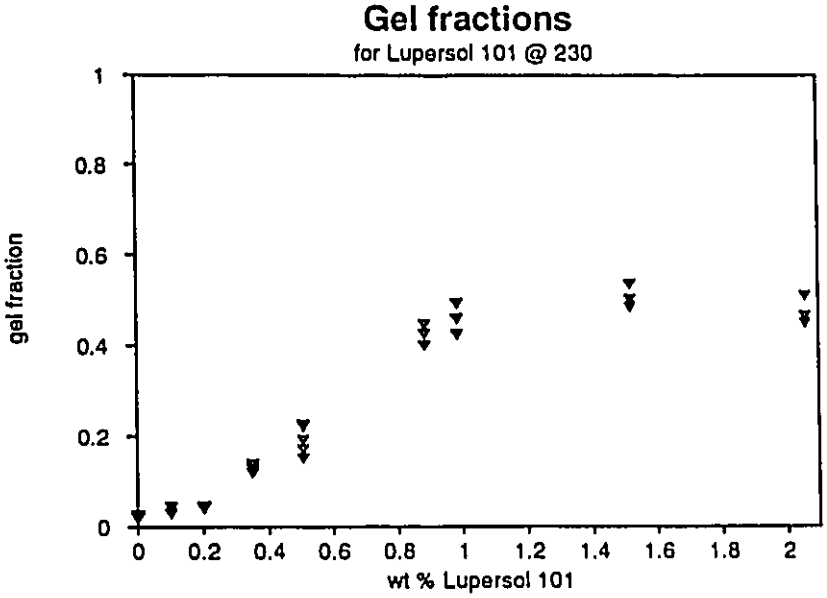

Figure 75. Gel fractions measured for minitruder experiments performed at 230°C using Lupersol 101 initiator.

Figure 76 and 77 show the gel levels for polymer extruded at 200 and 230°C in the presence of Lupersol 130. Unlike the difference found for Lupersol 101, the gel levels for both 200 and 230°C appear to be quite similar. In fact, except for the higher peroxide levels, the gel fractions are quite similar to that found for Lupersol 101 at 190 and 200 °C. This is further demonstrated in figure 78 which shows the *average* gel fractions of each extruder run plotted against the mmoles of peroxide per gram of polymer. For pure random crosslinking, one would expect (see appendix) that the only temperature dependence, and difference between peroxides, would be with respect to initiator efficiency. If the efficiency for Lupersol 101 and Lupersol 130 were to be equal, and independent of temperature, one would expect the same gel levels, for pure random crosslinking, for both initiators, at all temperatures. This seems to be true, for lower peroxide levels for all conditions except for Lupersol 101 at 230°C. The efficiency of the peroxide at 230°C seems to be markedly less than for all the other cases, Why? One could postulate that the efficiency for Lupersol 101 has a strong temperature dependence. However this is not demonstrated by the 190 and 200 °C curves which have statistically equal averages. The polymer could be experiencing more scission at 230°C, but this should be a function of the polymer and not the initiator, and the curve for Lupersol 130 at 230°C does not show this reduced gel level. Notice that this set of

conditions (Lupersol 101 at 230°C), has the shortest life time for the peroxide. It could be that the peroxide is being depleted before the polymer has had adequate time to melt and mix in the extruder. This should reduce the gel fraction.

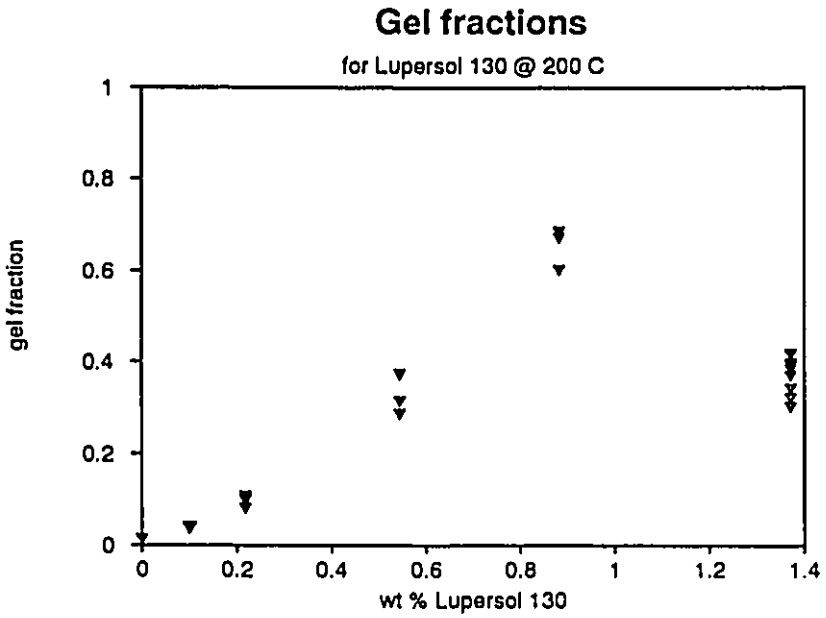

Figure 76. Gel fractions measured for minitruder experiments performed at 200°C using Lupersol 130 initiator.

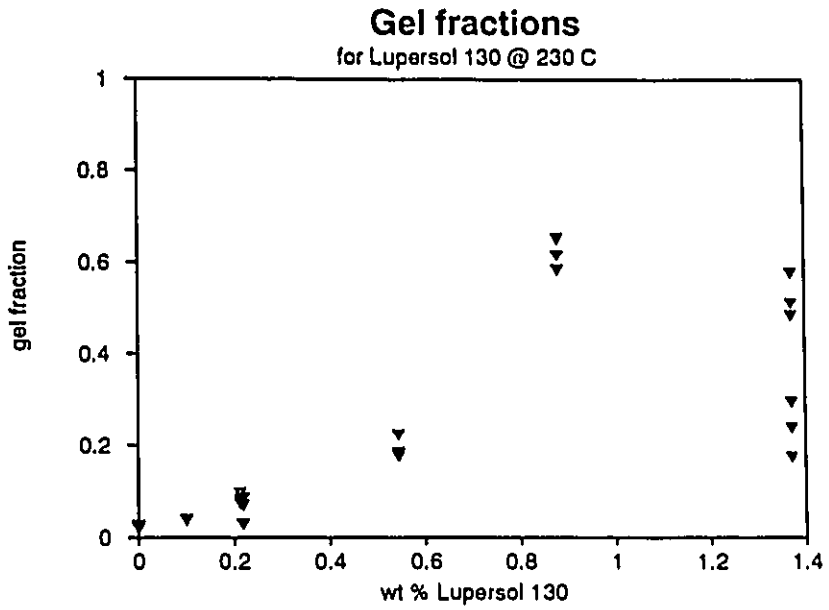

Figure 77. Gel fractions measured for minitruder experiments performed at 230°C using Lupersol 130 initiator.

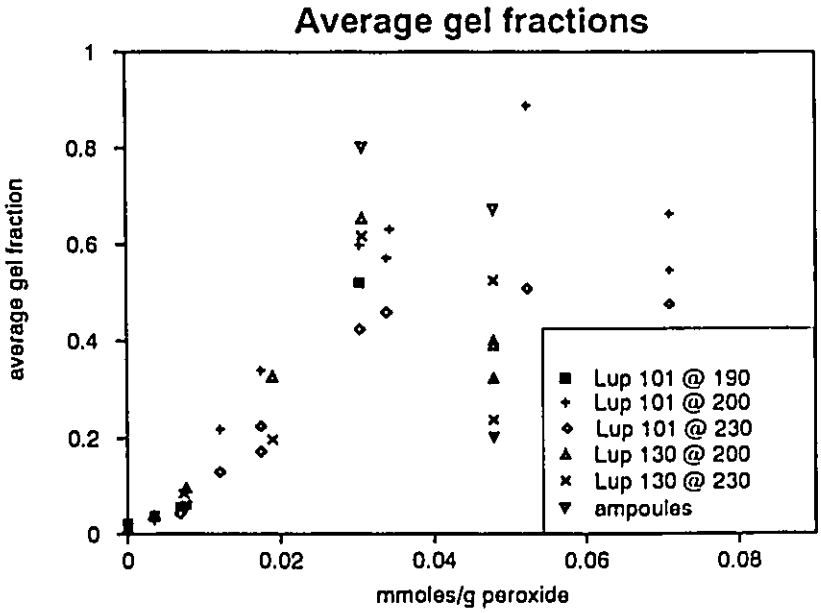

Figure 78. Average gel fractions measured for minitruder experiments performed at 190, 200 and 230°C using Lupersol 101 and 130 initiators and for the ampoules using Lupersol 130 at 200°C.

The second major observation is that the gel fraction seems to be reduced by high levels of peroxides. The reduction is shown for both peroxide types and at all temperatures, except 190°C where the higher peroxide level was not used. Moreover replicate experiments were performed to confirm the phenomena. One possible solution is that increased scission is occurring at the elevated peroxide levels, although this prediction is only borne out by a two step model and not by the solution to Zhu's equation (see modelling section). Another possibility is that this result is due to extruder effects. It was noted that the higher peroxide levels did not feed as well, or possibly the extruder was causing shear degradation of the gel. The variance of the high peroxide samples appeared to be larger.

The reasons for the ampoule experiments are two fold, firstly to determine if the extruder mixing plays a significant role in the level of gel formed, and secondly to shed some light on the reason for the reduction in the gel level at higher peroxide levels. These experiments were performed using Lupersol 130 at 200 °C. The gel levels obtained at 0.218 and 0.88 wt% agree quite well with the gel fractions obtained in the minitruder for those peroxide levels. The gel fractions observed are presented in figure 79. This indicates that the effect of extruder mixing is not a significant influence on the gel level for these peroxide concentrations. However, the ampoules also show a decline in the gel level at higher peroxide levels (1.37 wt%). Again the variability of these results are quite high relative to the results at lower peroxide concentrations.

The molecular weight of some sol material was measured to determine the trend. We must note that these values are not reliable estimates of the molecular weights, since they are branched, however they should be adequate to show the trends. Figure 80 shows the molecular weight averages vs. peroxide content for samples using Lupersol 130 and extruded at 200°C. Both the number and the weight average molecular weights decrease with peroxide level and the polydispersity of the polymer is also reduced. This is exactly the behavior that the theory predicts for the sol molecular weight averages.

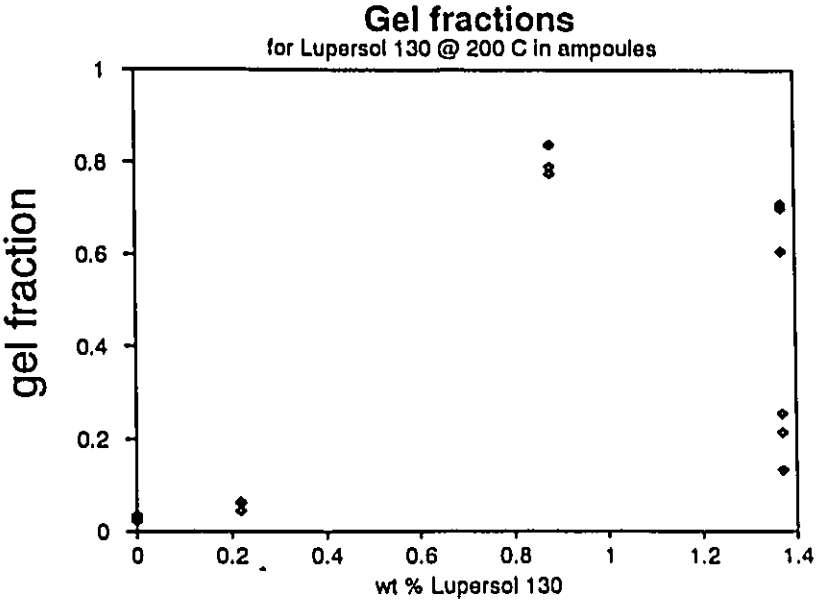

Figure 79. Gel fractions measured for ampoule experiments performed at 200°C using Lupersol 130.

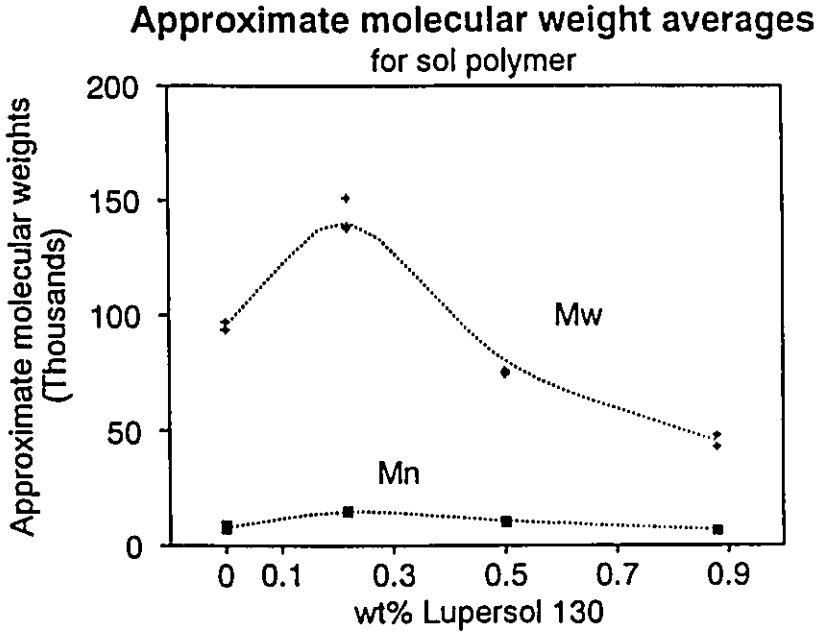

Figure 80. Approximate average molecular weights for sol polymer as measured by GPC. Polymer extruded in the presence of Lupersol 130 at 200°C. The lines are not model predictions.

4.6.3 Comparison between model predictions and experimental data

Parameter estimation method

If we consider either pure random scission, or pure random crosslinking, under isothermal conditions the model reduces to a single parameter model (see appendix).

$$dp/dt = \phi_p k_d^{1/2}[I]^{1/2}$$

or

$$dx/dt = \phi_x k_d[I]$$

where [I] is the initiator concentration, k_d is the initiator decomposition rate and is known, ϕ_p is the parameter for pure random scission and ϕ_x is the parameter for pure random crosslinking. p and x are the degrees of scission and crosslinking. Once we know either p or x we can calculate the desired quantities using either Saito's or Flory's equations and the initial molecular weight distribution.

We must simply estimate either ϕ_p or ϕ_x from molecular weight or gel fraction data. The non linear least squares package UWHAUS (Meeter 1965) that uses the Marquardt (1963) method was used. The program *2stepEst* was created to use the two step model to fit the parameters. The two step model is still valid for pure random crosslinking or pure random scission. For pure random scission, the molecular weight averages can be used and for pure random crosslinking, the gel fraction was used.

Polyethylene modification

The observation that reaction temperature does not influence the gel fraction, except for Lupersol 101 at 230°C, indicates that pure random crosslinking should be adequate to fit this data. In fact one should be able to fit all the data for a given peroxide, using the same crosslinking parameter. Moreover, no significant difference in the thermal properties was found by using different reaction temperatures. This implies that the degree of modification is independent of temperature and thus supports the pure random crosslinking hypothesis. In addition, if the peroxide efficiency is the same for both peroxides, a single crosslinking parameter value should represent all of the data.

The pure random crosslinking model was fit to a variety of the data (see table 14). Firstly, the parameter was estimated for each peroxide type and each temperature separately. Moreover, estimates were found neglecting the higher peroxide concentrations, where the gel levels fell. Considering Lupersol 101, the parameter estimates for data collected at 190 and 200 °C were not statistically different, however the data collected at 230°C was significantly lower. If the highest peroxide concentrations were neglected the crosslinking parameter values estimated were slightly higher.

Similarly, there was no significant difference in the crosslinking parameters found for Lupersol 130 at 200 and 230 °C both collected from the minitruder and from ampoules. Neglecting the higher peroxide levels also gave rise to slightly higher parameter values.

The gel data for Lupersol 101 at 190 and 200°C, neglecting the higher peroxide concentrations, were combined and the crosslinking parameter was found. Similarly the gel data for Lupersol 130 at 200 and 230°C, including the ampoule data, and neglecting the high concentration data, were combined to estimate the crosslinking parameter. It was found that the estimated values from these sets of data were not significantly different. To this point the only significantly different parameter value was for Lupersol 101 at 230°C, supporting the analysis that these data are somewhat suspect. Finally all the data, except Lupersol 101 at 230°C, was used to estimate a single crosslinking parameter having the value of 0.816 (l/mol). The data and the model are presented in figure 81.

Table 14. Parameter estimates for pure random crosslinking

Peroxide type	Temperature °C	Peroxide levels used	Crosslinking parameter	Approximate 95% confidence interval
Lupersol 101	190	all	0.69	(0.84, 0.54)
Lupersol 101	200	all	0.78	(0.88, 0.68)
Lupersol 101	230	all	0.49	(0.54, 0.43)
Lupersol 101	200	< 2 wt%	0.83	(0.93, 0.74)
Lupersol 101	230	< 1.0 wt%	0.57	(0.61, 0.53)
Lupersol 101	190 & 200	< 2 wt%	0.82	(0.90, 0.73)
Lupersol 130	200	all (no ampoules)	0.48	(0.62, 0.35)
Lupersol 130	230	all	0.46	(0.59, 0.34)
Lupersol 130	200	< 1 wt%	0.78	(0.95, 0.62)
Lupersol 130	230	< 1 wt%	0.85	(1.01, 0.69)
Lupersol 130	200	all ampoule data	0.64	(1.14, 0.14)
Lupersol 130	200	ampoule data < 1 wt%	1.06	(1.38, 0.75)
Lupersol 130	200 & 230	< 1 wt%, inc. ampoules	0.64	(0.80, 0.48)
Lupersol 101 & 130	190, 200, & 230	all	0.60	(0.66, 0.54)
Lupersol 101 & 130	all except Lupersol 101 @ 230	all except higher conc.	0.82	(0.89, 0.74)

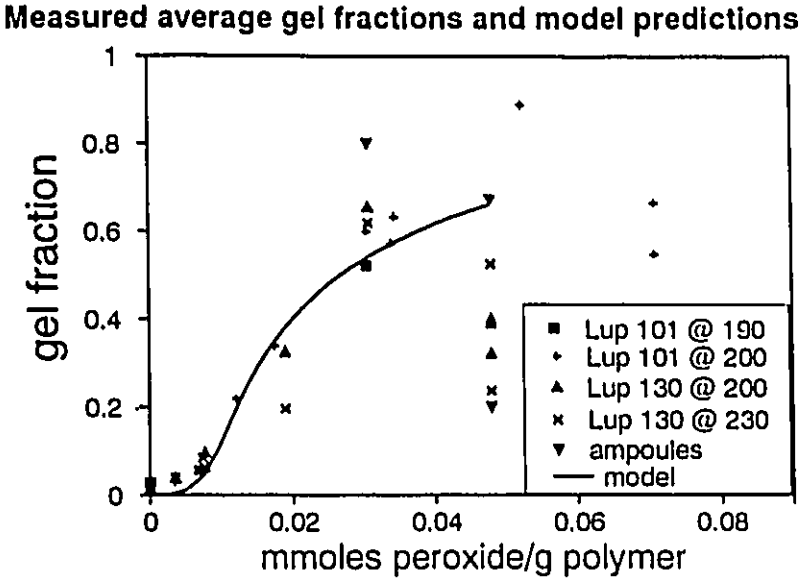

Figure 81. Pure random crosslinking model predictions, using a single crosslinking parameter and average gel fraction data.

This same set of data was used in an attempt to fit both crosslinking and scission, using the two step model, and the scission parameter found was not significantly different from zero. The pure random crosslinking model appears to be adequate to fit this gel fraction data. Moreover the initiator efficiency for Lupersol 101 and Lupersol 130 appear to be nearly equal, and independent of temperature.

Using the present model, one can predict the molecular weight averages of the sol polymer and compare them to the approximate molecular weights measured by GPC. Figure 82 shows that the comparison between the predicted and the measured values is reasonable. The predicted trends are observed. The measured average molecular weights must be considered only approximate since GPC is not strictly valid for branched polymer.

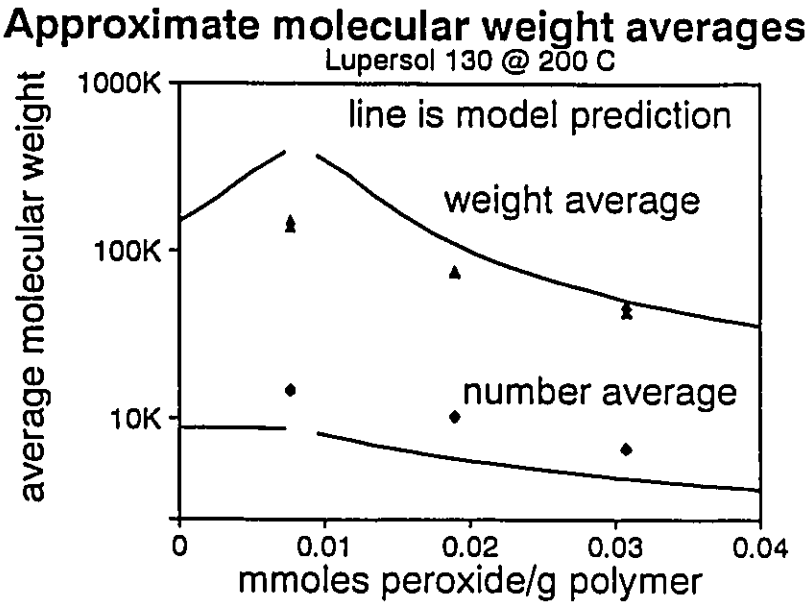

Figure 82. Pure random crosslinking model prediction for the sol molecular weight averages. The molecular weight data were measured by GPC and are therefore only approximate for branched polymer.

4.7 Concluding remarks

- The use of the classical Charlesby-Pinner equation to find the ratio of scission to crosslinking, for chemically induced modification is not valid. Some modifications in the two step approach may give rise to some improvement.
- A numerical solution to Zhu's equation for simultaneous random scission and crosslinking has been developed. This equation allows the calculation of the gel fraction and the entire molecular weight distribution for sol, both before and after the gel point, for any arbitrary initial distribution.
- Although the numerical solution to Zhu's equation agrees quite well with the classical solutions for pure random scission or crosslinking, it does demonstrate a significant difference for the simultaneous random scission and crosslinking case. Zhu's equation should more accurately represent the true behavior, since the assumptions made in its derivation are not a restrictive as the two step assumption. Modifications have been recommended to further improve the validity of the scission of branched molecules terms.

- The thermal properties, heats and temperatures of transitions, all decreased with increasing peroxide concentration, but do not appear to be functions of the modification temperature.
- A pure random crosslinking model is adequate to describe the gel formation of polyethylene, and the initiator efficiencies for Lupersol 101 and 130 are not significantly different from each other and independent of temperature. The pure random crosslinking hypothesis supported by the observation that the thermal properties, as measured by DSC, are not functions of the reaction temperature.
- It is important to use experimental conditions that allow adequate melting and mixing before the initiator is completely consumed when studying chemical modification of polymers via free radical mechanisms.

4.8 References

ASTM D2765 "Standard Test Methods for Determination of Gel Content and Swell Ratio of Crosslinked Ethylene Plastics" *Annual Book of ASTM Standards*

ASTM D3417 "Standard Test Method for Heats of Fusion and Crystallization of Polymers by Thermal Analysis" *Annual Book of ASTM Standards*

ATOCHEM "Halflife : peroxide selection based on half-life" ATOCHEM North America, Organic Peroxides Division, 1740 Military Rd. Buffalo NY.

Babic, D., Stannett, V. T. (1987) "Theoretical Considerations of Scission and Endlinking Reactions in Irradiated Polymers" *Radiat. Phys. Chem.* **30** 183-187

Ballauff, M., Wolf, B. A. (1981) "Degradation of Chain Molecules. 1. Exact Solution of the Kinetic Equations" *Macromolecules* **14** 654-658

Borsig, E., Szöcs, F. (1981) "High Pressure Effect on Polyethylene Crosslinking Initiated by Benzoyl Peroxide" *Polymer* **22** 1400-1402

Bremner, T., Rudin, R., (1990) "Modification of high density polyethylene by reaction with dicumyl peroxide" *Plast. Rubb. Process. Appl.* **13** 61-66

Callais, P. (1990) "The Maleic Anhydride Grafting of Polypropylene with Organic Peroxides" *Compalloy '90* 359-369

Capla, M., Borsig, E., (1980) "Simultaneous Degradation and Cross Linking Effect of Dicumyl Peroxide on Ethylene Propylene Copolymers" *Eur. Polym. J.* **16**, 611 - 613

Charlesby, A. Pinner, S. H., (1959) "Analysis of the Solubility Behavior of Irradiated Polyethylene and Other Polymers" *Proc. Roy. Soc.* **A249** 367-386

Chodak, I., Lazar, M. (1982) "Effect of the Type of Radical Initiator on Crosslinking of Polypropylene" *Die. Angew. Makromol. Chem.* **106**, 153-160

Chodak, I., Lazar, M. (1986) "Peroxide Initiated Crosslinking of Polypropylene in the Presence of p-Benzoquinone" *J. Appl. Polym. Sci.* **32**, 5431-5437

Chodak, I., Romanov, A. Ratzsch, M., Haudel, G. (1987) "Influence of the Additives on Polyethylene Crosslinking Initiated by Peroxides" *Acta Polymerica* **38** 672,674

Dawkins, J. V. "Calibration of separation systems" in "Steric exclusion liquid chromatography of polymers", Janca, J. (ed), Marcel Dekker, NY 1984 p. 85

De Boer, J., Pennings A. J., (1981) *Makromol. Chem., Rapid Commun* **2**, 749-755

Demjanenko, M., Dusek, K., (1980) "Statistics of Degradation and Crosslinking of Polymer Chains with the Use of the Theory of Branching Processes" *Macromolecules* **13** 571-579

Flory, P. J. (1953) "Principles of Polymer Chemistry", Cornell Univ. Press. Ithaca NY.

Foster, G. N., MacRury, T. B., Hamielec, A. E., (1980) "Characterization of Polymers With Long Chain Branching- Development of the Molecular Weight and Branching Distribution Method" in *Liquid Chromatography of Polymers and Related Materials* Cazes, J. and Delamare, X. (eds.) Marcel Dekker, 143

Galiatsatos, V., Eichinger, B. E., (1988) "Computer Simulations of Radiation Cured Polyethylene" *J. Polym. Sci: Part B: Polym. Phys.* **26** 595-602

Giudici, R. Personal communication, McMaster University, Hamilton Ont. (1992)

Gordon, M., Malcolm, G. N., (1966) *Proc. R. Soc. London, Ser A* **295**, 29

Gordon, M., Temple W. B., (1976) in "Chemical Application of Graph Theory", A. T. Balaban, ed. Academic Press, NY.

Gordon, M. (1962) *Proc. R. Soc. London, Ser A* **268**, 240

Gordon, M. Ross-Murphy, S. B., (1975) *Pure Appl. Chem.* **43**, 1

Guaita, M., Chiantore, O., Luda, M. P. (1990) "Monte Carlo Simulations of Polymer Degradations. 1. Degradations without Volatilization" *Macromolecules* **23** 2087-2092

Hamielec, A. E., Gloor, P. E., Zhu, S., Tang, Y. (1990) "Chemical Modification of Polyolefins in Extruders - Chain Scission, Long Chain Branching and Crosslinking" *Compalloy '90* 85-145

Hamielec, A. E., Gloor, P. E., Zhu, S. (1991) "Free Radical Modification of Polyolefins in Extruders - Chain Scission, Crosslinking and Grafting" *Can. J. Chem. Eng.* **69** 611-618

Hendra, P. J., Peacock, A. J., Willis, H. A., (1987) "The Morphology of Linear Polyethylenes Crosslinked in their Melts. The Structure of Melt Crystallized Polymers in General" *Polymer* **28** 705-709

Hindmarsh, A. C. "ODEPACK, a systematized collection of ODE solvers" *Scientific Computing* S. Stepleman et al. (eds), North Holland, Amsterdam, (1983) - Volume 1 of IMACS Transactions on Scientific Computation pp. 55-64

Horii, F., Zhu, Q., Kitamaru, R., Yamaoka, H., (1990) " ^{13}C NMR Study of Radiation Induced Cross Linking of Linear Polyethylene", *Macromolecules* **23** 977-981

Hrymak, A. N. Personal communication, McMaster University, January (1993)

Hulburt, H. M., Katz, S. (1964) "Some Problems in Particle Technology, A Statistical Mechanical Formulation", *Chem. Eng. Sci. I* **19** 555-574

Hulse G. E., Kersting, J. R., Warfel, D. R (1981) *J. Polym. Sci. Polym. Chem Ed.* **19**, 655-667

Kampouris, E. M., Andreopoulos, A. G., (1987) "Benzoyl Peroxide as a Crosslinking agent for Polyethylene" *J. Appl. Polym. Sci.* **34** 1209-1216

Kampouris, E. M., Andreopoulos, A. G., (1989) "The Effect of the Gel Content of Crosslinked Polyethylene on its Physical Properties" *Eur. Polym. J.* **25** 321-324

Kampouris, E. M., Andrepoulos, A. G., (1989) "Gel Content Determination in Cross-Linked Polyethylene" *Biomaterials* **10**, 206-208

Kwei, T. K., Pearce, E. M., Schlecht, M. F., Cheung, W., (1991) "Crosslinking and Scission in Radical - Promoted Functionalization of Polyethylene" *J. Appl. Polym. Sci.* **42** 1939-1941

Lem, K-W., Han, C. D., (1982) "Rheological Properties of Polyethylenes Modified with Dicumyl Peroxide" *J. Appl. Polym. Sci.* **27**, 1367-1383

Lew, R., Balke, S. T. (1991) "The Reactive Compatibilization of Polypropylene- Polyethylene Blends and Near Infrared In-line Monitoring" Polymer Processing Society 7th annual meeting, April 21-24, Hamilton Ontario, Canada

Lew, R., Cheung, P., Balke, S. T. (1989) "Reactive Extrusion of Polypropylene - Elucidating Degradation Kinetics" *ACS Symp. Series.* **404**

Marquardt, D. "An algorithm for least squares estimation of non-linear parameters" *J. Soc. Ind. Appl. Math* 431-441 (1963)

Meeter, D. A., Wolfe, P. J. "Non linear least squares" University of Wisconsin Computing Center (1965)

Mukherjee, A. K., Tyagi, P. K., Gupta, B. D. (1989) "Conventional Crosslinking Studies on Low Density Polyethylene Monofilaments" *Die. Angew. Makromol. Chem.* **173** 205-212

Peacock, A. J., (1984) *Polymer Commun.* **25** 169

Peacock, A. J., (1987) *Polymer Commun.* **28** 259-260

Saito, O., (1958) "On the Effect of High Energy Radiation to Polymers", *J. Phys. Soc. Japan*, B13B, 198-206, 1451-1464, 1465-1475

Saito, O., (1972) "Statistical Theories of Crosslinking " in "The Radiation Chemistry of Macromolecules" M. Dole. ed., Academic Press, NY pp. 223-261

Schlecht, M. F., Pearce, E. M., Kwei, T. K., Cheung, W., (1988) " Chemical Reaction on Polymers: Radical Promoted Functionalization of Polyethylene" *ACS Symp. Ser.* **364**, chap. 22

Shiga, S., Sato, Y. (1987)"Characterization of Polymers by GPC-LALLS. III. Branching Structure of EPDM" *Rubber Chem. Tech.* **60**, 1-13

Shy, L. Y., Eichinger, B. E., (1986) "Computer Simulations of Radiation Cured Networks" *Macromolecules* **19** 2787-2793

Simunkova, D., Rado, R., Mlejnek, O (1970) "Mechanism and Kinetics of Polyethylene Crosslinking by $\alpha-\alpha'-$ bis(tert-butyl peroxy)-p-diisopropylbenzene" *J. Appl. Polym. Sci.* **14** 1825-1831

Song, Z., Baker, W. E., (1990) "Grafting of 2-(dimethylamino) ethyl methacrylate on Linear Low Density Polyethylene in the Melt" *Die Angew. Makromol. Chem.* **181** 1-22

Suwanda, D., Balke, S. T. (1989) "The Reactive Extrusion of Polyethylene", *ANTEC '89 Conf. Proc.*, 589-592

Suwanda, D., Balke, S. T. (1990) "The Reactive Extrusion of Polyethylene: Process Improvements for Initiator Dispersion", *ANTEC '90 Conf. Proc.*, 1908-1910

Suwanda, D., Lew, R., Balke, S. T. (1988a) "Reactive Extrusion of Polypropylene. 1. Controlled Degradation", *J. Appl. Polym. Sci.* **35** 1019-1932

Suwanda, D., Lew, R., Balke, S. T. (1988b) "Reactive Extrusion of Polypropylene. 2. Degradation Kinetic Modelling ", *J. Appl. Polym. Sci.* **35** 1033-1948

Tobita, H., (1990) "Crosslinking Kinetics in Free Radical Copolymerization", *Ph.D Thesis*, McMaster University, Hamilton, Ontario, Canada.

Triacca, V. J., Gloor, P. E., Zhu, S., Hrymak, A. N., Hamielec, A. E. (1991) "Numerical Solution for Simultaneous Random Scission and Crosslinking", Polymer Processing Society 7th annual meeting, April 21-24, Hamilton Ontario, Canada

Triacca, V. J., Gloor, P. E., Zhu, S., Hrymak, A. N., Hamielec, A. E. (1993) "Free Radical Degradation of Polypropylene: Random Chain Scission", in press *Polym. Eng. Sci.*

Tzoganakis, C. Tang, Y., Vlachopoulos, J., Hamielec, A. E. (1989) "Controlled Degradation of Polypropylene: A Comprehensive Experimental and Theoretical Investigation" *Polym. Plast. Technol. Eng.* **28**1 319-350

Tzoganakis, C. Vlachopoulos, J., Hamielec, A. E. (1988) "Modelling of the Peroxide Degradation of Polypropylene" *Intern., Polym., Process.* III 141-150

Wagner, H. L., *J. Phys. Chem. Ref. Data* **14** (2) 611-617 (1985)

Zabisky, R. C. M., Chan, W. -M. , Gloor, P. E., Hamielec, A. E. ,(1991), "A Kinetic Model for Olefin Polymerization in High Pressure Tubular Reactors - A Review and Update", *Polymer* (in press).

Zhu, S. (1991) "Advances in Free - Radical Polymerization Kinetics", *Ph.D Thesis*, McMaster University, Hamilton, Ontario, Canada.

Ziff, R. M., MacGrady, E. D. (1986) "Kinetics of Polymer Degradation" *Macromolecules* **19** 2513-2519

4.9 Appendix for chemical modification section

4.9.1 Calculation of the rates of peroxide induced scission or crosslinking

Consider a balance on total radicals, using the stationary state hypothesis gives,

$$[R] = (f/k_t)^{1/2}(k_d[I])^{1/2}$$

where [I] is the initiator concentration k_t is the overall termination rate constant, k_d is the initiator decomposition rate constant and f is the initiator efficiency and includes the number of radicals produced per initiator molecule. The initiator concentration is given by the differential equation

$$d[I]/dt = -k_d[I]$$

A balance on backbone and chain end radicals, using the SSH yields

$$[R_b] = \frac{k_{fp}Q_1[R]}{k_{fp}Q_1 + k_t[R] + k_\beta}$$

$$[R_e] = \frac{k_\beta[R_b]}{k_t[R] + k_{fp}Q_1}$$

where $[R_b]$ and $[R_e]$ back bone and chain end radicals, Q_1 is the first moment of the polymer molecular weight distribution, and is the number of polymer repeat units per unit volume. k_β is the beta-scission rate constant, and k_{fp} is the transfer to polymer rate constant. If we can say that $k_t[R]$ is $< k_{fp} \cdot Q_1$ then and substituting for [R] we get

$$[R_b] = \left(\frac{k_{fp}Q_1}{k_{fp}Q_1 + k_\beta}\right)\left(\frac{fk_d}{kt}\right)^{1/2}[I]^{1/2}$$

$$[R_e] = \left(\frac{k_\beta}{k_{fp}Q_1}\right)\left(\frac{k_{fp}Q_1}{k_{fp}Q_1 + k_\beta}\right)\left(\frac{fk_d}{kt}\right)^{1/2}[I]^{1/2}$$

The rates of scission and crosslinking are

$$\frac{dp}{dt} = \frac{k_\beta[R_b]}{Q_1}$$

$$= \left(\frac{k_\beta}{Q_1}\right)\left(\frac{k_{fp}Q_1}{k_{fp}Q_1 + k_\beta}\right)\left(\frac{fk_d}{kt}\right)^{1/2}[I]^{1/2}$$

$$= \phi_p k_d^{1/2}[I]^{1/2}$$

$$\frac{dx}{dt} = \frac{k_{tc}[R_b]^2}{Q_1} + \frac{k_{tc}[R_b][R_e]}{Q_1}$$

$$= \frac{k_{tc}}{Q_1}\left(1 + \frac{k_\beta}{k_{fp}Q_1}\right)[R_b]^2$$

$$= \left(\frac{k_{tc}}{Q_1}\right)\left(1 + \frac{k_\beta}{k_{fp}Q_1}\right)\left(\frac{k_{fp}Q_1}{k_{fp}Q_1 + k_\beta}\right)^2\left(\frac{fk_d}{kt}\right)[I]$$

$$= \phi_x k_d[I]$$

where k_{tc} is the termination by combination rate constant and p and x are the degrees of scission or crosslinking. This evaluation predicts that the rate of crosslinking will be first order in initiator concentration, and the rate of scission of half order. Higher initiator concentrations should give rise to increases crosslinking. For pure random crosslinking, the parameter reduces to the group

$$\phi_x = \frac{k_{tc}}{Q_1}\frac{f}{k_t}$$

This analysis assumes a) kinetic constants equal for all radical types, b) stationary state hypothesis for all radical types, c) $k_t[R]$ is $< k_{tp} \cdot Q_1$, d) random scission and random crosslinking, and e) constant volume and therefore Q_1 constant.

If we relax the $k_t[R]$ is $< k_{tp} \cdot Q_1$ assumption then we can write

$$[R_b] = \frac{\theta}{(\phi_1\theta + \phi_2)}$$

where $\theta = (k_d[I])^{1/2}$, $\phi_1 = k_t/k_{fp}Q_1$ and

$$\phi_2 = \left(\frac{k_{fp}Q_1 + k_\beta}{k_{fp}Q_1}\right)\left(\frac{k_t}{f}\right)^{1/2}$$

The rate of pure random scission is given by a three parameter model

$$\frac{dp}{dt} = \frac{k_\beta}{Q_1}\frac{\theta}{(\phi_1\theta + \phi_2)}$$

where the parameters are k_β, ϕ_1 and ϕ_2. The rate of pure random crosslinking is also given by a three parameter model

$$\frac{dx}{dt} = \frac{k_{fc}}{Q_1}\left(\frac{\theta}{\phi_1\theta + \phi_2}\right)^2$$

where the parameters are k_{fc}, ϕ_1 and ϕ_2. Now the rate of crosslinking will be less than first order with respect to initiator concentration and the rate of scission will be less than half order. However if $\phi_1\theta \ll \phi_2$ we return to a single parameter for crosslinking and a single parameter for scission. An *order of magnitude* analysis can be done to test this.

Basis: 1000 g of polyethylene, density 1000 g/l
0.1 wt% initiator of molecular weight 300 g/mol and having
$k_d = 8.73 \times 10^{15}$ exp (-37182/RT) or $6 \times 10^{-2}\ s^{-1}$ @ 200°C.
$k_t = 10^7$ (l/mol-s)
$k_{fp} = 10^3$ (l/mol-s)

We can calculate the group $\phi_1 = k_t/k_{fp}Q_1$ where Q_1= (1000 g/l)•(mol/28 g)= 36 mol/l so

$$\phi_1 = \frac{10^7}{10^3 \cdot 36} = 278$$

and

$$\theta^2 = k_d[I] = (6x10^{-2}s^{-1})(0.1wt\%/100)(1000g/l)(mol/300g)$$

$$= 2x10^{-4}(mol/l - s)$$

$$\theta = 1.4x10^{-2}$$

Therefore $\phi_1 \cdot \theta = (278) \cdot (1.4x10^{-2}) \cong 4$ and

$$\phi_2 = \left(\frac{k_{fp}Q_1 + k_\beta}{k_{fp}Q_1}\right)\left(\frac{k_t}{f}\right)^{1/2} \geq \left(\frac{k_t}{f}\right)^{1/2}$$

$$\cong (10^7)^{1/2} \cong 3000$$

Since $\phi_1\theta/\phi_2 = 4/3000 \ll 1$ we are justified in using $\phi_1\theta \ll \phi_2$ and therefore using a single parameter for scission and a single parameter for crosslinking.

4.9.2 Isothermal conditions to final states

Given the rates of scission and crosslinking derived above, and the initiator concentration $[I] = [I]_o \exp(-k_d t)$ one can integrate to find the final degree of scission and crosslinking. First for scission we can evaluate

$$p = \int_0^t \left(\frac{\phi_p}{Q_1} k_d^{1/2} [I]_o^{1/2} \exp(-k_d t/2) \right) dt$$

$$p = \frac{2\phi_p [I]_o^{1/2}}{k_d^{1/2}} (1 - \exp(-k_d t/2))$$

$$= \frac{2\phi_p [I]_o^{1/2}}{k_d^{1/2}} \qquad @t = \infty$$

Since the number average molecular weights, for pure random scission, are given by

$$\frac{M}{Mn} = \frac{M}{Mn_o} + p$$

where M is the molecular weight per repeat unit. Substitution in for p yields

$$\frac{M}{Mn} = \frac{M}{Mn_o} + \frac{2\phi_p [I]_o^{1/2}}{k_d^{1/2}}$$

Therefore a plot of M/Mn vs 2 $[I]_o\, k_d^{-1/2}$ should give a straight line with slope ϕ_p.

For pure random crosslinking

$$x = \int_0^t \left(\frac{\phi_x}{Q_1} k_d [I]_o \exp(-k_d t) \right) dt$$

$$x = \phi_x [I]_o (1 - \exp(-k_d t))$$

$$= \phi_x [I]_o \qquad @t = \infty$$

This analysis provides a very interesting result. Except for initiator efficiency, the final degree of crosslinking is independent of the initiator type. Initiators with vastly different decomposition rates, but similar efficiencies, would give the same final degree of crosslinking. Moreover if both the efficiency and termination are weak functions of temperature, the final degree of crosslinking will be independent of temperature. Scission will still depend on the initiator decomposition rate.

The final ratio of scission to crosslinking will then be a function of the initiator concentration and decomposition rate

$$\frac{p}{x} = \frac{2\phi_p}{k_d^{1/2}\phi_i[I]_o^{1/2}} \qquad @t = \infty$$

and thus p/x will not be constant for experiments using different initial peroxide concentrations and will tend to zero as $[I]_o$ increases.

4.9.3 Considerations for bifunctional initiators

Both Lupersol 101 and Lupersol 130 have two peroxide groups per initiator molecule, and thus are bifunctional initiators. This introduces some modifications to the equations as derived for a monofunctional initiator. These differences will only effect the modification vs. time profiles for either pure random crosslinking or pure random scission but should not influence the final degree of modification after all of the initiator is consumed. However for the bifunctional case we will have four radicals produced per initiator molecule instead of two for the monofunctional case. For the simultaneous random scission and crosslinking case, were the radical concentration influences the ratio of scission to crosslinking, the following analysis will be important. This derivation shows a proper way to account for the bifunctional initiators. Consider the following reactions:

$$I \xrightarrow{kd} R + R_1$$

$$R_1 \xrightarrow{kd} R + R_2$$

where R, R_1 and R_2 are primary radicals. R_1 is a radical with an unreacted peroxide group and R_2 in a diradical since both peroxide groups have decomposed. These radicals can react with polymer backbones to give macroradicals (Y_0) by transfer to polymer. X is a dead initiator product.

$$R + P \xrightarrow{kfp} X + Y_0$$

$$R_1 + P \xrightarrow{kfp} HR_1 + Y_0$$

$$R_2 + P \xrightarrow{kfp} R + Y_0$$

HR_1 is an initiator fragment, no longer a radical, but containing an unreacted peroxide group, which can decompose.

$$HR_1 \xrightarrow{kd} R + R$$

These radical species can undergo termination by combination with the macroradicals. Termination between primary radicals is neglected as this is accounted for by the initiator efficiency.

$$R + Y_0 \xrightarrow{kt} P$$

$$R_1 + Y_0 \xrightarrow{kt} P_1$$

$$R_2 + Y_0 \xrightarrow{kt} Y_0$$

P_1 is a macromolecule with a peroxide group that can decompose

$$P_1 \xrightarrow{kd} R + Y_0$$

Based upon this kinetic scheme, and assuming that the rate constants are equal for all peroxide and radical species, we can derive balances for all the species. Q_1 is the first moment of the molecular weight distribution for the dead polymer and is proportional to the concentration of repeat units in the polymer.

$$\frac{dR}{dt} = 2kdI + kdR_1 + 2kdHR_1$$

$$+ kdP_1 - kfpQ_1R - ktRY_0$$

$$\frac{dR_1}{dt} = 2kdI - kdR_1$$

$$- kfpQ_1R_1 - ktR_1Y_0$$

$$\frac{dR_2}{dt} = kdR_1 - 2kfpQ_1R_2 - 2ktR_2Y_0$$

$$\frac{dHR_1}{dt} = kfpQ_1R_1 - kdHR_1$$

$$\frac{dP_1}{dt} = ktY_0R_1 - kdP_1$$

$$\frac{dY_0}{dt} = (kfpQ_1 - ktY_0)(R + R_1 + 2R_2) - ktY_0^2$$

The balance on initiator is given by

$$\frac{dI}{dt} = -2kdI$$

and a balance on the total number of peroxide groups (PO) is given by

$$\frac{dPO}{dt} = -kdPO \qquad \{PO(t=0) = 2I(t=0)\}$$

and the total number of peroxide groups is also given by

$$PO = 2I + R_1 + P_1 + HR_1$$

The total primary radical concentration (R_t) can be found from

$$R_t = R + R_1 + 2R_2$$

$$\frac{dR_t}{dt} = \frac{dR}{dt} + \frac{dR_1}{dt} + 2\frac{dR_2}{dt}$$

$$\frac{dR_t}{dt} = 4kdI + 2kdHR_1 + kdP_1 - kfpQ_1R_t - kt(R + R_1 + 4R_2)Y_0$$

Solution of these equations (using LSODE and Gear's method), using kd=6x10^{-2} s^{-1}, kt=10^7 (l/mol-s), kfp=10^2 (l/mol-s) and Q1 =36 (mol/l) shows that the balance on primary radicals is adequately given by

$$\frac{dR_t}{dt} = 2kdPO - (kfpQ_1 + kt)R_tY_0$$

but not by

$$\frac{dR_t}{dt} = 4kdI - (kfpQ_1 + kt)R_tY_0$$

since PO does not equal 2xI over the entire course of the reaction since HR_1 rises to a significant level (see figure 83). The total macro radical concentration, given by solution of the differential equations can also adequately be described (using the stationary state hypothesis) by

$$Y_0 = \left(\frac{2kdPO}{kt}\right)^{(1/2)}$$

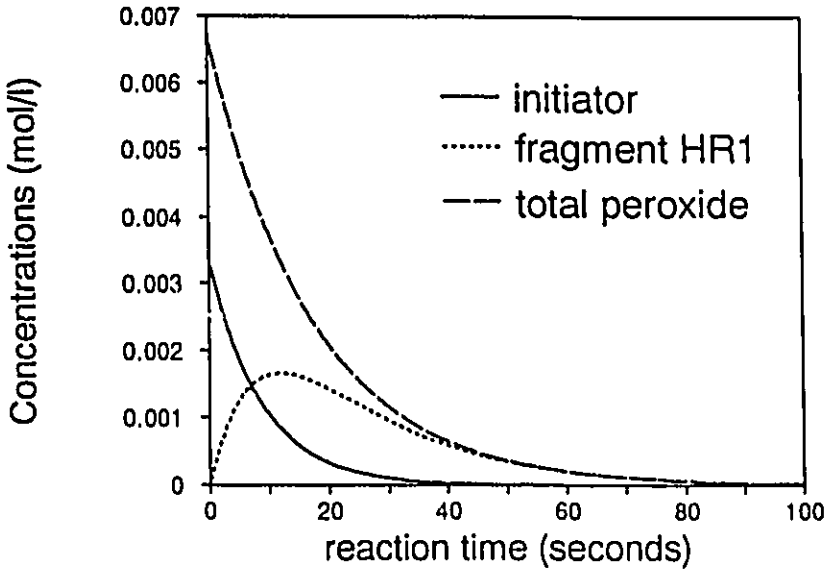

Figure 83. Concentrations of initiator, peroxide containing initiator fragment (HR_1) and total peroxides with reaction time.

Chapter 5 Concluding remarks

Comprehensive models have been developed for high pressure tubular and autoclave reactors and matched to data from industrial reactors. The molecular weight, branching frequency and gel predictions still need experimental verification. The presence oscillations in the gel content of the polymer produced in the continuous autoclave reactor may pose interesting problems for controlling process variability.

A mathematical model for Ziegler-Natta copolymerization has been developed accounting for multiple active site types. The model has been applied, in other studies, to both slurry type and UNIPOL type reactors. Further experimentation should be performed using TREF, GPC and NMR to completely characterize the active site distribution for a specific heterogeneous catalyst.

An algorithm to solve a model for simultaneous random scission and crosslinking has been developed that will calculate the gel fraction, the molecular weights both before and after the gel point, the branching frequencies as well as the degrees of scission and crosslinking. This model when compared to the classical two step solution, and the Charlesby-Pinner equation demonstrated serious deficiencies in the classical approaches. Although model modifications are suggested in this thesis, further work should be undertaken to improve the validity of scission term in this model to account for the random scission of branched chains of arbitrary structure.

Because insufficient data were available in the literature, experiments were performed using a high density polyethylene to gather data for the reactive extrusion model. A pure random crosslinking model was adequate to fit the data for HDPE, and was supported by thermal analysis. More information on the branch types, possibly from NMR must be obtained to quantify the degree of scission. Care must be taken to ensure that the reaction conditions minimize the effects of flow in the extruder. The gel fractions at higher peroxide levels appear to be lower than expected, however the variability is also larger. It is not clear what the cause of this reduction in gel level is, and further experiments should be performed to adequately explain, or discount the phenomenon. Modification experiments were performed with only one polymer type. Therefore the model should be tested using other types, including HDPE in a different molecular weight range and also LLDPE to test the effects of copolymer containing short branches.

Research projects seem to be never completely finished, there is always a new door opened or some unusual observation that could be investigated further. It is hoped that the findings of this thesis will inspire continuing research on the technology of polymer manufacturing processes.

Chapter 6 Appendix

6.1 Gel data.

Sample	bottle	wt%	peroxide type	temperature °C	gel fraction	screw speed (RPM)
MT39	14	0.2004	Lup 101	190	0.063	10
					0.055	
					0.05	
MT38	16	0.8838	Lup 101	190	0.484	10
					0.52	
					0.559	
MT32	24	0.1	Lup 101	200	0.021	10
					0.019	
					0.018	
MT01	14	0.2	Lup 101	200	0.056	5
					0.079	
					0.06	
					0.058	
					0.04	
					0.036	
MT20	8	0.3511	Lup 101	200	0.207	10
					0.209	

					0.239	
MT03	15	0.5062	Lup 101	200	0.295	5
					0.275	
					0.364	
					0.436	
					0.335	
					0.32	
MT02	16	0.8838	Lup 101	200	0.596	5
					0.714	
					0.563	
					0.579	
					0.693	
					0.45	
MT17	12	0.984	Lup 101	200	0.555	10
					0.631	
					0.531	
MT16	11	0.9964	Lup 101	200	0.628	10
					0.633	
					0.635	
MT14	21	1.5175	Lup 101	200	0.901	10
					0.851	
					0.913	
MT05	20	2.058	Lup 101	200	0.584	5
					0.66	
					0.644	
					0.572	
					0.63	

MT12	20	2.058	Lup 101	200	0.789 0.572 0.63 0.789	10
MT33	24	0.1	Lup 101	230	0.03 0.045	30
MT10	14	0.2004	Lup 101	230	0.03 0.042 0.041	30
MT19	8	0.3511	Lup 101	230	0.046 0.13 0.12	30
MT23	15	0.5062	Lup 101	230	0.139 0.17 0.192	30
MT24	15	0.5062	Lup 101	230	0.152 0.226 0.222	10
MT06	16	0.8838	Lup 101	230	0.222 0.426 0.447	30
MT18	12	0.984	Lup 101	230	0.4 0.46 0.425	30
MT15	21	1.5175	Lup 101	230	0.493 0.486	30

					0.502	
					0.536	
MT13	20	2.058	Lup 101	230	0.465	30
					0.45	
					0.51	
MT35	25	0.1	Lup 130	200	0.037	10
					0.041	
					0.037	
MT11	17	0.2183	Lup 130	200	0.107	5
					0.081	
					0.099	
MT21	18	0.5431	Lup 130	200	0.315	10
					0.373	
					0.287	
MT07	19	0.8806	Lup 130	200	0.687	10
					0.672	
					0.603	
MT26	22	1.37	Lup 130	200	0.383	10
					0.392	
					0.397	
MT30	23	1.37	Lup 130	200	0.416	10
					0.37	
					0.418	
MT31	23	1.37	Lup 130	200	0.322	10
					0.302	
					0.342	

AM02	17	0.218	Lup 130	200	0.045	0
					0.061	
					0.064	
AM01	19	0.8806	Lup 130	200	0.775	0
					0.837	
					0.79	
AM03	22	1.37	Lup 130	200	0.214	0
					0.134	
					0.255	
AM04	23	1.37	Lup 130	200	0.606	0
					0.699	
					0.710	
MT34	25	0.1	Lup 130	230	0.04	30
					0.037	
					0.037	
MT25	13	0.2113	Lup 130	230	0.083	30
					0.074	
					0.096	
MT09	17	0.2183	Lup 130	230	0.07	30
					0.086	
					0.03	
MT22	18	0.5431	Lup 130	230	0.177	30
					0.186	
					0.224	

MT08	19	0.8806	Lup 130	230	0.616	30
					0.586	
					0.653	
MT27	22	1.37	Lup 130	230	0.24	30
					0.176	
					0.296	
MT29	23	1.37	Lup 130	230	0.512	30
					0.485	
					0.578	
MT04	none	0	none	200	0.013	5
MT36	none	0	none	230	0.019	30
					0.026	
					0.024	
H01	none	0	none	not extruded	0.022	0
					0.026	
					0.035	

MT?? denotes minitruder experiments and AM?? denotes ampoule experiments. Experiments were performed in the order indicated by the sample number

6.2 Minitruder experiment summary

Polyethylene minitruder experiment summary.
Numbers indicate the bottle of the peroxide/ polymer mixture used for the experiment.

Level (wt%)	Peroxide type	Temperature 190	200	230
0.1	101		24	24
0.2	101	14	14	14
0.3511	101		8	8
0.5062	101		15	15,15
0.88	101	16	16	16
0.984, 0.9964	101		12,11	12
1.5175	101		21	21
2.058	101		20, 20	20
0.1	130		25	25
0.218, 0.2113	130		17	13,17
0.5431	130		18	18
0.8806	130		19	19
1.37	130		22,23,23	22,23